The Bystander Effect in Hepatitis C Virus Infection: Cellular Interactions Between Infected Cells and Uninfected Cells

Kate Rebecca Muller

B. Medicine, B. Surgery (Adel)

Department of Molecular and Cellular Biology

School of Biological Sciences

The University of Adelaide

THE UNIVERSITY of ADELAIDE

A dissertation submitted to The University of Adelaide

in candidature for the degree of

Doctor of Philosophy in the Faculty of Science

March 2015

Table of Contents

List of Figures

Chapter 3

List of Tables

Abstract

Hepatitis C virus (HCV) is a major cause of chronic liver disease worldwide that often results in progressive liver disease in the form of fibrosis, cirrhosis and in some cases, hepatocellular carcinoma. The mechanisms responsible for progression to advanced liver disease are poorly understood, but this primarily occurs as a result of chronic hepatic inflammation. Despite universal involvement of the liver in this inflammatory and fibrogenic process, only a small percentage of hepatocytes are infected. We therefore hypothesised that the pathological effect of the virus is extended beyond the infected hepatocyte to uninfected 'bystander' cells by cellular interactions between these cells. To study this hypothesis, we developed *in vitro* cell culture model systems to observe the interactions between HCV-infected and uninfected Huh-7 cells and stellate cells.

HCV permissive Huh-7 cells are relatively unresponsive to virus infection with regard to the innate immune response. This is due to a lack of expression of the pattern recognition receptor Toll-like receptor 3 (TLR3), which is known to play an important role in the innate immune response to HCV infection. To restore the response of infected Huh-7 cells to HCV we generated a Huh-7 cell line stably expressing functional TLR3. We subsequently demonstrated by microarray analysis upregulation of TLR3 response genes such as chemokines and classical interferon response genes (ISGs) in response to HCV infection of these cells.

To prevent HCV infection of Huh-7 'bystander' cells we also generated a line refractory to HCV infection by shRNA knockdown of the essential HCV entry

receptor CD81. This cell line was also tagged with GFP to allow for FACS sorting of uninfected cells in co-culture.

We subsequently employed these cell lines in conditioned media and co-culture model systems to examine the cell interactions mediated by soluble factors and cell-to-cell contact at the level of the transcriptome using Affymetrix microarray analysis. Although the effect of HCV-infected hepatocytes on uninfected 'bystander' hepatocytes was not dramatic, preliminary data suggested that suppressor of cytokine signalling 3 (SOCS3), a known inhibitor of endogenous interferon signalling pathways, is upregulated in uninfected Huh-7 cells co-cultured with HCV-infected TLR3-positive Huh-7 cells. Furthermore we also demonstrated that HCV-infected cells exert an antiviral effect on other infected cells, possibly via exosome-mediated signalling, and can increase expression of pro-fibrogenic markers in hepatic stellate cells. We also showed that TLR3-positive uninfected Huh-7 cells enhance chemokine expression in HCV-infected hepatocytes.

In summary, we have generated stable cell lines that can be employed in an *in vitro* cell culture model system to study the interactions between HCV-infected hepatocytes and other resident liver cells such as uninfected hepatocytes and hepatic stellate cells. We have demonstrated bidirectional cross-talk between cell types, and the observed exerted effects are likely to contribute to the pathogenesis of chronic liver disease in HCV infection by recruiting uninfected cells into the pro-inflammatory and pro-fibrogenic response to HCV infection. The knowledge gained from this work contributes to our understanding of the mechanisms underlying progression of liver disease in HCV infection.

Declaration

I certify that this work contains no material which has been accepted for the award of any other degree or diploma in my name in any university or other tertiary institution and, to the best of my knowledge and belief, contains no material previously published or written by another person, except where due reference has been made in the text. In addition, I certify that no part of this work will, in the future, be used in a submission in my name for any other degree or diploma in any university or other tertiary institution without the prior approval of the University of Adelaide.

I give consent to this copy of my thesis, when deposited in the University Library, being made available for loan and photocopying, subject to the provisions of the Copyright Act 1968.

I also give permission for the digital version of my thesis to be made available on the internet, via the University's digital research repository, the Library Search and also through web search engines.

Kate Rebecca Muller

March 2015

Acknowledgements

I would like to thank Associate Professor Michael Beard and all the members of the Hepatitis C Research Laboratory for the opportunity and support they have given me during the conduct of this PhD. In particular I would like to thank Dr Nicholas Eyre for his teaching, support and assistance over the last few years, and Dr Kylie van der Hoek for her help with microarray analysis. I would also like to thank Mehdi Ramezani-Moghadam from the Westmead Millennium Institute for Medical Research for his assistance with the stellate cell work.

I would like to thank my colleagues at Flinders Medical Centre for their encouragement and support that has allowed me to undertake these studies whilst continuing in a clinical role.

I would like to thank my parents, Di, Andrew, John and Gill and my sister Bree and brother Tom for their support over the years. I also wish to thank my friends for their encouragement and finally my partner, Chad, for his support and motivation.

I would like to dedicate this thesis to my late uncle, Dr Michael Nihill, who inspired me to follow him into academia.

Presentations, Publications and Awards

Presentations

HCV-induced changes in gene expression in non-infected ‘bystander’ Huh-7 cells. 18th International Symposium on Hepatitis C and Related Viruses, Seattle, USA, September 2011 (poster).

HCV-induced changes in gene expression in non-infected ‘bystander’ Huh-7 cells. ACH2 Workshop, Adelaide, Australia, June 2012 (oral).

HCV-induced changes in gene expression in non-infected ‘bystander’ Huh-7 cells. HCV 2012: 19th International Symposium on Hepatitis C and Related Viruses, Venice, Italy, October 2012 (poster).

The effect of hepatitis C infected Huh-7 cells on 'bystander' cells. Australian Gastrointestinal Week, Melbourne, Australia, October 2013 (poster of merit).

The effect of hepatitis C infected Huh-7 cells on 'bystander' cells. HCV 2013: 20th International Symposium on Hepatitis C and Related Viruses, Melbourne, Australia, October 2013 (poster).

Publications

TLR3-dependent cross-talk between HCV-infected and uninfected hepatocytes. Muller, K.R., Eyre, N.S., Van der Hoek, K.H., Li, K., Beard M.R. (in preparation).

Awards

MSD Hepatology Young Achiever Award, 2012

Abbreviations used

ATP	adenosine triphosphate
bp	base pairs
BSA	bovine serum albumin
°C	degrees Celsius
CCL	chemokine (C-C motif) ligand
cDNA	complementary DNA
CLDN	claudin
cm	centimetres
CMV	cytomegalovirus
COL1a1	collagen type 1 alpha 1
C_T	threshold cycle
CXCL	chemokine (C-X-C motif) ligand
CXCR	chemokine (C-X-C motif) receptor
Da	daltons
DAPI	4',6-diamidino-2-phenylindole
dATP	deoxyadenosine-5’-triphosphate
dCTP	deoxycytosine-5’-triphosphate
DDIT4	DNA damage inducible transcript 4
DDX60	DEAD (Asp-Glu-Ala-Asp) Box Polypeptide 60
dGTP	deoxyguanosine-5’-triphosphate
dH_2O	deionised water
DMEM	Dulbecco’s Modified Eagle Medium
DMSO	dimethyl sulfoxide
DNA	deoxyribonucleic acid
dNTP	deoxyribonucleotide triphosphate

dsRNA	double stranded RNA
dTTP	deoxythymidine-5’-triphosphate
ECM	extracellular matrix
EDTA	ethylenediaminetetraacetic acid
ELISA	enzyme-linked immunosorbent assay
EMCV	encephalomyocarditis virus
ER	endoplasmic reticulum
FACS	fluorescence-activated cell sorting
FBS	foetal bovine serum
ffu	focus-forming units
g	grams
GAGs	glycosaminoglycans
GFP	green fluorescent protein
HABP2	hyaluronic acid binding protein 2
HCV	hepatitis C virus
HCVcc	cell-culture propagated hepatitis C virus
HCC	hepatocellular carcinoma
HEPES	4-(2-hydroxyethyl)-1-piperazineethanesulfonic acid
HIV	human immunodeficiency virus
HRP	horseradish peroxidase
IFI6	interferon alpha-inducible protein 6
IFIT	interferon-induced protein with tetratricopeptide repeats
IFITM	interferon induced transmembrane protein
IFN-α	interferon alpha
IFN-β	interferon beta
IL	interleukin
IP-10	interferon gamma-induced protein 10
IRES	internal ribosome entry site

IRF	interferon regulatory factor
ISG	interferon stimulated gene
ISGF3	interferon-stimulated gene factor-3
ISRE	interferon-stimulated response element
JAK	janus kinase
kb	kilobases
kDa	kilo Daltons
kV	kilovolts
LDL	low-density lipoprotein
LDL-R	low-density lipoprotein receptor
µF	microfarad
µg	micrograms
µl	microlitres
µM	micromolar
mA	milliamps
MAVS	mitochondrial antiviral-signalling protein
MCP1	monocyte chemotactic protein-1
mg	milligrams
MIG	monokine induced by gamma interferon
MIP1β	macrophage inflammatory protein-1β
ml	millilitres
mM	millimolar
MOI	multiplicity of infection
mRNA	messenger RNA
MSR1	class A scavenger receptor type 1
MW	molecular weight
NCR	non-coding region
NF-κB	nuclear factor kappa-light-chain-enhancer of activated B cells

ng	nanograms
nm	nanometres
nM	nanomolar
NK	natural killer
NS	non-structural
OAS	2'-5'-oligoadenylate synthetase
OCLN	occludin
OD	optical density
ORF	open reading frame
PAGE	polyacrylamide gel electrophoresis
PAMP	pathogen-associated molecular pattern
PBS	phosphate buffered saline
PCR	polymerase chain reaction
PEG	polyethylene glycol
pg	picograms
pM	picomolar
pmol	picomoles
poly I:C	polyinosinic:polycytidylic acid
PKR	protein kinase R
PRR	pattern recognition receptor
qPCR	quantitative polymerase chain reaction
qRT-PCR	real-time reverse-transcription PCR
RANTES	Regulated on Activation, Normal T cell Expressed and Secreted
RdRp	RNA-dependent RNA polymerase
RELN	reelin
RIG-I	retinoic acid-inducible gene I
RIPA	radio-immunoprecipitation assay
RNA	ribonucleic acid

ROS	reactive oxygen species
rpm	revolutions per minute
SCID	severe combined immunodeficiency
SDS	sodium dodecyl sulfate
shRNA	short hairpin RNA
siRNA	small interfering RNA
SOC	super optimal broth with catabolite repression
SOCS3	suppressor of cytokine signalling 3
SPP	secreted phosphoprotein 1
SR-B1	scavenger receptor class B1
STAT	signal transducer and activator of transcription
SV40	simian virus 40
SVR	sustained virological response
TAE	Tris-Acetic Acid-EDTA
TARC	thymus and activation-regulated chemokine
TBS-T	Tris-buffered saline-Tween 20
TEMED	N,N,N’,N’-tetramethylethylenediamine
TfRTCA	transferrin receptor-truncated amino terminus
TGF-β	transforming growth factor beta
TIMP-1	tissue inhibitor of metalloproteinase 1
TIR	toll IL-1 receptor
TLR3	toll-like receptor 3
TNF	tumour necrosis factor
TRIF	toll-interleukin-1 receptor domain-containing adaptor inducing IFN-β
Tris	3,3,5,5-tetramethylbenzidine
U	units
uPA	urokinase-type plasminogen activator
UTR	untranslated region

UV	ultraviolet
V	volts
VLDL	very low-density lipoprotein
VSV	vesicular stomatitis virus
v/v	volume per volume
w/v	weight per volume
x g	G-force

Materials Providers

Addgene	Massachusetts, USA
Affymetrix	California, USA
Agfa	Mortsel, Belgium
AppliChem	Darmstadt, Germany
Beckman Coulter	Miami, FL, USA
Becton Dickinson	New Jersey, USA
Bioline	Sydney, Australia
BioRad Laboratories	California, USA
Biotium	California, USA
Biovision	California, USA
Clontech	California, USA
Corning	New York, USA
DAKO	California, USA
Eppendorf	Hamburg, Germany
GE Healthcare	Buckinghamshire, UK
GeneWorks	Adelaide, Australia
GeoSpiza	Washington, USA
GraphPad	California, USA
Imgenex	California, USA
Implen	München, Germany
Life Technologies	California, USA
Macherey-Nagel	Düren, Germany
Merck Millipore	County Cork, Ireland
Nikon	Tokyo, Japan
New England Biolabs	Massachusetts, USA

Olympus	Tokyo, Japan
Pall Life Sciences	New York, USA
Perkin Elmer	Massachusetts, USA
Promega	Wisconsin, USA
QIAGEN	Limburg, Netherlands
Roche	Indiana, USA
Rockland Immunochemicals	Pennsylvania, USA
Sartorius Stedim Biotech	Göttingen, Germany
Sigma-Aldrich	Missouri, USA
Thermo Scientific	Massachusetts, USA
UVP Inc	California, USA

Chapter 1
Introduction

1.1 Hepatitis C virus

1.1.1 Epidemiology

The hepatitis C virus (HCV) is a major cause of chronic liver disease worldwide and infects approximately 3% of the world's population. Liver disease secondary to HCV is the leading indication for liver transplantation (Brown 2005; Charlton 2005; Te and Jensen 2010). The HCV-related burden of chronic liver disease is set to rise over the coming years, resulting in a significant impact on global health systems (Wong *et al.* 2000; Law *et al.* 2003; Razali *et al.* 2007; Davis *et al.* 2010; Thomas 2012).

HCV is an enveloped RNA virus and is a member of the *Hepacivirus* genus in the *Flaviviridae* family. It infects humans and chimpanzees. The HCV genome was first identified in 1989 using a molecular biological approach (Choo *et al.* 1989). Prior to this HCV was the major cause of 'non-A, non-B hepatitis' (Choo *et al.* 1990). Current estimates suggest that greater than 180 million people worldwide have anti-HCV antibodies, and 350,000 HCV-related deaths occur annually. Prevalence is highest in regions of Asia and Africa (Perz *et al.* 2006; Mohd Hanafiah *et al.* 2013). In Australia, prevalence is approximately 1.3% (Sievert *et al.* 2011) (Figure 1.1).

NOTE:
This figure/table/image has been removed
to comply with copyright regulations.
It is included in the print copy of the thesis
held by the University of Adelaide Library.

Source: ©WHO, 2004

Figure 1.1 Global prevalence of HCV infection (Lavanchy 2008)

Transmission of HCV is via percutaneous exposure to infected blood or blood products. Since the adoption of blood and organ donor screening in developed countries as a result of diagnostics developed after the discovery of HCV, the incidence of acquisition of HCV from blood transfusion and organ transplantation is negligible, but this mode of transmission prior to 1990 accounts for 5-10% of infections in Australia. Haemodialysis is a risk factor for HCV positivity (Chak *et al.* 2011). The main mode of acquisition in developed countries is now via intravenous drug use (approximately 80%), with less common modes being through tattooing, piercing and occupational needle stick injuries (Dore *et al.* 2003). Vertical transmission rates are low (5-7%) but not negligible (Dore *et al.* 2003; Mohan *et al.* 2010). Whether sexual transmission occurs is controversial; rates are less than 1% (Terrault *et al.* 2013). In contrast, nosocomial transmission accounts for a significant number of infections in the developing world and endemic countries, via blood transfusion, reuse of syringes and needles and other medical procedures. A proportion of the HCV-infected population in Australia is represented by immigrants from these endemic areas (Sievert *et al.* 2011).

1.1.2 Natural history of HCV infection

Following acute exposure to HCV, only approximately 20% of individuals will successfully eradicate the infection, while the remaining 80% of individuals will develop chronic infection. The majority of acute infections are asymptomatic. Of those individuals who develop chronic HCV infection, approximately 20% will have progressive liver disease over a period of about 20-30 years, culminating in

liver cirrhosis and, in a small proportion (2%), hepatocellular carcinoma (HCC) (Alter 1995) (Figures 1.2 and 1.3). Liver disease occurs as a result of chronic hepatic inflammation, which is a consequence of the host response to the virus. The rate of progression to advanced liver disease is influenced by co-factors such as alcohol consumption and human immunodeficiency virus (HIV) co-infection.

1.1.3 Treatment

Treatment for hepatitis C virus infection became available in 1991. Initial treatment was with standard interferon-α, with response rates of only 10-20%. Interferon-α is a cytokine that stimulates the immune response and is anti-viral. When used in combination with the guanine nucleoside analogue ribavirin, response rates improved to 40% (Foster 2010). However, treatment was revolutionized in 2001 with the introduction of pegylated interferon-α. Pegylation enhances the antiviral activity of interferon-α by altering the pharmacokinetic and pharmacodynamic properties of the drug: increasing half-life, reducing clearance and altering volume of distribution. Sustained virological response (SVR, defined as undetectable HCV RNA in serum 6 months after cessation of treatment) rates in pharmaceutical registration trials improved to 40-50% in HCV genotype 1 infection and 75-85% for genotype 2 and 3 infection, when used in combination with ribavirin (Manns *et al.* 2001; Fried *et al.* 2002; Hadziyannis *et al.* 2004). Genotype has become a clear predictor of treatment response.

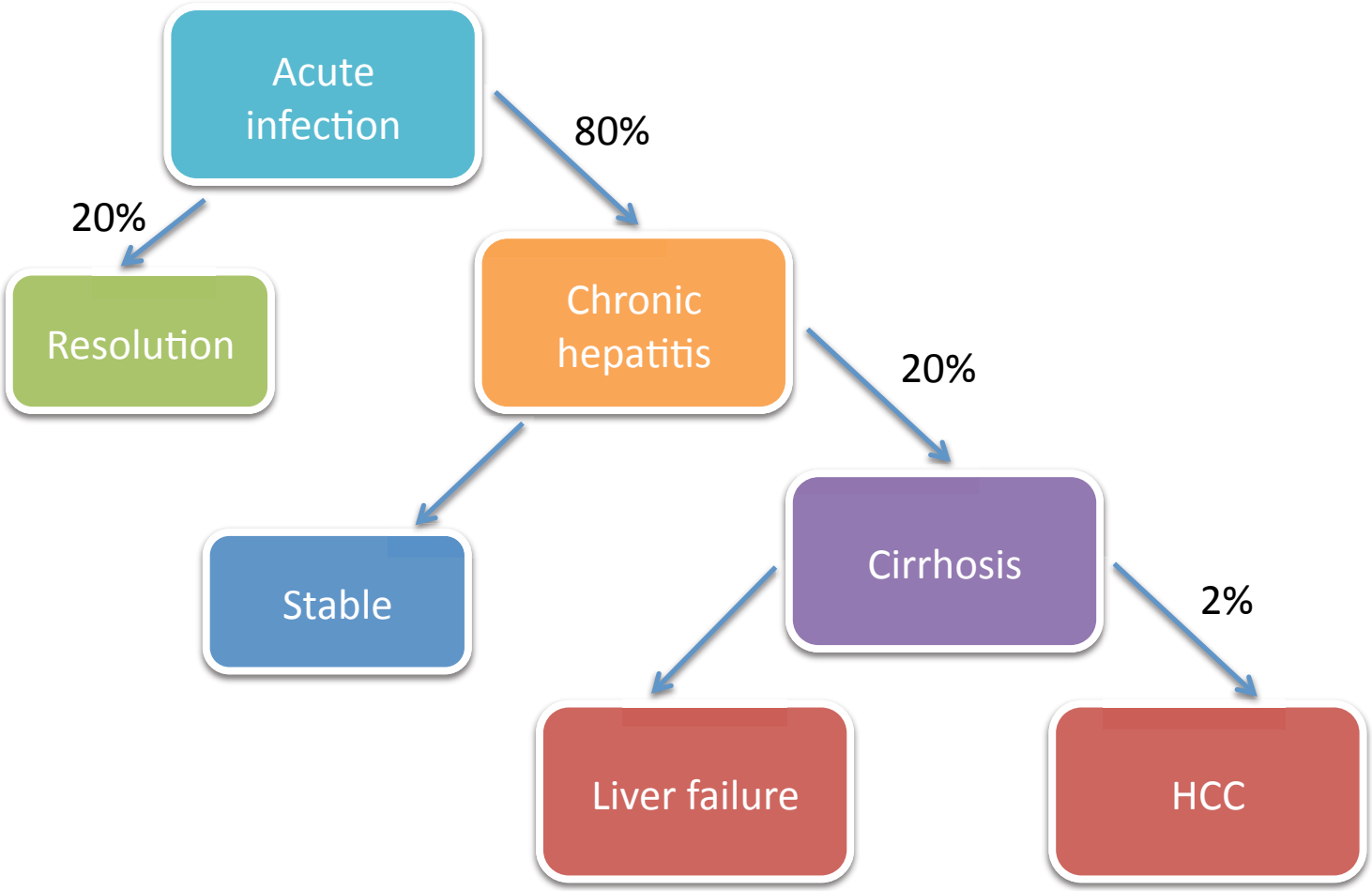

Figure 1.2 Natural history of HCV infection

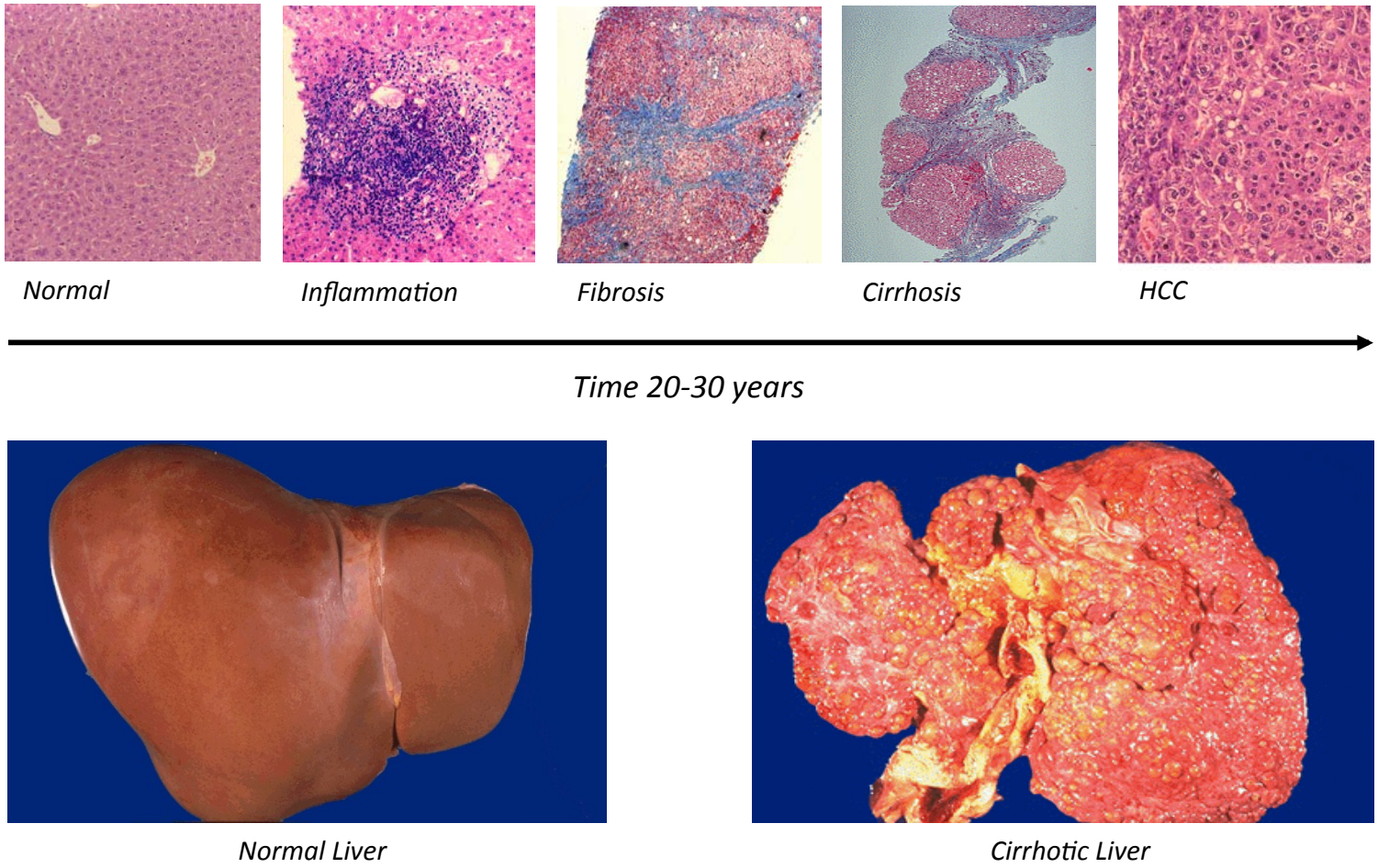

Figure 1.3 Progression of HCV induced liver disease

Treatment with pegylated interferon-α and ribavirin has now been the standard of care for a number of years. Treatment is given for a period of 24- or 48- weeks depending on genotype, and is associated with a number of side effects, including influenza-like symptoms, mood disturbances, insomnia, rash, anorexia and weight loss, and haematological disturbance (Fried 2002). The majority of side effects are attributable to interferon. Such side effects and treatment duration make treatment intolerable for some patients, particularly those with pre-existing psychiatric disorders and patients with advanced liver disease. Hence, a number of patients are not candidates for treatment or are unable to complete the full course. Additionally, patients with advanced liver disease or significant hepatic fibrosis, and patients with comorbidities such as insulin resistance, obesity, significant alcohol consumption and HIV co-infection tend to have lower SVR rates than patients who do not.

The poorer response rates in genotype 1 infection, lower response rates in patients with advanced liver disease and other co-morbidities and the poor tolerability of treatment in certain cohorts has led to an unmet need for treatment in a significant number of patients. Therefore, research has been directed at developing specific anti-virals with increased efficacy, particularly for genotype 1 infection.

Treatment was revolutionized again with the advent of the directly acting anti-virals (DAAs). The first generation of these, the NS3 serine protease inhibitors boceprevir and telaprevir, were added to standard therapy of patients with genotype 1 HCV infection. SVR rates in these patients improved to 70-80% with such triple therapy regimens (Marks and Jacobson 2012), although were not as promising in patients who have previously failed to respond to therapy or have advanced liver disease.

Unfortunately, there is rapid development of antiviral resistance to these compounds when used in monotherapy, hence interferon remained a key component of treatment (Aloia *et al.* 2012; Calle Serrano and Manns 2012). Additionally, these drugs increased the adverse effect profile of therapy. Multiple other compounds are in various stages of development, are undergoing clinical trials or have recently become available for clinical use, such as the second generation NS3/4A protease inhibitor simeprevir and the NS5B polymerase inhibitor sofosbuvir, among many others. It is likely that this next generation of directly-acting antivirals will form part of standard care within the next few years. Clinical trials suggest that these drugs are more efficacious, have improved side effect profiles and pan-genotypic activity (Pol *et al.* 2012; Fried *et al.* 2013; Jacobson *et al.* 2013; Lawitz *et al.* 2013; Zeuzem *et al.* 2013). Interferon-free, directly-acting antiviral combination regimens are likely to become standard therapy (Gane 2012), with promising clinical trial results reported (Kowdley *et al.* 2014; Sulkowski *et al.* 2014) and have been enthusiastically adopted into clinical practice.

1.1.4 The HCV genome

HCV is a single-stranded positive-sense RNA virus with a genome of 9.6 kb. The open reading frame (ORF) encodes a protein of approximately 3,000 amino acids and is flanked by 5'- and 3'-untranslated regions (UTRs). The encoded protein is a polyprotein precursor cleaved into a number of structural and non-structural proteins by both viral and host proteases, occurring co- and post-translationally (Figure 1.4).

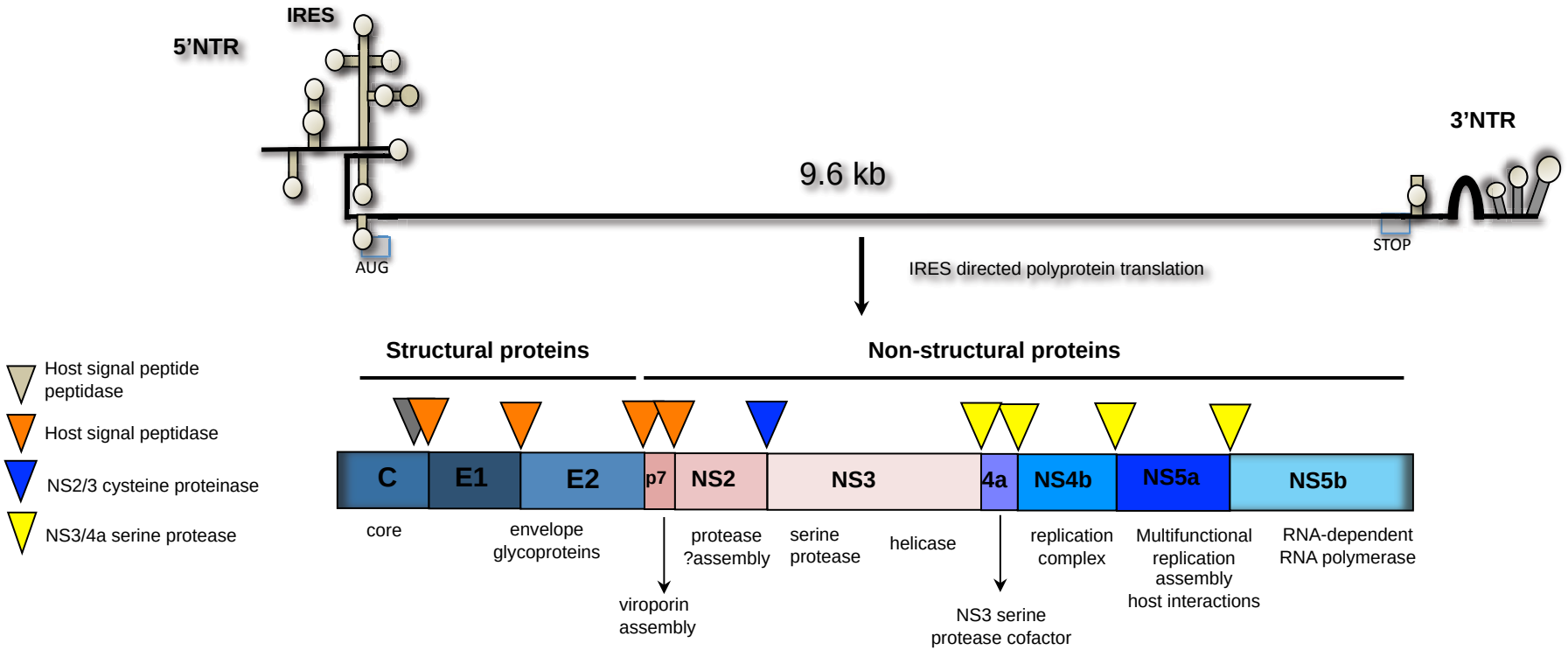

Figure 1.4 HCV genome and polyprotein

The 5'-UTR contains an internal ribosome entry site (IRES) which is required for cap-independent translation. The region also contains an additional sequence which plays a pivotal role in viral replication. The 5'-UTR is conserved across HCV isolates. The 3'-UTR is also conserved and appears to be essential for viral replication. It contains three domains, namely a variable region of approximately 40 nucleotides, a poly (U/UC) tract and a terminal segment (the 'X-tail') (Moradpour *et al.* 2007; Suzuki *et al.* 2007).

1.1.5 HCV genotypes

There are 7 major genotypes (designated 1-7) (Nakano *et al.* 2011) which vary in their geographical distribution and, as previously discussed, the response to treatment with pegylated interferon-α and ribavirin. They differ in their nucleotide sequence by 30-35%. Genotypes 1 and 3 predominate globally, including in Australia, where they account for approximately 55% and 35% of cases respectively (Dore *et al.* 2003). Genotypes 4-6 tend to be restricted geographically to regions of Africa, the Middle East and Asia (Bowden and Berzsenyi 2006) (Figure 1.5). HCV genotypes can be further classified into subtypes (a, b, c etc). The viral population within an individual is also heterogeneous in that it is formed of multiple closely related variants known as quasispecies. These variants arise due to the high mutation rate conferred by the error-prone HCV RNA-dependent RNA polymerase (NS5B) (Martell *et al.* 1992; Pawlotsky 2003).

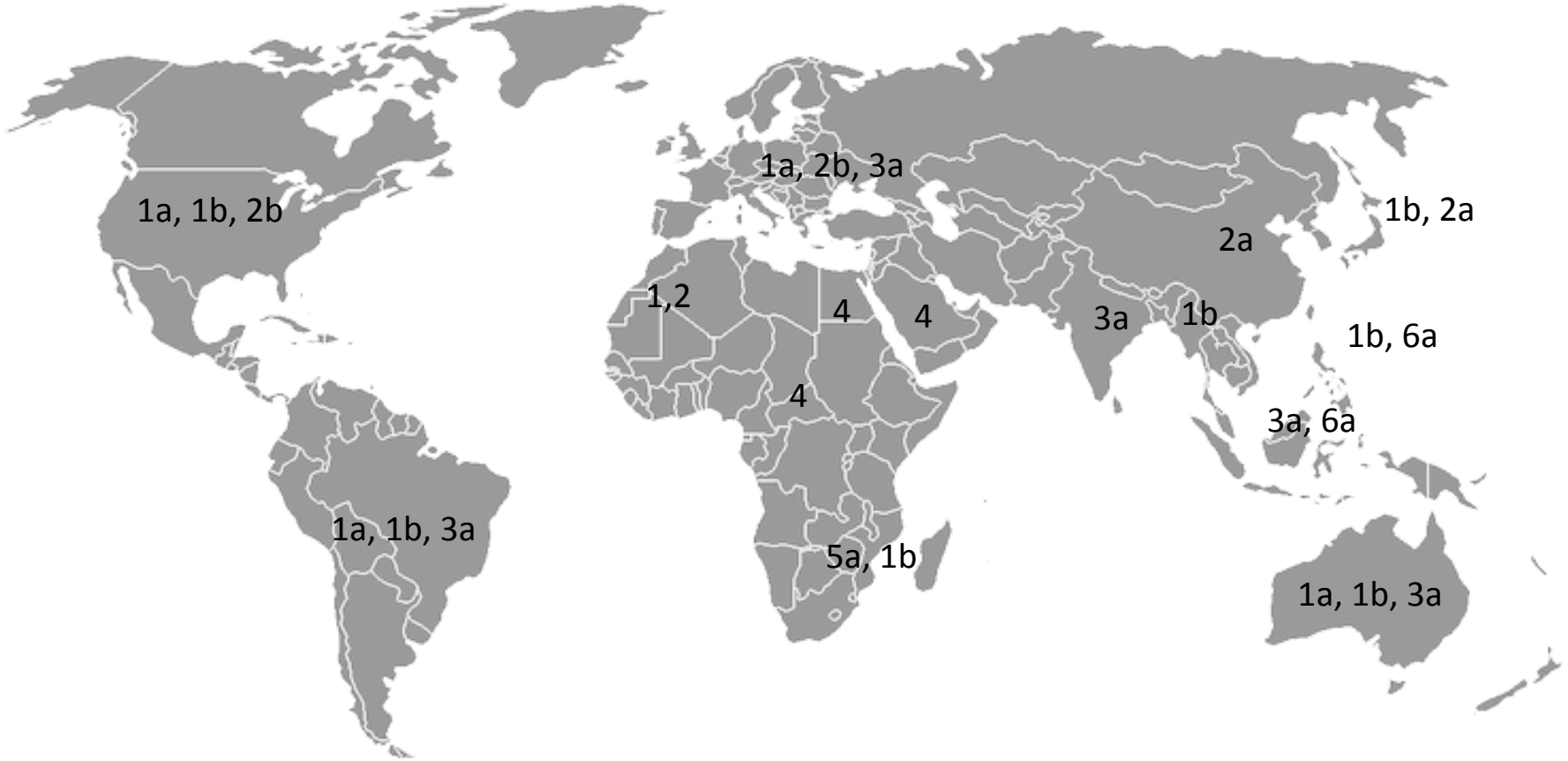

Figure 1.5 Global HCV genotype distribution

1.1.6 HCV proteins

The polyprotein precursor encoded for by the HCV RNA open reading frame is cleaved into 10 proteins by cellular and viral proteases. These are the structural proteins (core, E1 and E2), the p7 polypeptide and the non-structural proteins (NS2, NS3, NS4A, NS4B, NS5A and NS5B).

Core: The core protein is targeted to the endoplasmic reticulum (ER) but is also found to be associated with lipid droplets (Moradpour *et al.* 1996; Barba *et al.* 1997; Miyanari *et al.* 2007). It is located at the N-terminus of the precursor protein and is cleaved from this protein by the ER signal peptidase, along with the other structural proteins and p7. The mature protein (21-22 kDa) forms the viral nucleocapsid as well as playing roles in lipid metabolism and the development of HCC (Moriya *et al.* 1997; Moriya *et al.* 1998; Perlemuter *et al.* 2002; Dharancy *et al.* 2005; Yamaguchi *et al.* 2005; Akuta *et al.* 2007; Tanaka *et al.* 2008; Miyoshi *et al.* 2011; El-Shamy *et al.* 2013). There is also evidence to suggest that core is involved in host immune responses and other cellular pathways involved in pathogenesis, although data are somewhat contradictory (Marusawa *et al.* 1999; You *et al.* 1999; Dolganiuc *et al.* 2007; Park *et al.* 2012).

Envelope proteins, E1/E2: E1 and E2 form a non-covalent complex which is the basis of the viral envelope. They are glycosylated transmembrane proteins (30-35 kDa and 70-75 kDa, respectively) that mediate cell receptor binding and hence virion cell entry. (Hsu *et al.* 2003; Moradpour *et al.* 2007; Suzuki *et al.* 2007)

p7: The small p7 protein (63 amino acids) is thought to belong to the viroporin family. It has two transmembrane segments and a hydrophilic, cytoplasmic loop. It has been documented to function as a cation channel and is essential for viral replication. The exact role of p7 in replication is not well understood but it is probably involved in viral particle assembly and release (Gentzsch *et al.* 2013). It localizes to the ER and interacts with other HCV proteins such as NS2. (Sakai *et al.* 2003; Moradpour *et al.* 2007; Steinmann *et al.* 2007; Wozniak *et al.* 2010; Vieyres *et al.* 2013)

NS2: The NS2 protein (23 kDa) also localizes to the ER and functions along with NS3 as an autoprotease to cleave the NS2/NS3 junction (Santolini *et al.* 1995; Welbourn and Pause 2007). Its protease activity is located in the C-terminal portion of the protein, however its full length in the cleaved form also appears to play an important role in viral assembly and possibly egress (Jones *et al.* 2007; Jirasko *et al.* 2010; Popescu *et al.* 2011; de la Fuente *et al.* 2013).

NS3: The NS3 protein exhibits multiple functions. Located within the N-terminal portion of the protein is a serine protease which cleaves the remaining downstream non-structural proteins. NS4A acts as a cofactor for the protease and is important for membrane association of the complex. It is the NS3/4A serine protease that is the target of the first generation of directly acting antivirals against HCV, namely boceprevir and telaprevir (Morikawa *et al.* 2011), as well as the second generation drug simeprevir (Lin *et al.* 2009). It plays a role in evasion of the innate immune system and persistence of infection by cleavage of adaptor proteins involved in immune sensing, Toll-interleukin-1 receptor domain-containing adaptor inducing

IFN-β (TRIF) and mitochondrial antiviral signalling protein (MAVS) (Li *et al.* 2005; Meylan *et al.* 2005). In the C-terminus of NS3 is a viral helicase which unwinds double-stranded RNA in an ATP-dependent manner and is important in viral replication.

NS4A: As described above, NS4A forms a non-covalent complex with NS3 and acts as a cofactor for the serine protease, with roles in NS3 folding, membrane association and HCV replication and assembly (Lindenbach *et al.* 2007; Morikawa *et al.* 2011; Phan *et al.* 2011).

NS4B: NS4B is a hydrophobic protein that is highly conserved across genotypes. It induces membrane alterations in the ER to form the membranous web, which is the site of the HCV replication complex (Egger *et al.* 2002; Gosert *et al.* 2003). Formation of a membrane associated replication complex containing viral proteins and RNA is common to positive-sense RNA viruses. NS4B comprises four segments, flanked by N- and C-terminal helices, which traverse the ER membrane and it undergoes oligomerisation (Hugle *et al.* 2001; Lundin *et al.* 2003; Yu *et al.* 2006). It provides a platform for interaction with the other non-structural proteins and has a role in virus assembly (Jones *et al.* 2009; Gouttenoire *et al.* 2010).

NS5A: Also anchored to the ER, NS5A is a phosphoprotein with three domains which appears to have a number of essential roles in HCV replication (Blight *et al.* 2000; Lohmann *et al.* 2001) and virion assembly (Appel *et al.* 2008). It displays differential phosphorylation that dictates the efficiency of replication (Evans *et al.* 2004). NS5A has been shown to bind HCV RNA (Huang *et al.* 2005), other HCV proteins (Shimakami *et al.* 2004; Masaki *et al.* 2008) and host factors (Hamamoto *et*

al. 2005; Waller *et al.* 2010), functions that appear to be critical for replication. It is the target of a number of new directly-acting antiviral agents currently in development or recently made available for clinical use, such as daclatasvir and ledipasvir.

NS5B: This is an RNA-dependent RNA polymerase (RdRp), responsible for synthesis of both negative- and positive-strand RNA (Behrens *et al.* 1996). It is anchored to the ER membrane. NS5B is also a therapeutic target and the pangenotypic compound sofosbuvir is now in clinical use.

1.1.7 The HCV life cycle (Figure 1.6)

HCV virions are approximately 40-70nm in diameter. Their exact structure has not been determined, but they are thought to consist of an icosahedral nucleocapsid composed of oligomers of the core protein that encapsulate the RNA genome and is surrounded by a host-cell derived envelope studded with envelope proteins E1 and E2 (Moradpour *et al.* 2007). They exist in the circulation in association with low-density and very-low-density lipoproteins (LDLs and VLDLs) as well as immunoglobulins and as free particles. HCV infects hepatocytes, although infection of other cell types such as B-cells has been described.

Entry: HCV particles interact with a number of proteins on the hepatocyte cell surface (Figure 1.7). It is the specificity to these proteins that is thought to be responsible for the cell and species tropism of HCV. Receptors known to play a role in HCV entry into the hepatocyte include the low-density lipoprotein receptor

Figure 1.6 Life cycle of HCV (a) virus binding and internalisation **(b)** cytoplasmic release and uncoating (**c)** IRES-mediated translation and polyprotein processing **(d)** RNA replication **(e)** packaging and assembly (**f)** virion maturation and release. **(**Moradpour *et al.* 2007)

Figure 1.7 HCV entry (McCartney *et al.*2011)

(LDL-R) (Agnello *et al.* 1999; Monazahian *et al.* 1999) and scavenger receptor class B type I (SR-BI) (Scarselli *et al.* 2002), both involved in lipoprotein binding, glycosaminoglycans (GAGs) (Barth *et al.* 2003), CD81 (Pileri *et al.* 1998), Claudin-1 (CLDN1) (Evans *et al.* 2007) and Occludin (OCLN) (Ploss *et al.* 2009). These interactions appear to occur sequentially. Initially there is low-affinity binding to the LDL-R and GAGs, followed by a higher-affinity interaction with scavenger receptor class B1 (SR-B1), which has been shown to be critical for HCV cell entry. Binding to SR-B1 appears to facilitate interaction with the tetraspanin CD81, possibly by altering the conformation of the virion and exposing the CD81 binding site on envelope protein E2 (Kapadia *et al.* 2007; Zeisel *et al.* 2007; Bitzegeio *et al.* 2010; Ploss and Evans 2012).

CD81 is ubiquitously expressed and has multiple functions. It consists of four transmembrane domains separated by intra- and extra-cellular loops. Although not sufficient for HCV entry alone, CD81 has been shown to be an essential entry factor for HCV. HCV infection has been shown to be inhibited by anti-CD81 antibodies, soluble CD81 large extracellular loops and when expression is prevented by small interfering RNAs (siRNAs) (Zhang *et al.* 2004). Additionally, CD81-negative cell lines are permissive to HCV entry after expression of exogenous CD81 (McKeating *et al.* 2004). Although evidence has been published suggesting that CD81-independent routes of virus transmission between cells may occur (Timpe *et al.* 2008; Witteveldt *et al.* 2009), these findings have been subsequently refuted by the original authors (Brimacombe *et al.* 2010).

CLDN1 has also been shown to be an essential hepatocyte entry factor for HCV. Claudins are components of tight junctions and therefore have an important role in establishing cell polarity and regulating paracellular transport (Heiskala *et al.* 2001). Other members of the Claudin family, CLDN6 and CLDN9, have also been shown to permit cell entry (Zheng *et al.* 2007; Meertens *et al.* 2008), although it is not clear whether this is physiologically significant. HCV entry into primary human hepatocytes is not prevented by monoclonal antibodies against these claudins and expression *in vivo* is low (Fofana *et al.* 2013). HCV infection of hepatocytes can be prevented by anti-CLDN1 antibodies and siRNAs or permitted by CLDN1 expression in some SR-B1-positive, CD81-positive, CLDN1-negative cell lines (Evans *et al.* 2007; Fofana *et al.* 2010; Krieger *et al.* 2010). Evidence suggests that CLDN1 has a late role in entry, possibly at a similar time to virion binding with CD81. Although CLDN1 does not appear to directly interact with HCV, CD81-CLDN1 complexes appear to be critical and these two receptors act cooperatively to mediate viral entry into the cell (Harris *et al.* 2008; Krieger *et al.* 2010). It is suggested that this receptor association and interaction with HCV does not occur within tight junctions or at cell-cell contacts, but at the basolateral surface of the cell (Mee *et al.* 2008; Reynolds *et al.* 2008; Harris *et al.* 2010). Alternatively, transport of the complex to the tight junction after virion binding may occur (Brazzoli *et al.* 2008). CLDN1 is also essential for cell-cell spread of virus (Timpe *et al.* 2008; Brimacombe *et al.* 2010).

The expression of the essential entry factors SR-BI, CD81 and CLDN1 did not render all human cell lines susceptible to HCV infection. This suggested that an

additional entry factor existed and OCLN was hence identified from a Huh-7.5-cell line derived cDNA library screen. Along with CD81, OCLN is thought to be important for the species tropism of HCV. OCLN is also a tight junction protein and likely has a role late in the entry process (Benedicto *et al.* 2009; Liu *et al.* 2009; Ploss *et al.* 2009).

More recently it has been shown that receptor tyrosine kinases, epidermal growth factor receptor and ephrin receptor A2, act as co-factors in the process of HCV cell entry via their role in the formation of CD81-CLDN1 receptor complexes and viral glycoprotein-dependent membrane fusion (Lupberger *et al.* 2011).

Following interaction with these host factors, HCV is internalized by way of clathrin-mediated endocytosis (Blanchard *et al.* 2006). Acidification of the endosome in which the virion is contained stimulates membrane fusion and release into the cytoplasm.

Translation and polyprotein processing: Translation is initiated by the binding of the HCV IRES with the 40S ribosomal subunit and occurs directly from the HCV genome. A polyprotein is produced which is processed by cellular and viral proteases both during and after translation (Moradpour *et al.* 2007).

Replication: A membrane associated replication complex, known as the membranous web, is the site of HCV RNA replication. Its formation is induced by NS4B (although more recently other HCV proteins have been implicated (Romero-Brey *et al.* 2012)) and is derived from host ER membranes; the replication complex is also composed of viral proteins, viral RNA and other host factors. The NS5B

RdRp uses the positive-strand RNA genome as a template to synthesize a complementary negative-strand, and then synthesizes multiple copies of positive-strand RNA from this intermediate. These newly formed genomes are then utilized for translation, replication or formation of new virions (Moradpour *et al.* 2007).

Assembly and Release: Mechanisms of assembly of HCV particles have not been completely elucidated. It appears to occur in close association with lipid droplets and the ER. Both structural and non-structural HCV proteins play roles in this process. Core protein is important, in that it induces lipid droplet redistribution to a perinuclear location, and then other viral components can be recruited to these assembly sites on the cytosolic side of the ER membrane. NS5A appears to be crucial in this process. NS3 and NS2 participate in later steps of assembly, during which the envelope proteins are incorporated. Following formation of the nucleocapsid, budding into the luminal ER and maturation occur. Maturation appears to be coupled to VLDL formation. The new virion is then released from the cell by exocytosis, in a noncytolytic manner (Jones and McLauchlan 2010; Bartenschlager *et al.* 2011; Popescu *et al.* 2011).

1.1.8 HCV model systems

The study of HCV molecular virology and viral pathogenesis has been hindered by the lack of small animal models and cell culture models that faithfully recreate the complete lifecycle of the virus. Early work was performed using chimpanzees until the development of a subgenomic replicon system in 1999 (Lohmann *et al.* 1999).

Subsequently, a genomic replicon system was developed in 2002 (Ikeda *et al.* 2002). In 2005, the identification of an HCV isolate capable of replication in cell culture and production of infectious virus revolutionized the study of HCV, and now allows investigation of the complete HCV lifecycle *in vitro* (Lindenbach *et al.* 2005; Wakita *et al.* 2005; Zhong *et al.* 2005).

Animal models: Work in chimpanzees allowed for the initial identification of the virus (Choo *et al.* 1989) and this model has permitted the study of host immune responses and has a role in vaccine and drug development. However, there are ethical and financial barriers to the use of this model system, as well as some differences in the natural history of HCV infection in chimpanzees compared to humans, such as the high rate of clearance of acute infection in chimpanzees. A number of small animal models have also been developed, all with some limitations in their utility. Immunodeficient mice (such as severe combined immunodeficiency - uPA-SCID - mice) engrafted with human hepatocytes have been used in a number of studies but have the obvious limitation of a lack of adaptive immune responses. Other rodent models have been designed to overcome this limitation but these animals do not seem to develop HCV viraemia (Bukh 2012).

Cell culture systems (Figure 1.8): The subgenomic replicon system (Lohmann *et al.* 1999; Blight *et al.* 2000) and the genomic replicon system (Ikeda *et al.* 2002) utilize the human hepatoma cell line Huh-7 and have allowed for the study of HCV RNA and proteins as well as interactions with the host cell and in drug discovery. These systems, in which the HCV genome replicates autonomously under selective pressure, allow the study of HCV replication in culture, but fail to produce

Figure 1.8 HCV model systems (Tellinghuisen *et al.*2007)

infectious virus. This appears to be due to mutations which enhance replication but impact on assembly of virions (Pietschmann *et al.* 2009). Replicon systems generally consist of bicistronic RNA, where a neomycin resistance gene is encoded under the control of the HCV IRES in the first cistron, and the non-structural (subgenomic) or structural and non-structural (genomic) HCV proteins are encoded under the control of a encephalomyocarditis virus (EMCV) IRES. RNA is electroporated into cells and neomycin resistant clones are isolated (Tellinghuisen *et al.* 2007; Boonstra *et al.* 2009). The system has since been enhanced by the insertion of reporter genes such as luciferase and fluorescent proteins that allow high throughput quantification of HCV replication and tracking of HCV in living cells (Krieger *et al.* 2001; Moradpour *et al.* 2004; Ikeda *et al.* 2005).

The HCV pseudoparticle system has been important in HCV cell binding and entry studies and has been useful in the discovery of many of the HCV cell entry receptors. Pseudoparticles consist of a retroviral or lentiviral particles containing reporter genes and displaying HCV envelope proteins that drive entry of these particles (Bartosch *et al.* 2003; Drummer *et al.* 2003; Hsu *et al.* 2003). Expression of reporter genes allows for quantitation of entry when infecting permissive cell lines.

Until relatively recently it was not possible to produce infectious HCV in cell culture, but in 2005 an isolate capable of such was identified. This strain, isolated from a Japanese patient with fulminant hepatitis and termed JFH-1, was found to be infectious in both Huh-7-derived hepatoma cell lines in cell culture and in chimpanzees and chimeric mice (Lindenbach *et al.* 2005; Wakita *et al.* 2005; Zhong

et al. 2005; Lindenbach *et al.* 2006). Cell culture derived virus from this HCV genotype 2a clone was initially low titre, but the creation of chimeras of different genotypes produced higher titres in some cases, such as Jc1 (Pietschmann *et al.* 2006). The system has also been enhanced by the development of reporter systems such as luciferase and fluorescent protein tagged viruses (Vieyres and Pietschmann 2013). Since this advance, it has been possible to study the entire HCV life cycle in cell culture.

1.2 Disease progression in HCV infection

1.2.1 Background

In a proportion of individuals chronic HCV infection progresses to advanced liver disease. There is significant inter-individual variability in the rate of progression to cirrhosis, which may be related to host factors such as age, gender and co-morbid conditions. The mechanisms responsible for progression are not well understood, but liver disease in the form of fibrosis and subsequently cirrhosis appears to develop as a result of chronic hepatic inflammation.

1.2.2 Pathogenesis and pathophysiology of inflammation in HCV infection

Hepatic inflammation in chronic HCV infection is characterized by portal lymphoid aggregation, piecemeal and bridging necrosis, lobular inflammation and steatosis. The mechanisms underlying this inflammation are not completely understood. It is

recognised that hepatic injury is probably not a direct effect of the virus itself, but in fact secondary to the host immune response to the virus whereby the immune response attempts to remove HCV-infected hepatocytes (Pawlotsky 2004). In support of this, HCV is not cytopathic and hepatic damage and disease progression do not correlate with HCV viral load.

Innate immunity:

The host innate immune response is critical in HCV infection and plays an important role in initiation and magnitude of the adaptive immune response. Recognition of viral pathogen-associated molecular patterns (PAMPs) by specific host pattern recognition receptors (PRRs) initiates this response. HCV double stranded RNA (dsRNA) contains PAMPs and is recognised through two independent receptors: Toll-like receptor-3 (TLR3) and retinoic-acid-inducible gene I (RIG-I). More recently a third protein, protein kinase R (PKR) has been classified as a PRR (Arnaud *et al.* 2011). Activation of these pathways leads to transcription of Type I interferons (IFNs), α and β (Figure 1.9) (Gale and Foy 2005).

RIG-I is an ATP-dependent RNA helicase. On interaction with HCV dsRNA in the cytoplasm, caspase activation and recruitment domains within RIG-I are able to interact with mitochondrial antiviral signalling protein (MAVS), which in turn activates interferon regulatory factor 3 (IRF-3) and nuclear factor kappa-light-chain-enhancer of activated B cells (NF-κB). TLR3 is part of a family of PRRs and specifically recognises dsRNA. It is found in endosomes (Matsumoto *et al.* 2003)

Figure 1.9 Innate immune signaling in HCV infection (Gale and Foy 2005)

and recognises endosomal or extracellular dsRNAs. TLR3 activates IRF-3, IRF-7 and NF-κB via Toll-interleukin-1 receptor domain-containing adaptor inducing IFN-β (TRIF) (Gale and Foy 2005; Dustin and Rice 2007; Wang *et al.* 2009). Of note, HCV NS3/4A can cleave MAVS and TRIF, inactivating signalling (Foy *et al.* 2005; Li *et al.* 2005; Li *et al.* 2005; Meylan *et al.* 2005). Both the RIG-I and TLR3 pathways culminate in phosphorylation, dimerisation and translocation of IRF-3 to the nucleus, where interaction occurs with the IFN-β promoter and results in IFN-β production and subsequent secretion from the cell.

IFN-β, in an autocrine and paracrine manner, binds to IFN α/β receptors and activates the Jak-STAT pathway. In this signalling cascade, protein kinases Jak1 and Tyk1 catalyse phosphorylation of signal transducer and activator of transcription (STAT) -1 and -2. They then form a heterodimer and associate with IRF-9, forming the interferon-stimulated gene factor-3 (ISGF3) complex. ISGF3 is a transcription factor which localizes to the nucleus and binds to the interferon-stimulated response element (ISRE) on interferon-stimulated genes (ISGs). This leads to the up-regulation of hundreds of ISGs; these genes encode products with various functions, including chemokines, cell surface receptors and transcription factors (Gale and Foy 2005; Dustin and Rice 2007; Joyce and Tyrrell 2010). IRF-7 is one of these ISGs and is involved in a positive-feedback loop whereby IRF-7 is activated by TRIF and induces IFN-α production after phosphorylation, dimerisation (or heterodimerisation with IRF-3), translocation to the nucleus and interaction with a number of IFN-α promoter regions. IFN-α production further stimulates production of ISGs and stimulates cell-mediated immunity and cytokine

production (Gale and Foy 2005). An antiviral state results from ISG expression. However, like the ability to interfere with RIG-I and TLR3 pathways, it has been shown that HCV viral proteins are able to inhibit these interferon signalling pathways and host defences induced by interferons (Gale and Foy 2005; Sklan *et al.* 2009; Joyce and Tyrrell 2010). This leads to a chronic state of low-grade inflammation that is insufficient for viral clearance but causes chronic hepatic injury (Spengler and Nattermann 2007).

Additionally, through HCV stimulation of the TLR3 pathway, NF-κB induces transcription of pro-inflammatory cytokines and chemokines (Li *et al.* 2012). A number of cytokines and chemokines are upregulated in patients with HCV, such as CXCL10 (interferon gamma-induced protein 10, IP-10) and CCL5 (Regulated on Activation, Normal T cell Expressed and Secreted, RANTES), and have been associated with the severity of inflammation, progression to fibrosis and treatment response (Harvey *et al.* 2003; Helbig *et al.* 2004; Butera *et al.* 2005; Diago *et al.* 2006; Lagging *et al.* 2006; Zeremski *et al.* 2008; Berres *et al.* 2011). Chemokines are chemotactic cytokines responsible for T cell recruitment to the liver in HCV infection, and hence are important in establishing the adaptive immune response.

Natural Killer (NK) cells play an important role in the initial response to HCV infection. They may lyse infected cells, produce inflammatory cytokines and are another link between innate and adaptive immunity in that they stimulate maturation of dendritic cells. However, in chronic infection NK cells have downregulated cytolytic function and altered cytokine responses, such as excessive

production of interleukin 10 (IL-10) and transforming growth factor beta (TGF-β), contributing to fibrosis (Dustin and Rice 2007; Spengler and Nattermann 2007).

Adaptive immunity:

(a) Cell mediated immunity: In acute HCV infection, control of viraemia and clearance of virus is through a strong cytotoxic T-cell response. The onset of this response correlates with increases in serum transaminases, indicating liver injury. This involves both directly cytolytic processes and the production of cytokines and chemokines which attract non-specific inflammatory cells to the liver. The early T cell responses decline in chronic infection. T cells in chronic HCV infection exhibit abnormalities in function, contributing to persistence of infection (Guidotti and Chisari 2006; Dustin and Rice 2007; Spengler and Nattermann 2007).

(b) Humoral immunity: Anti-HCV antibodies form several weeks after acute infection and are present in chronically infected and previously exposed individuals but are not protective against re-infection and do not neutralize persisting infection. This may be related to the selective pressure exerted by these antibodies, with the development of viral escape mutants rendering the antibodies ineffective. The antibody response has been linked to the degree of hepatic injury through its effect on HCV evolution (Cerny and Chisari 1999; Dustin and Rice 2007; Spengler and Nattermann 2007).

Oxidative stress:

HCV is recognised to induce oxidative stress via chronic inflammation and direct induction of reactive oxygen species (ROS) by both HCV replication (Qadri *et al.* 2004) and specific HCV proteins (Gong *et al.* 2001; Moriya *et al.* 2001; Li *et al.* 2002; Okuda *et al.* 2002). ROS contribute to pathogenesis through a number of mechanisms including mitochondrial dysfunction, lipid peroxidation and activation of transcription factors. Reactive oxygen species may up regulate the pro-fibrogenic cytokine TGF-β, contributing to liver fibrosis (Poli 2000).

1.2.3 Pathogenesis and pathophysiology of fibrosis in HCV infection

Hepatic fibrosis occurs as a result of chronic liver inflammation. It is thought to be a physiologic attempt to limit the spread of inflammation. It is characterized by the deposition of collagen and other extracellular matrix (ECM) components, including other glycoproteins such as elastin and fibronectin as well as proteoglycans. Polymerisation occurs and the matrix is resistant to degradation. Initially this occurs in the periportal areas, followed by extension into the lobules towards the central vein. As this process progresses, fibrous septae form. The end result is cirrhosis, where these fibrous septae surround nodules of hepatocytes. This disrupts liver architecture, leading to alterations in hepatic function and blood flow (Figure 1.10) (Marcellin *et al.* 2002; Pawlotsky 2004; Friedman 2008; Joyce and Tyrrell 2010).

Figure 1.10 (A) Stages of fibrosis (Metavir scoring system) (B) The stellate cell in hepatic fibrosis (Asselah *et al.* 2009)

Multiple cells play a role in fibrogenesis, but it is the stellate cell that plays a central role. Quiescent stellate cells are found in the perisinusoidal space of Disse, which separates the hepatocytes from the sinusoidal endothelium and contains normal ECM which is important for normal hepatic function. Hepatocyte apoptosis, cytokine/chemokine production and reactive oxygen species from hepatocytes and Kupffer cells activate stellate cells. They are then transformed into a fibroblastic phenotype. Subsequent proliferation and migration of stellate cells, excess production of ECM proteins and a change in type of ECM are the main contributors to fibrogenesis (Figure 1.10). Fibrolysis is downregulated. Other than stellate cells, circulating and bone marrow derived fibroblasts are also implicated (Marcellin *et al.* 2002; Lee and Friedman 2011).

TGF-β is a major cytokine implicated in fibrosis and it is known to be increased in HCV infection (Paradis *et al.* 1996) and expression is activated by HCV (Presser *et al.* 2013). TGF-β is not only produced by hepatocytes but also activated stellate cells, so it may act in an autocrine or paracrine manner to further upregulate ECM production. The deposition of fibrillar collagen then further activates stellate cells, creating a positive feedback loop (Friedman 2000; Marcellin *et al.* 2002; Lee and Friedman 2011).

HCV has been shown to stimulate hepatic stellate cells in *in vitro* models. It has been demonstrated that the HCV core protein directly (Bataller *et al.* 2004; Coenen *et al.* 2011; Wu *et al.* 2013) and indirectly (Taniguchi *et al.* 2004; Shin *et al.* 2005; Clement *et al.* 2010) induces fibrogenic effects in stellate cells. Other HCV structural and non-structural proteins have also be implicated in fibrogenesis

(Bataller *et al.* 2004; Schulze-Krebs *et al.* 2005; Ming-Ju *et al.* 2011), as have HCV-positive apoptotic bodies (Gieseler *et al.* 2011) and HCV RNA (Watanabe *et al.* 2011). HCV has also been shown to increase reactive oxygen species, TGF-β and other pro-fibrogenic cytokine production (Lin *et al.* 2010; Nagaraja *et al.* 2012) and stellate cell activation and invasion occurs after exposure to conditioned media from HCV-infected Huh-7.5 cells, probably in response to secreted TGF-β from the infected cells (Presser *et al.* 2013).

Additionally, the stellate cell is now recognised to play a role in hepatic inflammation, producing pro-inflammatory cytokines and chemokines (such as CCL5, interleukin-6 and CCL2), thus stimulating further hepatic inflammation, stellate cell activation and fibrogenesis (Kisseleva and Brenner 2006; Friedman 2008; Joyce and Tyrrell 2010; Lee and Friedman 2011). Stellate cells have also been shown to stimulate HCV-infected hepatocytes, resulting in expression of inflammatory cytokines and chemokines (Nishitsuji *et al.* 2013).

1.3 Hepatic HCV burden *in vivo*

It is recognised that only a proportion of hepatocytes within the HCV infected liver are actually infected with HCV. A number of studies have examined this aspect of HCV infection, but it has been a point of controversy in the literature and appears to be somewhat dependent on the technique employed to detect infected hepatocytes.

Two-photon microscopy has been used to detect both viral proteins and viral double stranded RNA (Liang *et al.* 2009). This technique identified between 1.7% and 22%

of hepatocytes in liver biopsy specimens labelled positively for HCV core antigen. Where laser capture microdissection of liver biopsy samples has been used, 21-45% of hepatocytes were harbouring HCV RNA (Kandathil *et al.* 2013). *In situ* reverse transcription polymerase chain reaction techniques identified a median of 5% of hepatocytes were HCV-positive in liver biopsy specimens from HCV-positive patients (Lau *et al.* 1996). Similar results have been obtained by other techniques, such as immunohistochemistry or fluorescence microscopy (Krawczynski *et al.* 1992; Gonzalez-Peralta *et al.* 1994; Lau *et al.* 2008; Stiffler *et al.* 2009). In contrast, groups that have employed in situ hybridization to detect viral RNA have suggested that a greater proportion of positive hepatocytes, up to 100%, can be demonstrated (Agnello *et al.* 1998; Rodriguez-Inigo *et al.* 1999; Pal *et al.* 2006). However, this is not a consistent finding when the technique has been used by others, where only up to 15% of hepatocytes are HCV positive (Lau and Davis 1994).

1.4 The 'bystander' effect

Given the small percentage of hepatocytes infected in chronic HCV infection, it is unclear why hepatic inflammation and fibrosis affects the liver more globally. It has been suggested that the effect of HCV infection on non-infected hepatocytes and other cells within the liver extends the pathological effect of the virus beyond the infected cells, expanding liver injury and hence leading to the development of significant liver disease. However, the exact mechanisms underlying this bystander effect have yet to be established, and the literature examining this area is limited.

A number of groups have demonstrated cytotoxic T lymphocyte-mediated killing of bystander cells in HCV infection via perforin, Fas/Fas ligand and tumour necrosis factor (TNF) pathways (Ando *et al.* 1997; Gremion *et al.* 2004). Additionally, it was demonstrated that the non-structural protein NS4A was able to induce apoptosis in neighbouring non-transfected cells in cell culture (Madan *et al.* 2010). Other groups have also noted that HCV itself and HCV-infected cells exert effects on other cell types in the liver, such as dendritic and natural killer cells (Takahashi *et al.* 2010; Zhang *et al.* 2013). The effect on stellate cells has been previously discussed.

Alternatively, uninfected cells may exert an effect on HCV-infected cells. It has been previously shown that TLR3 expressed in uninfected hepatocytes senses HCV in neighbouring HCV-infected cells, stimulating a localized antiviral response that impacts on HCV replication in infected hepatocytes (Dansako *et al.* 2013). Hepatic stellate cells have also been shown to stimulate pro-inflammatory cytokines and chemokines in HCV-infected hepatocytes *in vitro* (Nishitsuji *et al.* 2013).

The amount of literature exploring this subject is small, and the lack of studies on the specific changes in gene expression in bystander hepatocytes is noted.

1.5 Hypothesis and Aims

We hypothesise that HCV-infected hepatocytes exert a bystander effect on neighbouring cells through either soluble factors or direct cell-cell contact, or vice versa (Figure 1.11). We suggest that this bystander effect expands the inflammatory response and hence injury. The aims of this thesis are therefore to determine the effect of HCV-infected hepatocytes on bystander cells, such as uninfected hepatocytes and stellate cells *in vitro,* and vice versa.

The specific aims of this thesis are:

1. To develop and characterize an *in vitro* model system to study the effect of HCV-infected hepatocytes on uninfected hepatocytes.
2. To study the effect of HCV-infected hepatocytes on hepatic stellate cells.
3. To study the effect of HCV-infected hepatocytes on HCV replication in other HCV-infected hepatocytes.
4. To study the effect of uninfected hepatocytes and hepatic stellate cells on HCV-infected hepatocytes.

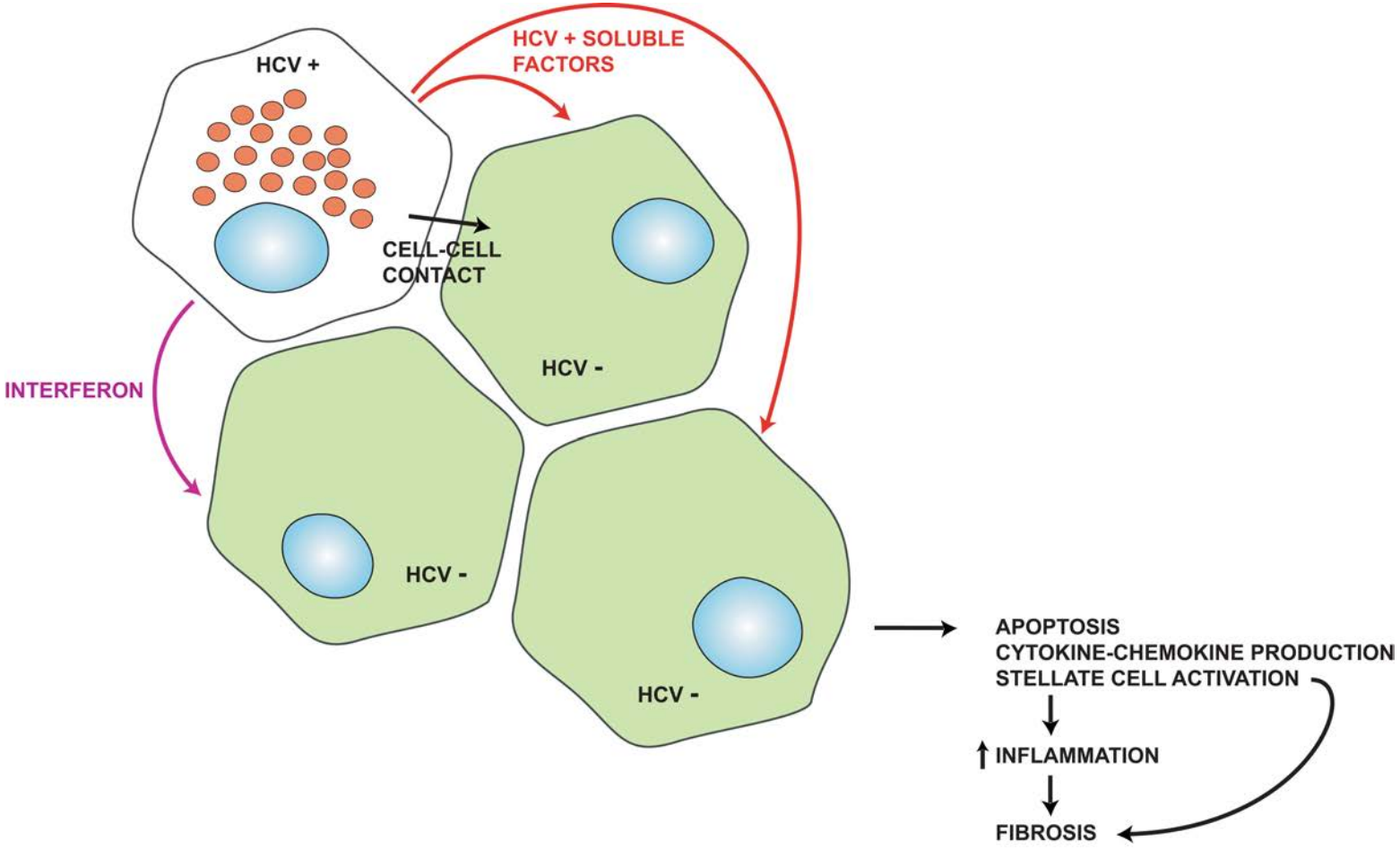

Figure 1.11 The bystander effect in HCV infection

Chapter 2
Materials and Methods

2.1 Molecular biology techniques

2.1.1 Synthetic oligonucleotides

Oligonucleotides of PCR/ sequencing purity were obtained from GeneWorks (Adelaide, South Australia) and diluted to 20μM or 9.6μM depending on application. Oligonucleotide concentration was determined by (assuming average MW of 330 Da per nucleotide):

Concentration (μM) = [concentration (mg/ml) x 10^6] / [length x nucleotide MW]

Primer sequences used were as follows:

Table 2.1 Primer sequences

Name	Sense primer (5'→ 3')	Anti-sense primer (5'→ 3')	Application
Claudin-1	CTGGGAGGTGCCCTACTTTG	CTTGGTGTTGGGTAAGAGGTTGT	RT-PCR
CD81	TGCCACCAGAAGATCGATGA	GGCAGCAATGCCGATGAG	RT-PCR
HCV	TCTTCACGCAGAAAGCGTCTAG	GGTTCCGCAGACCACTATGG	RT-PCR
IP-10 (CXCL10)	TCCACGTGTTGAGATCATTGC	TCTTGATGGCCTTCGATTCTG	RT-PCR
RANTES (CCL5)	CTGCATCTGCCTCCCCATA	GCGGGCAATGTAGGCAAA	RT-PCR
MIP1β (CCL4)	CAGCGCTCTCAGCACCAA	AGCTTCCTCGCAGTGTAAGAAAA	RT-PCR
IL8 (CXCL8)	TCACTGTGTGTAAACATGACTTCCA	TTCACACAGAGCTGCAGAAATCA	RT-PCR
DDX60	ACATGAAAATTATGGAGGAC	ACAGCACTGGAGCCTGAGAG	RT-PCR
IFI6	CCTGCTGCTCTTCACTTGCA	CCGACGGCCATGAAGGT	RT-PCR
COL1a1	TTCACCTACAGCACGCTTGTG	TCTTGGTGGTTTTGTATTCGATGA	RT-PCR
TIMP-1	AAGGGCTACCAGAGCGATCA	GGTATTGCCAGGTGCACAAAT	RT-PCR
TGFβ	TCGACATGGAGCTGGTGAAA	GAGCCTTAGTTTGGACAGGATCTG	RT-PCR
SOCS3	TGGATGGAGCGGGAGGAT	CATAGTCAGGAGGCACAGAGTAGAAT	RT-PCR
36B4 (RPLP0)	AGATGCAGCAGATCCGCAT	GGATGGCCTTGCGCA	RT-PCR
TfRTCA	CCTGGATCCACCATGATGGTAGATGGCG ATAACAGT	ACTGCTAGCGATCCTGTTTCTCCAGGTCC ATCAGAACTCTTACAATAGCCCAAGTAG CCAATCATAAATC	Cloning
CMV	CGCAAATGGGCGGTAGGCGTG		Sequencing

2.1.2 Plasmids (Appendix I)

Lentiviral plasmids: These plasmids are used for packaging of lentiviral vectors and production of lentiviral particles. psPAX2 (Addgene) is a second generation packaging plasmid encoding HIV-1 gag-pol. pMD2.G (Addgene) is an envelope plasmid encoding the VSV-G envelope protein.

pGIPZ lentiviral vector: The pGIPZ lentiviral vector (Open Biosystems, Thermo Scientific) was used to generate cell lines with stable short hairpin RNA (shRNA) knockdown of HCV entry factors. The plasmid also encodes green fluorescent protein (GFP) allowing for monitoring of shRNA expression. It contains a puromycin resistance gene for selection in mammalian cells. Five lentiviral vectors encoding different shRNAs targeting CD81 were screened for effective knockdown of CD81 using fluorescence microscopy, flow cytometry and qRT-PCR. Six lentiviral vectors encoding different shRNAs targeting Claudin-1 were screened for effective knockdown of Claudin-1 using fluorescence microscopy, Western blotting and qRT-PCR.

pLenti6/V5-D-TOPO: This is a lentiviral vector purchased from Invitrogen (Life Technologies) used for generation of the lentiviral-mediated expression of mCherry on the cell surface of Huh-7 cells. It contains a blasticidin resistance gene for selection in mammalian cells.

Retroviral plasmids: Plasmids used in production of retroviral vectors for stable expression of TLR3 were pCL-10A1 (Imgenex), a packaging plasmid providing gag-pol and an envelope protein; pCX4bsr-TLR3, encoding wild-type TLR3; and

pCX4bsr-ΔTIR, encoding mutant TLR3 in which the TIR (toll IL-1 receptor) signalling domain has been deleted. These plasmids contain a blasticidin resistance gene for selection. The plasmids were a kind gift from Dr Kui Li, University of Tennessee Health Science Center, USA.

pJc1: This plasmid encodes a chimeric genome of HCV, J6/JFH1 (Appendix II), kindly provided by Professor Ralf Bartenschlager, University of Heidelberg, Germany (Pietschmann *et al.* 2006).

2.1.3 Bacterial transformation

Chemically competent *E.coli* cells (α-Select, Bioline. See Appendix III) were thawed on ice and 10ng of plasmid DNA was added to 50µl of competent cells. After gentle mixing they were incubated on ice for 30 minutes. The cells were then heat shocked by placing on a heating block at 42°C for 30 seconds. The cells were then returned to ice and incubated for a further 2 minutes. 950µl of SOC (see Appendix III) was added to each tube and they were incubated on a shaking platform at 37°C for 45 minutes. The cells were centrifuged (18,000 x *g* for 1 minute) and the pellet resuspended in 100µl of 0.85% (w/v) saline. Cells were then plated onto Luria agar plates containing the appropriate selection antibiotic (ampicillin 100µg/ml, kanamycin 50µg/ml) and incubated at 37°C overnight.

2.1.4 Plasmid DNA preparation

Single colonies (from section 2.1.2) were inoculated into 10ml of sterile Luria broth containing an appropriate antibiotic and incubated at 37°C overnight on a shaking platform. 5ml of this culture was transferred to a disposable plastic centrifuge tube and centrifuged at 18,000 x *g* for 5 minutes. Small-scale plasmid DNA preparation was then performed using the QIAprep® Spin Miniprep Kit (QIAGEN) as per the manufacturer's instructions.

For large-scale plasmid DNA preparation, 200µl of the starter culture was inoculated into 200ml of Luria broth containing the appropriate antibiotic and incubated overnight at 37°C on a shaking platform. The culture was transferred to a large centrifuge tube and bacteria were pelleted by centrifugation at 6000 x *g* for 15 minutes at 4°C. Plasmid DNA was then prepared using the QIAGEN Plasmid Maxi Kit (QIAGEN) or NucleoBond® Xtra Maxi (Macherey-Nagel) as per the manufacturer's instructions.

DNA concentration was quantified using a spectrophotometer. Plasmid DNA was stored at -20°C.

2.1.5 Restriction endonuclease digestion

Restriction endonucleases were purchased from New England Biolabs. Digests were performed using 10U of the appropriate enzyme or enzymes, combined with 2µl of the corresponding 10x reaction buffer, 1µg of DNA and MilliQ water to a final volume of 20µl. Samples were incubated at 37°C overnight.

2.1.6 Agarose gel electrophoresis

Gel electrophoresis was performed using 1% agarose gels. Gels were made by dissolving DNA grade agarose (Agarose low EEO, AppliChem) in 1 x TAE (see Appendix III) and then cast in trays in a Mini-Gel Caster (BioRad). Samples were mixed with 6 x Loading Dye (New England Biolabs) and loaded into wells of the gel; 5µl of an appropriate DNA ladder (New England Biolabs) was also loaded. Gels were run in a Mini-Sub® Cell GT Cell or a Wide Mini-Sub® Cell GT Cell (BioRad), in 1 x TAE at 100 V until the desired separation had been achieved.

Gels were stained in GelRed™ Nucleic Acid Gel Stain (Biotium) for 15 minutes. DNA was visualized under ultraviolet (UV) light using a Gel Doc XR system and Quantity One® 1-D analysis software (BioRad) or a BioDoc-It® Imaging System (UVP).

2.1.7 Gel extraction of DNA

To extract DNA from agarose gels, DNA bands were excised from gels using a scalpel blade whilst being visualized under UV light and placed in weighed Eppendorf tubes. The QIAquick Gel Extraction Kit (QIAGEN) was then used to purify DNA, as per the manufacturer's instructions.

2.1.8 Dephosphorylation with Antarctic Phosphatase

To prevent re-ligation of digested DNA and hence re-circularization of cloning vectors, dephosphorylation was performed with Antarctic Phosphatase (New England Biolabs). Antarctic Phosphatase (5 units) was added to 1-5µg of DNA and 2µl of 10x Antarctic Phosphatase Reaction Buffer with dH_2O to a final volume of 20µl. The sample was incubated at 37°C for 60 minutes followed by heat inactivation at 65°C for 10 minutes.

2.1.9 Oligonucleotide annealing

Guidelines published by Roche Applied Science were followed when performing cloning using adaptor-duplexes. Complementary oligonucleotides containing the peptide of interest were designed. Single-stranded overhangs were incorporated into the oligonucleotides; these were designed to be complementary to the insertion site in the appropriately digested plasmid to be used. For annealing, forward (5µl) and reverse (5µl) oligonucleotides (at a concentration of 20µM) were mixed with 35µl dH_2O and 5µl of 10x Buffer 2 (New England Biolabs) and incubated at 95°C for 4 minutes. The sample was then incubated at 70°C for 10 minutes then slowly cooled to room temperature.

2.1.10 DNA ligation

To ligate digested DNA inserts into digested plasmids, 1µl of T4 DNA Ligase (New England Biolabs) and 2µl of the supplied 10x ligation buffer were added to a mixture of DNA insert and plasmid (in a 3:1 ratio); in cases of adaptor-duplex cloning, 2µl of the annealed oligonucleotides was added. dH_2O was added to a final volume of 20µl. Samples were then incubated at 16°C overnight. In order to check background re-ligation of plasmids, control ligations (in which no insert was added to the mixture) were performed in parallel.

2.1.11 DNA sequencing

DNA sequencing was performed at the Australian Genome Research Facility (AGRF; Adelaide, South Australia). Samples were prepared by adding 1µg of DNA to 1µl of the appropriate forward or reverse primer (at a primer concentration of 9.6µM). Milli-Q water was added to a final volume of 13µl before submission of samples to AGRF for BigDye® Version 3 sequencing (Applied Biosystems) and capillary separation.

2.1.12 RNA extraction

Total cellular RNA was extracted using TRIzol® Reagent (Invitrogen, Life Technologies) as per the manufacturer's instructions. For extraction of RNA where the downstream application was microarray analysis, extraction was performed

using a RNeasy® Mini Kit (QIAGEN) or a RNAqueous® -4PCR kit (Ambion, Life Technologies), as per the manufacturer's instructions. Where tubes were not provided with kits, RNase-Free 1.5ml Microfuge Tubes (Ambion, Life Technologies) were used.

Depending on the downstream application and method of RNA extraction, some RNA samples were DNaseI treated to remove contaminating DNA. For 20µl samples, 2 units of DNaseI (RNase-free, Ambion, Life Technologies) and 2.1µl of 10 x DNaseI buffer (Ambion, Life Technologies) were added to each sample. Tubes were incubated at 37°C for 15 minutes. DNase Inactivation Reagent (2.1µl, Ambion, Life Technologies) was then added. Tubes were centrifuged at 10,000 x *g* for 1 minute and the supernatant was transferred to a new tube. All RNA samples were stored at -80°C.

2.1.13 Estimation of DNA and RNA concentrations

DNA and RNA were quantified using a UV spectrophotometer (NanoPhotometer™, Implen). Purity of RNA was estimated by the OD_{260nm}/OD_{280nm} ratio, with ratios above 1.80 considered acceptable.

2.1.14 cDNA preparation

Preparation of cDNA from RNA by reverse transcription was performed using M-MLV Reverse Transcriptase (Promega). 1µg of RNA and 1µg of Random Hexamer

Primer (GeneWorks) were diluted in water to a final volume of 14µl. Samples were incubated at 70°C for 5 minutes and then 4°C for 5 minutes. Subsequently, the following were added to each tube: 5µl of 5 x M-MLV RT Buffer (Promega), 10mM dNTPs (dATP, dCTP, dGTP, dTTP, Promega), 40 units rRNasin® RNase Inhibitor (Promega), 200 units M-MLV RT RNase H(-) Point Mutant (Promega) and 3.25µl dH_2O. Samples were incubated at 42°C for 50 minutes then placed on ice. Samples were diluted to a final volume of 100µl and stored at -20°C.

2.1.15 Polymerase Chain Reaction

Polymerase Chain Reactions (PCR) were performed using Platinum® *Taq* DNA Polymerase High Fidelity (Invitrogen, Life Technologies). DNA template (10ng) was combined with 5µl 10x High Fidelity PCR Buffer, 1µl of 10mM dNTP mixture, 2µl of 50mM $MgSO_4$, 1µl each of 20µM forward and reverse primers, 0.5µl Platinum® *Taq* High Fidelity and dH_2O to a final volume of 50µl. Reactions were carried out as follows: denaturation at 94°C for 1 minute, 30 cycles of 94°C for 20 seconds, 55°C for 20 seconds and 68°C for 2 minutes, followed by cooling at 4°C. Reactions were performed using a MyCycler™ Thermal Cycler (BioRad) or a S1000™ Thermal Cycler (BioRad).

2.1.16 PCR purification

PCR products were purified using a MinElute PCR Purification Kit (QIAGEN) as per the manufacturer's instructions.

2.1.17 Real-Time Quantitative RT-PCR

Relative levels of mRNA or HCV RNA were determined using real-time RT-PCR by the comparative C_T method. 10µl of SYBR® Green Master Mix (Applied Biosystems, Life Technologies), 0.3µl each of forward and reverse primers (20µM concentration), 4.4µl dH_2O and 5µl cDNA were combined in each well (MicroAmp Fast Reaction Tubes, Applied Biosystems, Life Technologies). Each cDNA sample was run in duplicate. 5µl of each cDNA sample was also combined with 10µl of SYBR® Green Master Mix and 0.3µl each of forward and reverse primers for a housekeeping gene (36B4) to normalize cDNA input. A StepOnePlus™ Real-Time PCR System (Applied Biosystems, Life Technologies) was used to control reaction conditions (denaturation at 95°C for 10 minutes, 40 cycles of 95°C for 15 seconds and 60°C for 1 minute, one cycle of 95°C for 15 seconds, 60°C for 1 minute and 95°C for 15 seconds to produce a melt curve (0.3°C increments). Data were analysed using StepOne™ Software v2.0.2 (Applied Biosystems).

2.1.18 PCR Array

An Human Antiviral Response RT^2 Profiler PCR Array (96-well format, QIAGEN) was used to assess a panel of genes involved in the innate immune response in a TLR3-positive cell line in response to stimulation with polyinosinic:polycytidylic acid (Poly I:C) or HCVcc. The kit was used as per the manufacturer's instructions.

2.1.19 Microarray

Microarray analysis was performed at the Adelaide Microarray Centre (Adelaide, South Australia). Affymetrix Genearrays (Affymetrix GeneChip® Hu1.0ST and Hu2.0ST) were used and additional analysis was performed using GeneSifter® Analysis Edition software (Geospiza).

2.2 Cell culture techniques

2.2.1 Cell lines

Huh-7: A human hepatocellular carcinoma cell line, isolated from a well-differentiated hepatocellular carcinoma in a 57 year old Japanese male (Nakabayashi *et al.* 1982).

Huh-7.5: Subgenomic replicon cells cured of HCV RNA by treatment with IFN-α (Blight *et al.* 2002). They are highly permissive for HCVcc infection and RIG-I signalling in these cells is deficient (Sumpter *et al.* 2005).

PH5CH8: Derived from the non-neoplastic hepatocyte cell line PH5CH. The PH5CH8 cell line is immortalized with the simian virus 40 (SV40) large T antigen (Ikeda *et al.* 1998). It is not permissive to HCV infection.

NNeoC-5B: Huh-7 cell line containing the full HCV genome and replicating the HCV polyprotein without production of infectious virions (see Section 1.1.8) (Ikeda *et al.* 2002). This cell line was a kind gift from Professor Stanley Lemon (University of North Carolina, North Carolina, USA). NNeoC-5B cells cured of

replicating HCV were also used (cells were cured by incubating with interferon α-2b at 200 units/ml for 2 weeks).

SGH-JFH1-RLuc: An HCV-replicon harbouring Huh-7.5 cell line. The HCV subgenomic replicon encodes a Renilla luciferase reporter of HCV non-structural protein expression. This cell line was generated by selection of replicon-harbouring cells using blasticidin. The SGR-JFH1-RLuc replicon construct was a kind gift from Dr Kui Li (University of Tennessee Health Science Center, Memphis, TN, USA).

HEK293T: A derivative of the Human Embryonic Kidney 293 cell line that constitutively expresses the SV40 large T antigen, allowing for replication of transfected plasmids with an SV40 origin of replication.

LX2: A human hepatic stellate cell line, derived from primary hepatic stellate cells and spontaneously immortalized in low serum conditions. It retains characteristics of hepatic stellate cells (Xu *et al.* 2005).

Primary Rat Hepatic Stellate cells: Isolation was performed by Mehdi Ramezani-Moghadam at the Westmead Millennium Institute for Medical Research, Sydney, Australia. Cells were isolated by *in situ* pronase-collagenase perfusion followed by density gradient centrifugation.

2.2.2 Stable cell lines generated and used in this thesis

A number of stable cell lines were generated during this project.

Huh-7 + CD81 shRNA: A Huh-7 cell line demonstrating stable shRNA knockdown of the essential HCV entry factor CD81, generated via a lentiviral approach.

Huh-7 + Claudin-1 shRNA: A Huh-7 cell line demonstrating stable shRNA knockdown of the essential HCV entry factor Claudin-1, also generated via a lentiviral approach.

Huh-7 + CD81 shRNA + cell surface targeted mCherry: The Huh-7 cell line with stable CD81 knockdown was used to generate this cell line, which was used in the development of a cell sorting system (see section 2.7 and Chapter 6). This cell line stably expresses mCherry on the cell surface. Localisation of mCherry to the cell surface was achieved by fusing the mCherry coding sequence (in-frame) to that of the membrane targeting sequence of the transmembrane protein, human transferrin receptor, as previously described (Winnard *et al.* 2007).

Huh-7 + TLR3: Huh-7 cells (which normally lack TLR3 expression) stably expressing TLR3 (or TLR3 lacking the signalling domain ΔTIR) were generated using a retroviral system (Wang *et al.* 2009).

2.2.3 Cell culture medium

Mammalian cells in culture were maintained in Dulbecco's Modified Eagle Medium (DMEM) containing 4.5g/L D-Glucose, 25mM HEPES and 2 mM L-

glutamine (Gibco, Life Technologies). Where appropriate, cells were maintained in DMEM-F12, GlutaMAX™ (DMEM + Ham's F-12 Nutrient Mix (1:1) + GlutaMAX™-I, Gibco, Life Technologies). Media was supplemented with foetal bovine serum (FBS), penicillin (50 units/ml) and streptomycin (50µg/ml). Media according to cell line and additional supplements were as follows:

Table 2.2 Cell lines, culture media and supplements

Cell line	Media	Additional Supplements
Huh-7	DMEM, FBS 10%, penicillin/streptomycin	
Huh-7.5	DMEM, FBS 10%, penicillin/streptomycin	
PH5CH8	DMEM-F12, FBS 1%, penicillin/streptomycin	Per 500ml: -Epidermal Growth Factor 100ng (Sigma) -Insulin Transferrin and Selenium 100x stock solution, 5ml (Life Technologies) -Hydrocortisone 25mM solution 1ml (Sigma) -Linoleic Acid 2.5mg (Sigma) -Prolactin 50ng (Sigma)
NNeoC-5B	DMEM, FBS 10%, penicillin/streptomycin	G418 800µg/ml
293T	DMEM, FBS 10%, penicillin/streptomycin	
Huh-7 + CD81 shRNA or Claudin-1 shRNA	DMEM, FBS 10%, penicillin/streptomycin	Puromycin 3µg/ml
Huh-7 + CD81 shRNA + mCherry	DMEM, FBS 10%, penicillin/streptomycin	Puromycin 3µg/ml Blasticidin 3µg/ml
Huh-7 + TLR3 or ΔTIR	DMEM, FBS 10%, penicillin/streptomycin	Blasticidin 3µg/ml
SGH-JFH1-RLuc	DMEM, FBS 10%, penicillin/streptomycin	Blasticidin 3µg/ml
LX2	DMEM, FBS 10%, penicillin/streptomycin	

2.2.4 Maintenance of cell lines

Cells were maintained in sterile plastic cell culture flasks (0.2µm vented; 25cm^2, 75cm^2, 175cm^2), dishes (3.5cm^2, 6cm^2, 10cm^2) or trays (6-, 12-, 24-, 96-well) (Corning or BD Falcon). Cells were incubated at 37°C, 5% CO_2. Cells were

passaged every 3 to 4 days by removal of culture media, washing once with phosphate buffered saline (PBS) and then detaching the cells by incubating in Trypsin-EDTA for approximately 3 minutes followed by gentle tapping. Cells were then resuspended in complete culture medium, counted and diluted in an appropriate amount of medium before adding to a new flask.

2.2.5 Trypan blue exclusion

Cell counts were performed by mixing cells in suspension with an equal volume of Trypan Blue (0.4% w/v, Sigma) and counting using a haemocytometer. The cell concentration was calculated by:

Concentration (cells/ml) = cells in a 5x5 grid x 2 (dilution factor) x 10^4

2.2.6 Cryopreservation of cells

Trypsinized and re-suspended cells were transferred to sterile 50ml tubes (Falcon) and centrifuged at 200 x *g* for 10 minutes. Culture media was removed and cells were resuspended in fresh culture medium at a concentration 5 x 10^6 to 1 x 10^7 cells per ml. An equal volume of cold freezing mix (50% medium, 30% FBS, 20% dimethyl sulfoxide (DMSO, Sigma), filter sterilized) was added drop-wise and mixed. 1ml aliquots were added to each sterile 1.8ml CryoTube (Nunc, Thermo Scientific) and tubes were transferred to a freezing chamber (Nalgene, Thermo

Scientific) containing isopropanol. The chamber was placed in a -80°C freezer. Long term storage was in liquid nitrogen.

2.2.7 Resuscitation of frozen cells

Tubes containing frozen cells were thawed rapidly in a 37°C water bath. An equal volume of fresh culture medium was added to each tube and then the suspension was transferred to a culture flask containing fresh culture medium. The flask was then incubated as previously described.

2.2.8 Transfection

Cells were transfected with plasmid DNA using FuGENE 6 Transfection Reagent (Roche) as per the manufacturer's instructions. 24 hours prior to transfection cells were seeded into 6-, 12- or 24-well trays at a suitable concentration to achieve 50-70% confluency at the time of transfection. Serum free Opti-MEM (Gibco, Life Technologies) and FuGENE 6 were mixed, followed by plasmid DNA, in ratios recommended by the manufacturer. After 15 minutes incubation at room temperature the mixture was added drop-wise to each well and the cells were returned to culture. Assays were performed 24 to 72 hours later.

2.2.9 Lentivirus production

To produce lentivirus with which to develop stable cell lines expressing shRNAs or genes, 3.5 x 10^5 HEK293T cells were seeded per well in a 6-well tray and incubated at 37°C overnight. Transfection was then performed as described in section 2.2.7, with packaging plasmids psPAX2 and pMD2.G and the appropriate vector.

Cells were incubated at 37°C overnight. The following day, culture media was aspirated and replaced with 2ml of fresh media in each well. After further incubation overnight, supernatant was aspirated and stored at 4°C; a further 2ml of fresh media was added to each well and cells were again incubated at 37°C overnight. The following day, supernatant was aspirated and pooled with supernatant collected the previous day. Samples were cleared of cellular debris by centrifugation at 1500 rpm for 5 minutes. Each sample was then filtered through a 0.4 µm filter (Minisart® Syringe Filter, Sartorius Stedim Biotech), aliquoted and stored at -80°C.

2.2.10 Lentivirus infection

To transduce lentiviral particles into the target cell line (see Table 2.3), target cells were seeded at 2 x 10^5 per well in a 6-well plate and cultured overnight. The following day, lentivirus (from section 2.2.8) was diluted at a ratio of 1:5 in complete media with Polybrene 4µg/ml (Sigma). Media was aspirated from target cells and 1ml of the diluted lentivirus was placed on each well. After incubation at 37°C for 6 hours, lentiviral media was aspirated and replaced with complete culture

media, and the plate was returned to culture for 48-72 hours. Where the construct contained a fluorescent protein, transduction efficiency was checked by fluorescence microscopy. Media was aspirated and replaced with complete media containing the appropriate selection antibiotic (see section 2.2.2). A well containing uninfected cells was used as a control. The cells were then serially passaged under selection for 2-3 weeks before enrichment by fluorescence-activated cell sorting (FACS), where applicable, and analysis of gene expression or shRNA-mediated gene knockdown, as appropriate.

2.2.11 Retrovirus production

To produce retrovirus with which to develop stable cell lines expressing TLR3, 3.5 x 10^5 HEK293T cells were seeded per well in a 6-well tray and incubated at 37°C overnight. The next day, culture medium was replaced with complete medium without antibiotics. Transfection was performed by diluting 6µl of Lipofectamine 2000 (Invitrogen, Life Technologies) into 150µl Opti-MEM (Gibco, Life Technologies) and incubating for 5 minutes at room temperature. 1.5µg of pCX4bsr (TLR3 or ΔTIR plasmid) and 1.5µg of pCL-10A1 (packaging plasmid) were mixed in 150µl Opti-MEM. The Lipofectamine and plasmid dilutions were then combined and incubated for 15-20 minutes at room temperature. This mixture (300µl per well) was added drop-wise to cells and gently mixed. The cells were incubated at 37°C overnight.

The following day, culture medium was replaced with 1ml fresh medium containing antibiotics and cells incubated overnight at 37°C. Supernatant was collected and stored at 4°C and replaced with 1ml culture media; cells were incubated overnight at 37°C and supernatant was collected again. The two collections were not pooled. Supernatants were cleared of cellular debris and filtered as described in section 2.2.8. Supernatant was stored at 4°C for immediate use to avoid freeze-thaw related loss of viral titre, but any extra supernatant was stored at -80°C.

2.2.12 Retrovirus infection

To infect target cells with retrovirus to produce TLR3-expressing cell lines, target cells (Huh-7) were seeded in 6-well plates to achieve a 30-50% confluency at the time of infection, and cultured at 37°C overnight. Culture media was replaced with 2ml of retroviral supernatant containing Polybrene at a concentration of 8µl/ml. The following day media was aspirated and the infection repeated with the second collection of supernatant. After 72 hours media was replaced with complete media containing the appropriate selection antibiotic (see section 2.2.2), with a well of uninfected cells acting as a control.

2.2.13 Treatment of cells with dsRNA

To assess TLR3 responses to dsRNA stimulation, cells were treated with Poly I:C, a synthetic dsRNA analogue. Treatment was with Poly I:C (Sigma) in complete culture media, 50µg/ml for 24 hours.

2.2.14 Inhibition of exosomes

To inhibit the secretion of exosomes from cells, cells were treated with the exosome inhibitor GW4869 (Sigma). GW4869 was used at a 10μM concentration in serum free media for 16 hours.

2.2.15 Production of conditioned media

Huh-7 or Huh-7+TLR3 cells were infected with HCVcc (Jc1, MOI 0.25-2.0) or mock-infected. Media from these cells was harvested after 72 hours of infection, cleared of cellular debris by centrifugation or filtration through a 0.45μm filter (Acrodisc® Syringe Filter, Pall Life Sciences or Minisart®, Sartorius Stedim Biotech) and then supplemented with fresh media at a ratio of 4:1 if required. Conditioned media was then used immediately on target cells or stored at -20°C for later use.

Conditioned media was also prepared by stimulating Huh-7+TLR3 cells or Huh-7+ΔTIR cells with Poly I:C for 24 hours and then harvested as above.

2.2.16 Fractionation of conditioned media

To fractionate prepared conditioned media, centrifugal filters of differing molecular weight cut-off (50K and 100K) were used as per the manufacturer's instructions (Amicon® Ultra-15 Centrifugal Filter Devices, Merck Millipore).

2.2.17 Co-culture of cell lines

Huh-7+TLR3 cells were infected with HCVcc (Jc1, MOI 1.0-2.0) or mock-infected. Cells were then returned to culture for 48-72 hours to allow infection to become established. Cells were then harvested, counted and mixed with Huh-7+CD81 knockdown cells (± cell surface mCherry) in a 1:1 ratio. The HCV infection rate of infected or transfected cells was determined by immunofluoresence in parallel culture. Co-cultured cells were incubated for 24-72 hours, at which time they were harvested and separated by fluorescence activated cell sorting (Section 2.5.3) or magnetic bead separation (Section 2.6).

2.3 Cell-culture propagated HCV (HCVcc)

2.3.1 Preparation of HCV RNA

5µg of plasmid DNA containing an HCV clone (Jc1, Appendix II) was linearised by digesting with the restriction enzyme MluI at 37°C overnight. *In vitro* transcription of RNA was performed using the MEGAscript® T7 *in vitro* transcription kit (Ambion, Life Technologies) or the T7 High Yield RNA Synthesis Kit (New England Biolabs) as per the manufacturer's instructions. DNase treatment was performed for 15 minutes at 37°C using the provided TURBO DNase. TRIzol® Reagent (1ml, Invitrogen, Life Technologies) was added and RNA isolated as per the manufacturer's instructions. The RNA was resuspended in 20µl of RNAse-free water and the concentration was determined using a spectrophotometer. RNA integrity was checked by agarose gel electrophoresis.

2.3.2 HCV RNA transfection and preparation of viral stocks

Huh-7.5 cells were cultured in two 175cm^2 flasks to near confluence, harvested by trypsinization and washed twice with 10ml Opti-MEM (Gibco, Life Technologies). Cells were resuspended in Opti-MEM at a concentration of 1 x 10^7 cells/ml. 0.4 ml of cells and 10µg of RNA was added to each electroporation cuvette (Gene Pulser® Cuvette, BioRad), on ice, and gently mixed. Cells were electroporated with a single pulse at 0.27 kV, 100 ohms, 960 µF (Gene Pulser® electroporation system, BioRad). Cells from each electroporation was immediately plated into a 175cm^2 flask containing complete culture medium and cultured for 2-10 days, subculturing into new flasks when cells approached confluence. Virus containing supernatants were collected into 50ml tubes (BD Falcon) and cleared of cellular debris by centrifugation at 3900 x *g* for 5 minutes.

2.3.3 Concentration of HCV (PEG precipitation)

Cleared virus-containing supernatants in 50ml tubes (BD Falcon) were adjusted to 40ml with complete culture medium, if necessary. 10ml of 40% (w/v) polyethylene glycol (PEG, MW: 8000, in PBS, Sigma) was added to achieve a final concentration of 8% (w/v). Tubes were inverted to mix well and incubated at 4°C overnight. Samples were centrifuged at 3900 x *g* for 30 minutes at 4°C. Supernatant was removed and the pellet resuspended in 1-2 ml of complete culture medium; samples were aliquoted into screw cap microcentrifuge tubes and stored at -80°C.

2.3.4 Amplification of viral stocks

Huh-7.5 cells were seeded at 1.6 x 10^6 cells per 75cm^2 flask and cultured overnight. The culture medium was removed and replaced with 2 x 10^4 focus-forming units (ffu) of HCV (cell-culture propagated, HCVcc) in 2-3ml of complete media. After returning the cells to culture for 3 hours, complete media was added to a final volume of 10ml and the cells returned to culture for 3 days. Culture supernatant was collected and the cells sub-cultured into a 175cm^2 flask. Cells were returned to culture for 2-3 days and supernatant was again collected, cleared and aliquoted.

2.3.5 Titration of infectious HCV

Huh-7 or Huh-7.5 cells were seeded at 2 x 10^4 cells/well in a 96-well plate and cultured overnight. Serial 10-fold dilutions of virus-containing supernatants or concentrated virus were prepared in 100µl volumes of complete medium (1 in 10, 1 in 100, 1 in 1000, 1 in 10,000). Media was removed from the seeded cells and replaced with 40µl of inoculum (in duplicate for each dilution). Cells were returned to culture for 3 hours, then inoculum was removed and cells were washed with PBS (100µl/well). After washing, PBS was replaced with 100µl/well of complete culture medium and the plate returned to culture for 3 days. Cells were fixed with acetone/methanol and stained for HCV as described in section 2.4. HCV-positive cells were visualized by fluorescence microscopy and HCV-positive foci (distinct

clusters of HCV-positive cells) in each well were counted. Duplicates were averaged. The virus titre was calculated by:

Titre (ffu/ml) = number of foci × dilution factor × 25

2.3.6 General infection protocol

Cells were plated in 6-, 12- or 24-well plates at a density such that they would be confluent at the time of harvesting (generally 6, 24, 48 or 72 hours). After culturing overnight, culture media was aspirated and HCVcc (Jc1) diluted in an appropriate volume of culture medium was added to each well, at an MOI of 0.25-2.0, depending on the experiment. After 3 hours incubation at 37°C, culture medium was increased to an appropriate final volume and plates returned to culture at 37°C. When harvesting at each time point, infection rates were also determined by immunofluorescence analysis of parallel cultures. All experiments were performed in triplicate.

2.4 Fluorescence microscopy techniques

2.4.1 Cell fixation

Cells were seeded at an appropriate density according to planned time course in 96-well plates or 24-well plates with coverslips. Culture medium was removed and the cells were washed with PBS before addition of the fixation solution.

For cells fixed with acetone/methanol, a 1:1 mix of ice-cold acetone and methanol was added to each well (100µl per well in 96-well plates, 500µl per well in 24-well plates) and incubated at 4°C for 15 minutes. The fixation solution was then replaced with PBS.

For cells fixed with 4% paraformaldehyde in PBS, the appropriate volume of paraformaldehyde was added to each well and the plates were incubated at room temperature for 20 minutes. They were then washed twice with PBS. If the cells were to be permeabilized for labelling of intracellular antigens, an appropriate volume of 0.1% Triton in PBS was added to each well and the plates were incubated at room temperature for 10 minutes, followed by two washes with PBS. Blocking was performed by incubating with 2% FBS in PBS for 2 hours at room temperature, followed by two washes with PBS.

2.4.2 Antigen labelling

PBS was removed from each well and cells were incubated with an appropriate volume of primary antibody (40µl per well in 96-well plates, 200µl per well in 24-well plates) diluted in 1% bovine serum albumin (BSA, Sigma) in PBS. Incubation was at room temperature for 1 hour.

Table 2.3 Primary antibodies used in fluorescence microscopy

Name	Dilution	Manufacturer
Pooled inactivated HCV positive human serum	1 in 50	
Anti-NS5A Mouse (mAb 9E10)	1 in 800	Gift, Charles Rice (Rockefeller University)
Rabbit anti-Claudin 1	1 in 200	Invitrogen
Purified mouse anti-human CD81	1 in 200	BD Pharmingen
Anti-Flag Mouse IgG	1 in 200	Sigma
Anti-mCherry Rabbit IgG	1 in 200	BioVision
Anti-TLR3 Mouse IgG1	1 in 200	Imgenex
Biotinylated Anti-GFP Rabbit IgG	1 in 500	Rockland Immunochemicals
Anti-Smooth Muscle Actin	1 in 100	Dako

The primary antibody was removed and cells washed with PBS. Appropriately diluted secondary antibody fluorescent conjugate in 1% BSA was added to each well and plates were incubated in the dark for 1 hour at 4°C.

Table 2.4 Secondary antibodies used in fluorescence microscopy

Name	Dilution	Manufacturer
Alexa Fluor® 488 goat anti-human IgG	1 in 50 to 1 in 150	Invitrogen
Alexa Fluor® 488 goat anti-rabbit IgG	1 in 50 to 1 in 150	Invitrogen
Alexa Fluor® 488 goat anti-mouse IgG	1 in 50 to 1 in 150	Invitrogen
Alexa Fluor® 555 goat anti-human IgG	1 in 50 to 1 in 150	Invitrogen
Alexa Fluor® 555 goat anti-rabbit IgG	1 in 50 to 1 in 150	Invitrogen
Alexa Fluor® 555 goat anti-mouse IgG	1 in 50 to 1 in 150	Invitrogen

Secondary antibody was removed and cells were washed twice with PBS. If nuclear staining was required, cells were incubated in the dark for 10 minutes at room temperature with 4',6-diamidino-2-phenylindole (DAPI, Sigma) diluted 1 in 1000 in water, followed by washing with PBS. Coverslips were mounted on glass slides with Prolong® Gold antifade reagent (Invitrogen, Life Technologies).

2.4.3 Light fluorescence microscopy

Cells were visualized using an Eclipse Ti Inverted Wide-field Fluorescence Microscope (Nikon) and NIS-Elements Advanced Research Imaging Software (Nikon).

2.4.4 Confocal fluorescence microscopy

Confocal microscopy was performed at the Detmold Family Cell Imaging Facility (SA Pathology, Adelaide, South Australia) using a BioRad Radiance 2100 confocal system coupled to an Olympus IX70 inverted microscope.

2.5 Flow cytometry techniques

2.5.1 Labelling of cell surface antigens

Indirect immunofluorescence was used to label cell surface antigens. Labelling was performed at 4°C or on ice. Cells were harvested by trypsinization and approximately 1 x 10^6 cells were transferred to each FACS tube (Becton Dickinson). Tubes were centrifuged at 200 x *g* for 10 minutes and cells were resuspended in 3ml of cold FACS wash buffer (see Appendix III). The cells were centrifuged again as above and then resuspended in 50µl of primary antibody (diluted to 1 in 100 in 10% FBS (v/v) in PBS) and incubated on ice for 1 hour. Cells were washed twice with cold FACS wash buffer then resuspended in 50µl of secondary antibody fluorescent conjugate (diluted in 10% FBS (v/v) in PBS). Cells

were incubated on ice in the dark for 1 hour, washed twice with cold FACS wash buffer and resuspended in 0.5ml of FACS fixative solution (see Appendix III). Tubes were stored at 4°C in the dark until analysis was performed.

Table 2.5 Primary and Secondary antibodies used in Flow Cytometry

Name		Manufacturer
Mouse anti-human CD81	Primary	BD Pharmingen
Alexa Fluor® 555 goat anti-mouse IgG	Secondary	Invitrogen
Purified Mouse IgG1, κ	Isotype control	BD Pharmingen

2.5.2 Flow Cytometric Analysis

Analysis of cell-associated fluorescence was performed using a BD FACSCanto™ Flow Cytometer (Becton Dickinson). Cells were gated based on forward-scatter and side-scatter properties. Voltages for fluorophores were set using unlabelled cells or isotype-matched control antibody labelled cells. BD FACSDiva™ Software (Becton Dickinson) was used to control acquisition and for data analysis.

2.5.3 Fluorescence-activated Cell Sorting

Cell sorting by flow cytometry was performed at the Detmold Family Cell Imaging Facility (SA Pathology, Adelaide, South Australia). Sorting was performed with an Epics Altra HyperSort cell sorter, using Expo MultiComp Software version 1.2B (Beckman Coulter), except for experiments described in Chapter 6 where a MoFlo Astrios High Speed Cell Sorter using Summit Software version 6.2 (Beckman Coulter) was used. Cells were prepared as above but final resuspension was in

FACS sort buffer (see Appendix III) and cells were collected in complete culture media.

2.6 Magnetic bead cell separation

Magnetic separation of co-cultured cell lines was performed using a CherryPicker™ Reagent Kit (Clontech). After co-culture of Huh-7 + CD81shRNA + mCherry cells with HCVcc-infected or uninfected Huh-7+TLR3 cells (as described in section 2.2.17), cells were harvested with Cell Dissociation Solution Non-enzymatic 1x (Sigma) and resuspended in culture medium. The cells were centrifuged at 200 x *g* for 5 minutes at 4°C, media was aspirated and the cells were resuspended in cold PBS. The suspension was passed through a 70µm cell strainer (BD Falcon) and cells counted using a haemocytometer. 5 x 10^5 cells were aliquoted into 1.5ml microcentrifuge tubes and volumes adjusted to 1ml if necessary.

Samples were placed on ice and 10µl of CherryPicker Antibody (0.5mg/ml) was added to each tube. No antibody was added to one tube as a negative control. Tubes were mixed gently by inversion and incubated on ice for 30 minutes, with gentle mixing every 10 minutes. The cells were then centrifuged at 200 x *g* for 4 minutes at 4°C, supernatant aspirated and cells washed twice with 1ml cold PBS. The cells were then resuspended in 1ml cold 1x CherryPicker Wash Buffer (supplied).

During cell incubation with antibody, the required amount of Mag Capture Bead stock (40µl per 5 x 10^5 cells, Clontech) was transferred to a 1.5ml microcentrifuge tube and washed twice with 1ml of 1x wash buffer. After each wash, the tube was

placed on a magnetic stand (MagnaRack™, Invitrogen, Life Technologies) to attract the beads and associated cells to the side of the tube before the wash buffer was aspirated. The beads were then resuspended in 1x wash buffer and 100µl of the washed bead suspension was added to each sample. The samples were placed on a shaker at slow speed for 30 minutes at room temperature.

After a 30 minute incubation the tubes were placed on the magnetic stand. Once the beads had been attracted to the wall of the tube the supernatant was aspirated and the beads washed once with cold wash buffer. The tubes were then placed on the magnetic stand again, and when the beads had been attracted to the wall of the tube the supernatant was aspirated. The cells captured on the beads were then lysed for RNA extraction (section 2.1.6). Capture efficiency was assessed by fluorescence microscopy and flow cytometry.

2.7 Protein chemistry techniques

2.7.1 Extraction of cellular protein

Culture medium was removed from cell monolayers in 6- or 12-well culture trays and cells were washed with ice cold PBS. Proteinase Inhibitor Cocktail (Sigma) was added to RIPA buffer (1 in 100, see Appendix III) and 150µl of this mix was added to each well. Plates were incubated on ice for 20 minutes. Lysates were then collected by scraping and passed through a fine needle and syringe (29 gauge) followed by centrifuging in 1.5ml microcentrifuge tubes at 21,000 x *g* for 10 minutes at 4°C. Supernatant was collected and stored at -20°C.

2.7.2 SDS-PAGE

12% separating gels with 5% stacking gels (see Appendix III) were cast using a BioRad Mini PROTEAN® Tetra Cell casting stand. The separating gel solution was loaded first, and layered with approximately 500µl-1ml of water. After allowing the gel to set for 30 minutes, excess water was poured off and the stacking gel was loaded on top of the separating gel. A comb was inserted to form wells.

Markers (Precision Plus Protein™ Kaleidoscope Standards, BioRad) and protein samples containing 1x Loading Buffer (see Appendix III) were heated to 95°C for 5 minutes before loading. Gels were assembled in tanks and tanks were filled with running buffer (see Appendix III). Samples were loaded and separated by electrophoresis (120 V, 1-2 hours).

2.7.3 Western blotting

Following electrophoresis, gels were equilibrated in cold transfer buffer for 15 minutes. To transfer proteins to a Hybond™Amersham™ -ECL membrane (GE Healthcare), gels and membranes were inserted into a Mini Trans-Blot® Electrophoretic Transfer Cell (BioRad). Electrophoresis was performed in cold transfer buffer (see Appendix III) overnight (25 V, 4°C) or for 1 hour (100 V, room temperature).

After transfer, membranes were blocked with 5% skim milk powder (Diploma) in TBS-T (see Appendix III) for 1 hour on a shaking platform. Membranes were then

incubated overnight at 4°C in an appropriate concentration of primary antibody diluted in 1% skim milk powder in TBS-T.

Table 2.6 Primary antibodies used in western blotting

Name	Dilution	Manufacturer
Rabbit anti-Claudin 1	1 in 500 to 1 in 1000	Invitrogen
Anti-TLR3 Mouse IgG1	1 in 500	Imgenex
Anti-Flag Mouse IgG	1 in 1000	Sigma
Mouse anti-β-actin	1 in 10,000	Sigma

Membranes were washed three times in TBS-T (15 minutes per wash) and then incubated on a shaking platform for 1 hour at room temperature with the appropriate horseradish peroxidase-conjugated secondary antibody diluted in 1% skim milk powder in TBS-T.

Table 2.7 Secondary antibodies used in western blotting

Name	Dilution	Manufacturer
Stabilized Peroxidase Conjugated Goat Anti-Rabbit (H + L)	1 in 10,000	Thermo Scientific
Stabilized Peroxidase Conjugated Goat Anti-Mouse (H + L)	1 in 10,000	Thermo Scientific
Donkey anti-mouse HRP	1 in 10,000	Rockland Immunochemicals

The membrane was then washed six times in TBS-T. Bound antibody was detected using SuperSignal® West Femto Maximum Sensitivity Substrate (Thermo Scientific) as per the manufacturer's instructions and Curix Ortho HT-G X-ray Film (Agfa).

2.7.4 Enzyme-linked immunosorbent assay (ELISA) Array

Qualitative ELISA (Multi-analyte ELISArray, Human TLR-induced cytokines: viral-induced, QIAGEN) was used as per the manufacturer's instructions to assess qualitative cytokine expression in a TLR3-positive cell line in response to stimulation with Poly I:C or HCVcc.

2.8 Luciferase assays

To assess the effect of conditioned media from HCV-stimulated (or mock-stimulated) TLR3-positive Huh-7 cells on HCV replication, luciferase activity of SGH-JFH1-RLuc cells was measured using the *Renilla* Luciferase Assay System (Promega). Cells were seeded at a density of 7 x 10^4 cells per well in a 12-well plate. The following day culture media was aspirated and replaced with conditioned media.

After 48 hours, media was aspirated and cells washed once with PBS. Passive Lysis Buffer (100µl per well, Promega) was added and then lysates were collected 15 minutes later. 20µl of each cell lysate (in duplicate) was added to each well of an optical tray (OptiPlate™-96, PerkinElmer). *Renilla* Luciferase Assay Reagent was prepared by adding *Renilla* Luciferase Assay Substrate to *Renilla* Luciferase Assay Buffer as per the manufacturer's instructions (Promega). Luciferase output was measured on a GloMax® 96 Microplate Luminometer (Promega).

2.9 Data analysis

Data analysis with unpaired Student's *t*-tests was performed using GraphPad Prism software (Versions 5 and 6).

Chapter 3

An *in vitro* model system to examine the bystander effect in HCV infection

3.1 Introduction

Progression of liver disease to cirrhosis and hence liver failure in individuals with HCV infection is a significant clinical problem and the burden of chronic liver disease secondary to HCV is increasing. Chronic liver disease in the form of cirrhosis occurs after many years of HCV infection (Alter 1995) and is preceded by hepatic inflammation and as a result, fibrosis. Liver disease occurs despite the low number of hepatocytes within the liver that are infected with the virus (Liang *et al.* 2009; Kandathil *et al.* 2013). HCV is not thought to be directly cytopathic and it is the host immune response to the HCV-infected hepatocyte that is the cause of liver injury in HCV infection (Pawlotsky 2004; Guidotti and Chisari 2006; Spengler and Nattermann 2007). However, the mechanisms that drive progression of HCV-related liver disease have not been completely elucidated. The lack of a small animal model and, until relatively recently, the inability to study the full HCV life cycle in cell culture have hampered efforts to study molecular mechanisms that underpin progressive liver disease.

We hypothesise that it is the interaction between the HCV-infected hepatocyte and uninfected 'bystander' cells in the liver (including hepatocytes, stellate cells and Kupffer cells) that expands the liver injury and thus contributes to the progression of liver disease. In this hypothesis, the effect of host innate immune responses to

HCV infection of hepatocytes, resulting in the production of cytokines, chemokines and interferon stimulated genes, is not isolated to infected cells but effects are also exerted on 'bystander' cells. The aim of this chapter was to generate an *in vitro* model system to examine the cross-talk between infected and uninfected 'bystander' cells to further our understanding of how HCV may cause progression of liver disease.

3.2 Generation of stable cell lines refractory to HCV infection

Our initial studies focused on the cross-talk between HCV-infected Huh-7 cells and uninfected Huh-7 cells. However, our experimental model, in which uninfected Huh-7 cells are either co-cultured with infected Huh-7 cells or cultured in conditioned media from infected cells, would result in infection of 'bystander' Huh-7 cells that could confound interpretation of results. Previous work has shown that knockdown of the HCV-specific cell entry receptors CD81 and Claudin-1 can inhibit HCV entry into the hepatocyte and cell-cell spread of virus (McKeating *et al.* 2004; Zhang *et al.* 2004; Evans *et al.* 2007; Brimacombe *et al.* 2010; see section 1.1.7). Therefore, to overcome infection of 'bystander' Huh-7 cells by HCV in our model system, cell lines were generated that demonstrated stable knockdown of known HCV entry factors Claudin-1 and CD81. The rationale for generating knockdown cell lines for both of these entry factors was two-fold. Firstly, it has been suggested that there are CD81-independent routes of cell-cell spread of HCV (Timpe *et al.* 2008; Witteveldt *et al.* 2009) and hence Claudin-1 was initially chosen as an ideal target in the model system as cell-cell spread of virus would not occur.

However, subsequent work has suggested that CD81-independent viral spread may not be the case (Brimacombe *et al.* 2010). Secondly, the knockdown of Claudin-1 was insufficient for use in this model system whereas the knockdown of CD81 was more robust, as discussed in section 3.2.1.

3.2.1 Generation of stable Claudin-1 and CD81 knockdown cell lines

To generate stable Claudin-1 and CD81 knockdown cell lines, shRNAs targeting Claudin-1 or CD81 were employed (Appendix IV). The pGIPZ lentiviral vectors (Appendix I) encoding various shRNAs were purchased from Open Biosystems (Thermo Scientific). A non-silencing shRNA control was also purchased. Expression cassettes that contain the shRNAs also encode a puromycin resistance gene and GFP, allowing for monitoring of shRNA expression. Six pGIPZ constructs encoding different shRNAs targeting Claudin-1 and five clones targeting CD81 were used to produce lentivirus as described in section 2.2.8. The lentiviral particles were then used to transduce Huh-7 cells as described in section 2.2.9. Following selection with puromycin, 10 polyclonal stable cell lines were produced (five Claudin-1 knockdown cell lines and five CD81 knockdown cell lines) which were then screened for effective knockdown of the appropriate target entry factor. All comparisons were made to the non-silencing shRNA control.

The five Claudin-1 shRNA knockdown cell lines were screened for effective shRNA knockdown at both the mRNA and protein level. Total protein was harvested and Western blots specific for Claudin-1 were performed (Figure 3.1).

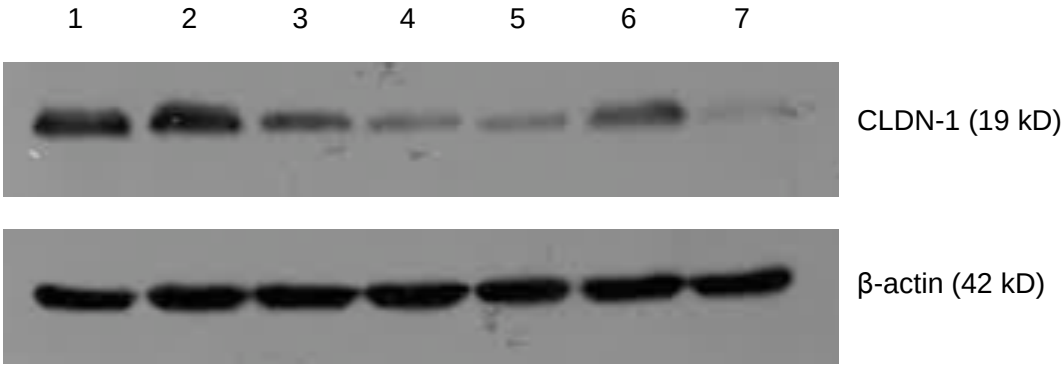

1. WT Huh-7
2. Huh-7 + Control shRNA
3. Huh-7 + A-10 shRNA
4. Huh-7 + A-12 shRNA
5. Huh-7 + F-7 shRNA
6. Huh-7 + G-11 shRNA
7. Huh-7 + H-4 shRNA

Figure 3.1 Claudin-1 expression by western blot in Huh-7 Claudin-1 knockdown cell lines.

Knockdown was most effective in the two cell lines designated ‘A-12’ and ‘H-4’ (lanes 4 and 7). Based on the protein data we extracted total RNA from ‘A-12’ and ‘H-4’ cells, synthesized cDNA and quantitated mRNA by qRT-PCR using primers specific for Claudin-1. As expected based on the protein data, the strongest knockdown of Claudin-1 mRNA was confirmed in both cell lines (Figure 3.2), with approximately 50% knockdown observed. The polyclonal nature of the isolated cells could indicate that there is a mixed population of cells with varying degrees of Claudin-1 expression. To investigate this we examined Claudin-1 expression *in situ* by immunofluorescence. While we noted an overall decrease in Claudin-1 expression there were populations of cells in which there was significant Claudin-1 expression (Figure 3.3). Expression was at the cell surface and in the cytoplasm, as would be expected. Collectively, these results suggested that the most effective knockdown at both the mRNA and protein level was in the ‘H-4’ cell line. However, after further cell passage, repeat analysis by qRT-PCR suggested less effective knockdown (less than 50%, Figure 3.4). The degree of knockdown in these cells was felt to be suboptimal for the cell line to be used as a bystander cell in our model system and hence the CD81 knockdown cell lines (described below) were used in preference in subsequent work.

The efficacy of shRNA knockdown of CD81 mRNA in the five cell lines developed was initially determined by qRT-PCR. RNA was isolated, cDNA produced and qRT-PCR was performed to determine mRNA levels of CD81. These results indicated that the most effective knockdown was seen in the ‘C-10’ and ‘H-8’ clones (Figure 3.5), with approximately 90% and 80% knockdown respectively. As

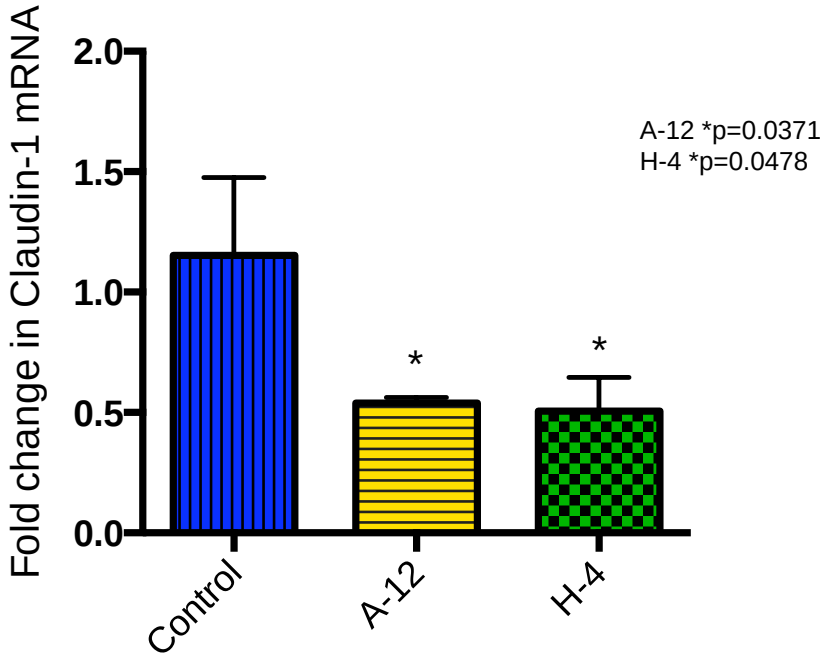

Figure 3.2 Real time RT-PCR demonstrates Claudin-1 knockdown in Huh-7 Claudin-1 shRNA knockdown cell lines. A statistically significant reduction in Claudin-1 mRNA expression was noted in both cell lines, with approximately 50% knockdown achieved (n=3, Student's *t*-test).

A

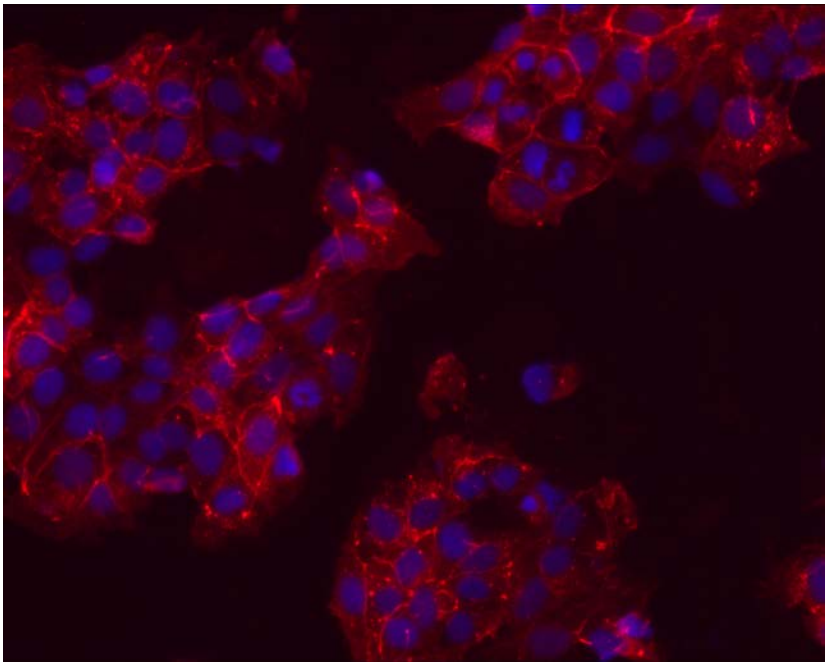

B

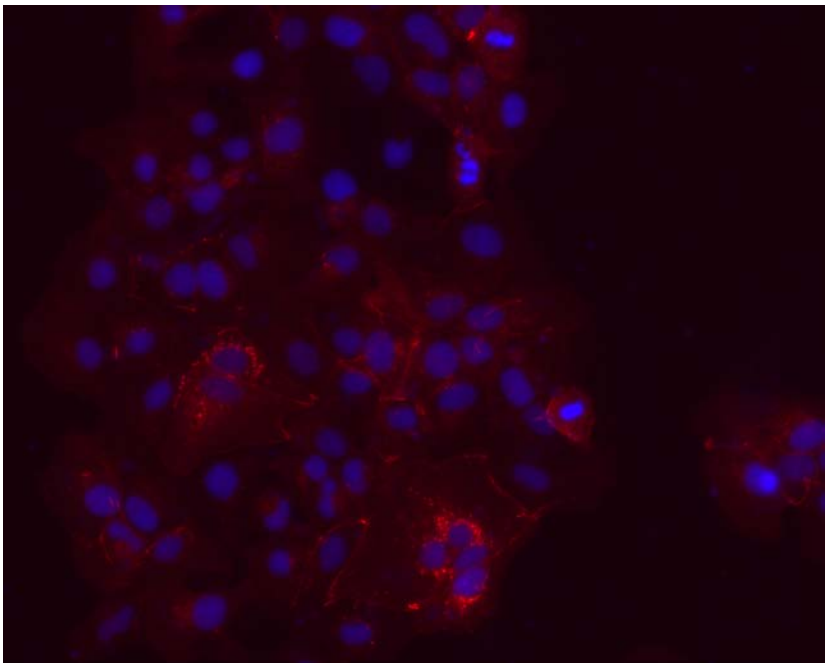

Figure 3.3 Claudin-1 expression demonstrated by immunofluorescence. 20x magnification. **(A)** Huh-7 + Control shRNA and **(B)** Huh-7 + Claudin-1 knockdown (Clone 'H-4').

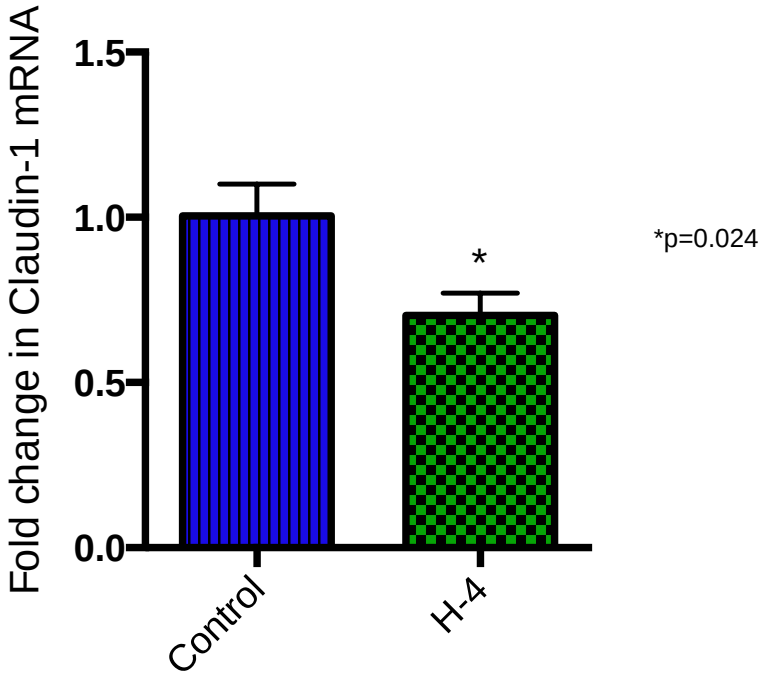

Figure 3.4 Repeat qRT-PCR analysis suggests less than 50% Claudin-1 knockdown in the Huh-7 + 'H-4' Claudin-1 shRNA cell line (n=3, p=0.024, Student's t-test).

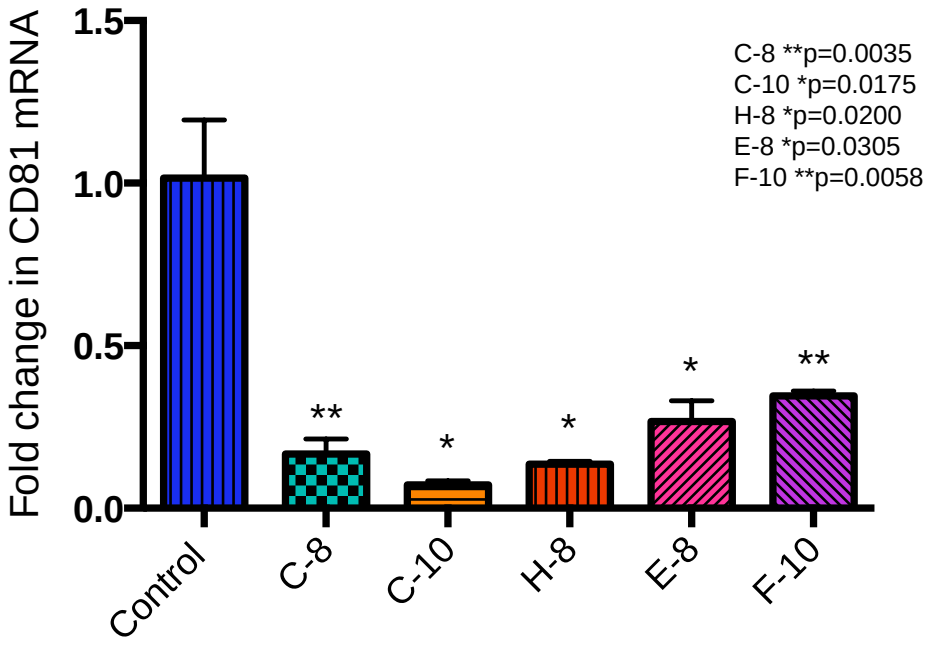

Figure 3.5 Real time RT-PCR demonstrates CD81 knockdown in Huh-7 CD81 knockdown cell lines. A statistically significant reduction in CD81 mRNA expression was noted in all cell lines, with the most effective knockdown in the 'C-10' cell line (n=3, Student's *t*-test).

CD81 is a cell surface molecule, further analysis of these two cell lines was performed by flow cytometry, with similar results for both cell lines (Figure 3.6). Flow cytometry demonstrated 87.5% and 83.6% of cells in the ‘H-8’ and ‘C-10’ groups respectively had low levels of CD81 expression and high levels of GFP (lower right quadrant). In comparison, 57.7% of control cells showed high levels of CD81 expression, as opposed to 4.7% and 3.5% in the ‘H-8’ and ‘C-10’ groups. When the results of the qRT-PCR and flow cytometry studies were taken together, the ‘C-10’ cell line was chosen for downstream use. A reduction in CD81 expression was also demonstrated by immunofluorescence microscopy using a specific anti-CD81 antibody. In comparison to the parent Huh-7 cell line, in which we demonstrated cell surface expression of CD81, we could detect no such expression in the C-10 cell line (Figure 3.7). Collectively these results indicated successful stable knockdown of CD81 expression in these cells.

3.2.2 Fluorescence-activated cell sorting of knockdown cell lines

While the degree of CD81 knockdown was more efficient than for Claudin-1, a small number of cells retain CD81 expression (as seen by flow cytometry and immunofluorescence microscopy), as would be expected given this was a polyclonal cell line. In order to improve the degree of CD81 knockdown homogeneity, we sorted cells as per section 2.5.3 according to GFP expression, given that the IRES-driven GFP cassette is encoded by the same RNA transcript that contains the shRNA. Claudin-1 knockdown cells were also sorted. The top 8% of cells according to GFP intensity were isolated and cultured, and qRT-PCR of

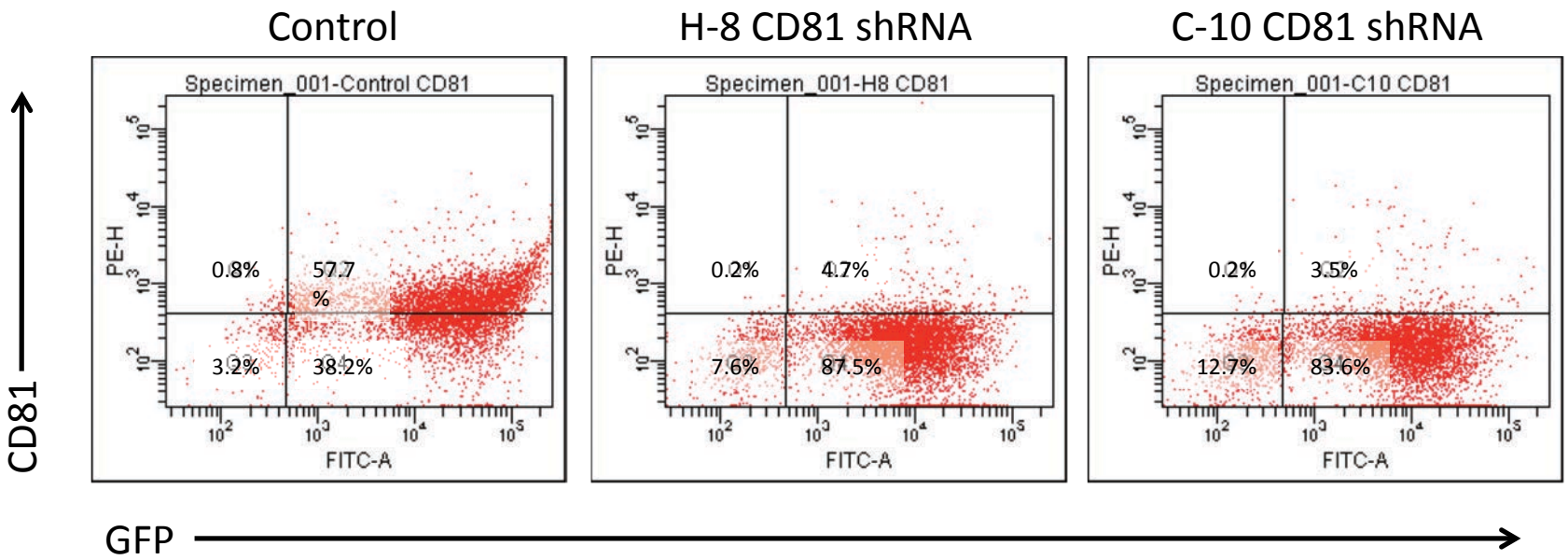

Figure 3.6 Flow cytometry demonstrates similar reduction in CD81 expression in 'H-8' and 'C-10' Huh-7 CD81 knockdown cell lines.

A

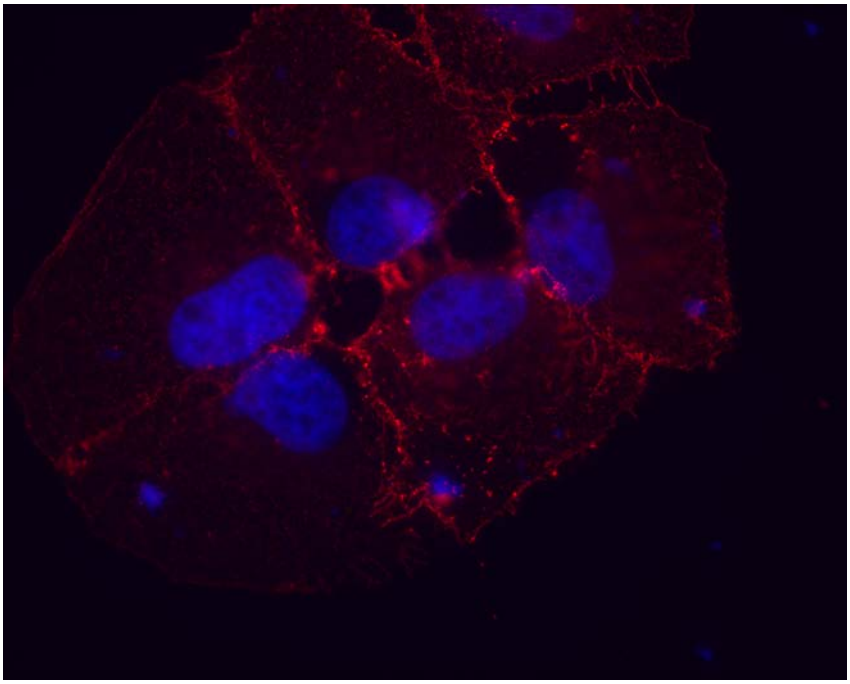

B

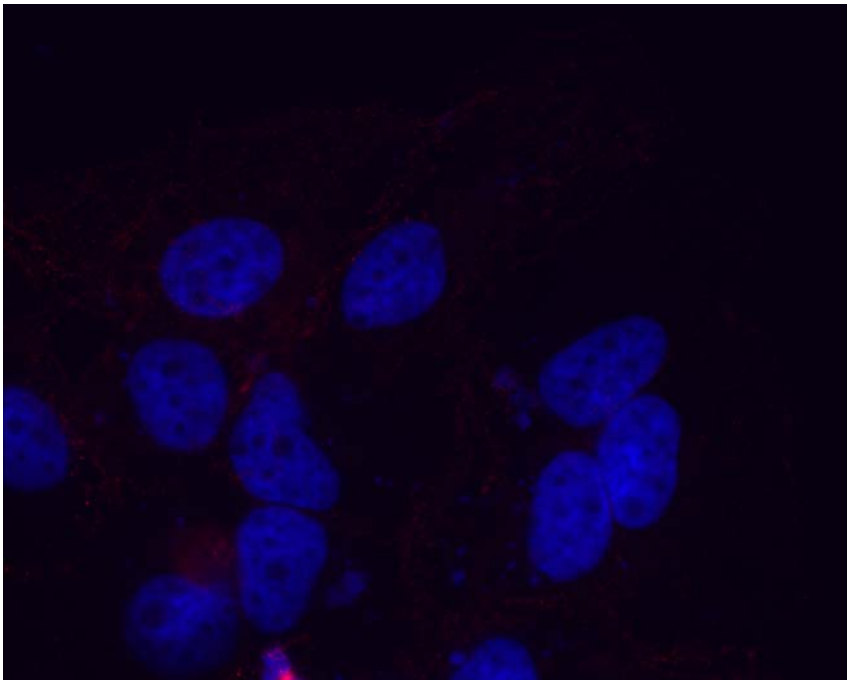

Figure 3.7 CD81 expression demonstrated by immunofluorescence. 60x magnification. **(A)** Huh-7 + Control shRNA and **(B)** Huh-7 + CD81 knockdown. Nuclei were stained with DAPI.

both Claudin-1 and CD81 knockdown cell lines was repeated. Unfortunately this method of selection did not result in a further decrease in mRNA expression in the Claudin-1 cell line (Figure 3.8a). However there remained significant knockdown in the CD81 knockdown cell lines (Figure 3.8b) and hence this cell line was chosen for downstream use and further characterized as described in section 3.3.

3.3 Huh-7 CD81 knockdown cell lines are refractory to HCV infection

To determine whether the Huh-7 CD81 knockdown cell line 'C-10' was refractory to HCV infection and could therefore be used in the proposed model system as a bystander cell, the permissiveness of these cells for infection with HCV Jc1 was determined by an infection assay and qRT-PCR.

Huh-7 CD81 knockdown cells (Clone C-10) and wild-type Huh-7 cells were seeded in a 96-well plate for a focus-forming unit assay as described in section 2.3.5. HCV antigens were subsequently labelled by indirect immunofluorescence using pooled anti-HCV serum and visualized by fluorescence microscopy. Distinct HCV-positive foci were counted and it was observed that there was almost 100% reduction in the infection rate in the CD81 knockdown cell line (Figure 3.9a). Cells were also infected (MOI 0.5) for a period of 72 hours with HCV Jc1 at which time there was a 95% reduction in HCV RNA in CD81 knockdown cells as determined by qRT-PCR (Figure 3.9b). Taken together, these results suggested that the Huh-7 CD81 knockdown cell line was refractory to HCVcc infection and was therefore suitable for use as a bystander cell in the model system.

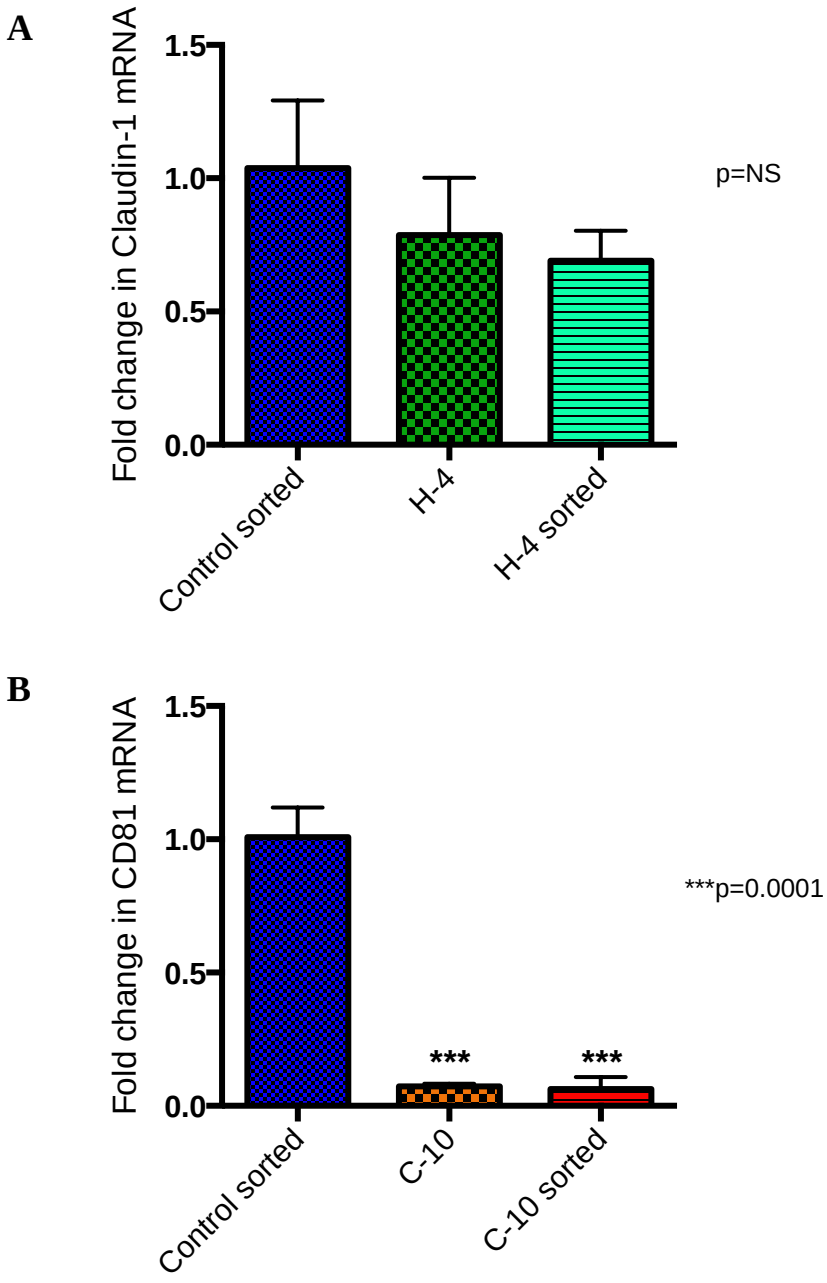

Figure 3.8 Entry factor knockdown post-fluorescence-activated cell sorting **(A)** Claudin-1 mRNA expression in Claudin-1 knockdown cell lines (n=3, *p*=NS, Student's *t*-test) **(B)** CD81 mRNA expression in CD81 knockdown cell lines (n=3, *p*=0.0001, Student's *t*-test).

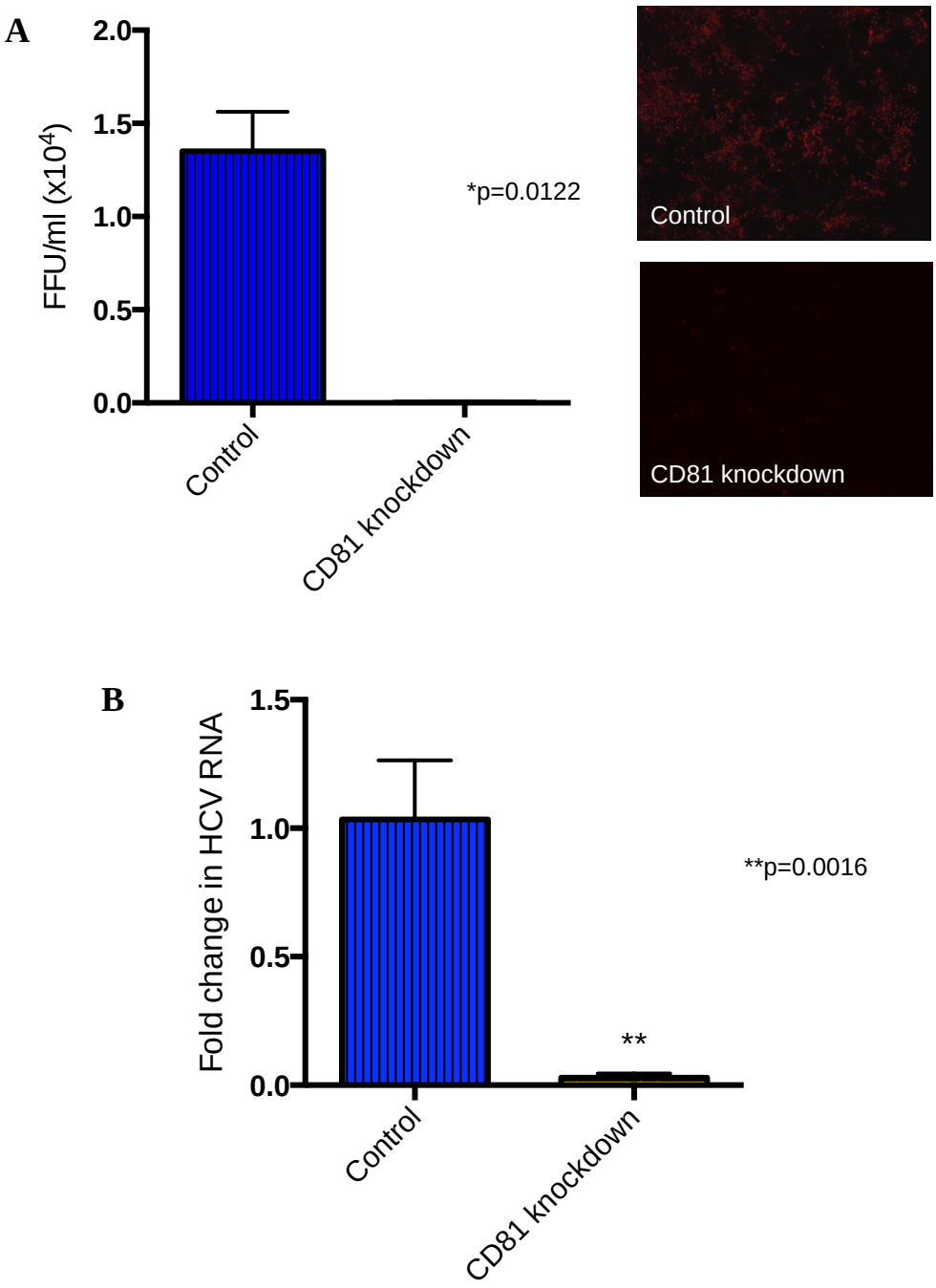

Figure 3.9 Huh-7 CD81 knockdown cell lines are refractory to HCV Jc1 infection (A) Focus-forming assay. Immunofluorescence panels show infection rates with HCV Jc1, with minimal infection observed in the CD81 knockdown cells compared to control, 4x magnification. **(B)** qRT-PCR (n=3, Student's *t*-test).

3.4 Conditioned media from HCV-infected Huh-7 cells has minimal impact on the transcriptome of uninfected Huh-7 cells

The rationale that underpins the HCV-related effect on bystander cells that is the focus of this chapter is that soluble factors produced as a result of HCV replication can have an effect on the bystander cell resulting in a change in the transcriptome. To determine the effect of HCV Jc1-infected Huh-7 cells on uninfected Huh-7 CD81 knockdown cells, Huh-7 cells were infected with HCV Jc1 (MOI 0.25) and returned to culture for 72 hours. After 72 hours a 30-40% infection rate was confirmed by immunofluorescence using pooled inactivated HCV-positive human serum as the primary antibody (Figure 3.10). Conditioned media was harvested as described in section 2.2.13; media was also harvested from uninfected Huh-7 cells after incubation for 72 hours and used as a control. Huh-7 CD81 knockdown cells were cultured in conditioned media from both control and test groups for 72 hours at which time total RNA was extracted and the transcriptomes were analysed by microarray analysis. This experimental design is summarized in Figure 3.11. Financial costs associated with microarrays prohibited the analysis of multiple time points and hence we chose 72 hours post inoculation of media to analyse the transcriptome. RNA quality was assessed by bioanalyser (Figure 3.12). Microarrays were performed at the Adelaide Microarray Centre (Adelaide, South Australia) using Affymetrix Genearrays (Affymetrix GeneChip® Hu1.0ST). Immunofluorescence in parallel cultures confirmed the absence of HCV infection at the time of harvesting (results not shown).

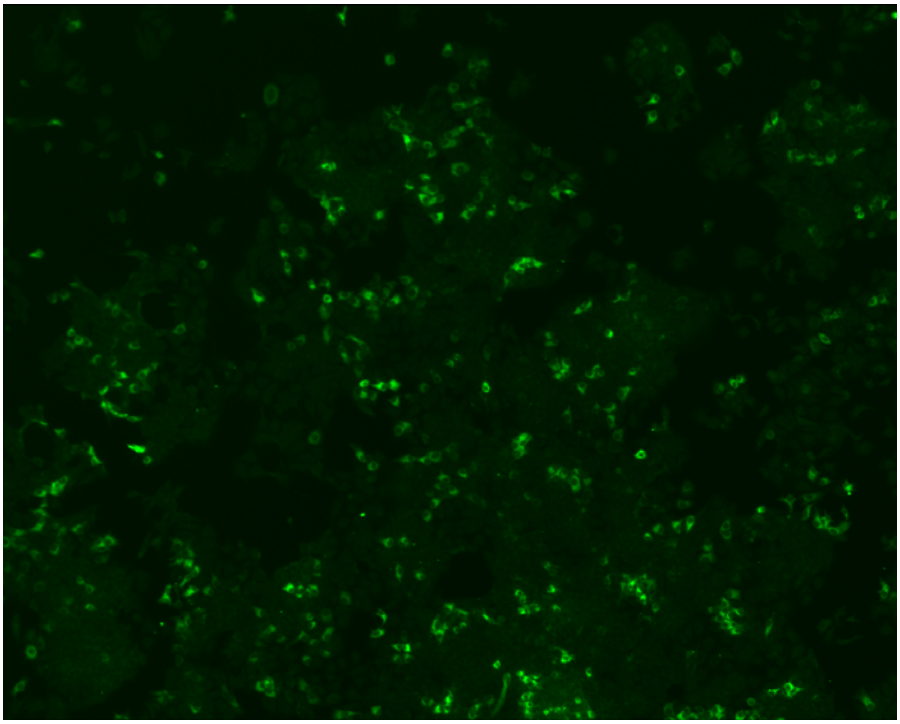

Figure 3.10 Infection rate in Huh-7 cells infected with HCV Jc1 for 72 hours, at which time media was harvested. HCV antigens were labelled with pooled inactivated HCV-positive human serum as the primary antibody followed by an appropriate fluorescent secondary antibody.

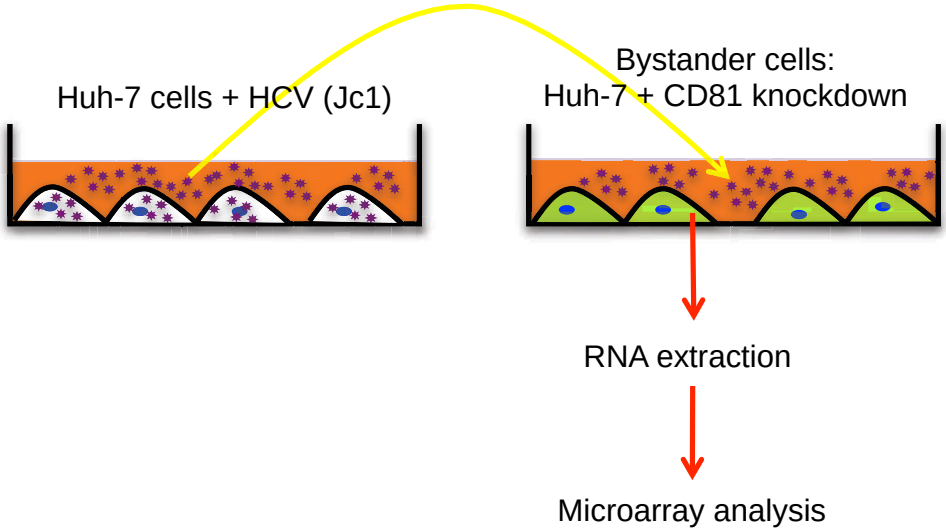

Figure 3.11 Experimental design of conditioned media studies to determine the effect of HCV-infected Huh-7 cells on bystander Huh-7 cells. After incubation of Huh-7 cells infected with HCV Jc1 for 72 hours, conditioned media was harvested and Huh-7 CD81 knockdown cells were incubated in this media for 72 hours. Following this, RNA was extracted and the transcriptome analysed by microarray analysis.

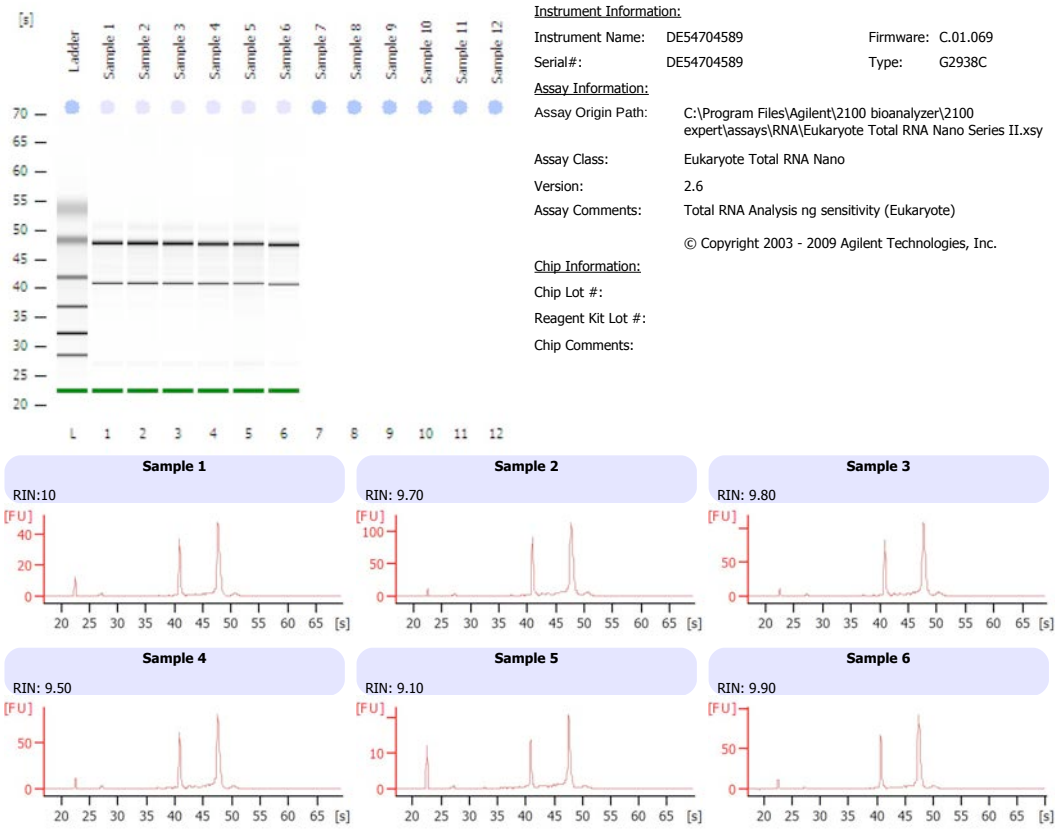

Figure 3.12 Bioanalyser assessment of RNA quality. Prior to microarray analysis, RNA quality and concentration was determined by bioanalyser. Analysis was performed prior to all microarrays discussed in this thesis.

Comparison of the transcriptome of Huh-7 CD81 knockdown cells exposed to conditioned media from HCV-infected cells to the transcriptome of Huh-7 CD81 knockdown cells cultured in media from uninfected cells revealed little differential expression. Analysis using Affymetrix software revealed that approximately 75% of the cellular transcripts (27,118 of 36,079) were designated as present. Principal component analysis (PCA) is shown in Appendix V. Surprisingly, cells exposed to conditioned media from infected cells did not exhibit any fold changes in gene expression more than two times that observed in the uninfected group. While we believe that a HCV Jc1 infection rate of approximately 40% should have been sufficient see an effect in bystander cells, as an alternative strategy we also investigated the effect of conditioned media from Huh-7 cells harbouring the full-length HCV replicon. Huh-7 cells were cultured for 72 hours in conditioned media taken from the HCV replicon-harbouring cell line NNeo-C5B (or NNeo-C5B cells cured of replicating HCV). These cells do not produce infectious HCV virions and hence infection of bystander hepatocytes is not of concern. Similar to the previously discussed work using HCV Jc1, only low level differential gene expression was observed (Figure 3.13). Of the few genes that demonstrated fold changes >2, DNA damage-inducible transcript 4 (DDIT4) was upregulated 2.7-fold and has been previously described as an anti-HCV ISG (Schoggins *et al.* 2011). There were a number of genes significantly downregulated. SPP1, otherwise known as osteopontin, was 2.11-fold downregulated, and is known to correlate with hepatic fibrosis (Huang *et al.* 2010; Patouraux *et al.* 2012; Urtasun *et al.* 2012), as is Reelin (RELN), which was recently evaluated as a serum biomarker for hepatic fibrosis in HCV-infected patients (Mansy *et al.* 2014). It is difficult to draw conclusions from

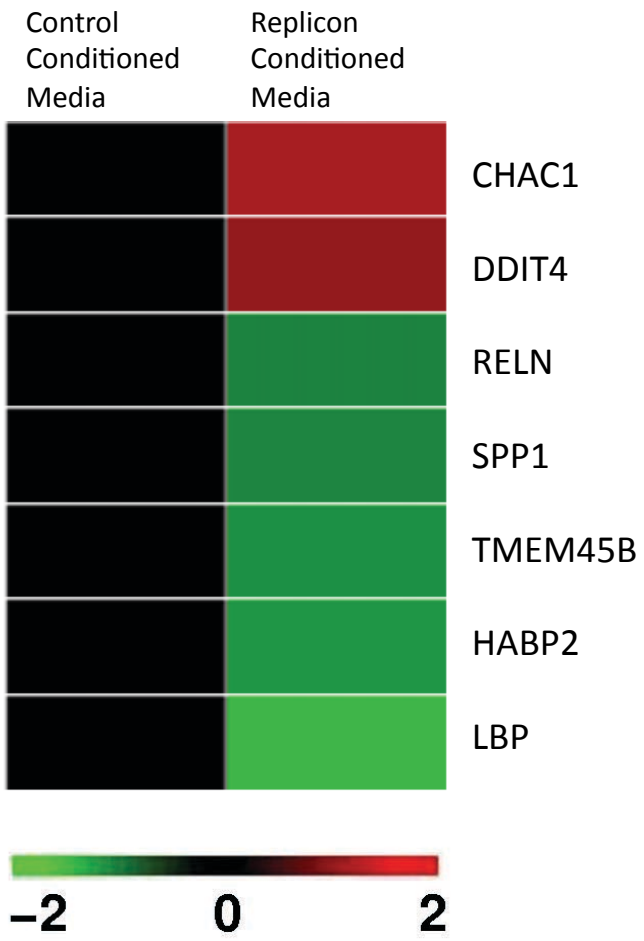

Figure 3.13 Microarray analysis of Huh-7 cells exposed to conditioned media from Nneo-C5B (Replicon) cells for 72 hours. Low level differential gene expression was observed in bystander cells, fold changes > 2 shown (Range -3.04 to -2.0 and 2.0 to 2.62).

this small data set, however this pattern of differential gene expression suggests an anti-inflammatory and anti-fibrogenic phenotype of bystander cells. In contrast, hyaluronic acid binding protein (HABP2) was also downregulated (2.32-fold). This protein plays a role in fibrinolysis and is downregulated in fibrogenesis (Roderfeld *et al.* 2009), hence its downregulation in bystander cells would potentially promote disease progression. Polymorphisms in this gene have been associated with severe HCV-induced liver fibrosis (Wasmuth *et al.* 2009).

3.5 Discussion

Progression to advanced liver disease occurs in a approximately 7-20% of persons chronically infected with HCV after 20 years (Alter 1995; Thein *et al.* 2008). Chronic liver disease associated with HCV is associated with substantial morbidity and mortality and is rising in incidence (Wong *et al.* 2000; Law *et al.* 2003; Davis *et al.* 2010; Thomas 2012). Cirrhosis secondary to HCV and its complications is a leading indication for liver transplantation worldwide (Brown 2005; Charlton 2005; Te and Jensen 2010). Thus, HCV infection and the burden of disease is a significant world-wide problem.

The mechanisms whereby liver disease progression occurs in chronic hepatitis C have not been fully elucidated, but we do know that there is a complex interplay between the resident and infiltrating cells of the liver that drives pathogenesis. It is well established that hepatic inflammation occurs in the HCV-infected liver, probably as a result of the host response to the virus-infected hepatocyte rather than

a direct cytopathic effect of the virus itself (Pawlotsky 2004). The innate immune response to HCV infection plays an important role in establishing an antiviral state. The recognition of HCV RNA via the innate immune sensors Toll-like receptor-3 (TLR3) and retinoic-acid-inducible gene I (RIG-I) (Sumpter *et al.* 2005; Wang *et al.* 2009) aims to control viral replication by transcription of the Type I interferons, interferon-α and -β. It is interferon-α and -β that subsequently stimulate pathways that lead to the production of hundreds of antiviral interferon stimulated genes (ISGs) and proinflammatory cytokines (Horner and Gale 2013). This innate response is also important in the initiation of adaptive immunity as the strength of the innate response can ultimately shape the adaptive response. Chronic hepatic inflammation also stimulates a fibrogenic response, leading to deposition of extracellular matrix, hepatic fibrosis and ultimately cirrhosis (Marcellin *et al.* 2002). However, only a low proportion of cells in the HCV-infected liver actually harbour the virus. Two-photon microscopy demonstrated between 1.7% and 22% of hepatocytes were infected in liver biopsy samples (Liang *et al.* 2009) and laser capture microdissection of liver biopsy samples identified 21 to 45% of hepatocytes were HCV RNA positive (Kandathil *et al.* 2013). Given that hepatocytes are not universally infected with HCV, it is unclear why the liver is more extensively affected by the inflammatory and fibrogenic response. It is hypothesised that liver injury is extended to uninfected, 'bystander' cells via an interaction with infected cells, either through a direct interaction or through the production of soluble factors. Furthermore, infiltrating mononuclear cells will also play a role in the pathogenic process. The literature suggests that both direct and indirect mechanisms may play a role in the cross-talk between HCV-infected and uninfected cells. It has been

previously demonstrated that the hepatocyte produces chemokines in response to HCV infection, particularly the CXCR3-associated chemokines such as CXCL10, CXCL11 and CCL5, and these play a role in recruitment of inflammatory cells to the liver (Harvey *et al.* 2003; Helbig *et al.* 2004; Apolinario *et al.* 2005; Zeremski *et al.* 2008). It has also been shown that CXCL8 (IL-8) is produced by Huh-7 cells expressing the HCV core protein, inducing α-smooth muscle expression in stellate cells and therefore encouraging a pro-fibrogenic state (Clement *et al.* 2010). Hence, the hepatocyte plays a central role in driving the pathogenic process, through the production of soluble factors. Other resident liver cells also play a role. The soluble factor IL-1 produced by the hepatic stellate cell line LX2 has been shown to stimulate the production of the chemokine CCL4 (MIP1β) by HCV-infected Huh-7.5 cells in a conditioned media model (Nishitsuji *et al.* 2013). Other interactions are extremely localized. Cell contact has been shown to be important for sensing of HCV in infected cells by TLR3 residing in adjacent uninfected cells via a Class A Scavenger Receptor 1 (MSR1) mediated mechanism, with subsequent production of an antiviral state (Dansako *et al.* 2013).

Thus far the interactions between HCV-infected and uninfected cells have been difficult to study due to the lack of both *in vitro* model systems and small animal models. The model system described in this chapter allows for the examination of this interaction *in vitro* between infected and uninfected hepatocytes, in both conditioned media and co-culture approaches.

An integral aspect of the model system generated in this thesis is the production of a ‘bystander’ cell line that is refractory to HCV infection. HCV exploits a number of

essential host entry factors that render hepatocytes permissive to infection, namely SR-BI, Claudin-1, CD81 and Occludin (Pileri *et al.* 1998; Scarselli *et al.* 2002; Evans *et al.* 2007; Ploss *et al.* 2009). It has been previously shown that HCV infection *in vitro* can be prevented by knockdown of Claudin-1 and CD81 or by use of anti-Claudin-1 or -CD81 antibodies (Zhang *et al.* 2004; Evans *et al.* 2007; Timpe *et al.* 2008; Brimacombe *et al.* 2010; Fofana *et al.* 2010; Krieger *et al.* 2010). We adopted a two-pronged approach to entry receptor knockdown in this thesis. While we were able to knockdown Claudin-1, the degree of knockdown was felt to be insufficient for the cell line to be used in our model. In this chapter it is demonstrated that with significant CD81 knockdown using shRNAs, infection of the HCV-permissive cell line Huh-7 can be prevented. Although some literature suggests that CD81-independent routes of cell-cell spread of HCV can occur (Timpe *et al.* 2008; Witteveldt *et al.* 2009), there was no perceivable spread of virus through the culture from the small number of cells that were infected. Knockdown of HCV entry factors in HCV permissive cell lines was performed in preference to using hepatocyte cell lines that are known to be refractory to HCV infection, such as HepG2 (human hepatocellular carcinoma-derived cell line) and PH5CH8 (immortalized non-neoplastic hepatocyte cell line) cells. This approach was chosen given the experience with the Huh-7 cell line and its characteristics in our laboratory, and so that both infected and uninfected hepatocytes were of the same cell type, allowing for identical culture conditions. The PH5CH8 cell line was used in work described later in this thesis.

Having developed a CD81 negative cell line that was not permissive to HCV infection we were now in a position to assess the HCV 'bystander' effect in these cells at the transcriptional level using Affymetrix Genechip technology. In this model system no significant differential gene expression was observed in bystander CD81 knockdown Huh-7 cells exposed to conditioned media from HCV Jc1 infected Huh-7 cells. There are a number of potential explanations for the lack of response in our bystander cell population. Firstly, while Huh-7 cells can be infected with HCV, they are relatively unresponsive at the innate immune response level to HCV infection. It has been previously shown that the transcriptome of Huh-7 cells harbouring autonomously replicating HCV was not significantly different to HCV-cured clonally related cells, when assessed by microarray analysis (Scholle *et al.* 2004). Results of microarray analysis obtained in our own laboratory confirm this finding (unpublished data). Although Huh-7 cells retain a RIG-I pathway, RIG-I expression is low. Additionally, they are deficient in TLR3 and thus lack TLR3 responses (Li *et al.* 2005). Hence, HCV infected cells do not respond as a primary hepatocyte would and may not produce a number of ISGs and cytokines that mediate interactions with uninfected cells. It is for these reasons that the Huh-7.5 cell line is highly permissive to HCV infection, as it is both RIG-I and TLR3 deficient (Sumpter *et al.* 2005). Secondly, the infection rate in Huh-7 cells from which conditioned media was taken may not have been sufficiently robust to induce a response. However, given little response was seen in bystander cells exposed to conditioned media taken from a replicon-harbouring cell line in which all cells harbour replicating HCV, the infection rate is less likely to be solely responsible for the lack of response seen. The choice of a single time point at which to harvest

conditioned media may play a role here. Media was harvested at 72 hours post-infection as it was felt that the infection rate would be significantly robust at this time, and with ongoing infection this would mean continued expression of effector molecules. The significant financial cost, particularly of microarray analysis, is a limiting factor in assessing multiple time points. However, early infection events and cellular responses are potentially missed by this approach and hence any impact on bystander cells by early responses will not be seen. However, HCV infection appears to activate TLR3 signalling and cytokine production three or four days after infection (Wang *et al.* 2009; Li *et al.* 2012). Thirdly, the model system described here examines the effect of soluble factors and cell-free virus on uninfected cells but there is no direct cell-cell contact between infected and uninfected cells. It is possible that any effect may only be mediated by interaction over short distances and thus the conditioned media approach may not impact on the bystander cell. This has been previously shown to be the case by Dansako et al., where cross-talk between HCV-infected and uninfected cells occurred in a localized environment, and may have required direct cell-cell contact, as previously discussed (Dansako *et al.* 2013). Finally, the model does not allow for examination of the role of the adaptive immune response in the bystander effect on uninfected hepatocytes.

Low-level differential gene expression was seen in Huh-7 bystander cells exposed to conditioned media harvested from HCV replicon-harbouring cells (NNeo-C5B). These replicon-harbouring cells are also a Huh-7 based cell line and are related to those described by Scholle et al. (2004), where the presence of replicating HCV had little impact on the transcriptome as assessed by microarray. It is therefore not

surprising that they are also relatively unresponsive to replicating HCV. Despite this, a number of genes were identified that differed in expression in bystander cells. Those genes noted to be greater than two-fold up- or downregulated in bystander cells exposed to conditioned media in this experiment appear to have roles in inflammation, apoptosis and TLR signalling pathways. As previously noted, the 2.7-fold upregulated DDIT4 is an anti-HCV ISG. SPP1, or osteopontin, is a known chemo-attractant for T lymphocytes (Weber *et al.* 1996) and was noted to be downregulated in the current study. Osteopontin has been shown to up-regulate Collagen-I and levels correlate with hepatic fibrosis in HCV-related and alcoholic liver disease (Huang *et al.* 2010; Patouraux *et al.* 2012; Urtasun *et al.* 2012). HCV core protein has been previously shown to down-regulate osteopontin, which may be an underlying mechanism of viral persistence and suppression of the inflammatory response to HCV (Nguyen *et al.* 2006). Down-regulation of osteopontin in bystander cells may suggest an effect of HCV or soluble factors on uninfected hepatocytes in a similar manner, expanding the suppression of the inflammatory response to uninfected cells. Of interest, two other downregulated genes in this study, RELN and HABP2, also have roles in hepatic fibrogenesis in HCV-infected patients, as previously discussed.

In conclusion, we have successfully generated a stable cell line refractory to HCV infection and used this in our bystander cell model. We were unable to demonstrate a marked response in bystander Huh-7 cells exposed to conditioned media from HCV-infected cells, most likely reflecting the unresponsive nature of the Huh-7 cell line. In subsequent chapters the model system described here has been modified to

include a TLR3 expressing cell line that is more responsive to HCV infection and used the cell lines generated in this chapter to examine the bystander effect in the context of both soluble factors from and direct cell-cell contact with TLR3-positive HCV-infected cells.

Chapter 4

The Toll-like receptor 3 response to HCV infection in Huh-7 cells

4.1 Introduction

The early host innate immune response is essential in the sensing of HCV infection by the hepatocyte. After entry into the cell and uncoating of the viral genome, translation of the viral polyprotein occurs and replication is initiated. During viral replication, specific pathogen-associated molecular patterns (PAMPs) within viral components are recognised by host pattern recognition receptors (PRRs). In the case of HCV, PAMPs in the HCV genome constitute dsRNA and are recognised by the host PRRs retinoic acid inducible gene-I (RIG-I) and toll-like receptor 3 (TLR3). This binding initiates downstream signalling resulting in the induction of antiviral and proinflammatory genes (reviewed in Horner and Gale 2013). More recently, protein kinase R (PKR) has been identified as an additional PRR for HCV (Arnaud *et al.* 2011). A more in-depth discussion of PRRs and their activation is outlined in Chapter 1.

The human hepatoma cell line Huh-7, the only cell line that robustly supports HCV infection and replication *in vitro* does not express Toll-like receptor 3 (TLR3) and is thus deficient in TLR3 responses to dsRNA (Li *et al.* 2005). It is likely that the lack of TLR3 expression in Huh-7 cells confers permissiveness to HCV infection. However, it has been previously demonstrated that stable TLR3 expression in Huh-7.5 cells (an interferon-cured HCV replicon cell line that has defective RIG-I

signalling and hence more permissive for HCV infection than Huh-7 cells (Sumpter *et al.* 2005)) allows sensing of HCV via TLR3 and subsequent induction of IRF-3 and upregulation of interferon stimulated genes (ISGs) as well as activation of chemokines and inflammatory cytokines (Wang *et al.* 2009; Li *et al.* 2012). We reasoned that the low levels of differential gene expression in response to conditioned media from HCV infected Huh-7 cells described in Chapter 3 may be related to the inability of these cells to adequately sense HCV RNA due to the lack of TLR3 expression. To overcome this lack of response we reasoned that reintroduction of TLR3 by ectopic expression into Huh-7 cells should re-establish HCV sensing and subsequent ISG and chemokine/cytokine production, with enhanced effect on bystander cells in our model system.

4.2 Generation of a TLR3-positive Huh-7 cell line

The pCX4bsr retroviral expression plasmid encoding human TLR3 (FLAG-tagged) and pCX4bsr encoding the TLR3 mutant ΔTIR (FLAG-tagged, TIR signalling domain deleted) (a kind gift from Dr Kui Li, University of Tennessee Health Science Center, Memphis, TN, USA) (Wang *et al.* 2009) were used to generate Huh-7 cell lines that stably express wild-type TLR3 or ΔTIR-TLR3 (Figure 4.1). These stable polyclonal cell lines were generated via a retroviral approach as per the method described in sections 2.2.10 and 2.2.11. Briefly, target cells were cultured in retrovirus-containing supernatant containing Polybrene. After infection, TLR3 or ΔTIR expressing cells were selected using blasticidin.

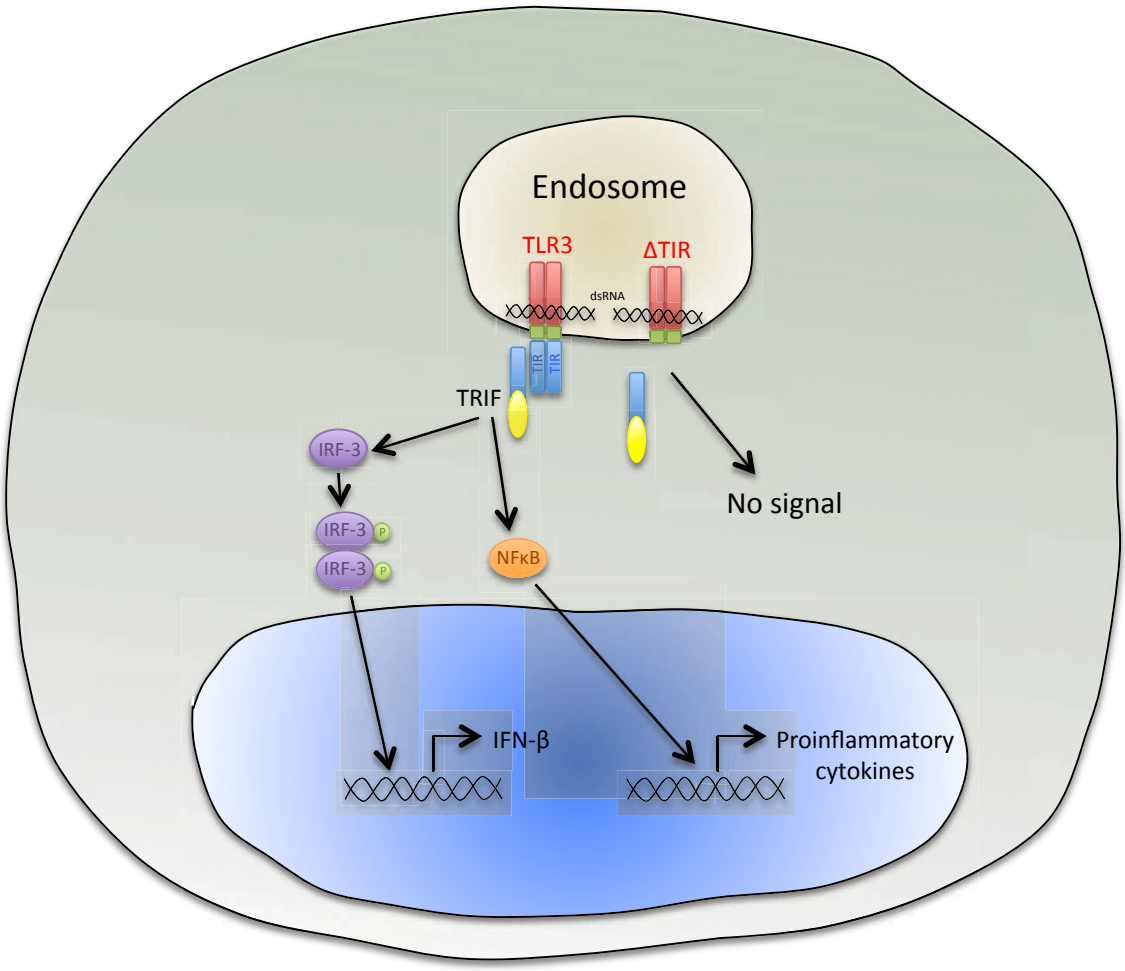

Figure 4.1 Schematic diagram showing TLR3 and the TLR3 mutant ΔTIR. After interaction of dsRNA to TLR3, TRIF binds to the TLR3 TIR domain, activating downstream signaling pathways that upregulate IFN-β and proinflammatory cytokines, via IRF-3 and NFκB respectively. In the case of ΔTIR, the TIR signaling domain has been deleted, thus the binding of dsRNA to TLR3 does not lead to an interaction with TRIF and downstream signaling does not occur.

To confirm stable expression of TLR3 and the ΔTIR mutant in Huh-7 cells, cells were seeded, fixed with acetone and methanol, and labelled with anti-TLR3 or anti-Flag primary antibody as described previously (section 2.4). Immunofluorescence microscopy confirmed TLR3 and ΔTIR expression, in a cytoplasmic pattern with a tendency towards perinuclear distribution (Figure 4.2). TLR3 and ΔTIR expression were also confirmed by harvesting total protein from cells and performing Western blots specific for both TLR3 and FLAG (Figure 4.3). As expected, the parent Huh-7 cell line did not express detectable levels of TLR3, whereas both the wild-type and mutant TLR3 cell lines demonstrated positive TLR3 expression, with a band of approximately 120 kDa in size. As expected, the band expressed by the mutant cell line (ΔTIR) was slightly smaller. Neither the wild-type or mutant TLR3-expressing cell lines showed any differences in cell morphology or growth characteristics when compared to the parent Huh-7 cell line. Taken together, these results demonstrate stable expression of TLR3 in Huh-7 cells.

4.3 Reintroduction of TLR3 into Huh-7 cells restores dsRNA-induced cytokine and chemokine expression

To determine whether the stable cell lines generated expressed functional TLR3, cells were stimulated with the synthetic dsRNA analogue Poly I:C, a well known TLR3 agonist, at 50μg/ml for 24 hours. Total RNA was subsequently extracted, cDNA generated and qRT-PCR performed to determine mRNA levels of various cytokines and chemokines that had been previously demonstrated to be induced by HCV in a TLR3-positive Huh-7.5 cell line (Li *et al.* 2012). Results were normalized

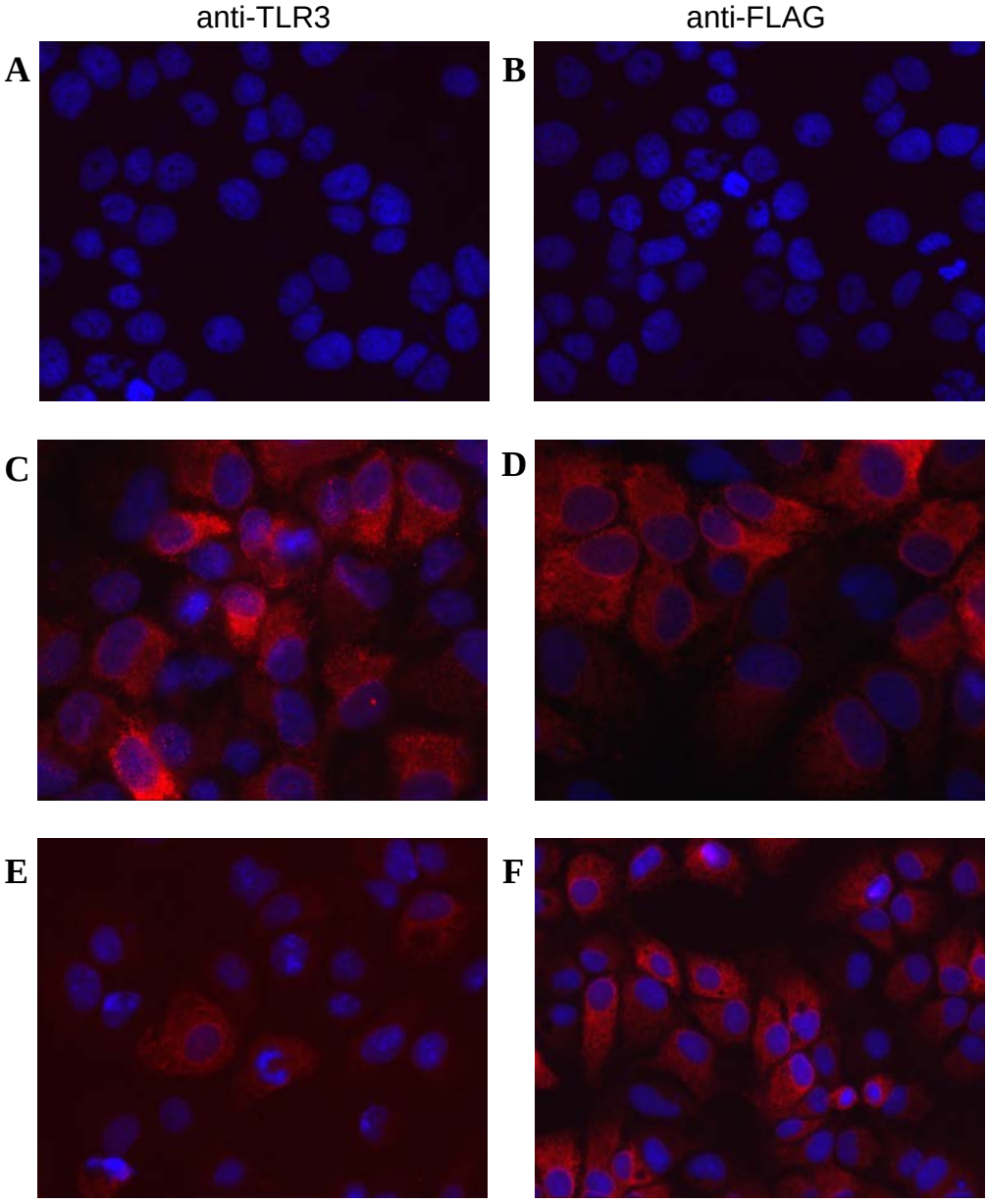

Figure 4.2 TLR3 and ΔTIR expression in Huh-7 cells by immunofluorescence. 20x magnification. **(A)** Huh-7 WT, anti-TLR3 **(B)** Huh-7 WT, anti-FLAG **(C)** Huh-7+TLR3, anti-TLR3 **(D)** Huh-7+TLR3, anti-FLAG **(E)** Huh-7+ΔTIR, anti-TLR3 **(F)** Huh-7+ΔTIR, anti-FLAG.

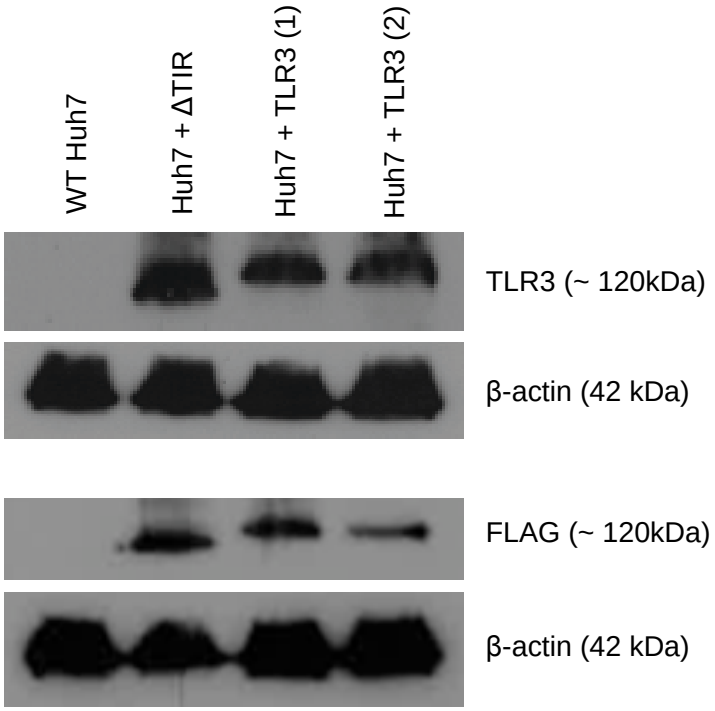

Figure 4.3 Detection of TLR3 in Huh-7+TLR3 and Huh-7+ΔTIR cell lines by western blot. The parental cell line WT Huh-7 does not express detectable TLR3.

to those of the housekeeping gene 36B4. Cells expressing wild-type TLR3 had a significant increase in the mRNA of the TLR3 response genes CXCL10, CCL5, CCL4 and IFI6 after stimulation with Poly I:C (Figure 4.4), with fold changes in mRNA relative to parent Huh-7 cells or Huh-7+ΔTIR cells ranging from 6 times for CXCL10 to 800 times for CCL5. There was no significant difference in the baseline expression of these cytokines between Huh-7+TLR3 and Huh-7+ΔTIR cells when mRNA levels were assessed by qRT-PCR (data not shown).

Increases in mRNA expression do not always correlate to downstream increases in protein expression. Therefore, to investigate protein expression in response to Poly I:C, qualitative ELISA was used to confirm cytokine protein expression in TLR3-expressing Huh-7 cells. A panel of cytokines as represented in the Multi-Analyte ELISArray (QIAGEN) described in section 2.6.4 were assessed. In response to stimulation with Poly I:C 50μg/ml for 24 hours, IL-6, RANTES (CCL5) and IP-10 (CXCL10) were increased in expression in Huh-7+TLR3 cells when compared to Huh-7+ΔTIR cells stimulated in parallel (Table 4.1). The assay used is qualitative in nature and thus the degree to which the expression of these cytokines was increased could not be determined by this method. Interestingly, we would have expected that interferon-α and other inflammatory cytokines represented in the ELISArray, such as MIG (CXCL9) and TNFα, would have been induced by Poly I:C stimulation of TLR3, but this was not observed. Possible reasons for this include low-level induction below the level of detection of the ELISA, induction at a time point not captured in this experiment, or loss of the positive feedback loop whereby IRF7 stimulates IFN-α production.

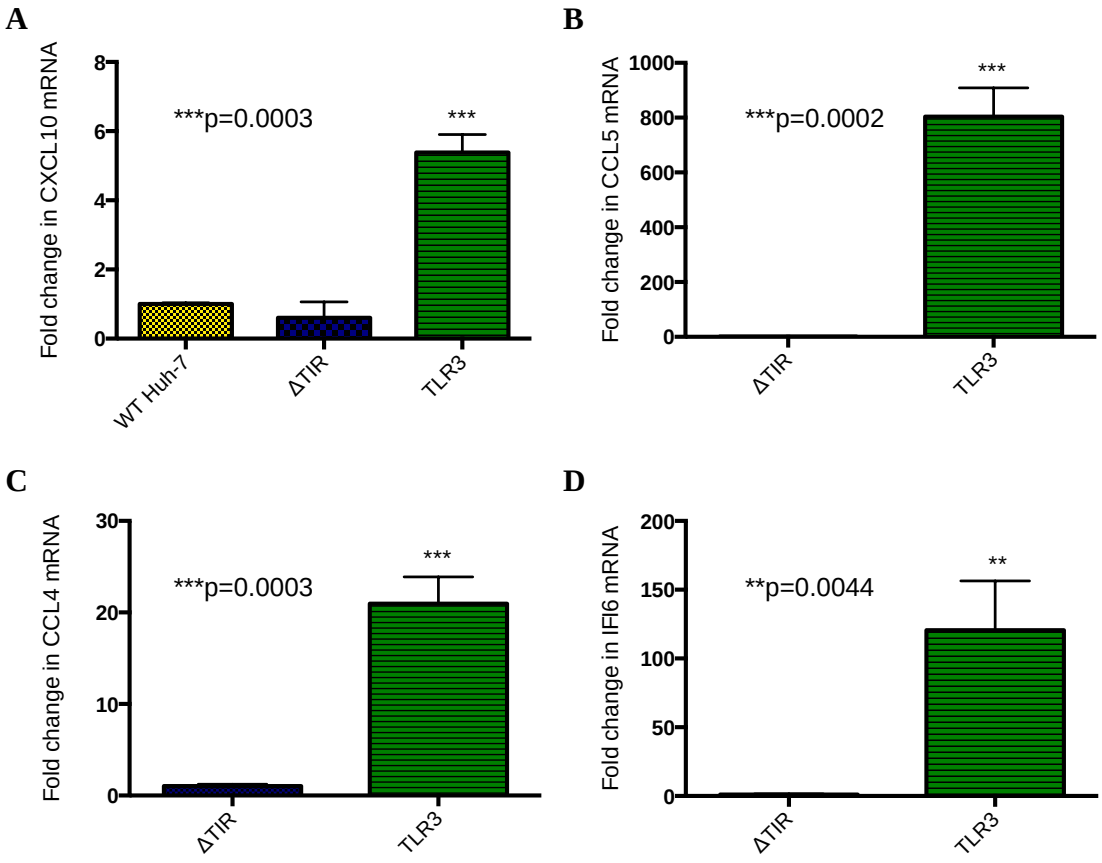

Figure 4.4 Expression of TLR3 in Huh-7 cells restores cytokine and chemokine production in response to stimulation by dsRNA. Huh-7+TLR3 cells were stimulated with Poly I:C 50μg/ml for 24 hours. Significant upregulation of **(A)** CXCL10 **(B)** CCL5 **(C)** CCL4 and **(D)** IFI6 mRNA was observed in Huh-7+TLR3 cells in comparison to Huh-7+ΔTIR stimulated in parallel, as determined by real-time RT-PCR (n=3, Student's *t*-test).

Table 4.1 ELISA confirms expression of cytokines in response to Poly I:C stimulation

Cytokine	Huh-7 ΔTIR + Poly I:C	Huh-7 TLR3 + Poly I:C
TNFα	-	-
IL1B	-	-
IL6	-	+
IL12	-	-
IL17A	-	-
IL8 (CXCL8)	+	+
MCP-1 (CCL2)	-	-
RANTES (CCL5)	-	+
IP-10 (CXCL10)	-	+
MIG (CXCL9)	-	-
TARC (CCL17)	-	-
IFNα	-	-

Collectively, the results of the qRT-PCR and ELISA experiments suggest that reintroduction of TLR3 in this system is functional in responding to a dsRNA stimulus.

4.4 Reintroduction of TLR3 into Huh-7s restores HCVcc-induced cytokine and chemokine expression

Results above focused on stimulation of TLR3-positive Huh-7 cells with the dsRNA mimic Poly I:C. To determine the responsiveness of Huh-7+TLR3 cells to a productive HCV infection, Huh-7+TLR3 and Huh-7+ΔTIR cells were infected with HCV Jc1 (MOI 1.0-2.0) for 72 hours. It was observed that a high MOI was required to achieve an adequate infection rate in TLR3-expressing cells (Figure 4.5). This is most likely related to the enhanced innate TLR3 sensing and related downstream signalling generated in response to HCV infection, with generation of an antiviral state. This observation is consistent with previous studies (Wang *et al.* 2009). RNA

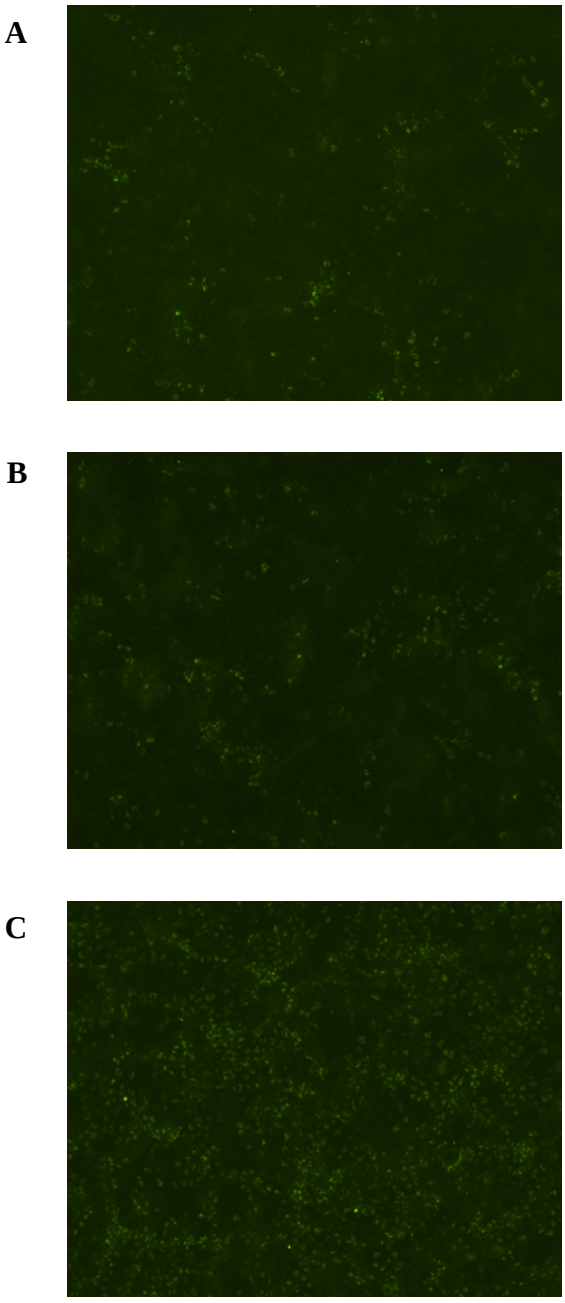

Figure 4.5 Immunofluorescence demonstrates high MOI is required to achieve a robust HCV Jc1 infection of Huh-7+TLR3 cells. After 72 hours infection with HCV Jc1, cells were fixed with acetone and methanol and labeled with an anti-HCV antibody as described in section 2.4.2. 4x magnification. **(A)** HCV Jc1 MO1 0.5 **(B)** HCV Jc1 MOI 1.0 **(C)** HCV Jc1 MOI 2.0.

was subsequently extracted and qRT-PCR performed to assess mRNA levels of the cytokines and chemokines previously noted to be upregulated in response to Poly I:C stimulation. In comparison to Huh-7+ΔTIR cells infected in parallel, CXCL10, CCL5 and CCL4 mRNA was significantly upregulated in Huh-7+TLR3 cells, although the fold changes in mRNA were somewhat less marked than those seen in the Poly I:C stimulated cells (Figure 4.6). The weaker response observed may be related to the ability of HCV to inhibit signalling downstream of TLR3, via cleavage of TRIF by NS3/4A (Li *et al.* 2005), as discussed in more detail in Chapter 1. It is also likely that there is significantly more dsRNA available with Poly I:C stimulation compared to HCV infection. Nevertheless, infection of TLR3-expressing cells resulted in an innate immune response to viral infection.

As performed after stimulation with Poly I:C, we also used qualitative ELISA to confirm cytokine protein expression in TLR3-expressing Huh-7 cells in response to HCV Jc1 infection. The same panel of cytokines was assessed as described in section 4.3. In response to infection with HCV Jc1 for 72 hours, IL-6, RANTES (CCL5) and IP-10 (CXCL10) were again expressed by Huh-7+TLR3 cells when compared to Huh-7+ΔTIR cells infected in parallel. IL-8 (CXCL8) was expressed in both control and TLR3-expressing cell lines (Table 4.2).

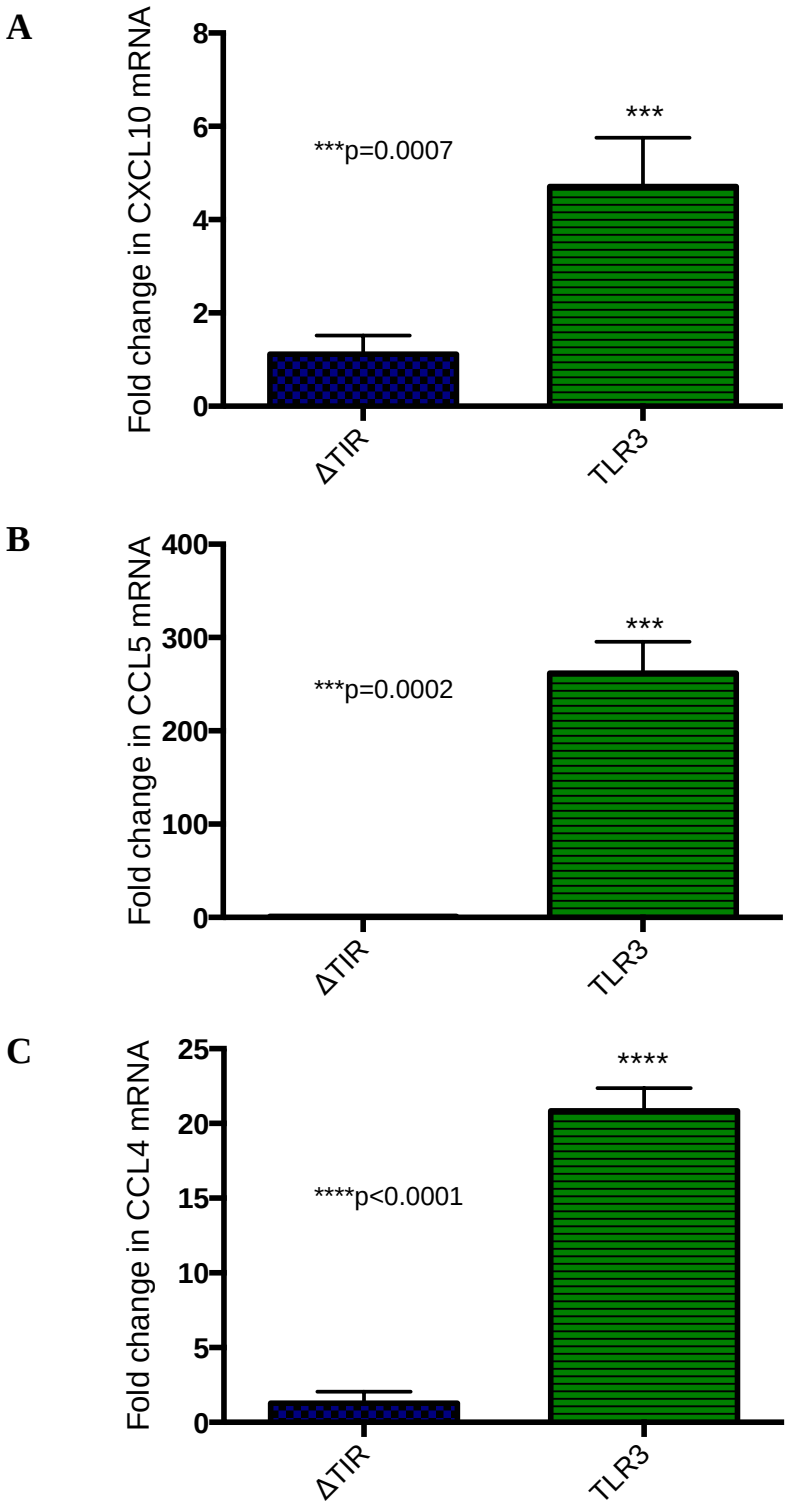

Figure 4.6 Expression of TLR3 in Huh-7 cells restores cytokine and chemokine production in response to infection with HCVcc. Huh-7+TLR3 cells were infected with HCV Jc1 for 72 hours. Significant upregulation of **(A)** CXCL10 **(B)** CCL5 and **(C)** CCL4 mRNA was observed in Huh-7+TLR3 cells in comparison to Huh-7+ΔTIR infected in parallel as determined by real-time RT-PCR (n=3, Student's *t*-test).

Table 4.2 ELISA confirms expression of cytokines in response to HCV Jc1 infection

Cytokine	Huh-7 ΔTIR + HCV Jc1	Huh-7 TLR3 + HCV Jc1
TNFα	-	-
IL1B	-	-
IL6	-	+
IL12	-	-
IL17A	-	-
IL8 (CXCL8)	+	+
MCP-1 (CCL2)	-	-
RANTES (CCL5)	-	+
IP-10 (CXCL10)	-	+
MIG (CXCL9)	-	-
TARC (CCL17)	-	-
IFNα	-	-

4.5 Multiple genes are upregulated in Huh-7+TLR3 cells in response to dsRNA and HCVcc

To obtain a more global view of TLR3-dependent gene expression in Huh-7+TLR3 cells, total RNA from cells stimulated with Poly I:C 50μg/ml for 24 hours or infected with HCV Jc1 for 72 hours was analysed by an antiviral pathway-focused PCR array (QIAGEN) and human microarray using Affymetrix gene expression analysis. Comparison was made with Huh-7+ΔTIR cells stimulated or infected in parallel. To our knowledge there have been no studies investigating TLR3-dependent gene expression in Huh-7 cells using such an extensive panel of genes.

4.5.1 Pathway-focused Real-time PCR Array

To assess gene expression by a panel of genes related to the antiviral response, a Human Antiviral Response RT^2 Profiler PCR Array (QIAGEN) was used. This

PCR array assesses expression of 84 genes involved in human innate immune responses. Genes represented in this array are involved in pattern recognition receptor pathways (namely Toll-like receptors, Nod-like receptors and RIG-I-like receptors), type I interferon signalling or are interferon stimulated genes. For these experiments, Huh-7+TLR3 and Huh-7+ΔTIR cells were seeded into 12-well plates and cultured overnight. They were subsequently stimulated with Poly I:C for 24 hours as previously described, at which time RNA was harvested and cDNA prepared as per the kit instructions. In response to stimulation with Poly I:C, 15 genes were significantly upregulated in expression (fold change > 1.5) in Huh-7+TLR3 cells when compared to stimulated Huh-7+ΔTIR cells (Table 4.3 and Appendix VI); *p* values less than 0.05 were considered significant. The array also confirmed upregulation of expression of a number of the genes noted to be upregulated by qRT-PCR and ELISA in section 4.3.

Similarly, Huh-7+TLR3 cells infected with HCV Jc1 for 72 hours also upregulated multiple genes represented in the array (Table 4.3 and Appendix VI) in comparison to Huh-7+ΔTIR cells also infected for 72 hours. Again, *p* values less than 0.05 were considered significant. The pattern of genes upregulated was similar but not identical to those expressed in response to dsRNA stimulation.

Figure 4.7 depicts the pattern of differential gene expression after both Poly I:C stimulation and HCV Jc1 infection in a clustergram format. What is immediately apparent is the variability of the PCR array, suggesting that significant induction of TLR3 dependent genes may be missed in the assay. As an example (see arrow), CXCL10, which is positive in the ELISA analysis, is upregulated in Control-3,

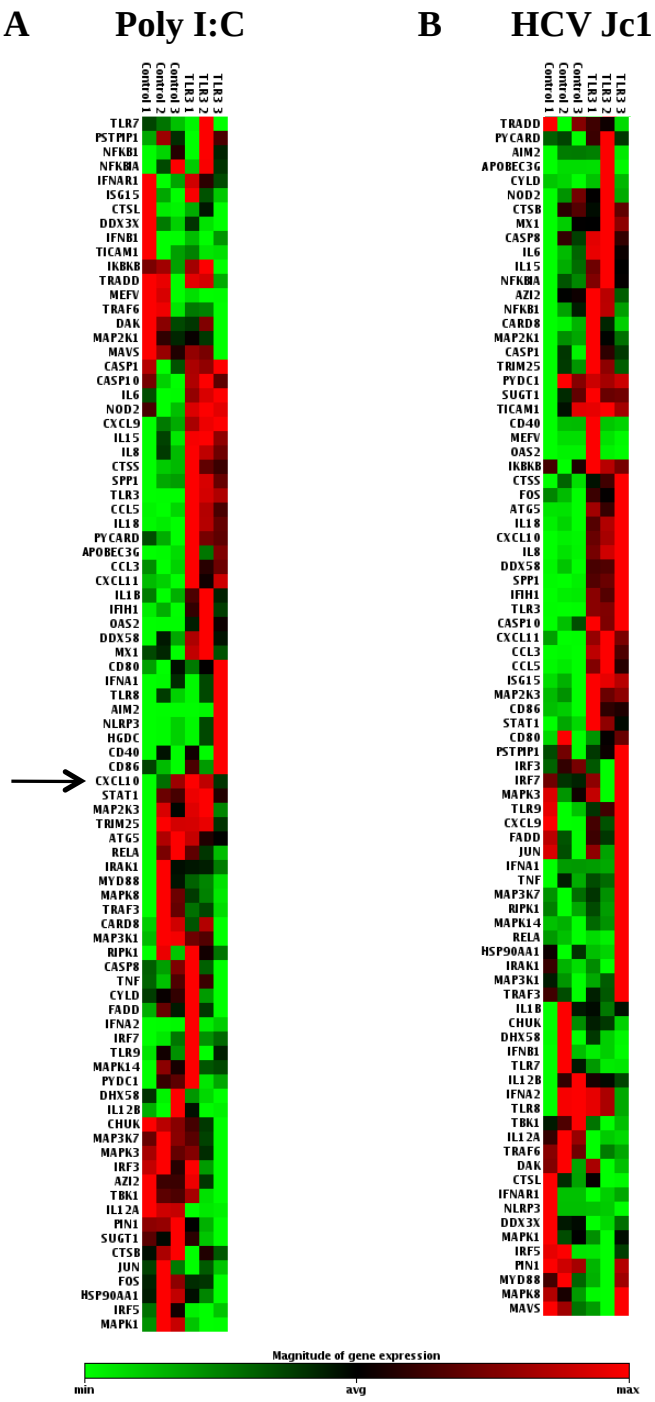

Figure 4.7 Human Antiviral Response PCR Array. Huh-7+ΔTIR and Huh-7+TLR3 cells were **(A)** stimulated with Poly I:C for 24 hours or **(B)** infected with HCV Jc1 for 72 hours. The heatmaps show somewhat different patterns of differential gene regulation when the response to Poly I:C is compared to the response to HCV infection. In both groups many of the upregulated genes are cytokines and chemokines.

TLR3-1 and TLR3-2 but not TLR3-3, and as such does not register in statistical analysis. However, there are genes where there is significant differential expression between control cells and TLR3-postive cells. The pattern of genes differentially regulated is different between Poly I:C and HCV infection, but chemokines and cytokines feature highly in both groups, such as CCL3, CCL5, CXCL9, IL-6, IL-8 (CXCL8) and IL-18. These results confirm the qRT-PCR and ELISA results above. Upregulation of TLR3 by both Poly I:C and HCV infection is noted. Poly I:C has been previously shown to upregulate TLR3 expression (Tissari *et al.* 2005; Wang *et al.* 2013). Variable expression of TLR3 in hepatocytes in the setting of HCV infection has been reported, both in patients chronically infected with HCV and *in vitro* (Sato *et al.* 2007; Benias *et al.* 2012). TLR3 expression has been observed to increase with other types of viral infection, such as respiratory syncytial virus and simian immunodeficiency virus (Sanghavi and Reinhart 2005; Groskreutz *et al.* 2006). TLR3 upregulation observed in our work may relate to the acute rather than chronic HCV infection in this *in vitro* model; whether TLR3 downregulation occurs with longer periods of infection was not tested. As this is a commercial array and the sequence of the TLR3 PCR primers is unknown, another possible explanation for this observation could be that the primers are specific for the ΔTIR region of TLR3. Hence, TLR3 would not be detected in the control cells where the ΔTIR region has been deleted. It is not entirely clear why TLR3 is upregulated to a greater degree in response to HCV infection as compared to Poly I:C stimulation.

Table 4.3 Human Antiviral Response PCR Array

Gene		Fold change	
		Poly I:C	HCV Jc1
ATG5	ATG5 autophagy related 5 homolog (S. cerevisiae)	ns	1.73
CASP10	Caspase 10, apoptosis-related cysteine peptidase	ns	2.41
CCL3	Chemokine (C-C motif) ligand 3	4.66	205.24
CCL5	Chemokine (C-C motif) ligand 5	60.09	41.19
CD86	CD86 molecule	ns	2.43
CTSS	Cathepsin S	2.16	1.48
CXCL10	Chemokine (C-X-C motif) ligand 10	ns	4.16
CXCL11	Chemokine (C-X-C motif) ligand 11	18.55	19.42
CXCL9	Chemokine (C-X-C motif) ligand 9	15.84	ns
DDX58	DEAD (Asp-Glu-Ala-Asp) box polypeptide 58	ns	2.312
FOS	FBJ murine osteosarcoma viral oncogene homolog	ns	1.506
IFIH1	Interferon induced with helicase C domain 1	1.63	2.00
IL12A	Interleukin 12A (natural killer cell stimulatory factor 1, cytotoxic lymphocyte maturation factor 1, p35)	0.39	0.59
IL15	Interleukin 15	1.34	2.34
IL18	Interleukin 18 (interferon-gamma-inducing factor)	2.69	2.09
IL1B	Interleukin 1, beta	1.82	ns
IL6	Interleukin 6 (interferon, beta 2)	2.70	4.24
IL8	Interleukin 8	1.94	3.35
ISG15	ISG15 ubiquitin-like modifier	ns	2.01
MAP2K3	Mitogen-activated protein kinase kinase 3	ns	2.21
NFKBIA	Nuclear factor of kappa light polypeptide gene enhancer in B-cells inhibitor, alpha	ns	1.78
NOD2	Nucleotide-binding oligomerization domain containing 2	2.49	ns
OAS2	2'-5'-oligoadenylate synthetase 2, 69/71kDa	23.39	ns
PIN1	Peptidylprolyl cis/trans isomerase, NIMA-interacting 1	0.66	ns
PYCARD	PYD and CARD domain containing	1.74	ns
SPP1	Secreted phosphoprotein 1	2.10	2.69
STAT1	Signal transducer and activator of transcription 1, 91kDa	ns	1.94
TLR3	Toll-like receptor 3	647.22	1876.72

ns not significant

4.5.2 Microarray

Our previous qRT-PCR analysis was limited to the 84 genes 'cherry-picked' as antiviral response genes that constituted the QIAGEN Human Antiviral Response RT^2 Profiler PCR Array. To extend our analysis further we interrogated the transcriptome of Huh-7+TLR3 or Huh-7+ΔTIR cells stimulated with Poly I:C and HCV Jc1, using Affymetrix GeneChip analyses. To our knowledge, the

transcriptome of stimulated TLR3-expressing Huh-7 cells has not been previously studied, and adds to what is currently known about TLR3 responses, particularly considering that TLR3 responses to stimulation vary across cell types (Lundberg *et al.* 2007). RNA quality and concentration were determined prior to microarray by bioanalyser. PCA plots are shown in Appendix V. Further analysis was performed using Genesifter software. Hundreds of differentially expressed genes (574 greater than two-fold change) were noted in TLR3-expressing cells compared to Huh-7+ΔTIR stimulated with Poly I:C (Appendix VII). A heat-map displaying genes with fold-changes greater than five (37 genes) in response to Poly I:C is shown in Figure 4.8. Fold changes in response to HCV infection were not as marked as those seen in response to Poly I:C and the pattern of gene expression was somewhat different, consistent with the qRT-PCR results previously described (Figure 4.9). Seventy-four genes were greater than two-fold differentially expressed in TLR3-expressing cells infected with HCV Jc1, when compared to HCV Jc1-infected Huh-7+ΔTIR cells (Appendix VIII). Common to both analyses (Table 4.4) were a number of cytokines and chemokines, including CCL5, CXCL10, IL-8 (CXCL8), and CXCL6 (GCP2), as well as interferon stimulated genes such as IFI44 and the IFIT proteins. The response to Poly I:C was broader, with genes such as IFI6, CXCL11, IL-6, IL-1B, IL-18, OAS1, SPP1 and the IFITM proteins amongst the upregulated genes. Members of the Jak-STAT pathway such as STAT1, SOCS3 and IRF9 were also differentially expressed.

Gene Identifier	Gene Name	Fold Change	adj. *p* value
NM_004139	Lipopolysaccharide binding protein	36.2	0.000021
NM_002985	Chemokine (C-C motif) ligand 5	32.93	0.000083
NM_138938	Regenerating islet-derived 3 alpha	25.01	0.000311
NM_002038	Interferon, alpha-inducible protein 6	24.35	0.000038
NM_017631	DEAD (Asp-Glu-Ala-Asp) box polypeptide 60	19.75	0.000002
NM_030754	Serum amyloid A2	17.1	0.000101
NM_005143	Haptoglobin	15.67	0.000041
NM_001910	Cathepsin E	13.87	0.000041
NM_007231	Solute carrier family 6 (amino acid transporter), member 14	11.68	0.000021
NM_006398	Ubiquitin D	10.89	0.000086
NM_006398	Ubiquitin D	10.82	0.000086
NM_004585	Retinoic acid receptor responder (tazarotene induced) 3	9.54	0.000043
NM_002423	Matrix metallopeptidase 7 (matrilysin, uterine)	9.48	0.000077
NM_000610	CD44 molecule (Indian blood group)	9.44	0.000076
NM_001565	Chemokine (C-X-C motif) ligand 10	8.54	0.000083
NM_002543	Oxidized low density lipoprotein (lectin-like) receptor 1	7.97	0.000522
NM_001085	Serpin peptidase inhibitor, clade A (alpha-1 antiproteinase, antitrypsin), member 3	7.53	0.000021
NM_006417	Interferon-induced protein 44	7.28	0.000156
NM_002960	S100 calcium binding protein A3	7.28	0.000402
NM_020995	Haptoglobin-related protein	7.24	0.000086
NM_002462	Myxovirus (influenza virus) resistance 1, interferon-inducible protein p78 (mouse)	7.24	0.000014
NM_018284	Guanylate binding protein 1, interferon-inducible, 67kDa	7.09	0.000064
NM_002994	Chemokine (C-X-C motif) ligand 5	6.82	0.000014
NM_078625	Vanin 3	6.7	0.000214
NM_004079	Cathepsin S	6.63	0.000181
NM_001486	Glucokinase (hexokinase 4) regulator	6.44	0.000467
NM_001548	Interferon-induced protein with tetratricopeptide repeats 1	6.08	0.000190
NM_005564	Lipocalin 2	6.06	0.000059
NM_014391	Ankyrin repeat domain 1 (cardiac muscle)	5.95	0.000101
NM_001785	Cytidine deaminase	5.85	0.000062
NM_001710	Complement factor B	5.8	0.000043
NM_001710	Complement factor B	5.7	0.000043
NM_001165	Baculoviral IAP repeat-containing 3	5.67	0.000113
NM_001733	Complement component 1, r subcomponent	5.58	0.000021
NM_005195	CCAAT/enhancer binding protein (C/EBP), delta	5.17	0.000055
NM_001710	Complement factor B	5.06	0.000126
NM_006061	Cysteine-rich secretory protein 3	-6.69	0.000260

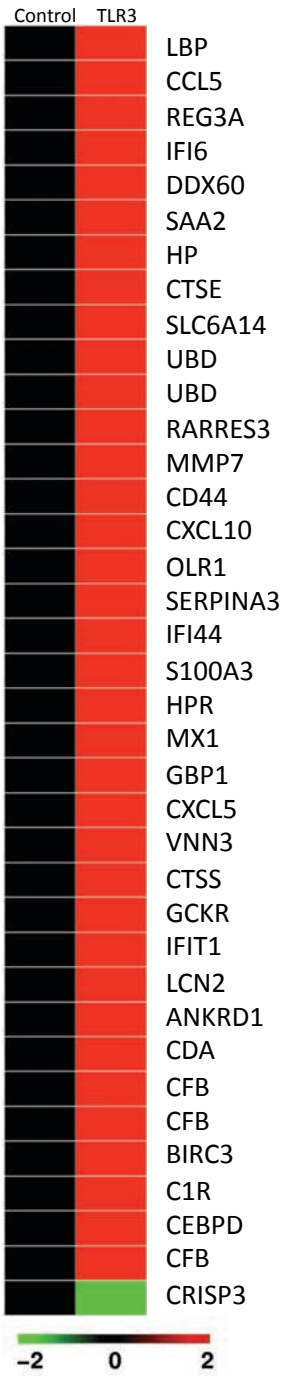

Figure 4.8 Microarray analysis reveals multiple differentially expressed genes in TLR3-expressing Huh-7 cells in response to stimulation with dsRNA.
Huh-7+TLR3 cells were stimulated with Poly I:C 50μg/ml for 24 hours. The heat map shows up- and down- regulated genes in Huh-7+TLR3 cells in comparison to Huh-7+ΔTIR stimulated in parallel. Fold changes > 5, range -6.69 to 36.19, $p < 0.05$.

Gene Identifier	Gene Name	Fold Change	adj. *p* value
NM_004139	Lipopolysaccharide binding protein	10.87	0.000088
NM_017631	DEAD (Asp-Glu-Ala-Asp) box polypeptide 60	7.76	0.000170
NM_001565	Chemokine (C-X-C motif) ligand 10	5.6	0.000081
NM_021187	Cytochrome P450, family 4, subfamily F, polypeptide 11	4.29	0.000283
NM_001785	Cytidine deaminase	3.97	0.001100
NM_000583	Group-specific component (vitamin D binding protein)	3.4	0.007420
NM_001031683	Interferon-induced protein with tetratricopeptide repeats 3	3.38	0.000283
NM_001001435	Chemokine (C-C motif) ligand 4-like 1	3.34	0.001870
NM_030787	Complement factor H-related 5	2.97	0.001560
NM_005143	Haptoglobin	2.97	0.001150
NM_005807	Proteoglycan 4	2.96	0.000470
ENST00000377050	ubiquitin D	2.94	0.002030
NM_001548	Interferon-induced protein with tetratricopeptide repeats 1	2.84	0.000403
ENST00000477922	maltase-glucoamylase-like pseudogene	2.83	0.001800
NM_020119	Zinc finger CCCH-type, antiviral 1	2.78	0.000258
ENST00000477922	maltase-glucoamylase-like pseudogene	2.77	0.000694
NM_002993	Chemokine (C-X-C motif) ligand 6 (granulocyte chemotactic protein 2)	2.73	0.001320
NM_006512	Serum amyloid A4, constitutive	2.73	0.008010
NM_002984	Chemokine (C-C motif) ligand 4	2.66	0.002010
NM_003733	2-5-oligoadenylate synthetase-like	2.65	0.000694
ENST00000477922	maltase-glucoamylase-like pseudogene	2.64	0.003740
ENST00000477922	maltase-glucoamylase-like pseudogene	2.57	0.001850
NM_001142883	Inositol hexakisphosphate kinase 3	2.55	0.001420
ENST00000477922	maltase-glucoamylase-like pseudogene	2.52	0.051400
ENST00000477922	maltase-glucoamylase-like pseudogene	2.5	0.001600
NM_001547	Interferon-induced protein with tetratricopeptide repeats 2	2.49	0.003080
NM_000584	Interleukin 8	2.49	0.000564
NM_001165	Baculoviral IAP repeat-containing 3	2.48	0.001250
NM_001775	CD38 molecule	2.43	0.000470
NM_021006	Chemokine (C-C motif) ligand 3-like 1	2.43	0.001100
ENST00000477922	maltase-glucoamylase-like pseudogene	2.43	0.000610
NM_006417	Interferon-induced protein 44	2.37	0.010300
NM_177551	Niacin receptor 1	2.32	0.008120
NM_001086	Arylacetamide deacetylase (esterase)	2.31	0.003790
NM_002985	Chemokine (C-C motif) ligand 5	2.31	0.005600
NM_001910	Cathepsin E	2.31	0.000502
ENST00000477922	maltase-glucoamylase-like pseudogene	2.3	0.000470
NR_033807	cytochrome P450, family 3, subfamily A, polypeptide 5	2.3	0.002320
NM_000610	CD44 molecule (Indian blood group)	2.28	0.000283
NM_000715	Complement component 4 binding protein, alpha	2.23	0.000170
NM_004668	Maltase-glucoamylase (alpha-glucosidase)	2.21	0.002240
NM_201442	Complement component 1, s subcomponent	2.19	0.000670
NM_130786	Alpha-1-B glycoprotein	2.18	0.001620
NM_005651	Tryptophan 2,3-dioxygenase	2.17	0.004910
NM_021258	Interleukin 22 receptor, alpha 1	2.15	0.000694
NM_000602	Serpin peptidase inhibitor, clade E (nexin, plasminogen activator inhibitor type 1), member 1	2.13	0.001250
NM_005711	EGF-like repeats and discoidin I-like domains 3	2.12	0.000383

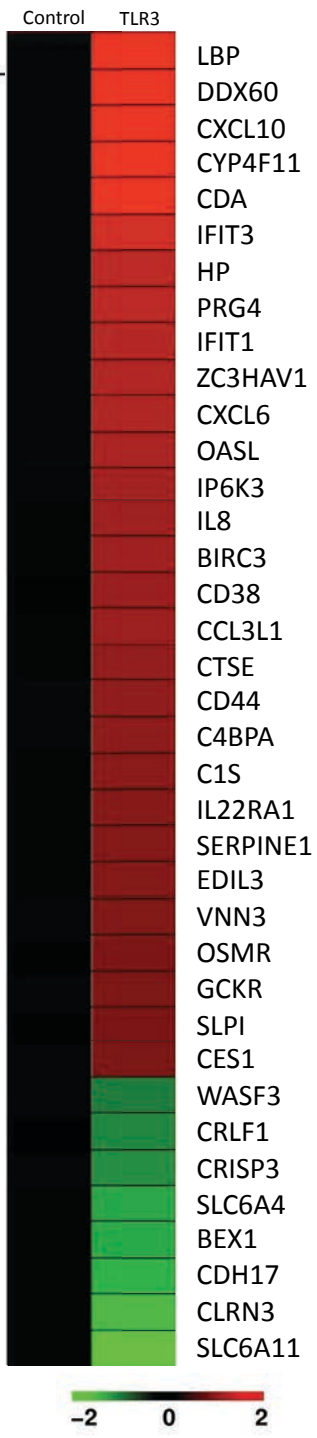

Figure 4.9 Microarray analysis reveals multiple differentially expressed genes in TLR3-expressing Huh-7 cells in response to infection with HCV Jc1.
Huh-7+TLR3 cells were infected with HCV Jc1 for 72 hours. The heat map shows up- and down- regulated genes in Huh-7+TLR3 cells in comparison to Huh-7+ΔTIR infected in parallel. Fold changes > 2, range -4.69 to 10.87, $p < 0.05$.

Table 4.4 Selected differentially expressed genes – Affymetrix Microarray

Gene	Fold change	
	Poly I:C	HCV Jc1
Claudin-6	-2.06	
Chemokine (C-C motif) ligand 4 (CCL4)		2.66
Chemokine (C-C motif) ligand 5 (CCL5)	32.93	2.3
Chemokine (C-C motif) ligand 20 (CCL20)	2.34	
Chemokine (C-X-C motif) ligand 1 (CXCL1)	4.57	
Chemokine (C-X-C motif) ligand 2 (CXCL2)	3.74	
Chemokine (C-X-C motif) ligand 5 (CXCL5)	6.82	
Chemokine (C-X-C motif) ligand 6 (CXCL6, GCP2)	4.71	2.73
Chemokine (C-X-C motif) ligand 10 (CXCL10)	8.54	5.6
Chemokine (C-X-C motif) ligand 11 (CXCL11)	4.19	
DEAD (Asp-Glu-Ala-Asp) box polypeptide 58 (DDX58, RIG-I)	2.35	
DEAD (Asp-Glu-Ala-Asp) box polypeptide 60 (DDX60)	19.75	7.76
Guanylate binding protein 2, interferon inducible	2.61	
Interferon alpha-inducible protein 6 (IFI6)	24.35	
Interferon gamma receptor 1	2.75	
Interferon induced with helicase C domain 1 (IFIH1, MDA5)	3.91	
Interferon induced protein 44 (IFI44)	7.28	2.37
Interferon-induced protein with tetratricopeptide repeats 1 (IFIT1)	6.08	2.84
Interferon-induced protein with tetratricopeptide repeats 2 (IFIT2)		2.49
Interferon-induced protein with tetratricopeptide repeats 3 (IFIT3)	3.46	3.38
Interferon induced transmembrane protein 1 (IFITM1)	4.61	
Interferon induced transmembrane protein 2 (IFITM2)	2.15	
Interferon induced transmembrane protein 3 (IFITM3)	2.03	
Interleukin 18 (interferon-gamma-inducing factor) (IL18)	4.92	
Interleukin 1, beta (IL1B)	2.41	
Interleukin 2 receptor, gamma	2.26	
Interleukin 32 (IL32)	3.03	
Interleukin 6 (interferon, beta 2, IL6)	2.92	
Interleukin 8 (IL8)	4.8	2.49
Interferon regulatory factor 1 (IRF1)	2.22	
Interferon regulatory factor 9 (IRF9)	4.95	
2'-5'-oligoadenylate synthetase 1 (OAS1)	4.22	
2'-5'-oligoadenylate synthetase 3 (OAS3)	2.79	
Secreted phosphoprotein 1 (SPP1)	2.08	
Suppressor of cytokine signalling 3 (SOCS3)	3.0	
Signal transducer and activator of transcription (STAT1)	2.44	
Tumor necrosis factor, alpha-induced protein 2 (TNFAIP2)	2.3	
Tumor necrosis factor, alpha-induced protein 3 (TNFAIP3)	3.31	
Tumor necrosis factor receptor superfamily, member 9	3.48	

Of interest, the DEAD box RNA helicase DDX60 featured highly in both lists (fold-changes were 19.75 and 7.76 in response to Poly I:C and HCV respectively). There is a limited amount of literature regarding DDX60 and it has only relatively recently been shown to have antiviral activity, including against HCV (Miyashita *et*

al. 2011; Schoggins *et al.* 2011). We are not aware of any previously published data indicating that DDX60 is a TLR3 response gene.

Claudin-6 was downregulated by Poly I:C in Huh-7+TLR3 cells. It has been suggested that this tight junction protein may mediate HCV cell entry in cell lines (Zheng *et al.* 2007; Meertens *et al.* 2008), however claudin-6 monoclonal antibodies do not prevent HCV infection of primary human hepatocytes and claudin-6 expression in hepatocytes *in vivo* is low (Fofana *et al.* 2013).

Given this antiviral pattern of gene expression in response to TLR3 stimulation, it is not surprising that these cells are not particularly permissive to HCV infection, as we and others have observed (Wang *et al.* 2009).

4.6 Discussion

After HCV infection of the hepatocyte, pattern recognition receptors (PRRs) sense pathogen-associated molecular patterns (PAMPs) within the virus, initiating the innate immune response and resulting in the production of pro-inflammatory and anti-viral factors such as interferons and cytokines, the ultimate aim being eradication of the virus. HCV is specifically sensed by the independent PRRs RIG-I and TLR3, triggering the innate immune response against the virus.

The hepatoma-derived cell line Huh-7 commonly used in *in vitro* studies of HCV is relatively unresponsive to HCV infection at the innate immune response level due to these cells being TLR3-deficient (Sumpter *et al.* 2005; Preiss *et al.* 2008), which probably explains in part the permissiveness of these cells to HCV infection.

Interestingly, the Huh-7.5 cell line, which is highly permissive to HCV infection is also defective in RIG-I signalling, indicating that innate recognition of HCV RNA is important in control of viral replication. In contrast, in the liver hepatocytes express functional TLR3 and RIG-I. Thus, reconstitution of TLR3 into Huh-7 cells is a valid strategy to study the *in vivo* physiological response to viral infection. TLR3 recognises dsRNA and sensing of the HCV PAMP, dsRNA intermediates, by TLR3 initiates downstream pathways. Unlike the HCV PAMP for RIG-I, which derives from the 3'NTR, HCV dsRNA that can be recognised by TLR3 does not appear to derive from a specific part of the genome and it is the dsRNA structure that is imperative. The minimum length of HCV dsRNA that activates TLR3 signalling pathways is 80-100bp (Li *et al.* 2012). Once TLR3 senses the PAMP, it initiates the activation of IRF-3, IRF-7 and NF-κB via Toll-interleukin-1 receptor domain-containing adaptor inducing IFN-β (TRIF) (Gale and Foy 2005; Dustin and Rice 2007; Wang *et al.* 2009). Subsequent phosphorylation, dimerisation and translocation of IRF-3 to the nucleus leads to interaction with the IFN-β promoter and results in IFN-β production. IFN-β, in an autocrine and paracrine manner, binds with IFN α/β receptors and activates the Jak-STAT pathway (Figure 1.9). This leads to the up-regulation of hundreds of interferon stimulated genes (ISGs); these genes encode products with various functions, including chemokines, cell surface receptors and transcription factors (Gale and Foy 2005; Dustin and Rice 2007; Joyce and Tyrrell 2010). An antiviral state results from ISG expression, although the exact factors that contribute to this state are not well understood.

It has been previously shown that reconstitution of TLR3 in Huh-7.5 cells restores the ability of these cells to sense dsRNA and initiate the antiviral response to HCV infection (Wang *et al.* 2009). Additionally, HCV infection in TLR3-postive Huh-7.5 cells stimulates a cytokine response that occurs via NF-κB, independently of the induction of interferons (Li *et al.* 2012). In this chapter, a Huh-7 cell line was generated that stably expresses TLR3. The rationale for developing this cell line was to generate a cell line responsive to HCV infection, with a view to using this in our bystander cell model system. We reasoned that an HCV-responsive cell line would have a greater effect on bystander cells in the model through the production of soluble mediators. We demonstrated that stable expression of TLR3 in Huh-7 cells restored the ability of these cells to respond to synthetic dsRNA (Poly I:C) and HCV infection using HCV Jc1. Stimulation of Huh-7 cells expressing functional TLR3 with Poly I:C and infection with HCV induced expression of chemokines/cytokines such as CCL5, CCL4 and CXCL10, as shown by qRT-PCR. This supports the findings of Li and colleagues where the authors demonstrated similar results by Bio-Plex Cytokine Assay and qPCR in TLR3-positive Huh-7.5 cells (Li *et al.* 2012). Also consistent with the observations of Li and colleagues, we were able to demonstrate expression of IL-6, CXCL10 and CCL5 in response to both Poly I:C and HCV infection by ELISA. Although a number of the cytokines represented in the ELISA are known to be TLR3 response genes (TNFα, IL-1B, IL-12, IL-17A, CCL2, CXCL9, CCL17, in addition to those above), not all were differentially expressed in this experiment. This may in part be related to the cell type, as it is known that various cell types respond differently to TLR3 stimulation (Lundberg *et al.* 2007). Li and colleagues were also able to demonstrate

upregulation of TNFα, and low-level upregulation of IL-1B and IL-17A in Huh-7.5 cells infected with HCV JFH-1 (Li *et al.* 2012), however none of these factors were differentially expressed in our work. A number of factors, such as the variation in cell type, virus, and assay sensitivity may be responsible for this discrepancy.

To our knowledge, there are no published data examining the TLR3-dependent transcriptome in Huh-7 cells. Therefore, to determine a global picture of the TLR3-related cellular transcriptome response to dsRNA and HCV infection, PCR array and microarray analyses were performed. On a PCR array panel of 84 genes involved in the innate immune response, 17 genes demonstrated statistically significant differential expression (fold changes > 1.5) in TLR3-expressing cells stimulated by Poly I:C compared to control (Table 4.3). Of those genes upregulated, a number are noted to be cytokines or chemokines (CCL3, CCL5, CXCL9, CXCL11, IL-1B, IL-6, IL-8 (CXCL8), IL-18), ISGs (including IFIH1, OAS-2, SPP-1) or are involved in antigen presentation (CTSS). A similar but not identical pattern of differential gene expression was noted in TLR3-positive Huh-7 cells infected with HCV Jc1 for 72 hours (21 genes differentially expressed, fold changes > 1.5). Again, many of these genes were cytokines or chemokines (CCL3, CCL5, CXCL10, CXCL9, IL-6, IL-8 (CXCL8), IL-15, IL-18). Interestingly, TLR3 was upregulated in both groups. The somewhat different profile of upregulated genes observed when Poly I:C stimulation is compared to HCV infection has been previously observed and may relate to the different timing of cytokine induction by these two PAMPs (within 24 hours in the case of Poly I:C, versus several days after HCV infection), as well as implying specificity of the interaction with TLR3 (Wang

et al. 2009; Li *et al.* 2012; Horner and Gale 2013). The later time point at which HCV induces TLR3-mediated cytokine production is most likely related to the fact that TLR3 recognises HCV dsRNA replicative intermediates, which are present later in viral replication, rather than during viral entry or early replication (Li *et al.* 2012; Horner and Gale 2013).

Microarray analysis revealed over 500 genes (fold change > 2) differentially expressed in TLR3-positive Huh-7 cells stimulated with Poly I:C for 24 hours. Again, chemokines and interleukins featured highly, as well as RIG-I, ISGs and members of the Jak/STAT pathway. Similar results were observed in TLR3-positive Huh-7 cells infected with HCV Jc1 for 72 hours, however the fold changes were not as marked and there were less genes differentially expressed overall. This may relate to the ability of HCV to inhibit signalling downstream of TLR3 via NS3/4A cleavage of TRIF (Li *et al.* 2005). Chemokines such as CXCL10, CXCL6 and IL-8 (CXCL8) were common to both analyses. Also upregulated were interferon-induced genes such as the IFIT, IFITM and OAS proteins, known to be anti-viral (Itsui *et al.* 2006; Raychoudhuri *et al.* 2011; Wilkins *et al.* 2013). Of note, the DEAD box RNA helicase DDX60 featured highly in both lists. This protein has not been widely characterized in the literature, but has been shown to be an antiviral factor that positively promotes RIG-I binding to dsRNA and was shown to be antiviral against HCV in an over-expression screen (Miyashita *et al.* 2011; Schoggins *et al.* 2011). The overall TLR3-related response to Poly I:C and HCV observed in these studies appears to be antiviral and corresponds with the observation that these cells are not particularly permissive to HCV infection.

Taken together, these results suggest that reconstitution of functional TLR3 in Huh-7 cells enhances the cell responsiveness to dsRNA and HCV infection. TLR3 recognition of HCV infection stimulates a proinflammatory and antiviral response with multiple cytokines and ISGs upregulated in response to infection. It has been previously shown that levels of a number of these chemokines or their receptors (such as CXCL10, CCL2, CXCL9, CCL3 and IL-8 (CXCL8)) are upregulated in HCV-infected individuals and are associated with the degree of hepatic inflammation (Napoli *et al.* 1996; Harvey *et al.* 2003; Wald *et al.* 2007; Zeremski *et al.* 2007; Helbig *et al.* 2009). TLR3 hence plays a crucial role in the host response to HCV infection.

The TLR3-positive cell line generated in this chapter will allow further evaluation of the bystander effect, with enhanced cellular responses to HCV infection hypothesised to augment the effect on bystander cells in subsequent experiments.

Chapter 5
The bystander effects mediated by soluble factors

5.1 Introduction

As previously discussed in Chapter 3, it is proposed that HCV-infected hepatocytes exert an effect on 'bystander' cells in the HCV-infected liver. These cells may include uninfected hepatocytes, stellate cells, Kupffer cells and infiltrating immune cells. Given that only 2-20% of hepatocytes are infected with HCV, the effect exerted on these bystander cells is proposed to contribute to inflammatory injury expansion and hence progression of liver disease in HCV infection. As demonstrated in Chapter 3, a minimal effect on gene expression profiles was seen in uninfected Huh-7 cells when exposed to conditioned media from HCV-infected Huh-7 cells. It was suggested that this was due to the relative unresponsiveness of Huh-7 cells to HCV infection because of a lack of TLR3 expression. A TLR3-expressing Huh-7 cell line was subsequently generated and enhanced response to HCV infection of these cells was demonstrated in Chapter 4.

It was proposed that by using the TLR3-positive Huh-7 cell line generated in our model system, an enhanced bystander effect would be seen due to the re-establishment of sensing of HCV infection. In this chapter, a conditioned media system to observe the effect of soluble factors produced by infected cells on various bystander cell types, or vice versa, is described.

5.2 Conditioned media from HCV-infected cells does not affect the transcriptome of bystander hepatocytes

To examine the effect of HCV Jc1-infected Huh-7+TLR3 cells on uninfected Huh-7 CD81 knockdown cells, Huh-7+TLR3 cells were infected with HCV Jc1 (MOI 1.0-2.0) and returned to culture for 72 hours. The infection rate was confirmed by immunofluorescence to detect HCV antigen and we routinely achieved a hepatocyte infection rate of 30-50% (Figure 5.1). Conditioned media from these cells was harvested as previously described and was also harvested from uninfected Huh-7+TLR3 cells as a control after incubation for 72 hours. Huh-7 CD81 knockdown cells were cultured in conditioned media from both groups for 24-72 hours at which time total RNA was extracted. RNA quality and concentration were assessed by bioanalyser, and the transcriptome was analysed by microarray analysis using an Affymetrix GeneChip. Immunofluorescence in parallel cultures confirmed the absence of HCV infection at the time of harvesting (not shown).

Microarray analysis revealed no significant differential gene expression in Huh-7 CD81 knockdown cells exposed to conditioned media from HCV-infected, TLR3-positive cells when compared to media from TLR3-positive uninfected cells (not shown). This was despite adequate infection rates and appropriate response to HCV-infection in TLR3-positive Huh-7 cells as determined by qRT-PCR analysis of CCL5 mRNA expression in which we showed that HCV infection of Huh-7+TLR3 cells resulted in an increase of approximately 130-fold at the mRNA level (Figure 5.1).

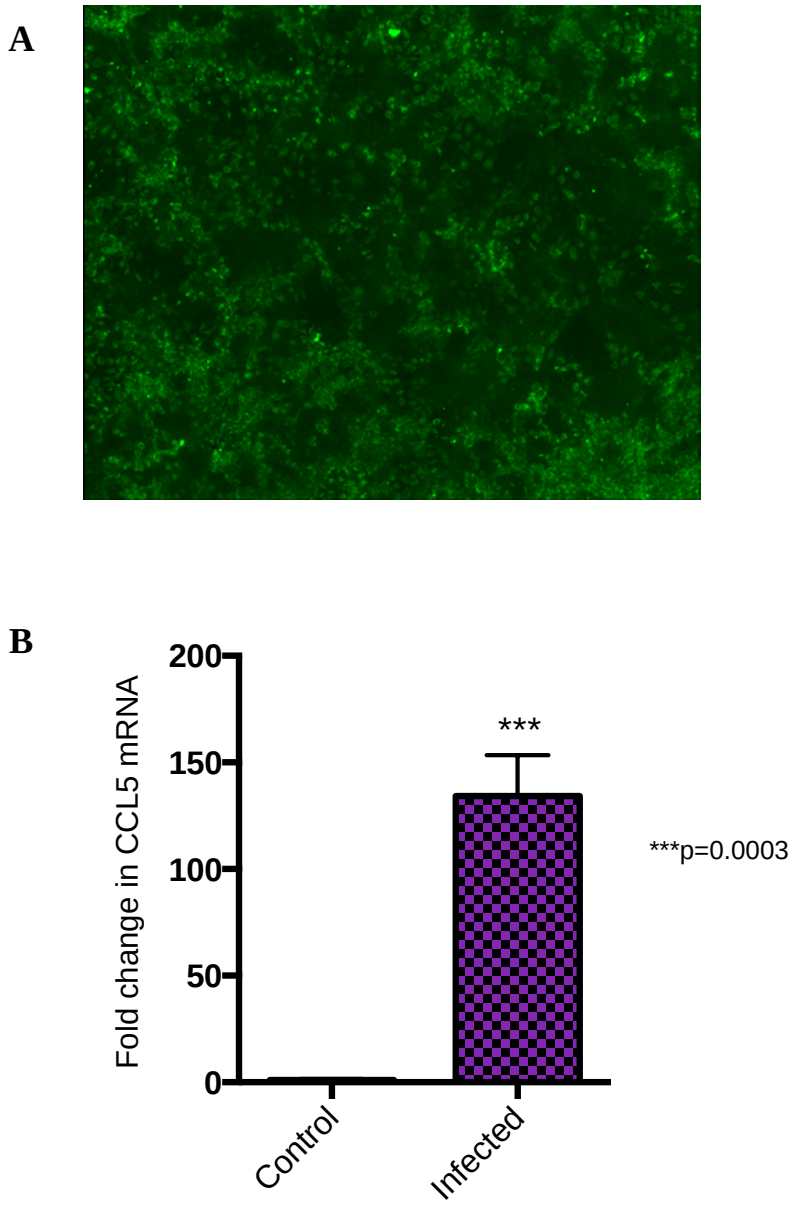

Figure 5.1 Characteristics of conditioned media used to stimulate Huh-7+CD81 knockdown cells or PH5CH8 cells. (A) HCV Jc1 infection in Huh7+TLR3 cells at 72 hours as shown by immunofluorescence **(B)** qRT-PCR shows CCL5 upregulation in HCV-infected Huh7+TLR3 cells from which conditioned media was harvested.

The hepatocyte cell line PH5CH8 (a simian virus 40 (SV40) large T antigen-immortalized non-neoplastic human hepatocyte cell line) was also cultured in conditioned media (as above) for 6-24 hours. This cell line is not permissive to HCV infection but expresses functional TLR3 and is more similar to the hepatocyte than the Huh-7 cell line (Li *et al.* 2005; Dansako *et al.* 2013) and was used in this instance to investigate the response of a non-neoplastic hepatocyte cell line. Consistent with the results observed in the Huh-7+CD81 knockdown cell line, no significant differential gene expression was observed despite the demonstration of a strong upregulation of CCL5 mRNA response to HCV infection (Figure 5.1).

Hence, even though the Huh-7+TLR3 cells respond to HCV infection by expressing a number of chemokines and cytokines, these do not seem to impact either Huh-7 or PH5CH8 cells at the level of the transcriptome. This result is surprising considering the chemokines and cytokines expressed in response to HCV infection and will be discussed further in the discussion section.

5.3 Conditioned media from HCV-infected cells decreases HCV-replication in sub-genomic replicon-harbouring Huh-7 cells

We were next interested to determine whether HCV-infected Huh-7+TLR3 cells could exert an antiviral effect. To test this, conditioned media (as generated above) was harvested and an HCV-replicon harbouring cell line (SGR-JFH1-RLuc, which encodes a Renilla luciferase reporter) was incubated in conditioned media for 48 hours. Interestingly, a small but reproducible reduction in luciferase activity was

observed in cells incubated in conditioned media from HCV-Jc1 infected TLR3-positive cells when compared to those incubated in media from uninfected cells (Figure 5.2). This indicated a reduction in HCV replication in the replicon cell line, suggesting an anti-viral effect of conditioned media from infected cells. This effect was at least in part mediated by TLR3 expression, as a significant reduction in HCV replication was observed when the effects of conditioned media from HCV Jc1-infected Huh-7+TLR3 cells were compared to those of conditioned media from HCV Jc1-infected control cells (Huh-7+ΔTIR, section 4.2) (Figure 5.3). As we had noted a more significant cellular response in TLR3-positive cells stimulated with Poly I:C, we repeated the experiment using conditioned media from Poly I:C stimulated cells. A similar effect to the HCV-infection experiments was observed when Huh-7+TLR3 cells were treated with Poly I:C for 24 hours, media was harvested and SGR-JFH1-RLuc cells were incubated in this media for 24 hours, as compared to either media from untreated Huh-7+TLR3 cells or media from Poly I:C treated Huh-7+ΔTIR cells (Figure 5.4).

These findings were subsequently confirmed in an infectious cell culture model by incubating HCV Jc1 infected Huh-7.5 cells in conditioned media from Poly I:C treated Huh-7+TLR3 cells. Briefly, Huh-7.5 cells were infected with HCV Jc1 and Huh-7+TLR3 cells were treated with Poly I:C. After 24 hours, media was harvested from Huh-7+TLR3 cells and the HCV-infected Huh-7.5 cells were incubated in this media for 72 hours. Media harvested from untreated Huh-7+TLR3 cells was used as a control. The level of HCV infection was determined by qRT-PCR, with a significant reduction in HCV RNA levels in cells exposed to media from Poly I:C-

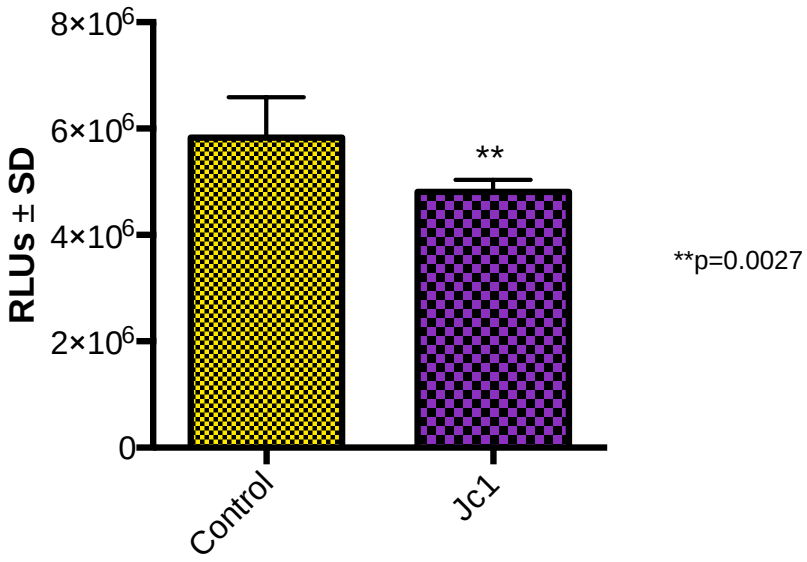

Figure 5.2 Conditioned media from HCV-infected Huh-7+TLR3 cells decreases viral replication in SGR-JFH1-RLuc cells. A statistically significant reduction in Renilla luciferase output was observed when cells harbouring a luciferase reporter HCV replicon were incubated in conditioned media from HCV Jc1-infected Huh-7+TLR3 cells for 48 hours, as compared to conditioned media from uninfected Huh-7+TLR3 cells (n=4, *p*=0.0027, Student's *t*-test).

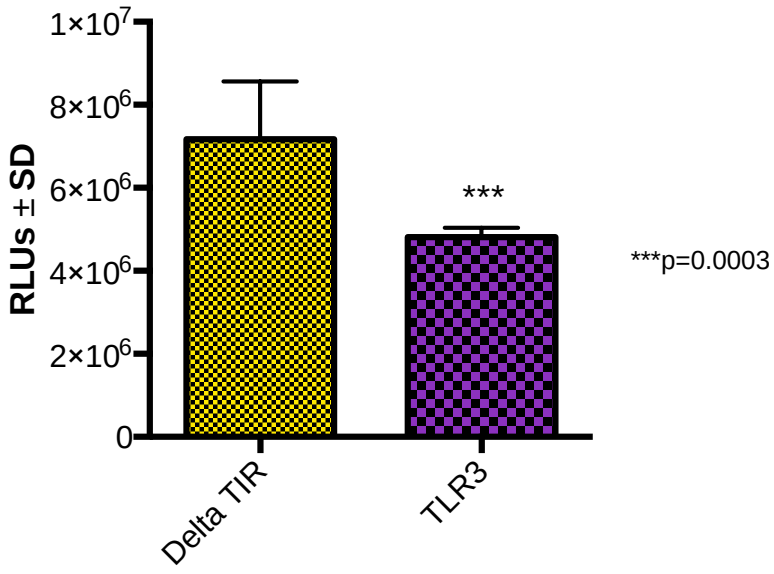

Figure 5.3 The decrease in viral replication in SGR-JFH1-RLuc cells in response to conditioned media from HCV-infected Huh-7+TLR3 cells is at least partially TLR3-dependent. A statistically significant reduction in Renilla luciferase output was observed when SGR-JFH1-RLuc cells were incubated in conditioned media from HCV Jc1-infected Huh-7+TLR3 cells for 48 hours, as compared to conditioned media from HCV Jc1-infected Huh-7+ΔTIR cells (n=4, p=0.0003, Student's t-test).

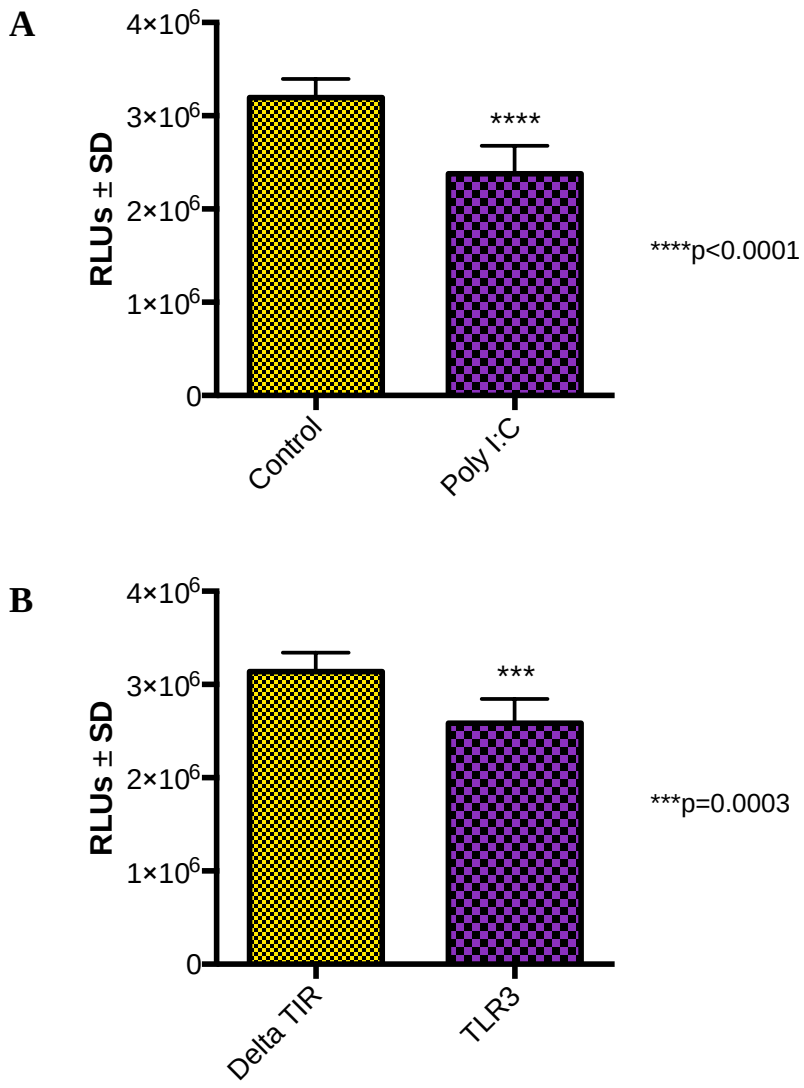

Figure 5.4 Conditioned media from dsRNA-treated Huh-7+TLR3 cells decreases viral replication in SGR-JFH1-RLuc cells. A statistically significant reduction in Renilla luciferase output was observed when cells harbouring a luciferase reporter-encoding HCV replicon were incubated in **(A)** conditioned media from Poly I:C-treated Huh-7+TLR3 cells compared to conditioned media from untreated Huh-7+TLR3 cells (n=4, $p<0.0001$, Student's *t*-test), or **(B)** conditioned media from Poly I:C-treated Huh-7+TLR3 cells compared to conditioned media from Poly I:C treated Huh-7+ΔTIR cells (n=4, $p=0.0003$, Student's *t*-test).

treated Huh-7+TLR3 cells, confirming the antiviral effect of this media previously observed using the luciferase system (Figure 5.5). Confirming these results by qRT-PCR implies the effect seen does not relate to the effect of conditioned media on target cell proliferation or viability. The greater effect seen by qRT-PCR compared to the luciferase experiments may relate to the longer incubation period in conditioned media or residual luciferase activity present after the reduction in replication has occurred.

5.3.1 Identification of antiviral mediators secreted from Huh-7+TLR3 cells

The obvious candidate mediating this antiviral effect is the production of Type I interferon, however we noted no significant increase in Type I interferon in HCV-infected or Poly I:C stimulated TLR3-positive cells, as seen in results presented in Chapter 4. Therefore, to identify the factor or factors in conditioned media from Poly I:C-stimulated TLR3 expressing Huh-7 cells, conditioned media was prepared as above and then fractionated using a 50 kDa centrifugal filter. This filter retains proteins greater than 50 kDa in size in the trap fraction whilst proteins of less than 50 kDa are collected in the flow-through. SGR-JFH1-RLuc cells were incubated in both flow-through and trap fractions for 48 hours and it was observed that HCV replication was significantly decreased in the cells treated with the trap fraction compared to the flow-through fraction. This indicated that the factor responsible for the antiviral effect was enriched in the trap fraction and hence larger than 50 kDa (Figure 5.6).

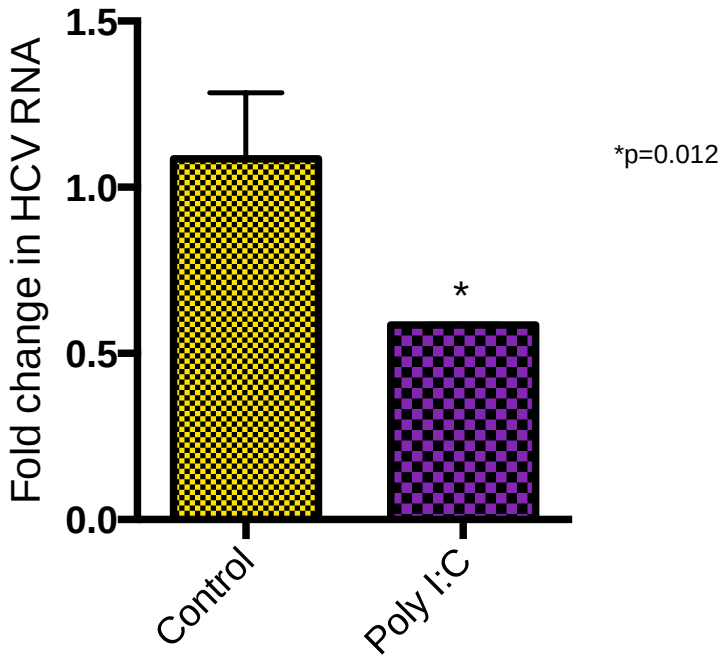

Figure 5.5 Conditioned media from dsRNA-treated Huh-7+TLR3 cells decreases viral replication in HCV Jc1-infected Huh-7.5 cells. A statistically significant reduction in HCV RNA, as determined by qRT-PCR, was observed when cells infected with HCV Jc1 were incubated in conditioned media from Poly I:C-treated Huh-7+TLR3 cells compared to conditioned media from untreated Huh-7+TLR3 cells (n=3, *p*=0.012, Student's *t*-test).

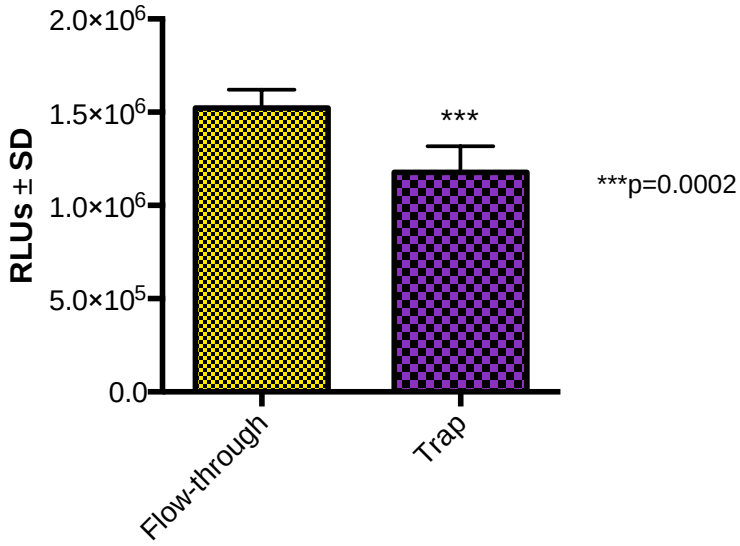

Figure 5.6 The factors responsible for the anti-viral effect of conditioned media from stimulated TLR3 expressing cells are greater than 50 kDa. Conditioned media from Poly I:C-treated Huh-7+TLR3 cells was fractionated using a 50 kDa centrifugal filter. A statistically significant reduction in Renilla luciferase output was observed when cells harbouring a luciferase reporter-encoding HCV replicon were incubated in the trap fraction compared to the flow-through fraction (n=4, *p*=0.0002, Student's *t*-test).

Given that we previously demonstrated that Huh-7+TLR3 cells stimulated with Poly I:C expressed a number of cytokines and chemokines, we had expected that the factor responsible for the antiviral effect would be smaller than 50 kDa as many cytokines and chemokines are smaller than 50 kDa. Therefore, based on the results of the fractionated conditioned media studies and precedents in the literature, we reasoned that exosomes containing antiviral factors may be responsible for the cross-talk between cells, accounting for the greater than 50 kDa size of the active factor. Exosomes are extracellular vesicles of 40-100nm in size which originate from cells and carry a number of the components of the parent cell, including RNA and proteins. They are known to play a role in cell signalling (reviewed in Robbins and Morelli 2014) and there is a precedent for exosomes transferring anti-viral activity in a hepatitis B virus infection model (Li *et al.* 2013). To test this hypothesis, we simultaneously treated Huh-7+TLR3 cells with Poly I:C and an exosome inhibitor, GW4869 (Sigma). The cells were washed prior to treatment to remove residual exosomes and the treatment was performed in serum-free conditions to eliminate the impact of serum-derived exosomes. After treatment for 16 hours with GW4869, conditioned media was harvested and filtered through a 0.45μm filter to remove cellular debris. To remove GW4869, which is toxic to cells after 24 hours, the media was fractionated using 50 kDa centrifugal filters. GW4869 is significantly smaller than 50 kDa and hence is removed by entering the flow-through fraction. Control media was also filtered in this way. SGR-JFH1-RLuc cells were incubated in media from the trap fraction (to which foetal bovine serum was added to 10% (v/v)) for 48 hours. It was observed that treatment with GW4869 abrogated the antiviral effect of the conditioned media, suggesting that exosomes

may indeed play a role (Figure 5.7). No significant difference in luciferase activity was noted in cells exposed to fractionated conditioned media from cells treated with GW4869 alone versus control media.

5.4 Conditioned media from HCV-infected cells increases expression of pro-fibrogenic markers in hepatic stellate cells

Our previous results revealing that the HCV-infected Huh-7 cell had little impact on bystander Huh-7 cells prompted us to investigate the effect on stellate cells. The stellate cell is the primary liver-derived cell that drives the fibrogenic process in the HCV-infected liver. Stellate cells are normally quiescent, but when activated produce extracellular matrix proteins such as collagen (Friedman 2008). In order to examine the effect of soluble factors from HCV Jc1-infected Huh-7+TLR3 cells on stellate cells, conditioned media was harvested as previously and frozen for subsequent use. Primary rat stellate cells were isolated by *in situ* pronase-collagenase perfusion as described in Chapter 2. Stellate cells two days post-isolation are considered to be quiescent, whereas cells cultured on plastic for seven days spontaneously activate (Rockey and Friedman 1992 and references therein). At two days or seven days post-isolation these cells were serum starved for 4 hours and then incubated in conditioned media from HCV Jc1-infected Huh-7+TLR3 cells or uninfected Huh-7+TLR3 cells for 24 hours. RNA was extracted and qRT-PCR performed to assess expression of pro-fibrogenic markers Collagen type-1 alpha-1 (COL1a1), Tissue inhibitor of metalloproteinase 1 (TIMP-1) and TGF-β, all of which are well described markers of stellate cell activation.

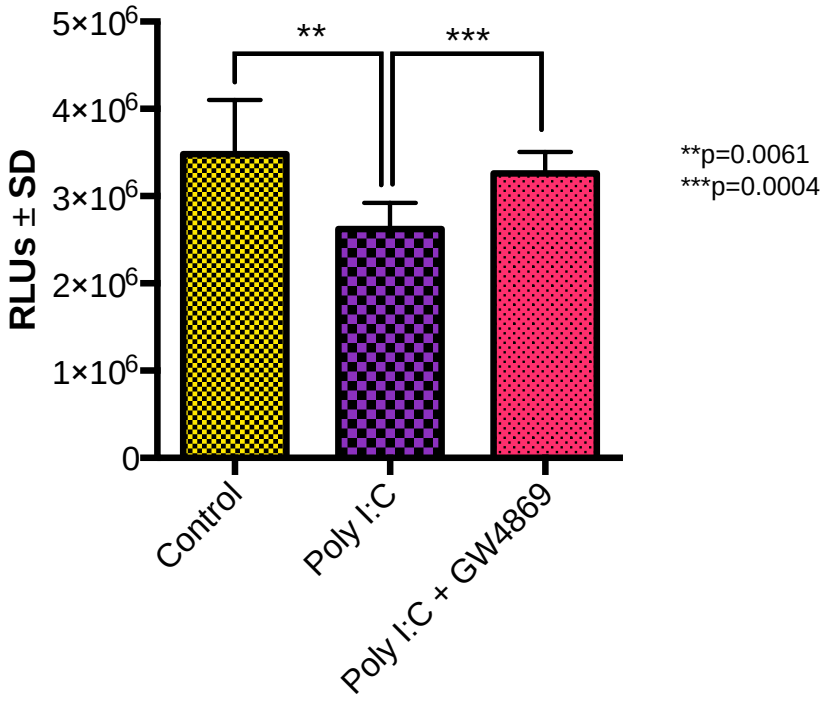

Figure 5.7 Exosomes mediate the anti-viral effect of conditioned media from stimulated TLR3 expressing cells. Huh-7+TLR3 cells were simultaneously treated with Poly I:C and the exosome inhibitor GW4869. Conditioned media was harvested from these cells and cells harbouring a luciferase reporter-encoding HCV replicon were incubated in this media for 48 hours. Comparison was made with media from Poly I:C-treated Huh-7+TLR3 cells (in the absence of GW4869) and control media from Huh-7+TLR3 cells without either Poly I:C or GW4869 treatment. A statistically significant reduction in Renilla luciferase output was observed when cells were incubated in media from Poly I:C-treated cells (n=4, *p*=0.0061, Student's *t*-test) but this effect was lost when GW4869 was added (n=4, *p*=0.0004, Student's *t*-test).

COL1a1 mRNA was significantly upregulated at day 2 post-isolation hepatic stellate cells incubated in conditioned media from infected Huh-7+TLR3 cells compared to stellate cells incubated in control media (Figure 5.8a). No significant difference was seen in day 7 post-isolation stellate cells (Figure 5.8b). In contrast, there was no significant difference in TIMP-1 expression in day 2 post-isolation stellate cells, however TIMP-1 was significantly upregulated in day 7 post-isolation hepatic stellate cells incubated in conditioned media from HCV-infected TLR3-positive Huh-7 cells (Figure 5.9). These results suggest that soluble factors or cell-free HCV in conditioned media from infected cells promote increased expression of pro-fibrogenic markers COL1a1 and TIMP-1 in primary rat hepatic stellate cells.

In contrast, TGF-β was significantly downregulated in day 2 post-isolation hepatic stellate cells exposed to conditioned media from HCV-infected Huh-7+TLR3 cells. No significant difference was seen in TGF-β expression in day 7 post-isolation stellate cells (Figure 5.10).

Collectively this work suggests that soluble factors from the HCV-infected hepatocytes can activate stellate cells, however more work is required to confirm this observation.

5.5 Conditioned media from bystander cells enhances chemokine expression in HCV-infected cells

It is also suggested that uninfected bystander cells such as hepatocytes, hepatic stellate cells and immune cells may exert an effect on HCV-infected cells that have

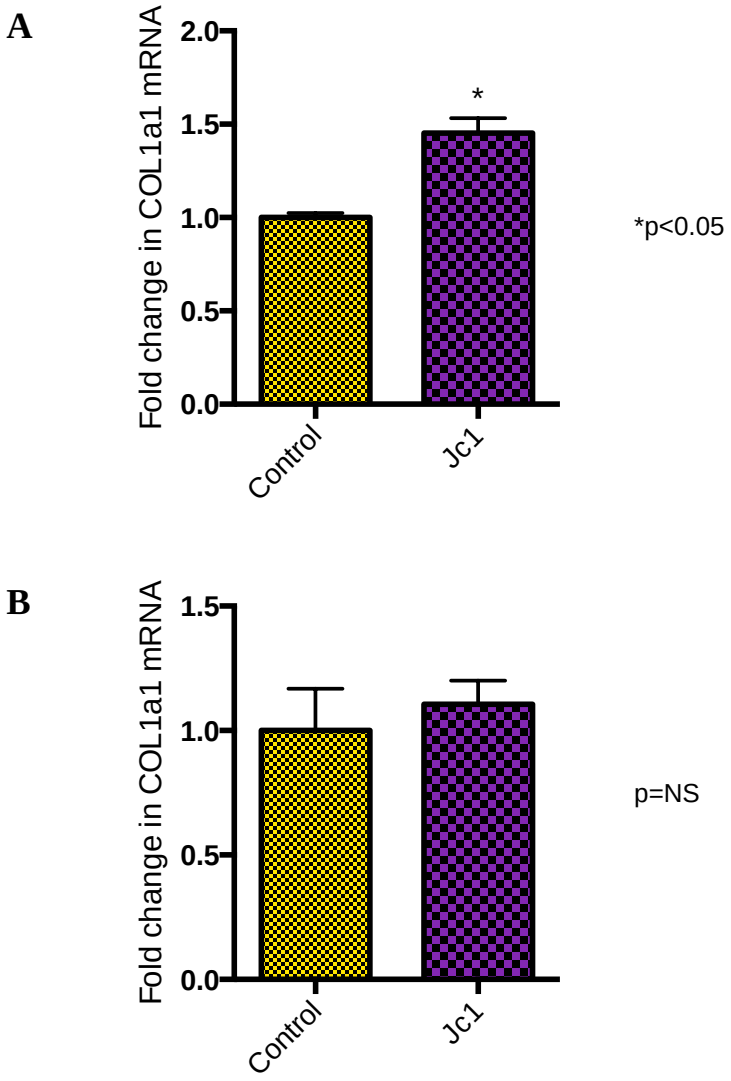

Figure 5.8 Conditioned media from HCV Jc1-infected Huh-7+TLR3 cells induces expression of the pro-fibrogenic marker COL1a1 in primary rat hepatic stellate cells. (A) Primary rat hepatic stellate cells at day 2 post-isolation were incubated in conditioned media from HCV Jc1-infected Huh-7+TLR3 cells for 24 hours. Significant upregulation of COL1a1 was observed by qRT-PCR in comparison to stellate cells incubated in conditioned media from uninfected Huh-7+TLR3 cells (n=2, $p<0.05$, Student's *t*-test). **(B)** Primary rat hepatic stellate cells at day 7 post-isolation were incubated in conditioned media from HCV Jc1-infected Huh-7+TLR3 cells for 24 hours. No significant difference in COL1a1 mRNA expression was observed in comparison to stellate cells incubated in conditioned media from uninfected Huh-7+TLR3 cells (n=2, p=NS, Student's *t*-test).

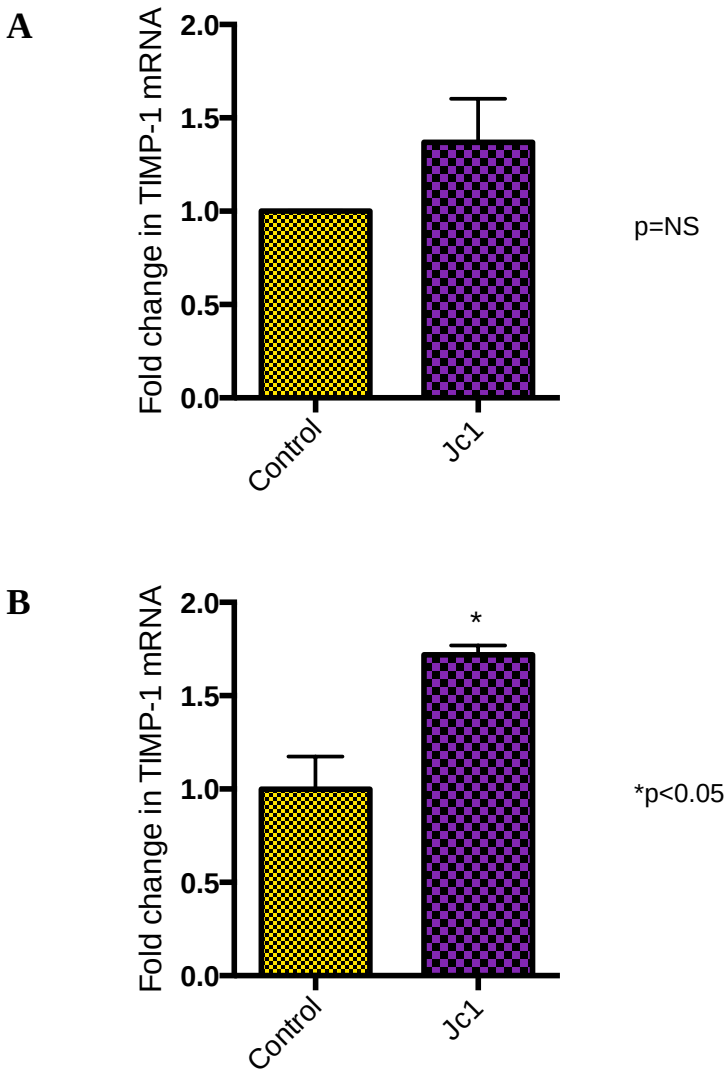

Figure 5.9 Conditioned media from HCV Jc1-infected Huh-7+TLR3 cells induces expression of the pro-fibrogenic marker TIMP-1 in primary rat hepatic stellate cells. (A) Primary rat hepatic stellate cells at day 2 post-isolation were incubated in conditioned media from HCV Jc1-infected Huh-7+TLR3 cells for 24 hours. No significant difference in TIMP-1 mRNA expression was observed by qRT-PCR in comparison to stellate cells incubated in conditioned media from uninfected Huh-7+TLR3 cells (n=2, *p*=NS, Student's *t*-test). **(B)** Primary rat hepatic stellate cells at day 7 post-isolation were incubated in conditioned media from HCV Jc1-infected Huh-7+TLR3 cells for 24 hours. Significant upregulation of TIMP-1 was observed by qRT-PCR in the Day 7 cells in comparison to stellate cells incubated in conditoned media from uninfected Huh-7+TLR3 cells (n=2, $p<0.05$, Student's *t*-test).

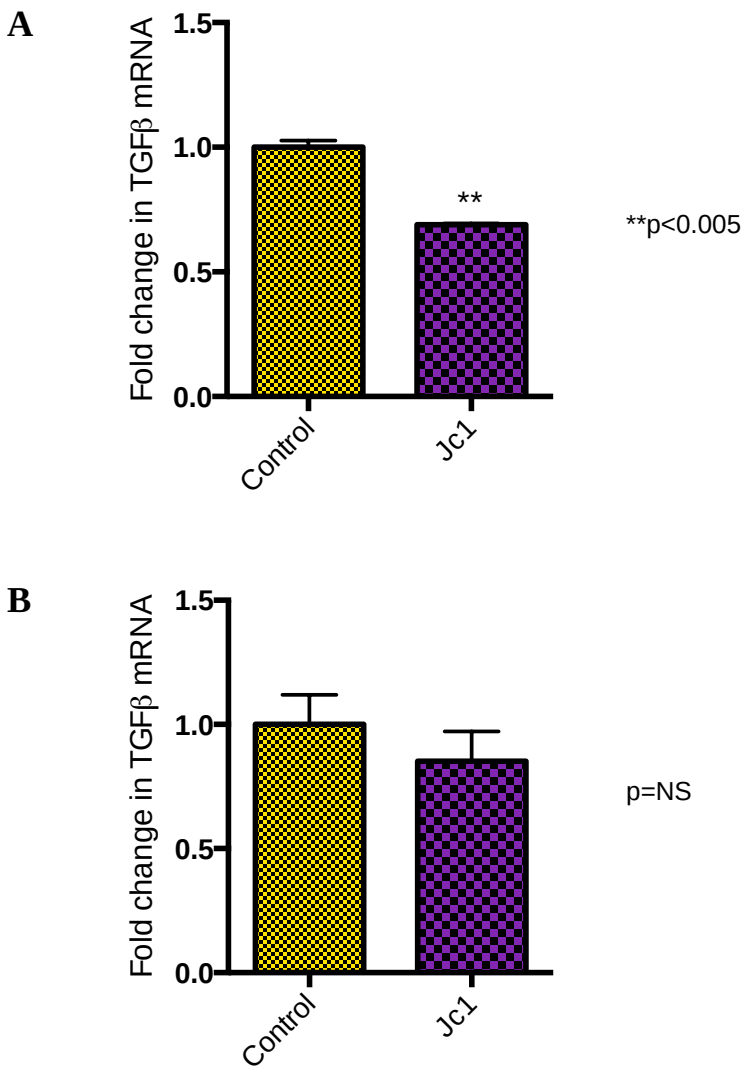

Figure 5.10 Conditioned media from HCV Jc1-infected Huh-7+TLR3 cells downregulates expression of the pro-fibrogenic marker TGF-β in primary rat hepatic stellate cells. (A) Primary rat hepatic stellate cells at day 2 post-isolation were incubated in conditioned media from HCV Jc1-infected Huh-7+TLR3 cells for 24 hours. Significant downregulation of TGF-β was observed by qRT-PCR in comparison to stellate cells incubated in conditioned media from uninfected Huh-7+TLR3 cells (n=2, $p<0.005$, Student's *t*-test). **(B)** Primary rat hepatic stellate cells at day 7 post-isolation were incubated in conditioned media from HCV Jc1-infected Huh-7+TLR3 cells for 24 hours. No significant difference in TGF-β mRNA expression was observed in comparison to stellate cells incubated in conditioned media from uninfected Huh-7+TLR3 cells (n=2, p=NS, Student's *t*-test).

been primed to respond to various stimuli due to their infected state. In addition to their significant role in the fibrogenic process, hepatic stellate cells also play a role in the inflammatory response, producing pro-inflammatory cytokines and chemokines and it has recently been shown that conditioned media from the stellate cell line LX2 is able to stimulate HCV JFH1-infected Huh-7.5 cells leading to significant expression of the chemokine MIP-1β (otherwise known as CCL4, but to avoid confusion will be referred to as MIP-1β in this section as per the original paper) (Nishitsuji *et al.* 2013). This suggests, as mentioned above, that the HCV-infected hepatocyte, while relatively unresponsive to the initial HCV infection, is primed to respond to additional stimuli.

To investigate whether this phenomenon occurs when conditioned media from other bystander cell types is used, Huh-7.5 cells were infected with HCV-Jc1 (MOI 0.25) for a period of 72 hours before being incubated with conditioned media from various uninfected bystander cell lines. Conditioned media was prepared as described by Nishitsuji and colleagues (Nishitsuji *et al.* 2013). Briefly, bystander cell lines (Huh-7.5, Huh-7, LX2, Huh-7+TLR3, Huh-7+ΔTIR) were seeded at $1x10^6$ in 100mm dishes in 10ml of complete medium without selection antibiotics for 3 days. Conditioned media was then harvested, filtered through a 0.45μm filter and immediately placed on the pre-HCV-infected Huh-7.5 cells described above. After returning these cells to culture for 24 hours, RNA was harvested for qRT-PCR. Immunofluorescence in parallel cultures confirmed adequate infection rates in Huh-7.5 cells (Figure 5.11).

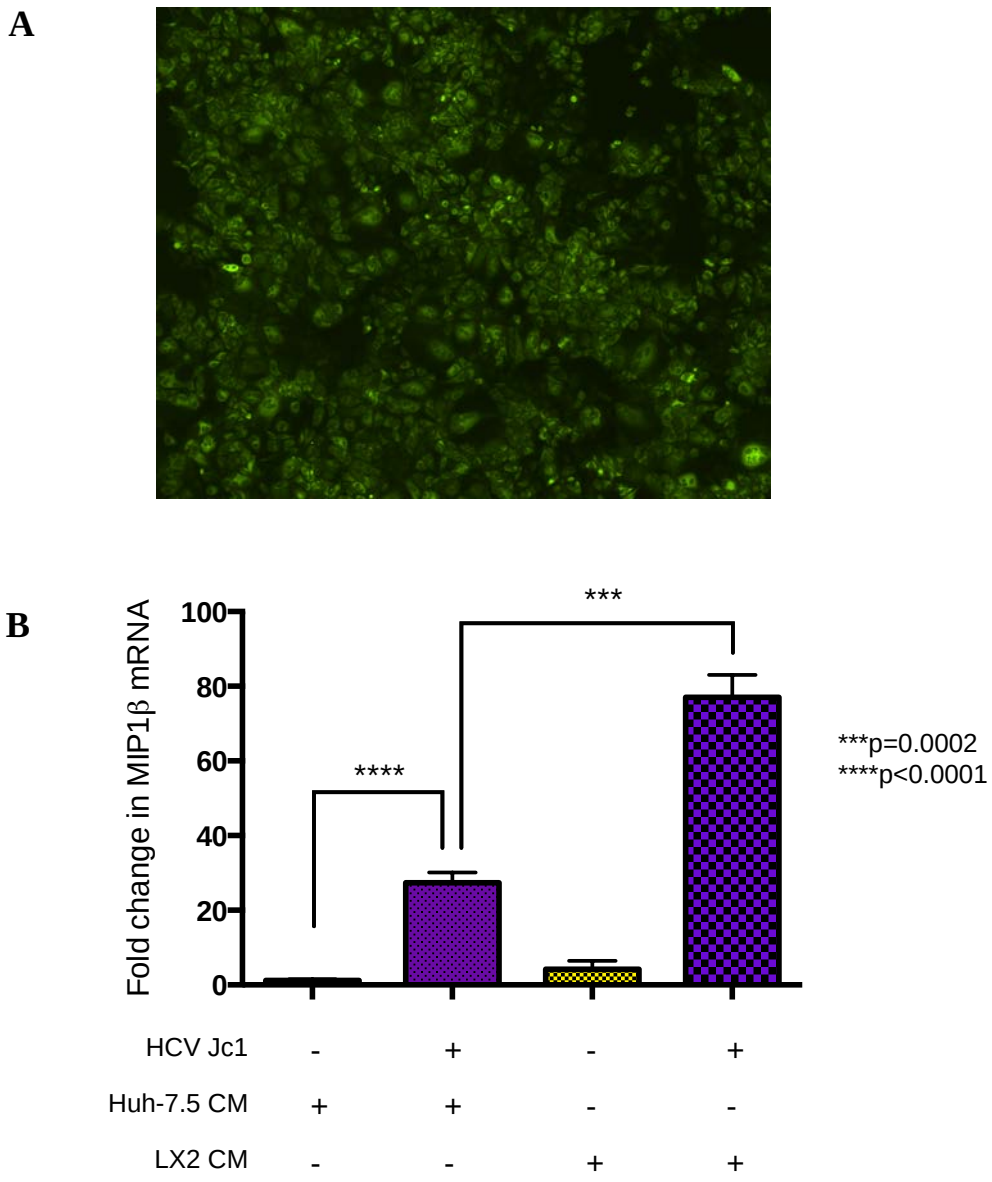

Figure 5.11 Conditioned media from LX2 cells enhances MIP1β expression in HCV-infected Huh-7.5 cells. (A) Huh-7.5 cells were infected with HCV Jc1 for 72 hours and the infection rate is shown by immunofluorescence analysis of parallel cultures. **(B)** MIP1β expression is upregulated in HCV-infected Huh-7.5 cells, as shown by qRT-PCR. Conditioned media from LX2 cells enhanced MIP1β expression in infected but not uninfected Huh-7.5 cells (n=3, Student's *t*-test).

By performing qRT-PCR to determine expression of MIP1β mRNA, we were able to replicate the observation of Nishitsuji and colleagues in that conditioned media from LX2 cells stimulated MIP1β expression (approximately 80-fold) in HCV-infected Huh-7.5 cell but not uninfected cells (Figure 5.11). Interestingly, in contrast to the published results, we also saw an upregulation of MIP1β in HCV-infected Huh-7.5 cells incubated in media from uninfected Huh-7.5 cells. The above suggests that the HCV-infected hepatocyte is primed to respond to stimuli more so than the uninfected hepatocyte.

Interestingly, we observed a significant enhancement of MIP1β expression when HCV-infected Huh-7.5 cells were incubated in conditioned media from uninfected Huh-7+TLR3 cells (500-fold) compared to LX2 conditioned media, which showed only 80-fold upregulation (Figure 5.12). In a subsequent experiment, it appeared that this observation was dependent on functional TLR3 as neither conditioned media from Huh-7+ΔTIR nor the parent cell line Huh-7 enhanced MIP1β expression in infected Huh-7.5 cells compared to conditioned media from Huh-7.5 cells (Figure 5.13). This may suggest that that the response seen to media from LX2 cells is also related to TLR3 activation.

5.5.1 Identification of the active factor secreted from LX2 and Huh-7+TLR3 cells

Nishitsuji *et al.* demonstrated that interleukin-1α (a 30 kDa protein) secreted from LX2 cells mediated the increase in MIP1β effect, despite observing that the

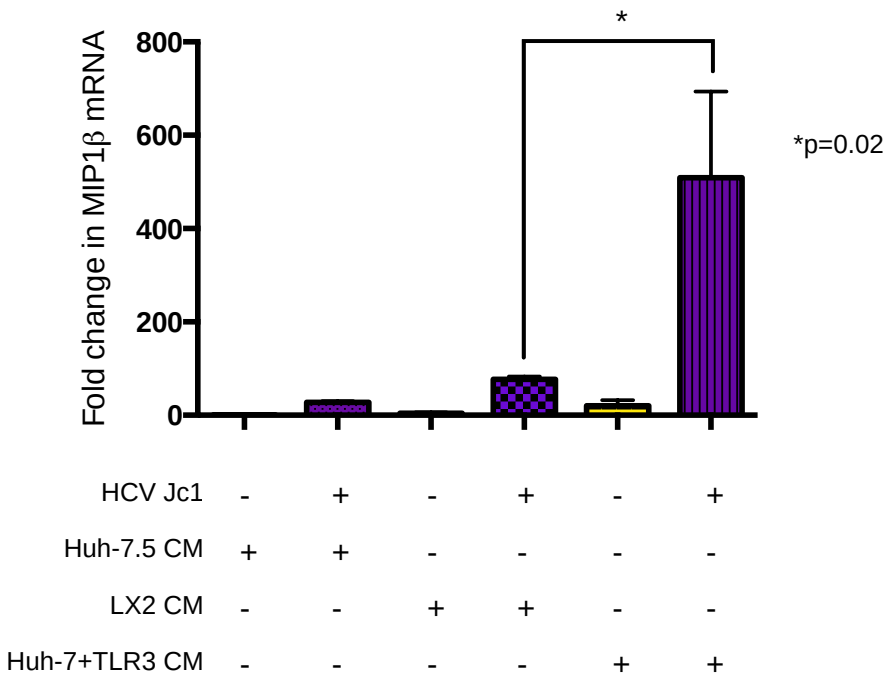

Figure 5.12 Conditioned media from Huh-7+TLR3 cells enhances MIP1β expression in HCV-infected Huh-7.5 cells to a greater degree than conditioned media from LX2 cells. qRT-PCR shows a significantly greater upregulation of MIP1β in HCV-infected Huh-7.5 cells exposed to conditioned media from TLR3-positive Huh-7 cells compared to conditioned media from LX2 cells (n=3, Student's *t*-test).

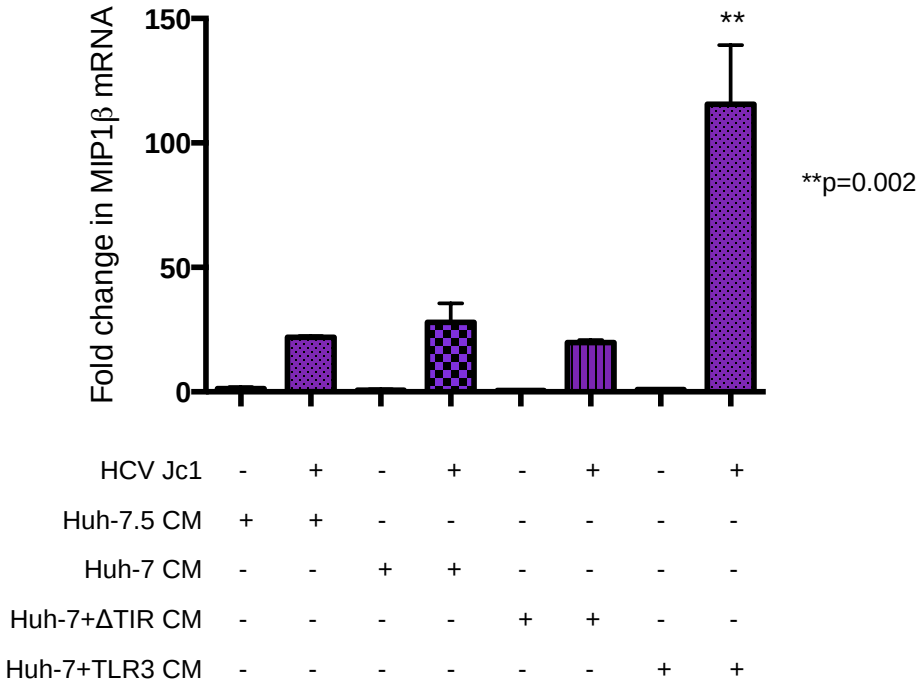

Figure 5.13 Enhanced upregulation of MIP1β in HCV-infected Huh-7.5 cells is dependent on functional TLR3 expression in bystander cells. qRT-PCR shows enhanced upregulation of MIP1β in HCV-infected Huh-7.5 cells exposed to conditioned media from TLR3-positive Huh-7 cells but not infected cells incubated in conditioned media from Huh-7+ΔTIR cells or the parent cell line Huh-7 (n=3, Student's *t*-test).

stimulator was enriched in the trap fraction of media passed through a 100 kDa filter (Nishitsuji *et al.* 2013). The authors hypothesised that the reason for this discrepancy was due to aggregates of protein containing IL-1α becoming trapped in the filter, although this hypothesis was not conclusively determined. We sought to determine whether this was also the case in our experiments. Regarding conditioned media taken from LX2 cells, the mediator of MIP-1β upregulation was enriched in the trap fraction of a 50 kDa filter, suggesting that the mediator was larger than 50 kDa, although there was still upregulation of MIP1β in the flow-through fraction compared to control. No significant difference was noted between the trap and flow-through fractions of a 100 kDa filter (Figure 5.14). In the case of proteins that have a molecular weight close to the size of the filter, the manufacturers suggest that there may only be partial retention of the protein, which may explain these results. In the case of media from TLR3-positive Huh-7 cells, no significant differences were seen between the trap and flow-through fractions of either the 50 kDa or the 100 kDa filters (Figure 5.15), although there was a slight trend to the mediator being enriched in the 50 kDa trap fraction and the 100 kDa flow-through, perhaps suggesting the mediator is between 50 and 100 kDa in size. We were therefore unable to confirm the results published by Nishitsuji *et al.* The hypothesis that protein aggregates accounted for the discrepancy in their work may also explain our observations, as it is conceivable that aggregates of different sizes may form, in addition to non-aggregated protein being present.

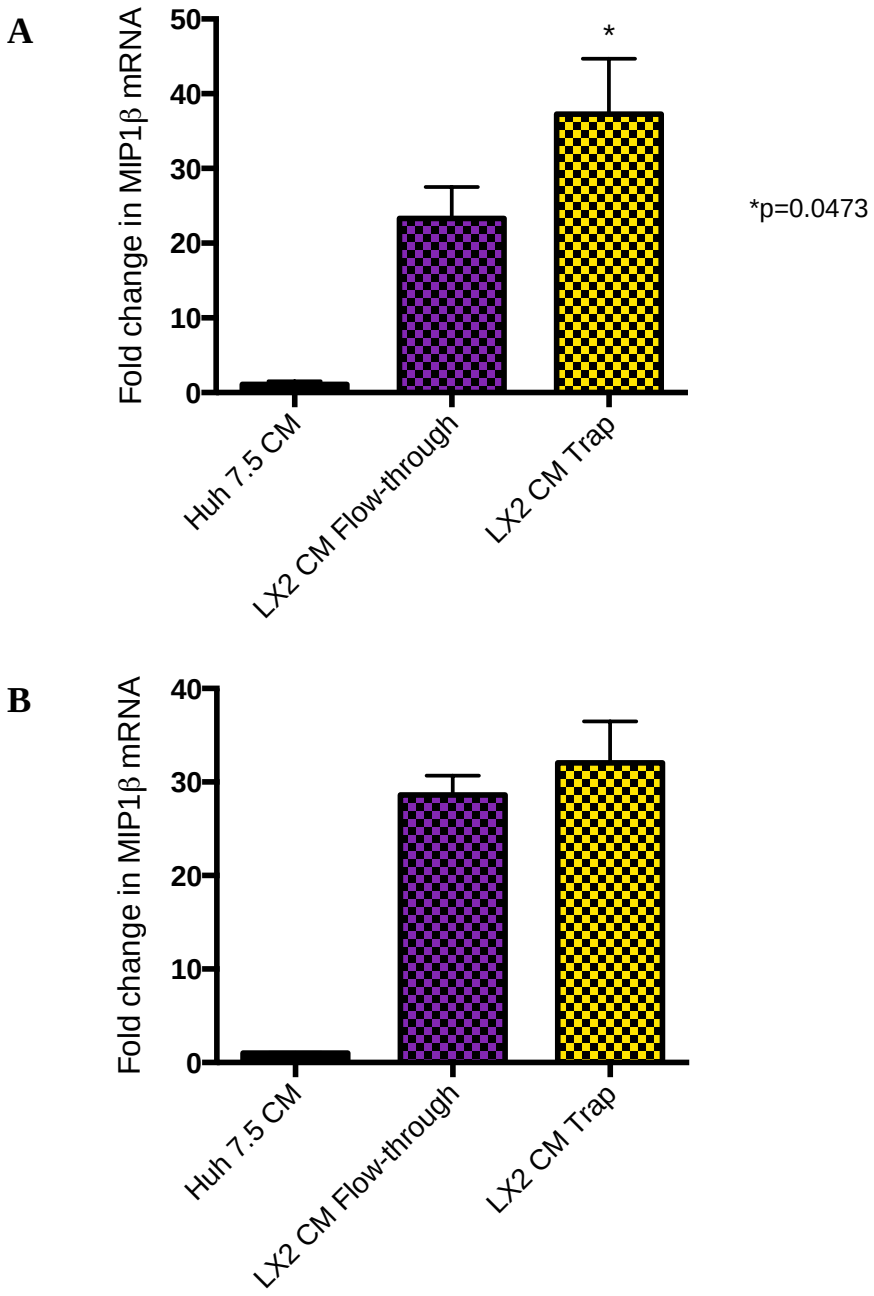

Figure 5.14 The mediator of upregulation of MIP1β in HCV-infected Huh-7.5 cells is enriched in the 50 kDa trap fraction of conditioned media from LX2 cells. (A) qRT-PCR shows enhanced upregulation of MIP1β in HCV-infected Huh-7.5 cells exposed to the 50 kDa trap fraction of conditioned media from LX2 cells (n=3, p=0.0473, Student's t-test). **(B)** No significant difference in MIP1β upregulation was observed in HCV-infected Huh-7.5 cells exposed to the 100 kDa trap fraction of conditioned media from LX2 cells, as compared to the 100 kDa flow-through fraction.

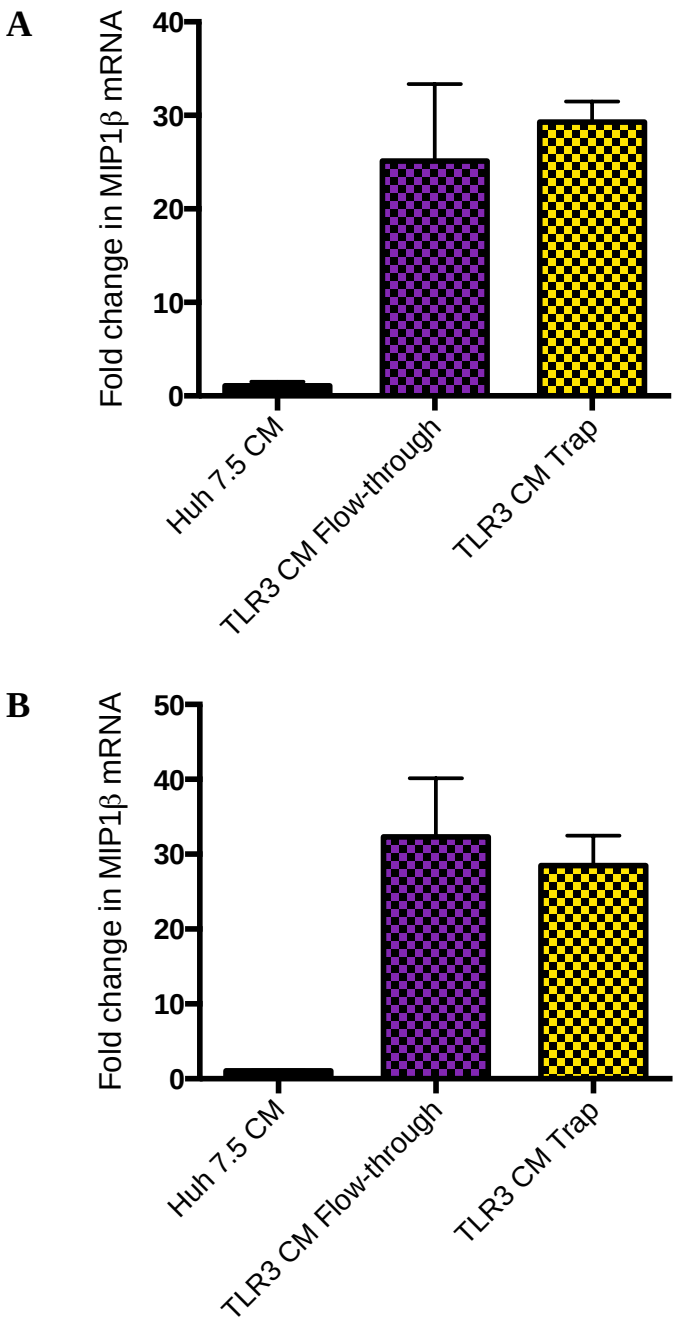

Figure 5.15 Upregulation of MIP1β in HCV-infected Huh-7.5 cells is not significantly altered by fractionation of media from Huh-7+TLR3 cells. There was no significant difference in MIP1β mRNA expression by qRT-PCR in HCV-infected Huh-7.5 cells culture in the trap and flow-through fractions of media from TLR3-positive Huh-7 cells **(A)** 50 kDa filter **(B)** 100 kDa filter.

5.6 Discussion

As previously discussed in Chapter 3, progression to advanced liver disease occurs in a significant proportion of individuals infected with HCV, however this occurs despite a low proportion (1.7-22%) of infected cells in the liver (Liang *et al.* 2009). The molecular mechanisms underlying this progression have not been fully elucidated. However, we and others propose that one of the mechanisms that leads to the development of advanced liver disease in HCV-infected individuals is the 'bystander effect', whereby uninfected cells in the liver become involved in the inflammatory and fibrogenic processes, driving disease progression. We propose that one of the mechanisms involved in disease progression is the cross-talk between the HCV-infected hepatocyte and uninfected bystander cells, amplifying the signals that drive disease progression. Understanding the mediators involved in this process may lead to novel anti-inflammatory and anti-fibrotic therapeutics, not to mention increasing our understanding of the liver cross-talk.

In this chapter, we sought to demonstrate an effect of HCV-infected hepatocytes on bystander cells including uninfected hepatocytes, other infected hepatocytes and stellate cells. We used the TLR3-expressing cell line developed in Chapter 4 in this model system, as we have demonstrated that this cell line has enhanced responsiveness to HCV infection, well over what is seen in TLR3-negative Huh-7 cells, consistent with published data (Wang *et al.* 2009; Li *et al.* 2012).

Despite the expression of TLR3 in HCV-infected Huh-7 cells and a robust response to infection, resulting in expression of numerous cytokines and chemokines, we could not demonstrate an effect at the transcriptional level in uninfected bystander

Huh-7 cells by microarray analysis. This finding parallels the results of similar experiments described in Chapter 3 in which we used conditioned media from TLR3-negative Huh-7 cell lines. It was proposed that this was a result of the relative unresponsiveness of the Huh-7 cell lines that support HCV infection due to a lack of TLR3 expression. However, this has been subsequently addressed by the use of Huh-7 cells stably expressing TLR3. We have previously demonstrated that TLR3-positive Huh-7 cells produce many chemokines and cytokines in response to stimulation by dsRNA or HCV infection, hence an additional issue may be that the bystander cells are simply unresponsive to these soluble factors. However, we were unable to demonstrate any response in an alternative bystander cell line, PH5CH8. These cell lines may lack the appropriate cell surface receptors to respond to the chemokines and cytokines produced.

As previously discussed, HCV-infection rates were relatively low in TLR3-positive Huh-7 cells and hence the concentration of soluble factors produced by these cells in the conditioned media may have been insufficient to stimulate an appreciable effect in bystander cells.

The potentially disease exacerbating effect of HCV-infected hepatocytes on uninfected cells may require direct cell-to-cell contact, rather than being mediated by soluble factors. It has been recently shown that uninfected ‘bystander’ TLR3-competent hepatocyte cell lines can sense HCV infection in neighbouring cells via HCV RNA released into the extracellular medium being detected by class A scavenger receptor type 1 (MSR1). This MSR1 recognition of HCV RNA activates the TLR3-mediated anti-viral pathways that can in turn restrict HCV-replication in

the infected ‘producer’ cells (Dansako *et al.* 2013). However, this effect was localized, being restricted to adjacent cells in direct co-culture, suggesting that cell-to-cell contact or cells in very close proximity are required for cross-talk between cells. The impact of cell-to-cell contact in our own model system is addressed in Chapter 6.

Additionally, the effect of HCV-infected hepatocytes on uninfected hepatocytes could be mediated by other cells involved in the immune response to HCV infection, such as dendritic cells and natural killer (NK) cells. Certainly, it has been shown that plasmacytoid dendritic cells are required for the cross-talk between HCV-infected Huh-7.5 cells and NK cells and these interactions are dependent on cell-to-cell contact (Zhang *et al.* 2013). Our model system does not address the possibility of an intermediary cell driving cross-talk between infected and bystander cells.

The lack of any appreciable effect of conditioned media from HCV-infected TLR3-positive Huh-7 cells on bystander hepatocytes prompted us to examine the effect of soluble mediators on primary rat hepatic stellate cells by investigating the expression of pro-fibrogenic markers COL1a1, TIMP-1 and TGF-β. Using qRT-PCR we have shown that COL1a1 and TIMP-1 mRNA was increased in expression in response to conditioned media from HCV-positive TLR3-positive Huh-7 cells at 24 and 72 hours respectively. Upregulation of COL1a1 and TIMP-1 in the stellate cell line LX2 in response to conditioned media from HCV replicon cells and HCV-JFH1 infected Huh-7.5.1 cells has been previously demonstrated in HCV-monoinfection and HCV-HIV co-infection (Schulze-Krebs *et al.* 2005; Lin *et al.*

2011). In contrast to this, in the present study we additionally observed downregulation of TGF-β mRNA in primary rat stellate cells. It has been previously shown that conditioned media from an HCV replicon cell line does not alter TGF-β expression in rat or human hepatic stellate cells (Schulze-Krebs *et al.* 2005). TGF-β is one of the major cytokines implicated in hepatic fibrosis. It is secreted by both hepatocytes and activated stellate cells, and acts in both an autocrine and paracrine manner to further stimulate stellate cells. HCV has been previously shown to upregulate TGF-β (Lin *et al.* 2008) and stellate cell activation and induction of a profibrogenic state occurs in response to conditioned media from HCV-infected Huh-7.5 cells (Presser *et al.* 2013) and HCV replicon cells (Schulze-Krebs *et al.* 2005). The downregulation of TGF-β in our experiments may be due to a negative feedback response to TGF-β secreted by HCV-infected Huh-7+TLR3 cells. TGF-β was statistically significantly upregulated in TLR3-expressing Huh-7 cells stimulated by Poly I:C (Fold change 1.51) and infected with HCV Jc1 (Fold change 1.61), compared to Huh-7+ΔTIR cells on the microarray analysis described in Chapter 4.

Whilst TLR3-positive hepatocyte cell lines replicate HCV, they do so less efficiently than TLR3-negative hepatocyte cell lines, as shown in our work (section 4.4) and by others (Wang *et al.* 2009). This suggests a TLR3-mediated antiviral state. We therefore instigated a study to investigate if this TLR3-related antiviral state could be transferred to neighbouring cells. We demonstrated that conditioned media from HCV-Jc1 infected Huh-7+TLR3 cells reduces luciferase output in a cell line harbouring a luciferase reporter-encoding HCV replicon. This implies that

HCV infection stimulates secretion of antiviral factors from infected cells that are able to impact on HCV replication in other infected cells. This effect appears to be at least in part related to the TLR3-mediated response to HCV-infection as the antiviral effect was not seen when HCV-infected Huh-7+ΔTIR cells were used. These results were confirmed when cells were stimulated with Poly I:C as opposed to infection with HCV, indicating that TLR3 sensing of HCV RNA is likely to be the major determinant of this effect. It has been previously shown that HCV replication is restricted by TLR3 expression in HCV-infected cells (Wang *et al.* 2009; Eksioglu *et al.* 2011). It has also been demonstrated that soluble factors from LX2 cells stimulated with Poly I:C have an anti-viral effect on HCV-infected cells via induction of interferon-λ (Wang *et al.* 2013). It is noteworthy that, as shown by microarray analysis in Chapter 4, interferon-λ was not upregulated in stimulated TLR3-expressing Huh-7 cells. It has not been previously demonstrated that TLR3-mediated antiviral effects occur via cross-talk between infected cells via soluble factors. We were able to confirm this finding in Huh-7.5 cells infected with HCV Jc1. As in the luciferase system, HCV replication (as determined by qRT-PCR) was reduced in cells incubated in conditioned media from Huh-7+TLR3 cells stimulated with Poly I:C. The molecular mechanisms behind this decrease in HCV replication in bystander cells is not immediately apparent, however, as mentioned previously, activation of TLR3 by viral infection does induce production of Type I interferon (Kawai and Akira 2008). Dansako *et al.* showed interferon-β message increased in response to HCV in TLR3-positive cells, although this increase was only two-fold (Dansako *et al.* 2013). Nevertheless, in our microarray experiments and qRT-PCR

analysis we did not see appreciable increases in type I interferon expression, suggesting that other, as yet unrecognised factors are involved.

In order to identify the antiviral factor or factors responsible, we subsequently performed fractionation of conditioned media and determined that the factors were larger than 50 kDa. As we had expected the soluble factor to be a TLR3-induced cytokine or chemokine, and thus smaller than 50 kDa, we hypothesised that exosomes carrying antiviral factors may be mediating the cross-talk between cells. Exosomes are extracellular vesicles that are able to transfer mRNA, microRNA and proteins between cells and it has previously been shown that antiviral activity can be transferred to neighbouring cells in the setting of HIV-1, hepatitis B and dengue virus. Tumne *et al.* demonstrated that exosomes purified from supernatant from a CD8-positive T-cell line, known to suppress HIV-1, suppressed HIV-1 replication *in vitro* (Tumne et al. 2009). It has also been previously shown that exosomes can transfer interferon-α-induced antiviral activity against HBV from non-permissive to permissive hepatocytes, with antiviral proteins and mRNAs such as APOBEC3G, IFI6 and IFITM1 transferred to permissive cells via exosomes, and that the anti-HBV activity of interferon-α can be inhibited by shRNA inhibition of exosome release in mice (Li *et al.* 2013). These authors also demonstrated similar results in the setting of HCV, where exosomes from interferon-α-treated macrophages and liver sinusoidal endothelial cells suppressed HCV replication *in vitro.* It has also been recently demonstrated that the anti-dengue activity of the ISG IFITM3 can be transferred between cells by exosomes (Zhu *et al.* 2014). In our work, this hypothesis was supported by demonstrating that HCV replication levels in target

cells were unchanged from baseline when exosome secretion was inhibited by GW4869, a known inhibitor of exosome release (Trajkovic *et al.* 2008; Kosaka *et al.* 2010). In HCV infection, viral RNA can be transferred to non-permissive plasmacytoid dendritic cells by exosomes, inducing immune responses (Dreux *et al.* 2012). However, as our work utilized Poly I:C, to which the target cells are not responsive, transfer of viral RNA does not appear to be responsible for the antiviral effect we have demonstrated and it is likely that transfer of TLR3-induced antiviral factors via exosomes is mediating the effect seen. This work is preliminary and further experiments are required to confirm our observations, such as shRNA knockdown of exosome release, exosome purification, and immunoblot and proteomics analysis of exosomes and how this relates to both TLR3 responses in the producer cell and anti-HCV activity in the recipient cell.

It is possible that cross-talk between the HCV-infected hepatocyte and bystander cells is not one-way traffic, and it is not inconceivable to envisage that bystander cells may impact the HCV-infected hepatocyte. In this case, the HCV-infected hepatocyte may be primed to respond to extracellular signals, not only from resident liver cells but also from infiltrating immune cells. Consistent with published data (Nishitsuji *et al.* 2013), we confirmed that conditioned media from the immortalized stellate cell line LX2 stimulates expression of MIP1β in HCV-infected Huh-7.5 cells but not in uninfected cells. However, a significantly greater upregulation of MIP1β was observed when HCV-infected Huh-7.5 cells were exposed to conditioned media from TLR3-expressing Huh-7 cells, with this phenomenon likely related to the presence of functional TLR3 as cells expressing a mutant form of

TLR3 (ΔTIR) did not show this effect. In the work from Nishitsuji *et al*., it was shown that this LX2 conditioned media effect was mediated by interleukin-1α (IL-1α), but despite IL-1α being 30 kDa in size, the effect was enriched in the trap fraction of media passed through a 100 kDa centrifugal filter. We were unable to confirm this observation. Nevertheless, collectively these observations suggest that the HCV infected hepatocyte is primed to respond to stimuli that may further enhance gene expression, driving liver disease.

In conclusion, it has been demonstrated in this chapter that there are interactions between TLR3-expressing, HCV-infected Huh-7 cells and bystander cells that are mediated by secreted factors. While we could not see changes at the mRNA level as a result of incubating bystander hepatocytes with conditioned media from stimulated TLR3-positive Huh-7 cells, we did note an antiviral effect of this conditioned media, as well as an effect on stellate cells and cells persistently infected with HCV. These interactions are summarized in Figure 5.16. These interactions are likely to contribute to the pathogenesis of HCV-related liver disease and support the hypothesis that the involvement of bystander cells in HCV infection expands the effect of HCV beyond the infected hepatocyte. Our work suggests that cross-talk between cells may be in part mediated by exosomes, but not entirely. The interplay between HCV-infected hepatocytes in cell contact with bystander cells is discussed in the subsequent chapter.

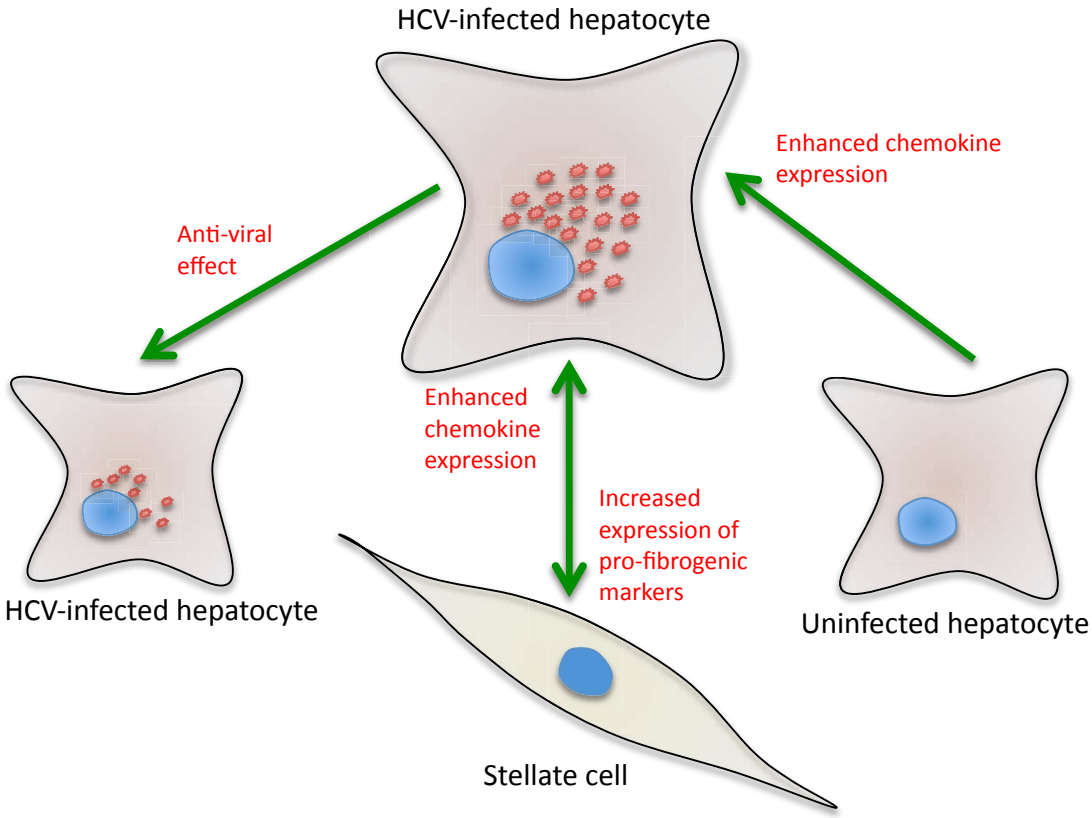

Figure 5.16 Summary of the interactions between HCV-infected hepatocytes and bystander cells as mediated by soluble factors.

Chapter 6

The bystander effects mediated by cell-to-cell contact

6.1 Introduction

Interactions between HCV-infected hepatocytes and bystander cells may be mediated, at least in part, by soluble factors. We hypothesise that additional interactions occur via direct cell-to-cell contact or that cells need to be in close proximity to exert an effect. Indeed, it has been previously shown that cell-to-cell contact is essential for class A scavenger receptor type 1 (MSR1)-mediated sensing of HCV infection in adjacent cells by uninfected cells and the resultant TLR3-mediated antiviral effect is localized (Dansako *et al.* 2013). Cell-to-cell contact was also shown to be important for interferon-α and -γ production mediated by interactions between HCV-infected hepatoma cells and dendritic and natural killer cells in co-culture (Zhang *et al.* 2013; Zhang *et al.* 2013).

Although previous studies have examined the interactions between HCV-infected hepatocytes and immune cells (NK cells, dendritic cells) in direct cell contact (Takahashi *et al.* 2010; Zhang *et al.* 2013; Zhang *et al.* 2013), the interactions between HCV-infected hepatocytes and other cells in direct cell-to-cell contact are poorly understood. In particular, the gene expression changes in uninfected hepatocytes in co-culture with HCV-infected hepatocytes have not been previously examined.

In this chapter, the interactions between bystander cells in direct cell contact with HCV-infected hepatocytes have been studied. Where HCV-infected hepatoma cells are cultured with uninfected hepatoma cells, the cells must be able to be separated after co-culture for downstream analysis of the two populations of cells in isolation and hence the development of cell separation methods is also described.

6.2 Generation of a stable cell line for use in a cell separation system

Following co-culture of HCV-infected and bystander cells using our previously described model system, it was necessary to separate the two cell types so that their transcriptome may be examined in isolation. In particular, it was important to ensure that there would be no contamination of the bystander cells by infected cells. This could have been achieved by the use of fluorescence-activated cell sorting to separate GFP-positive, CD81-knockdown Huh-7 cells from GFP-negative, TLR3-positive Huh-7 cells, however, restrictions were placed on the use of infectious virus in our flow cytometry facility. Therefore, an alternative strategy was employed in which we used a magnetic bead based separation system that could be used easily within our laboratory. This cell capture system uses the CherryPicker™ Reagent Kit (Clontech) whereby anti-mCherry labelled magnetic beads capture cells expressing the fluorescent protein mCherry on the cell surface, and is discussed below.

6.2.1 Generation of stable cell lines expressing cell surface mCherry

To positively select bystander cells in our co-culture model system, we initially generated Huh-7 CD81 knockdown cells that constitutively express cell surface mCherry. As previously described by Winnard *et al.* (Winnard *et al.* 2007), a transmembrane protein (human transferrin receptor) sequence was fused to the mCherry sequence, utilizing the pLenti6/V5-D-TOPO plasmid containing mCherry (Appendix I). This was used to produce lentivirus and Huh-7 CD81 knockdown cells were transduced. After selection with blasticidin, stable cell surface expression of mCherry was demonstrated by wide field and confocal fluorescence microscopy (Figures 6.1 and 6.2). As can be seen in Figure 6.1, 100% of cells express mCherry in a pattern that is consistent with cell surface expression. This was confirmed in Figure 6.2 in which immunofluorescence labelling of mCherry was observed in non-permeabilized cells.

Following generation of the stable mCherry-expressing cell line, it was necessary to demonstrate the ability to purify mCherry-positive cells using the CherryPicker™ system. Huh-7 cells infected with HCV Jc1 and mCherry-positive CD81 knockdown Huh-7 cells were mixed in a ratio of 1:1 and returned to culture for two days (Figure 6.3). The mCherry positive cells in the co-culture were then purified using the CherryPicker™ system as per the manufacturer's instructions described in Section 2.6. Capture efficiency and purity was assessed by fluorescence microscopy and flow cytometry. Immunofluorescence analysis revealed that all cells expressed mCherry (Figure 6.4). This was confirmed by flow cytometry analysis that

A

B

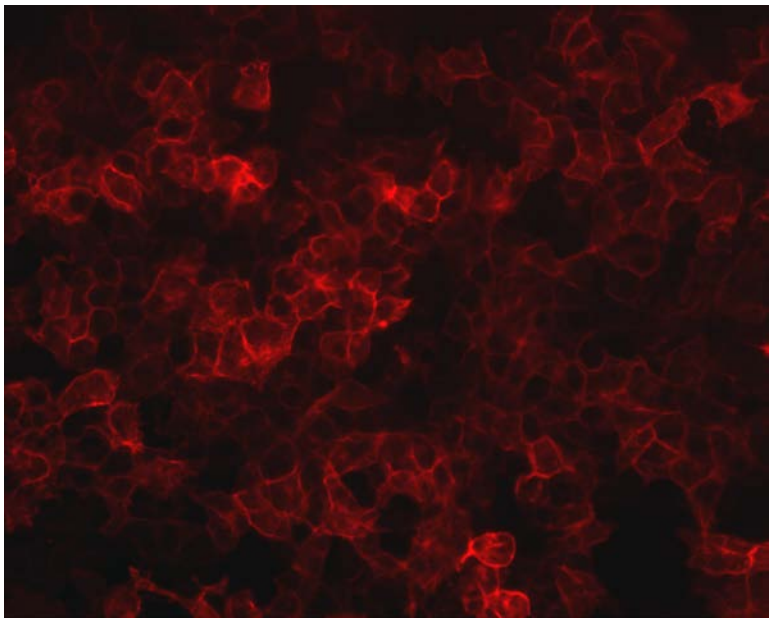

Figure 6.1 Fluorescence microscopy demonstrates stable mCherry expression in Huh-7+CD81 knockdown cells, in a cell-surface distribution. (A) Parent cell line Huh-7+CD81 knockdown **(B)** Huh-7 + CD81 knockdown + cell-surface mCherry.

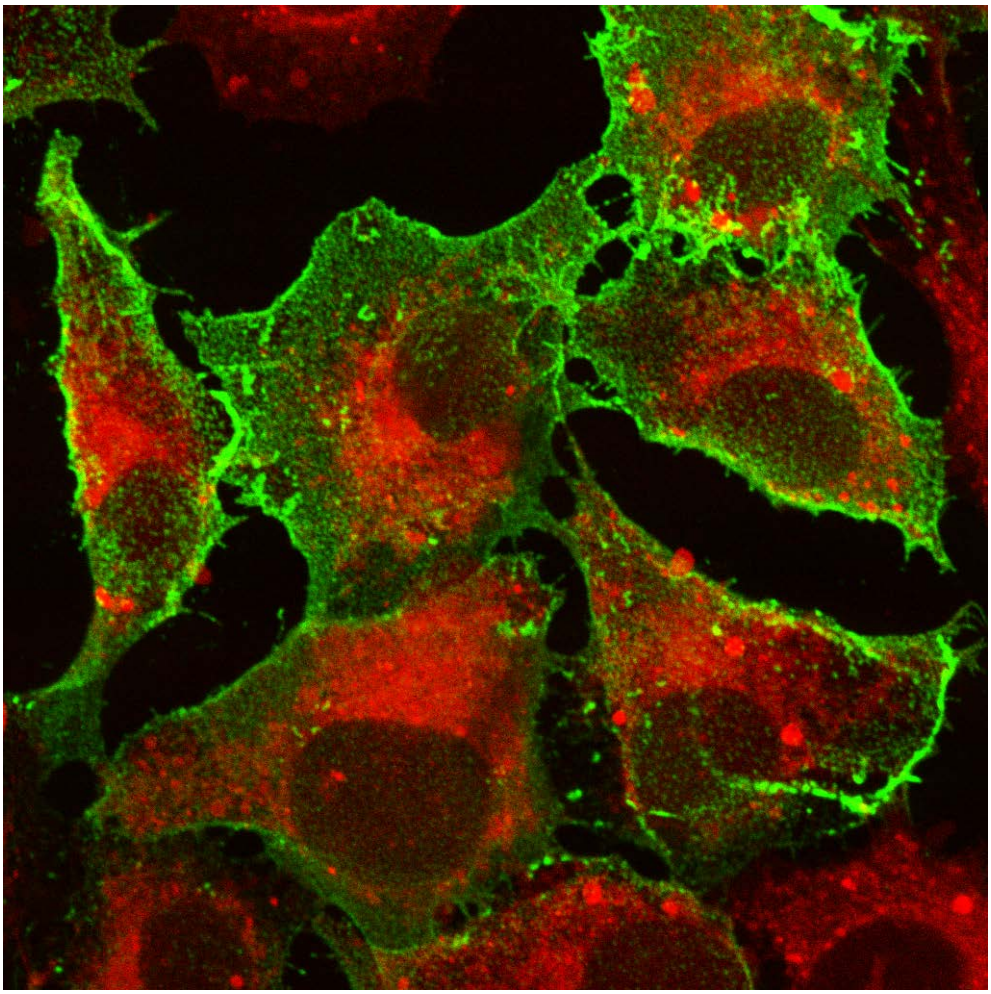

Figure 6.2 Confocal microscopy demonstrates cell-surface expression of mCherry. Non-permeabilized cells were labelled with anti-mCherry antibody followed by a secondary antibody with a green fluorescent conjugate. Unlabelled intracellular mCherry is also demonstrated by red fluorescence.

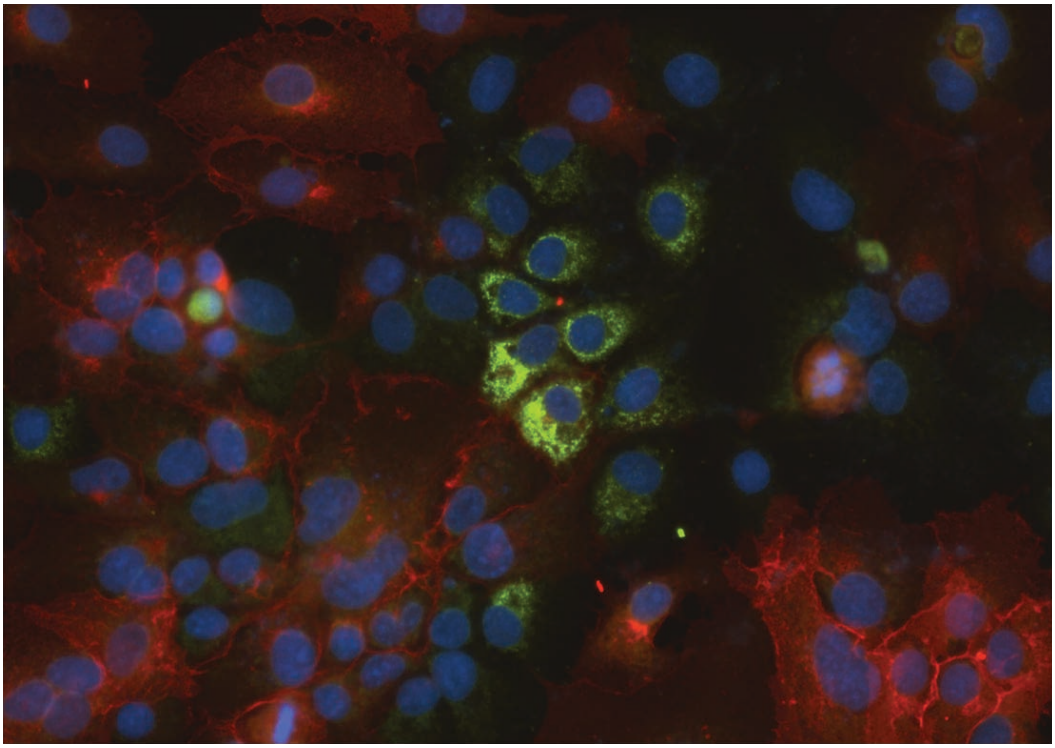

Figure 6.3 Fluorescence microscopy demonstrates mCherry-positive Huh-7+CD81 knockdown cells (red) **in co-culture with Huh-7+TLR3 cells infected with HCV Jc1** (green)**.** HCV antigen labelling was performed using pooled inactivated HCV-positive human serum as the primary antibody followed by an appropriate green fluorescent secondary antibody.

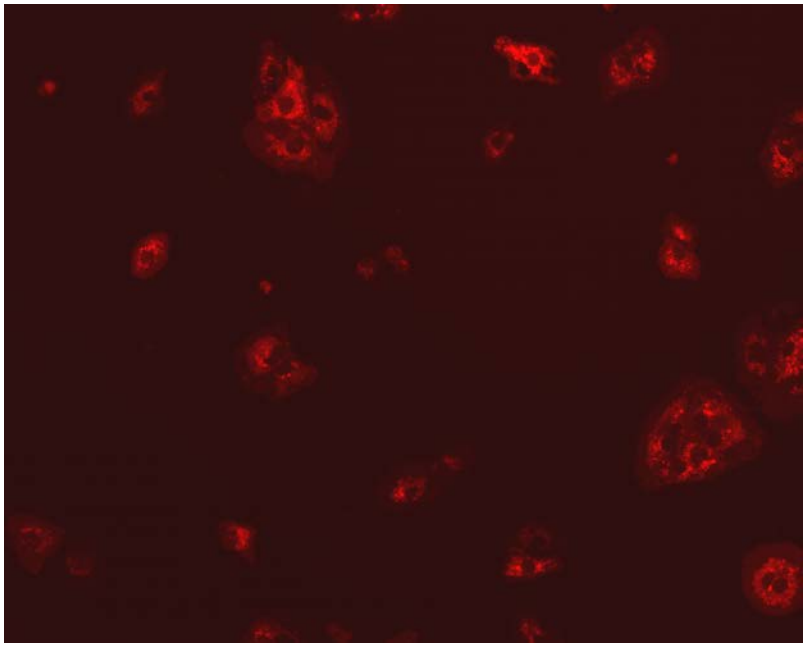

Figure 6.4 Fluorescence microscopy performed after magnetic bead sorting shows expression of mCherry by the captured cells.

demonstrated greater than 80% of cells in the captured sample were mCherry positive (Figure 6.5).

6.2.2 Utilization of the magnetic bead system in 'bystander effect' experiments

Subsequent to generation of the mCherry positive cell line and characterization of the system, restrictions on use of infectious samples in the flow cytometry facility were relaxed and it therefore became possible to use infected samples in the fluorescence-activated cell sorting equipment available. Hence, the magnetic bead separation system described was not used in further experiments in this Chapter. Nevertheless, this system could provide a viable alternative to FACS for purification of HCV-infected and uninfected cells.

6.3 Co-culture and fluorescence-activated cell sorting of HCV-infected and uninfected bystander cells

To assess the effect of HCV-infected hepatocytes on bystander hepatocytes in a co-culture setting, Huh-7+TLR3 cells were seeded into 75cm^2 cell culture flasks. The following day, the cells were mock infected or infected with HCV Jc1 at an MOI of 2 and returned to culture for 48 hours. Cells were then trypsinized and placed into co-culture with GFP-positive Huh-7 CD81 knockdown cells in a 1:1 ratio, in triplicate, and returned to culture for 24 hours. The HCV Jc1 infection efficiency was assessed at the time of seeding the cells into co-culture by fluorescence microscopy and was found to be approximately 30% (Figure 6.6). Following 24

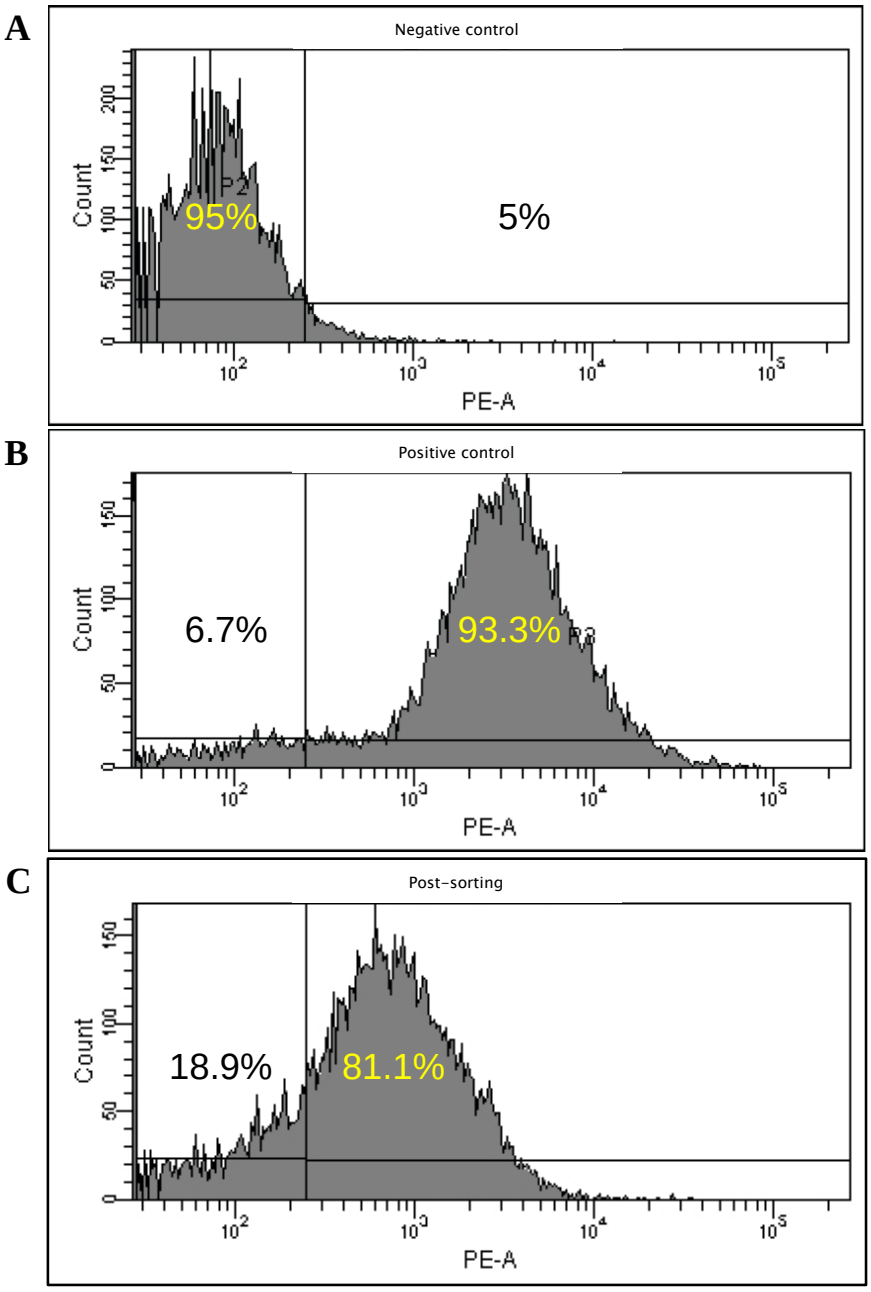

Figure 6.5 Flow cytometry demonstrates high purity of captured cells post-magnetic bead sorting. Following purification of mCherry-positive CD81-knockdown cells using the CherryPicker system, flow cytometry was performed to assess the purity of the captured cells. **(A)** Negative control **(B)** Positive control comprised of mCherry-positive cells taken from an unmixed cell culture sample, demonstrating 93% mCherry positive cells. **(C)** Captured cells. Greater than 80% of cells demonstrated expression of mCherry by flow cytometric analysis.

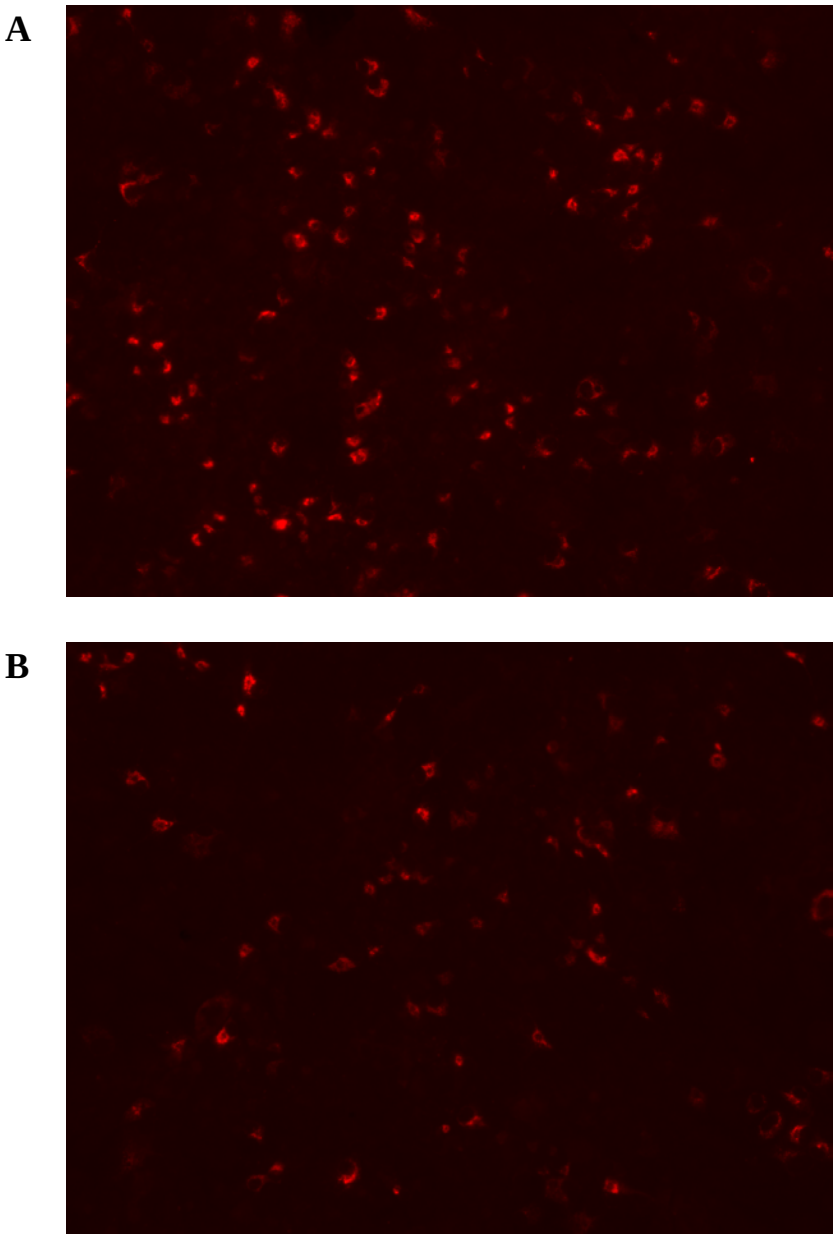

Figure 6.6 HCV-infection rate by immunofluorescence microscopy prior to cell sorting. To detect HCV-infected cells, HCV NS5A protein was labelled with an anti-NS5A monoclonal antibody and appropriate fluorescent secondary antibody. **(A)** Immunofluorescence microscopy indicates approximately 30% of Huh-7+TLR3 cells are infected prior to co-culture. **(B)** Immunofluorescence microscopy for HCV antigens following co-culture of HCV Jc1-infected Huh-7+TLR3 cells and Huh-7+CD81 knockdown cells prior to cell sorting.

hours of co-culture, cells were harvested and resuspended in FACS sort buffer and sorted on the basis of GFP positivity. Cell sorting was performed at the Detmold Family Cell Imaging Facility (SA Pathology, Adelaide, South Australia; section 2.5.3). After collecting both GFP-positive (bystander cells) and GFP-negative (HCV-infected cells) into normal media, cells were washed and RNA extracted as per section 2.1.12.

To assess the purity of the sorted sample, a small amount of sorted cells were plated and returned to culture, then subsequently fixed once they had become adherent for immunofluorescence analysis. To detect HCV-infected cells, HCV NS5A protein was labelled with an anti-NS5A monoclonal antibody and appropriate fluorescent secondary antibody, and visualized by fluorescence microscopy as described in section 2.4 (Figure 6.7a). This revealed that a small proportion of GFP-negative, HCV positive cells had been co-purified with the GFP-positive cell fraction. It was deemed that this low level of HCV-positive cells would not influence gene expression analysis.

We also confirmed that the Huh-7+TLR3 cells responded to HCV Jc1 infection by qRT-PCR analysis of CCL5 mRNA as we have shown previously (section 4.4). Comparison was made between HCV-positive/GFP-negative and HCV-negative/GFP-negative samples collected during FACS. CCL5 mRNA expression was increased approximately 10-fold in response to HCV infection (Figure 6.7b).

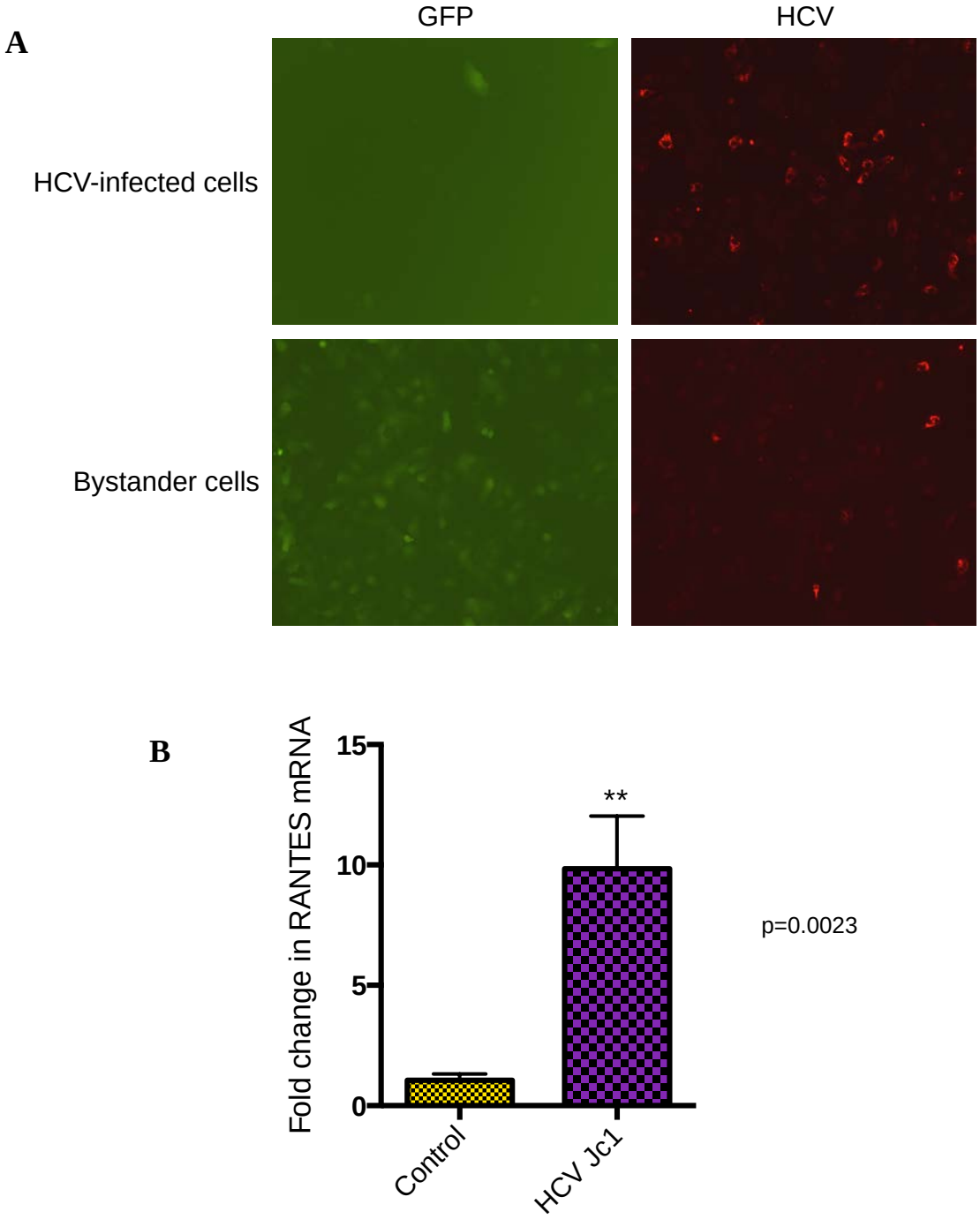

Figure 6.7 Immunofluorescence microscopy and qRT-PCR post-sorting.
(A) Immunofluorescence of GFP-positivity and HCV-infection in HCV-infected (top panels) and bystander cells (bottom panels). Immunofluorescence for GFP was acquired prior to cell fixation with acetone-methanol. Cells were then labelled for HCV antigens. It is observed that there is low-level GFP-positivity in the HCV-infected samples and low HCV contamination but high GFP in the bystander samples. **(B)** qRT-PCR demonstrates upregulation of RANTES in HCV-infected Huh-7+TLR3 cells (GFP-negative samples) post-sorting (n=3, *p*=0.0023, Student's *t*-test).

6.4 Co-culture with HCV-infected cells has a minor effect on the transcriptome of bystander hepatocytes

The RNA extracted from collected bystander cells (GFP-positive samples) was subjected to bioanalyser assessment and transcriptome analysis using Affymetrix Human Microarray and GeneSifter software to assess differential gene expression between Huh-7+CD81 knockdown bystander cells co-cultured with either HCV-infected or uninfected Huh-7+TLR3 cells. We could detect no statistically significant differences in gene expression between these two groups. Low-level, non-statistically significant fold changes were seen in approximately 150 genes (Appendix IX). The PCA plot is shown in Appendix V.

Following relaxation of analysis, one of the three genes noted to be upregulated greater than two-fold in bystander cells co-cultured with HCV-infected cells was suppressor of cytokine signalling 3 (SOCS3). SOCS3 is induced by cytokines, in particular interleukin 6 (IL-6) via the gp130 receptor (Carow and Rottenberg 2014). As demonstrated in the work described in Chapter 4, IL-6 is upregulated in Huh-7+TLR3 cells stimulated with Poly I:C or infected with HCV. SOCS3 negatively regulates cytokine signalling via the JAK-STAT pathway by binding to JAK, thereby inhibiting STAT3 activation as well as inhibiting IL-6 related activation of other STATs. SOCS3 has also been shown to be induced by HCV core protein (Bode *et al.* 2003). Given these roles in HCV infection and the JAK-STAT pathway, we elected to further evaluate the finding of SOCS3 upregulation. The samples analysed by microarray were subjected to qRT-PCR analysis of SOCS3 mRNA. A statistically significant upregulation of SOCS3 was demonstrated in

bystander cells that had been co-cultured with HCV-infected cells (Figure 6.8). Upregulation of SOCS3 in bystander cells may inhibit interferon signalling pathways in these cells, which would contribute to HCV persistence through suppression of the antiviral response.

6.5 HCV replication is decreased in hepatocytes co-cultured with TLR3-positive hepatocytes stimulated by dsRNA or infected by HCV

In the previous chapter it was shown that conditioned media from Huh-7+TLR3 cells infected with HCV or stimulated by dsRNA had an antiviral effect on an HCV-replicon harbouring cell line (SGR-JFH1-RLuc), with a small but reproducible reduction in HCV replication observed. In order to determine whether this effect is also seen, and possibly enhanced, when stimulated Huh-7+TLR3 cells are in cell-to-cell contact with SGR-JFH1-RLuc cells, the two cell lines were co-cultured and luciferase activity was measured.

For experiments where Huh-7+TLR3 cells were stimulated with dsRNA, Huh-7+TLR3 cells and SGR-JFH1-RLuc cells were mixed in a 1:1 ratio and plated in 12-well plates. After returning to culture overnight, cells were treated with Poly I:C for 16 hours and then harvested. In this instance, TLR3-positive Huh-7 cells will respond to dsRNA, whereas the SGR-JFH1-RLuc cells will not as they are TLR3 and RIG-I negative. Similar to the results seen in the conditioned media experiments discussed in Chapter 5, a small reduction in luciferase activity was observed in the Poly I:C-treated group, compared to cells that were not treated with

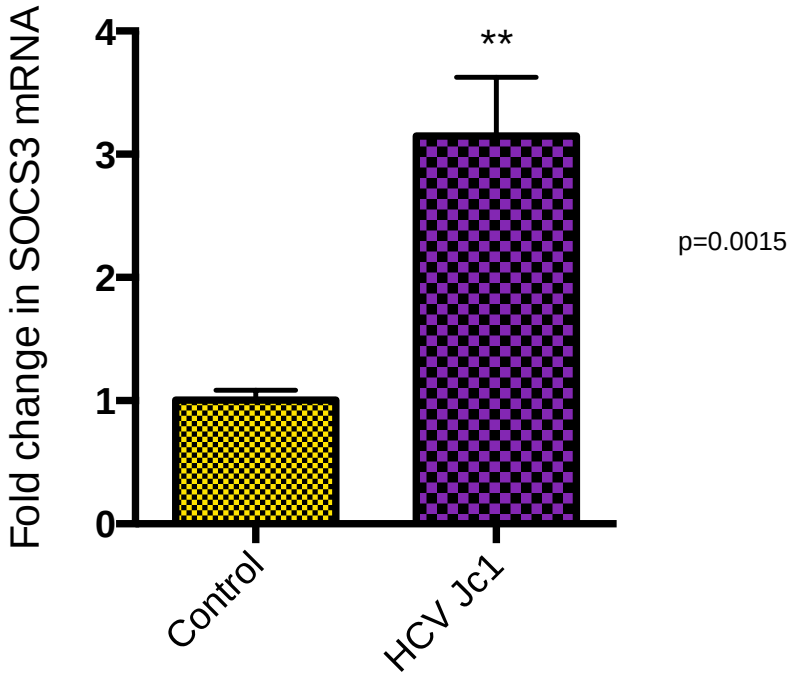

Figure 6.8 SOCS3 is upregulated in bystander hepatocytes co-cultured with HCV-infected Huh-7+TLR3 cells. When assessed by qRT-PCR, SOCS3 mRNA was significantly upregulated in bystander cells that were co-cultured with HCV Jc1-infected Huh-7+TLR3 cells for 24 hours, as compared to bystander cells that were co-cultured with uninfected Huh-7+TLR3 cells (n=3, *p*=0.0015, Student's *t*-test).

Poly I:C (Figure 6.9a). Treatment of SGR-JFH1-RLuc cells with Poly I:C in the absence of Huh-7+TLR3 cells had no impact on HCV-replication, suggesting the effect was related to stimulation of Huh-7+TLR3 cells in the co-culture and not a direct effect of Poly I:C on replicon-harbouring cells (Figure 6.9b).

Similarly we also demonstrated that there was a reduction in luciferase activity in SGR-JFH1-RLuc cells that were co-cultured with Huh-7+TLR3 cells that were infected with HCV Jc1. For these experiments, Huh-7+TLR3 cells were infected with HCV Jc1 (MOI 2.0) for a period of 72 hours. These cells were then harvested by trypsinization and placed into co-culture in 12-well plates with SGR-JFH1-RLuc cells for a further 48 hours. At this point cells were harvested and luciferase activity was measured. Again, a small but significant reduction in luciferase activity was observed in the cells co-cultured with HCV Jc1 infected cells compared to those co-cultured with uninfected Huh-7+TLR3 cells (Figure 6.10). Collectively, these results support the findings of the conditioned media experiments described in Chapter 5, suggesting that TLR3-positive, HCV-infected Huh-7 cells can exert an antiviral effect on other HCV-infected cells. However, it is not clear whether direct cell-to-cell contact is contributing to this effect.

6.6 Discussion

As previously discussed, progressive liver disease in chronic HCV infection occurs in a significant proportion of individuals but appears to occur despite the absence of universal infection of hepatocytes in the liver (Liang *et al.* 2009). The hypothesis

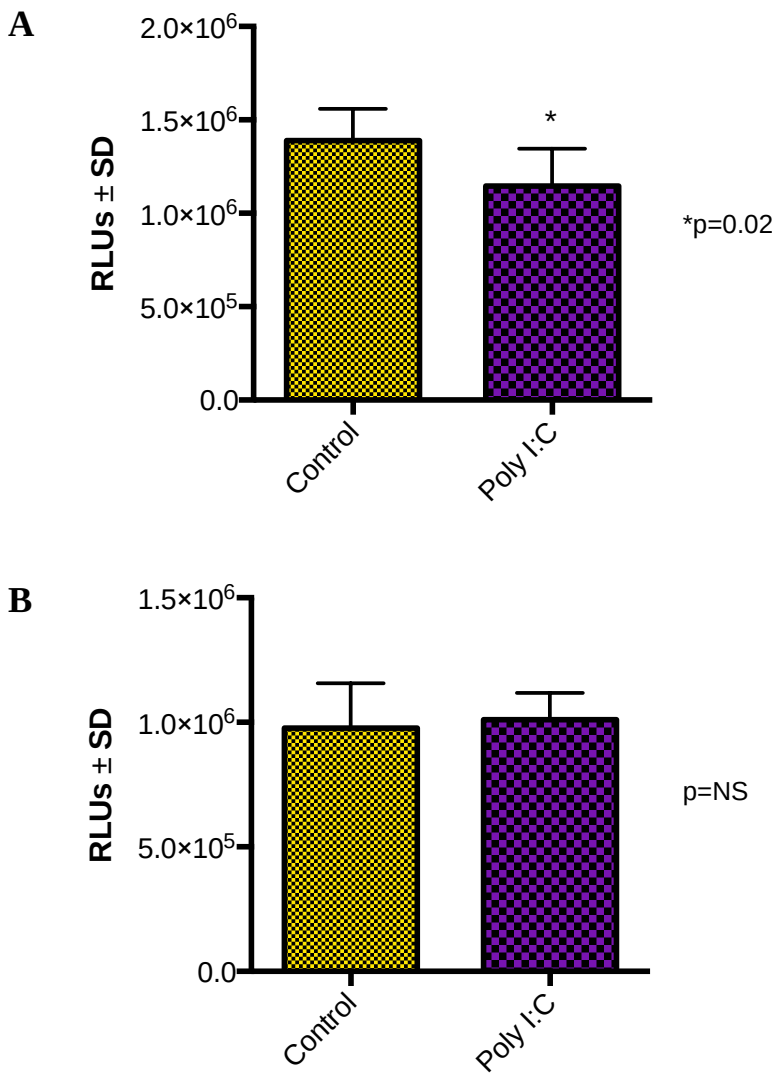

Figure 6.9 dsRNA-treatment decreases viral replication in SGR-JFH1-RLuc cells co-cultured with Huh-7+TLR3 cells. (A) Cells harbouring a luciferase reporter-encoding HCV replicon (SGR-JFH1-RLuc) were co-cultured with Huh-7+TLR3 cells. A statistically significant reduction in Renilla luciferase activity was observed when cells in co-culture were treated with Poly I:C for 16 hours compared to cells in co-culture that were not treated with dsRNA. (n=4, *p*=0.02, Student's *t*-test). **(B)** Treatment of SGR-JFH1-RLuc cells with Poly I:C in the absence of Huh-7+TLR3 cells had no effect on luciferase activity (n=4, *p*=NS, Student's *t*-test).

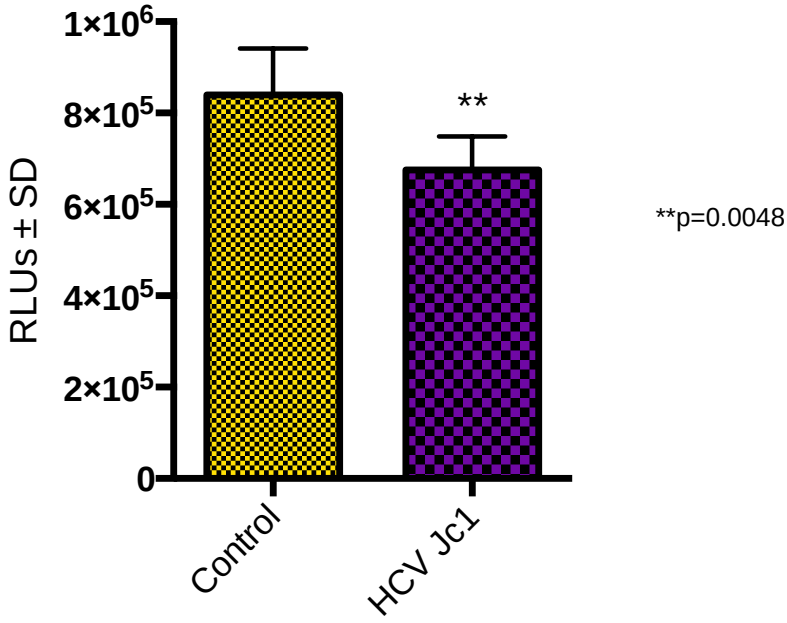

Figure 6.10 Viral replication is decreased in SGR-JFH1-RLuc cells co-cultured with Huh-7+TLR3 cells infected with HCV Jc1. Cells harbouring a luciferase reporter-encoding HCV replicon (SGR-JFH1-RLuc) were co-cultured for 48 hours with Huh-7+TLR3 cells infected with HCV Jc1. A statistically significant reduction in Renilla luciferase activity was observed when cells were in co-culture with HCV-infected cells compared to co-culture with uninfected cells. (n=4, *p*=0.0048, Student's *t*-test).

underlying this thesis is that the effect of HCV infection extends beyond the infected hepatocyte to 'bystander' cells, explaining why more widespread liver injury occurs. We have previously demonstrated that TLR3-positive HCV-infected hepatocytes exert, via soluble factors present in conditioned media, a pro-fibrogenic effect on stellate cells and an antiviral effect on other HCV-infected hepatocytes. Additionally, conditioned media from both stellate cells and uninfected hepatocytes exert a proinflammatory effect on HCV-infected hepatocytes. However, we were unable to demonstrate that soluble factors from HCV-infected, TLR3-positive Huh-7 cells exerted any effects on uninfected hepatocytes, at least at the level of the transcriptome.

It has been previously demonstrated that cell-to-cell contact or short-range interactions are important in the cross-talk between HCV-infected hepatocytes and adjacent uninfected hepatocytes, and these interactions are localized (Dansako *et al.* 2013). However, in that study co-cultured cells were not separated and therefore the transcriptome of the uninfected cells could not be examined. In this chapter we sought to develop a co-culture model which allowed for separation of co-cultured cells so that uninfected 'bystander' hepatocytes (Huh-7+CD81 knockdown cells developed in Chapter 3) could be examined in isolation after exposure to HCV-infected cells (Huh-7+TLR3 cells developed in Chapter 4). By examining the complete transcriptome of these cells it is possible to obtain a more global picture of the impact of HCV on uninfected bystander cells.

Our initial aim was to separate co-cultured cells using fluorescence-activated cell sorting (FACS) on the basis of the GFP-positivity of the CD81 knockdown cell line.

Unfortunately, due to restrictions on the use of HCV-infected material in flow cytometry equipment at our institution this was not possible and we therefore successfully developed a magnetic bead-based cell separation system whereby we could separate HCV-infected and bystander cells based on cell surface mCherry expression in the bystander Huh-7+CD81 knockdown cell line. Ultimately this system was not used in subsequent experiments as restrictions on use of infectious material in flow cytometry equipment were removed, but the model provides an alternative method of cell separation which can be utilized in situations where similar restrictions exist or flow cytometry-based cell sorting facilities are not available or appropriate.

Late in the course of this study we were able to use FACS to successfully separate HCV-infected Huh-7+TLR3 cells and uninfected 'bystander' Huh-7+CD81 cells that had been in co-culture for 24 hours. We were particularly interested in the uninfected bystander cells and subjected them to transcriptome analysis using Affymetrix Genearray analysis. Surprisingly, we observed only minor, non-statistically significant changes in gene expression in these cells compared to Huh-7 +CD81 knockdown cells co-cultured with HCV-negative Huh-7+TLR3 cells. There are several possible explanations for this finding. HCV-infection in the Huh-7 +TLR3 cells was approximately 30%, and therefore the infection rate in the co-culture was approximately 15% following mixing with bystander cells. Hence, the infection rate may not have been sufficiently robust to exert an observable effect on the uninfected cells and there may have been a number of 'bystander' hepatocytes that were not in direct cell-cell contact with HCV-infected cells. As shown in

Chapter 5, soluble factors do not appear to impact on the transcriptome of uninfected cells in a conditioned media model and therefore interactions may be localized and only occur with direct contact between infected and uninfected cells, as shown by others (Dansako *et al.* 2013). The CCL5 up-regulation in TLR3-positive cells, used here as a surrogate marker for overall response of these cells to HCV infection, was not as robust as has been previously demonstrated in our work. This may reflect the low infection rate, although as previously noted by us and others (Wang *et al.* 2009) a robust infection of TLR3-expressing hepatocytes is difficult to achieve, probably due to the generation of an antiviral state by the enhanced innate TLR3 sensing and its resultant downstream effects. Another potential reason for the lack of observable response in the bystander cell transcriptome is that a single time point, 24 hours, was performed in this experiment and hence effects in bystander cells may have occurred earlier or later than this time point and were therefore missed. Finally, as a neoplastic cell line, the 'bystander' Huh-7 cells may not be responsive to factors produced by infected cells. It has been shown that TLR3 in uninfected cells in close proximity to HCV-infected hepatocytes can sense HCV RNA and initiate an antiviral response (Dansako *et al.* 2013). As the bystander cells in our model do not express TLR3, they therefore would be unable to mount this antiviral response to HCV-infection in adjacent cells. Some of the aforementioned limitations of our model may be addressed by the use of other cell lines, ideally primary hepatocytes, although there are cost limitations associated with this approach.

Although no statistically significant changes in mRNA profile were observed in the microarray analysis, we noted that one of the most highly upregulated genes was suppressor of cytokine signalling 3 (SOCS3). SOCS3 is known to play a role in HCV infection and is upregulated by HCV core protein (Bode *et al.* 2003) and a number of the cytokines that we had demonstrated to be produced by stimulation of TLR3-expressing Huh-7 cells in Chapter 4, including IL-6 (Starr *et al.* 1997). We therefore examined the expression of SOCS3 in the bystander cells by qRT-PCR and found that there was a statistically significant three-fold upregulation of SOCS3 mRNA compared to control. SOCS3 inhibits the JAK-STAT pathway by binding to JAK and hence inhibiting STAT3 activation, interfering with interferon signalling pathways (Figure 6.11) (Bode *et al.* 2003; Croker *et al.* 2003; Duong *et al.* 2004; Huang *et al.* 2007; Carow and Rottenberg 2014). It has also been shown that hepatic SOCS3 expression is associated with poor response to interferon-based antiviral therapy against HCV (Walsh *et al.* 2006; Huang *et al.* 2007). The upregulation of SOCS3 in bystander cells may therefore have a number of implications. Firstly, inhibition of endogenous interferon signalling pathways in bystander cells by SOCS3 may contribute to the ability of HCV to inhibit antiviral responses, albeit indirectly, and to persist in an environment of low-level inflammation by allowing these cells to be more permissive to infection. Secondly, elevated SOCS3 expression in bystander cells may contribute to resistance to exogenous interferon therapy by preventing appropriate JAK-STAT signalling in these cells that may have otherwise had an antiviral effect on infected hepatocytes. These findings may also suggest that hepatic inflammatory responses in HCV infection are not enhanced by increased cytokine production in uninfected

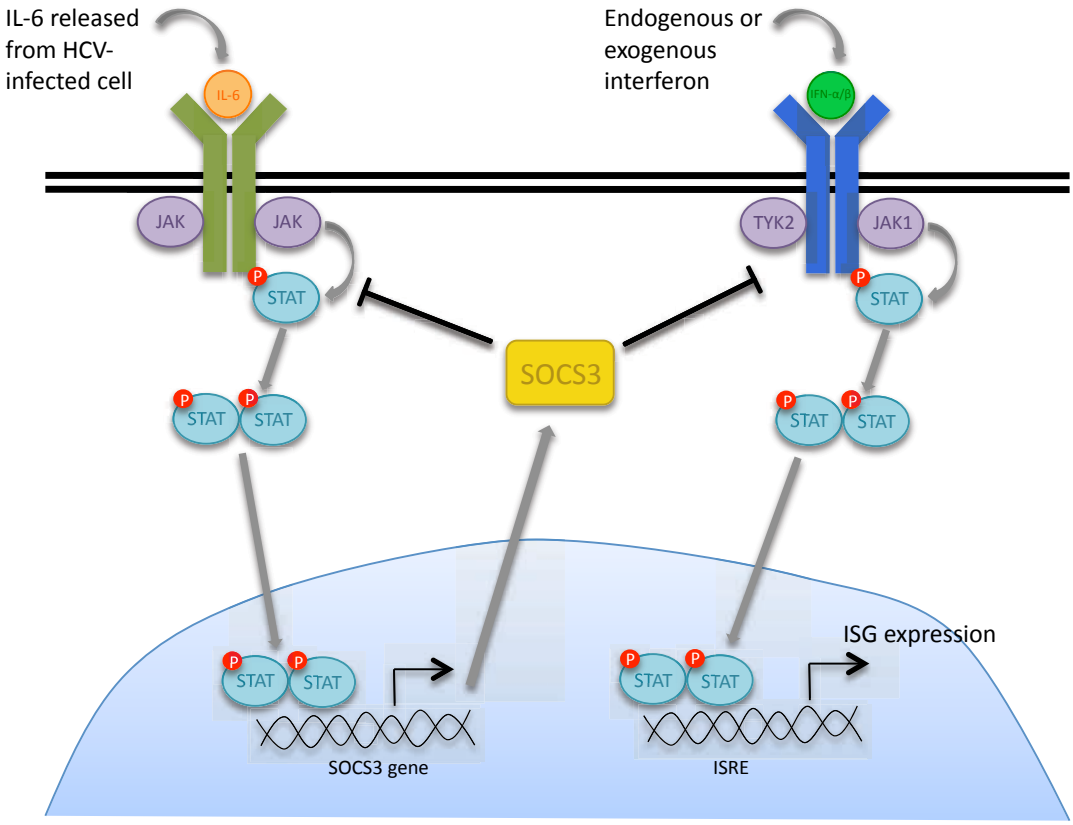

Figure 6.11 Suppressor of cytokine signaling 3 (SOCS3) pathways. Interleukin-6 (IL-6) stimulates the expression of SOCS3 which inhibits the JAK-STAT pathway. By inhibiting JAK-STAT signaling, SOCS3 suppresses the cellular response to endogenous and exogenous interferon and hence restricts interferon stimulated gene (ISG) expression, as well as having a negative feedback on cytokine signaling.

hepatocytes, although these cells may enhance cytokine responses to HCV in infected cells as discussed in Chapter 5.

In this Chapter, we have been able to extend our observation that conditioned media from HCV-infected Huh-7+TLR3 cells can exert an antiviral effect by demonstrating a similar effect in the co-culture setting. In a co-culture setting, HCV replication was suppressed in SGR-JFH1-RLuc cells co-cultured with Huh-7+TLR3 cells that were stimulated with Poly I:C or infected with HCV Jc1 compared to control. Co-culture did not appear to enhance the magnitude of this effect compared to the conditioned media work, perhaps suggesting that cell-to-cell contact does not play a major role in these effects although a contribution cannot be excluded.

It was not logistically possible during this study to perform cell contact studies between HCV-infected Huh-7 cells and stellate cells because major efforts were primarily directed towards development of the Huh-7 co-culture system. The hepatic stellate cell is known to reside in the space of Disse and is in close contact with hepatocytes (Friedman 2008). Cell contact studies to examine these interactions in the setting of HCV infection would therefore be of interest in future studies. As previously mentioned, using alternative hepatocyte cell lines such as the PH5CH8 cell line or primary hepatocytes in this model system in future studies will have advantages in addressing some of the limitations of the Huh-7 cell line.

In conclusion, we have developed cell culture models which allow for the co-culture of HCV-infected and uninfected Huh-7 cells and subsequent cell separation with high levels of purity, either through fluorescence activated cell sorting or using a magnetic bead-based cell separation system. Using these systems we have been

able to examine the transcriptome of uninfected cells that have been isolated from a co-culture with HCV-infected cells. We have observed in this Chapter that uninfected cells demonstrate increased expression of SOCS3 which is known to impair interferon signalling and hence bystander cells may contribute to HCV's persistence and ability to evade immune responses, as well as impair the response to exogenous interferon therapy.

Chapter 7
Conclusions and Future Directions

Hepatitis C virus infection is a major cause of chronic liver disease and hepatocellular carcinoma (HCC) worldwide. End-stage liver disease secondary to HCV infection is the leading indication for liver transplantation (Brown 2005; Charlton 2005; Te and Jensen 2010). Despite significant advances in research and treatment of HCV infection, much remains unknown regarding the pathogenesis of chronic liver disease due to HCV.

After the establishment of chronic HCV infection, which occurs in 70-80% of individuals acutely infected with HCV, a proportion of infected individuals will develop cirrhosis and/or HCC over the ensuing 20 to 30 years (Alter 1995). The mechanisms underlying this progression to advanced liver disease have not been fully elucidated. It is known that HCV causes hepatic inflammation via activation of innate and adaptive immunity as well as oxidative stress. The virus is able to evade these responses, leading to a state of low-grade, chronic inflammation in the infected liver. Hepatic inflammation stimulates fibrogenesis, leading to fibrosis and eventually cirrhosis (Pawlotsky 2004).

Interestingly, it has been shown that despite the apparent universal involvement of the liver in this process, only a small proportion of hepatocytes harbour replicating HCV (Liang *et al.* 2009; Kandathil *et al.* 2013). This seems to be dependent on individual patients and ranged from 1.7-45%. This raises the question of how HCV evokes such a significant pathological impact. Clearly, the infiltrating immune cells

and the associated proinflammatory cytokines that they produce can drive this progressive liver disease, however the role of the uninfected hepatocyte in this process has been largely ignored. We hypothesised that uninfected cells in the liver are recruited into the inflammatory milieu, expanding the effect of HCV beyond the infected hepatocytes. Particularly in the case of uninfected hepatocytes, there is a paucity of literature examining this phenomenon. Therefore, the aim of this study was to examine the effect of HCV-infected hepatocytes on uninfected 'bystander' cells and vice versa. We sought to develop cell culture models whereby HCV-infected and uninfected cells could interact via direct cell-to-cell contact but subsequently be examined separately.

To address some of the issues surrounding the role of the 'bystander' hepatocyte in HCV infection we developed a cell culture model that permits the examination of the effect of direct co-culture of HCV-infected and uninfected cells. Although there is an increasing body of work examining such interactions in conditioned media and 'Transwell' models, there is a paucity of literature examining the relationship between infected and uninfected cells in cell contact with each other. It has been shown that localized interactions between these cells do occur (Dansako *et al.* 2013), but the model described in this thesis is unique in that it allows for the infected and uninfected cells to be separated and the entire transcriptome of uninfected cells to be examined in isolation from infected cells. Future work to refine the model system, such as the use of primary hepatocytes and the extension of the model to other cell types such as stellate cells will improve its relevance to the *in vivo* situation and broaden its applications.

In order to prevent HCV infection of 'bystander' hepatocytes in co-culture with infected cells, we also generated a Huh-7 cell line that was refractory to HCV infection by knockdown of the essential HCV cell entry receptor, CD81. This cell line was not only employed in the co-culture system but also used in a number of conditioned media studies aimed at assessing the effect of soluble factors from HCV-infected cells on uninfected bystander hepatocytes. We also assessed the effect of conditioned media from HCV-infected cells on other cell types, including primary rat stellate cells and other HCV-infected cells.

During the course of this study, it became clear that the Huh-7 cell line commonly used in *in vitro* studies of HCV is relatively unresponsive to infection with HCV with regard to innate immune responses. It is this property to which the cell line probably owes its permissiveness to HCV infection. The lack of response likely relates to the fact that Huh-7 cells are Toll-like receptor 3 (TLR3)-deficient and express very little of the other RNA sensors such as RIG-I (Li *et al.* 2005). This thesis has added to the work of others (Wang *et al.* 2009; Li *et al.* 2012) by confirming the importance of TLR3 in the innate immune response to HCV infection. We have demonstrated upregulation of a large number of genes in response to both Poly I:C and HCV Jc1 infection in Huh-7+TLR3 cells, a number of which are cytokines and ISGs that are known to have antiviral activity against hepatitis C. It is these factors that are proposed to mediate effects on bystander cells. To our knowledge, this is the first report of microarray analysis of the response to HCV infection in TLR3-expressing cells. Interestingly, we report that HCV infection of these cells results in expression of many proinflammatory

cytokines and chemokines (e.g. CCL5, CXCL10, IL-8 (CXCL8)) that play a role in the recruitment of immune cells to sites of infection.

While the effects were not dramatic at the level of the transcriptome in bystander hepatocytes, we have demonstrated in this thesis that there is cross-talk between HCV-infected hepatocytes and uninfected hepatocytes, hepatic stellate cells and other HCV-infected hepatocytes. These interactions are bi-directional, and occur through both the release of soluble factors and direct cell-cell contact. These observations confirm the hypothesis that 'bystander' cells are involved in the response to HCV infection, despite not being directly infected with the virus.

The underlying mechanisms involved in these interactions are likely to be complex and multi-faceted. Due to time constraints it was not possible to characterize the precise mechanisms underlying our observations. However, preliminary data suggests that exosomes may play a role in cross-talk between cells and may exert an antiviral effect on HCV-infected cells, probably through transfer of antiviral or immunostimulatory factors between cells. Future work will seek to further define the role of exosomes in cell-cell interactions in HCV infection. It has previously been shown that exosomes may transfer HCV RNA to uninfected, non-permissive cells (Dreux *et al.* 2012). Additionally, exosomes have been shown to exert antiviral effects in HIV, hepatitis B and dengue virus infection (Tumne *et al.* 2009; Li *et al.* 2013; Zhu *et al.* 2014). To date, the antiviral effect of exosomes derived from infected hepatocytes in HCV infection has not been previously demonstrated and our work is novel in this regard, albeit preliminary. Future work is required to define the content of exosomes from HCV-infected hepatocytes. This could be

achieved through exosome purification and subsequent proteomics analysis or next-generation sequencing to determine RNA content.

We also sought to demonstrate that HCV-infected cells exerted effects on uninfected hepatocytes. We were unable to demonstrate significant changes in gene expression by microarray analysis in bystander hepatocytes either cultured in conditioned media from HCV-infected TLR3-positive Huh-7 cells or co-cultured with these cells. Further analysis of co-cultured bystander cells, however, suggested low-level but significant upregulation of SOCS3 in uninfected hepatocytes that had been co-cultured with HCV-infected Huh-7+TLR3 cells. As SOCS3 is known to inhibit the JAK-STAT pathway (Bode *et al.* 2003; Croker *et al.* 2003; Duong *et al.* 2004) and is associated with attenuated responses to exogenous interferon therapy against HCV (Walsh *et al.* 2006; Huang *et al.* 2007), it is possible that the expression of SOCS3 in some hepatocytes may provide a favourable environment for HCV infection through suppression of the JAK-STAT pathway and ISG expression. Furthermore, this observation shows that there is cross-talk occurring in our model system. It will be important to further optimize the cell culture model system that was used to demonstrate this effect so that more in-depth analysis of the role of upregulated SOCS3 in bystander cells can be performed.

Involvement of ‘bystander’ cells in HCV infection extends beyond other hepatocytes. It is well known that the stellate cell plays an important role in the fibrogenic response in the liver. We were able to demonstrate in this thesis that soluble factors secreted from Huh-7+TLR3 cells infected with HCV Jc1 exert effects on hepatic stellate cells, stimulating the expression of profibrogenic factors.

This confirms the work of other groups who have demonstrated that HCV itself and HCV-infected cells can activate stellate cells and stimulate a profibrogenic state (Bataller *et al.* 2004; Schulze-Krebs *et al.* 2005; Clement *et al.* 2010; Coenen *et al.* 2011; Presser *et al.* 2013). The stimulation of fibrogenesis by HCV and HCV-infected cells leads to hepatic fibrosis, with the end result of cirrhosis and its associated clinical manifestations. Stellate cells not only have a role in fibrogenesis but also play a role in the inflammatory response and they are known to secrete cytokines, such as CCL5 and CCL2 (Sprenger *et al.* 1997; Schwabe *et al.* 2003) which drive recruitment of immune cells to sites of infection. During the course of this thesis it was reported that conditioned media from LX2 cells could stimulate MIP-1β (CCL4) expression in HCV-infected Huh-7 cells, suggesting multiple levels of cross-talk in the HCV-infected liver (Nishitsuji *et al.* 2013). We confirmed that conditioned media from LX2 cells stimulated MIP-1β expression in HCV-infected Huh-7.5 cells, and hence stellate cells are recruited into the response to HCV infection in a bidirectional manner. We were able to add to the work of Nishitsuji et al. by demonstrating the same response in HCV-positive Huh-7.5 cells to conditioned media from TLR3-expressing Huh-7 cells, suggesting that uninfected hepatocytes also contribute to the inflammatory response to HCV infection in other cells. However, it is clear from this work that cells must be primed to respond in this manner, as uninfected cells do not respond in this way. This suggests that HCV infection must initiate the first step in order to allow the infected cell to then respond to factors secreted from other, uninfected cells.

In summary, it is clear that there are bidirectional interactions between HCV-infected hepatocytes and other resident liver cells such as hepatic stellate cells and uninfected hepatocytes, as well as interactions between infected hepatocytes. These interactions are summarized in Figure 7.1. These findings contribute to our knowledge of the pathogenesis of HCV-related liver disease in that they demonstrate wider involvement of other cells in the liver beyond those infected with the virus. The results of this work therefore assist in explaining why progression to chronic liver disease in HCV-infected individuals occurs in the absence of widespread hepatocyte infection. However, the underlying mechanisms of the interaction between cells warrant further study. In particular, our knowledge of these interactions in the context of cell-to-cell contact is limited and the model systems developed and described in this thesis will aid in future scrutiny of the cross-talk between cells.

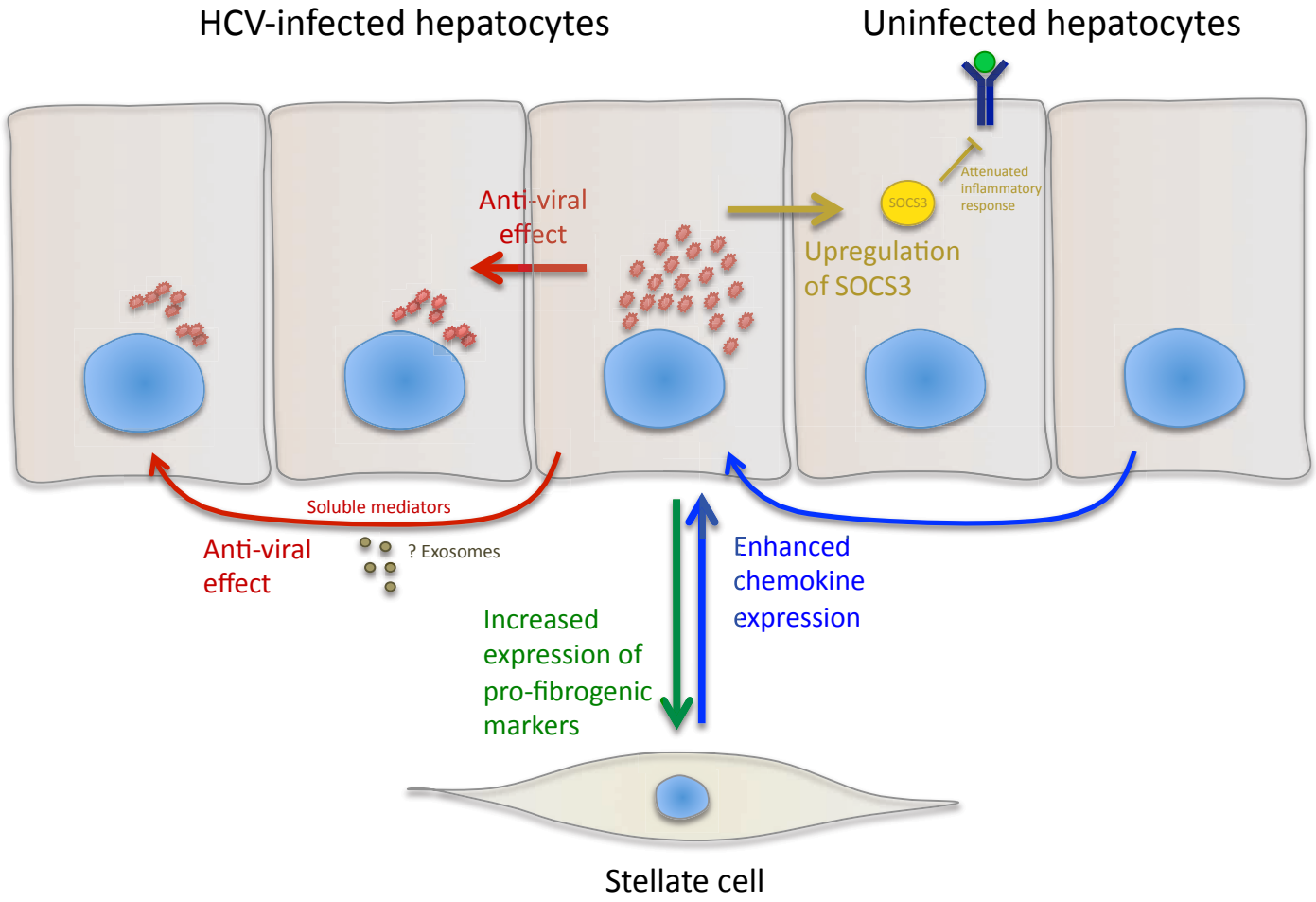

Figure 7.1 Summary of the interactions between HCV-infected hepatocytes and bystander cells

Appendix I

Plasmids

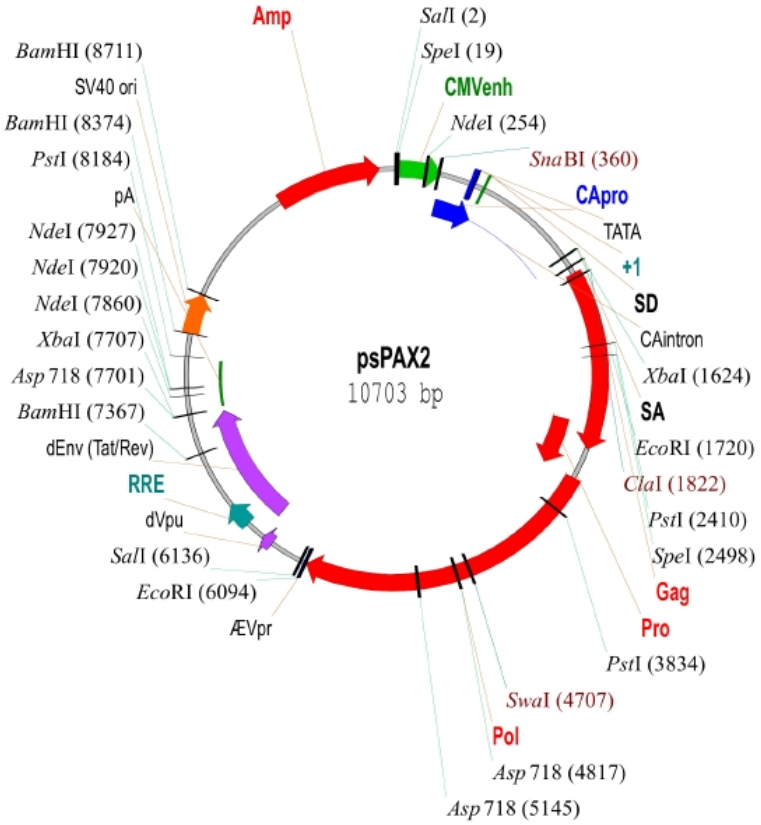

psPAX2

(Addgene)

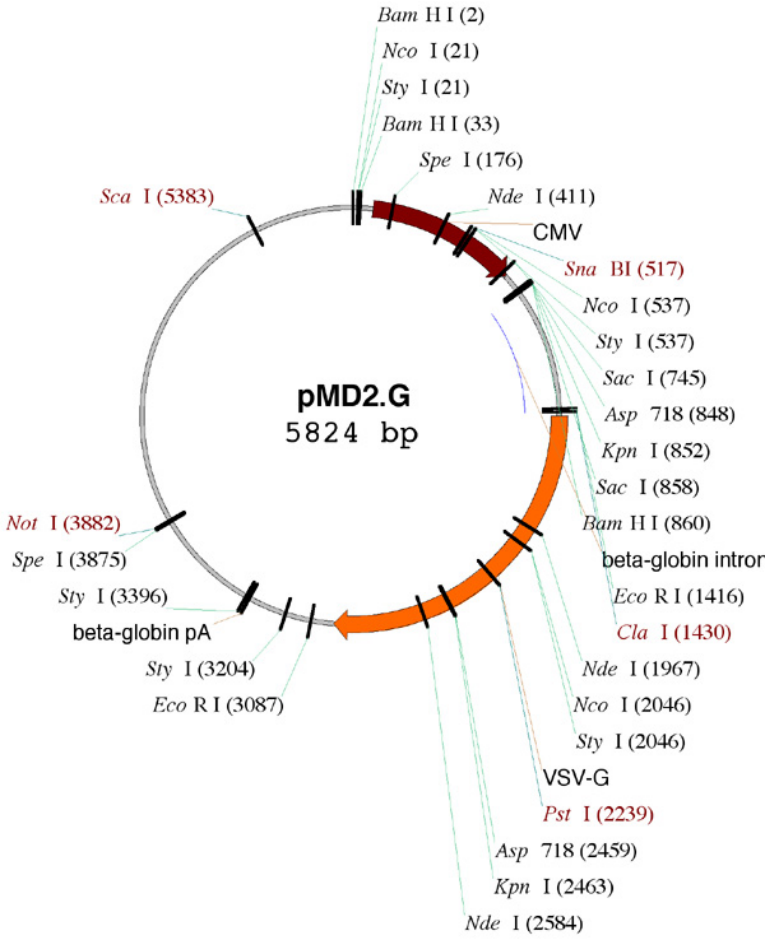

pMD2.G

(Addgene)

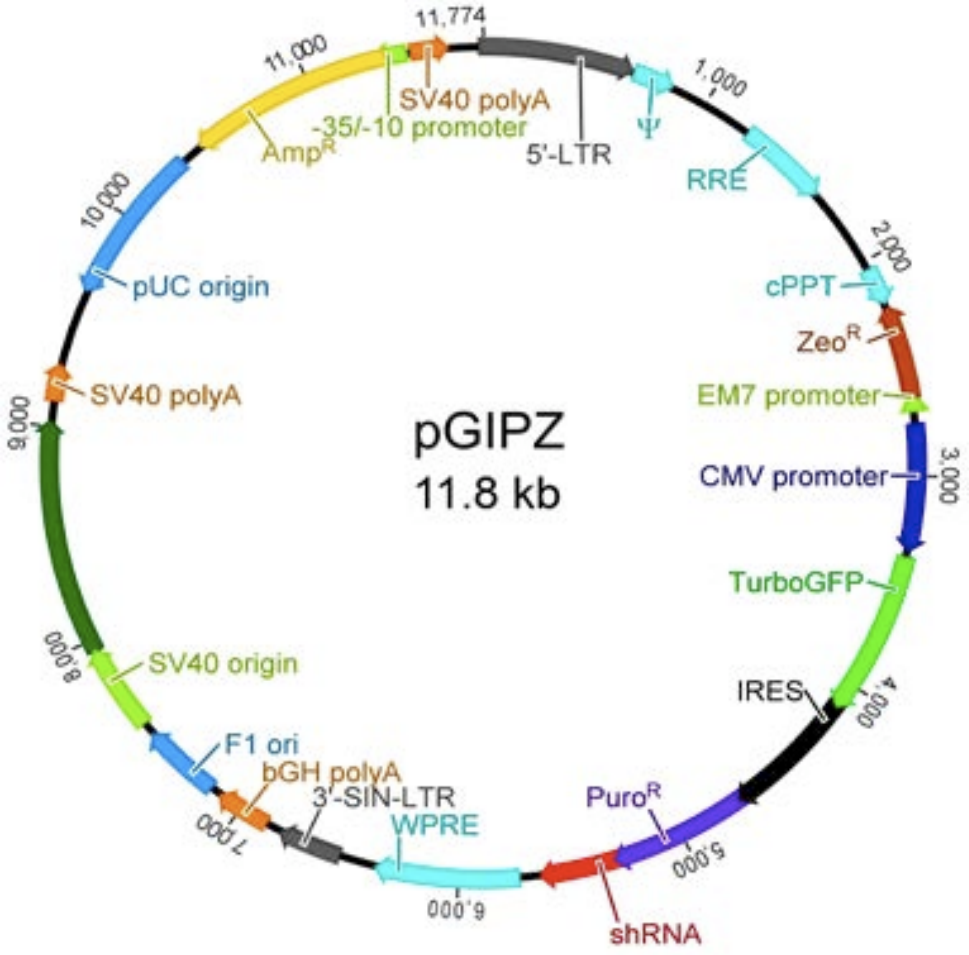

pGIPZ

(Open Biosystems, Thermo Scientific)

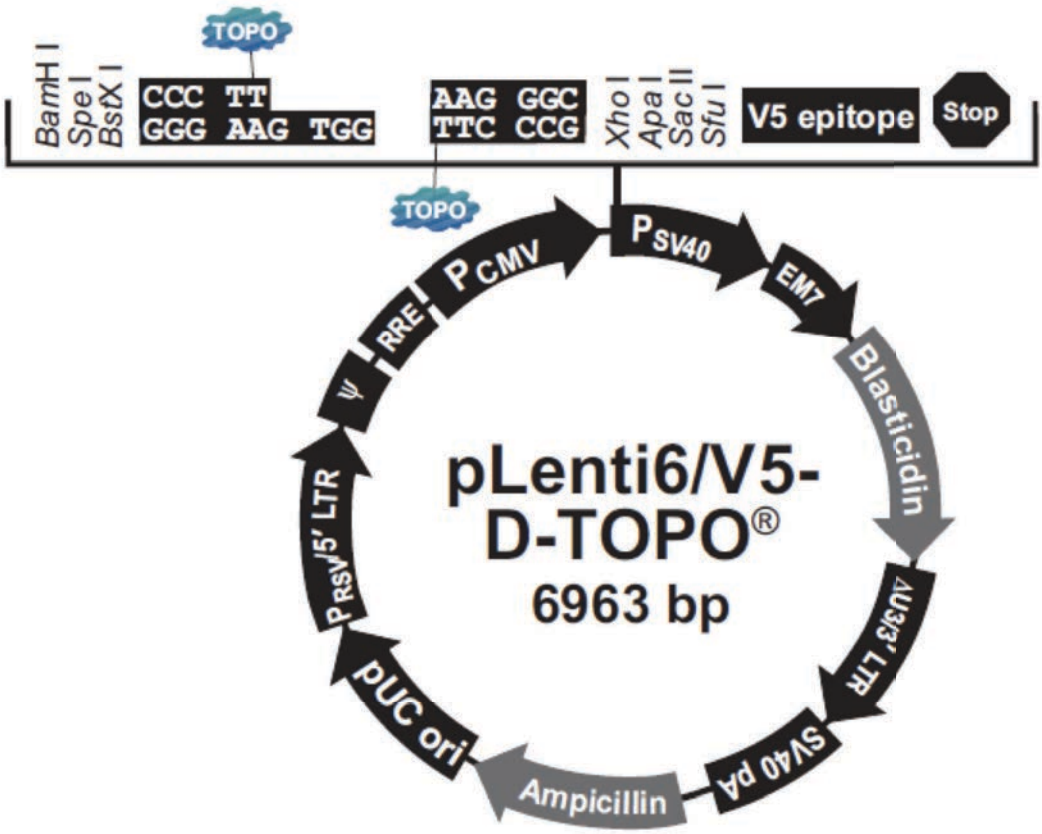

pLenti6/V5-D-TOPO

(Invitrogen, Life Technologies)

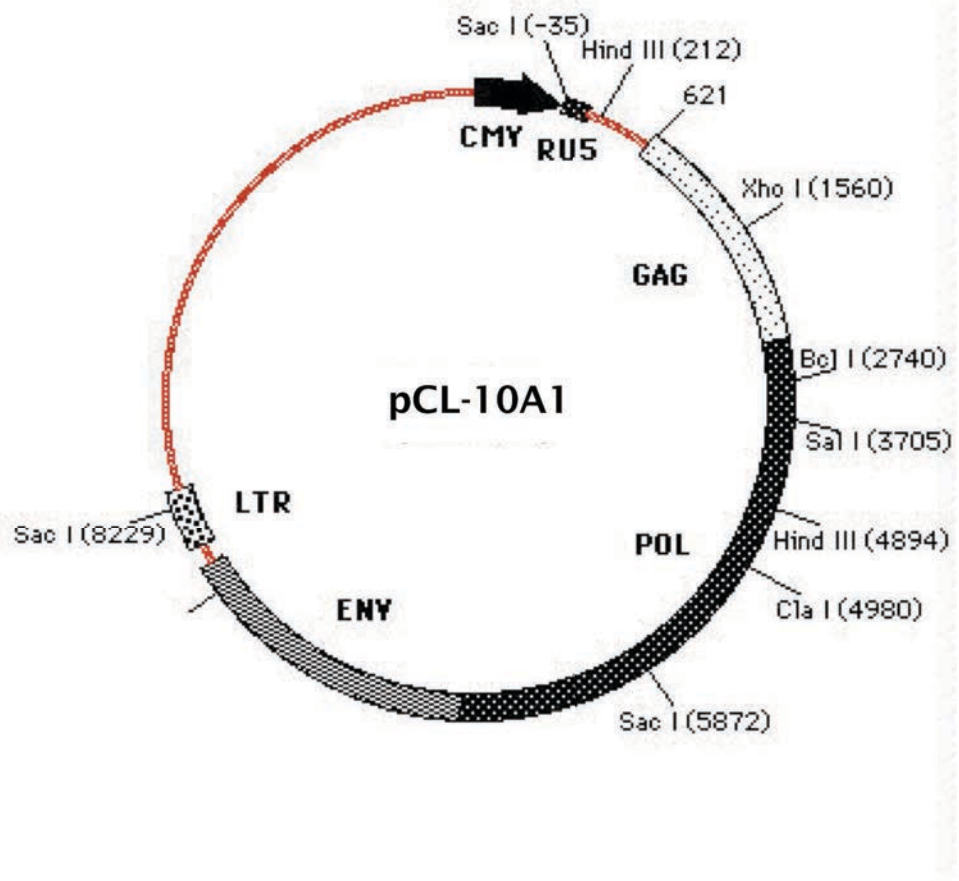

pCL-10A1

(Imgenex)

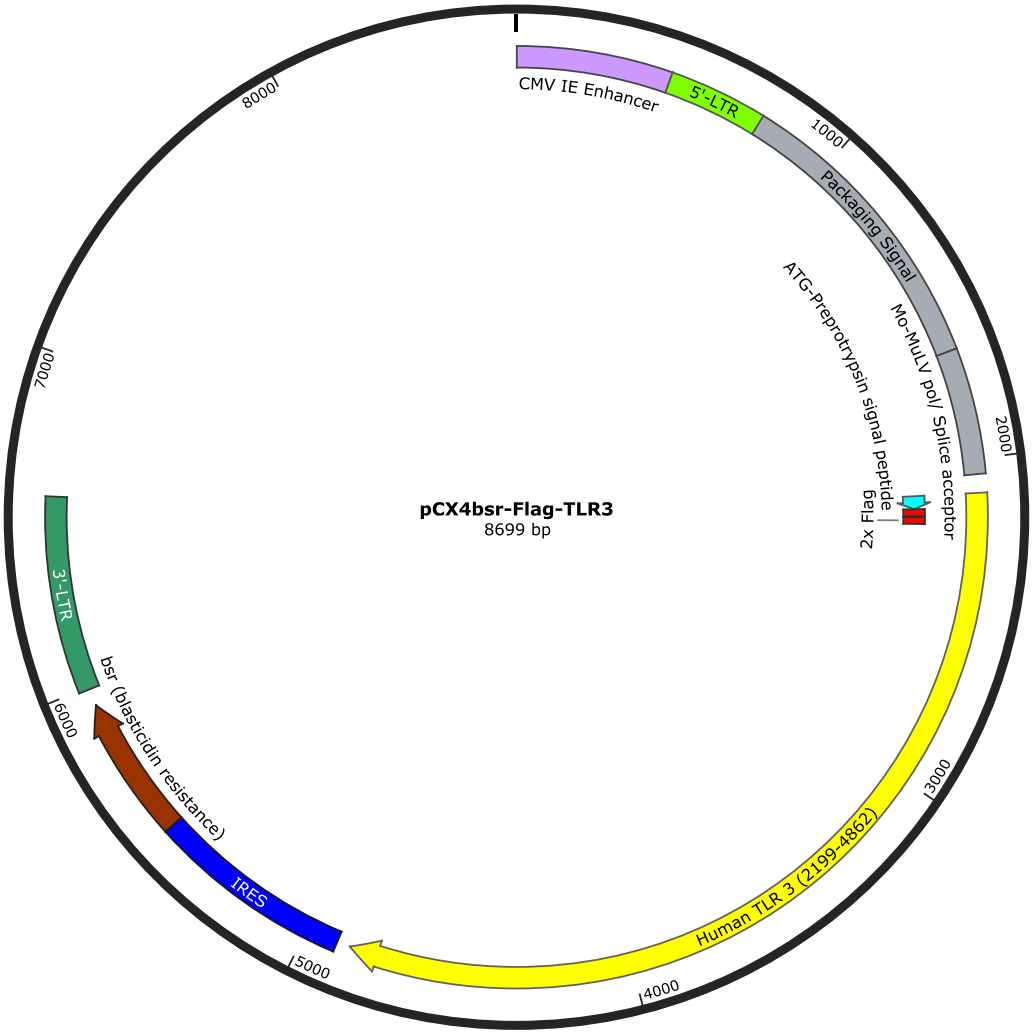

pCX4-bsr

pCX4bsr-ΔTIR is identical except codon 756-904 of human TLR3 has been deleted

Appendix II

Infectious HCV Constructs

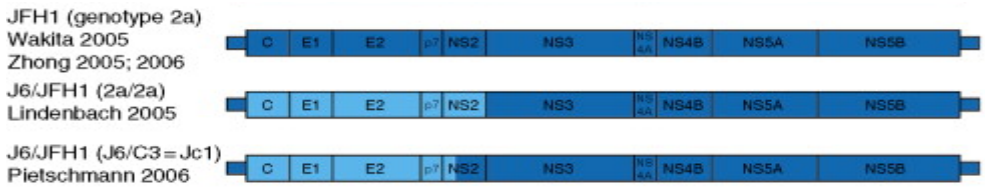

The chimeric Jc1 construct used in this thesis consists of sequences derived from the J6- and JFH1-genomes fused at a site located within NS2 (Pietschmann *et al.* 2006). *(Figure adapted from Gottwein and Bukh 2008).*

Appendix III

General Solutions and Buffers

Solutions obtained from the Central Services Unit, School of Molecular and Biomedical Science, University of Adelaide

Ethylenediaminetetraacetic acid, EDTA

Foetal bovine serum, FBS

Glycine-Tris-SDS, GTS

Luria Agar

Luria Agar + ampicillin plates

Luria broth

Phosphate buffered saline, PBS

0.85% saline

Sodium dodecyl sulfate, SDS

Super Optimal Broth with Catabolite Repression, SOC

Tris-acetic acid-EDTA, TAE

Tris buffered saline, TBS

Trypan Blue

Trypsin-EDTA

Solution components

RIPA buffer	1% NP-40 5% sodium deoxycholate 0.1% SDS in PBS
12% separating gel	12% acrylamide (Sigma) 0.4M Tris (pH 8.8) 0.1% SDS 0.1% ammonium persulfate (Sigma) 0.025% TEMED (Sigma)
5% stacking gel	5% acrylamide (Sigma) 0.13M Tris (pH 6.8) 0.1% SDS 0.1% ammonium persulfate (Sigma) 0.1% TEMED (Sigma)
5 x Loading buffer	3.8mL dH_2O 1mL 0.5M Tris-HCl (pH 6.8) 0.8mL hlycerol 1.6mL 10% (w/v) SDS 0.4mL 2-mercaptoethanol 0.4mL 1% (w/v) bromophenol blue
Running buffer (GTS)	0.3% glycine 14.4% Tris 1% SDS (w/v)
Transfer buffer	0.3% Tris (Amresco) 1.44% glycine (Amresco) 20% methanol (v/v)
TBS-T	50mM Tris 150mM NaCl 0.05% Tween 20 (Sigma)
FACS wash buffer	PBS 1% FBS (v/v) 10mM NaN_3
FACS fixative solution	PBS 0.1% formalin (v/v) 111mM D-glucose 10mM NaN_3
FACS sort buffer	DMEM 25mM HEPES 5mM EDTA 1% FBS

Competent cells

The genotype of the α-Select Chemically Competent Cells (Bioline) used was:

*deoR endA*1 *recA*1 *gyrA*96 *hsdR*17(r_k^- m_k^+) *supE*44 *thi*-1 *Δ(lacZYA-argFV*169) *Φ80δlacZΔ*M15 F^- γ^-

Appendix IV

Short hairpin RNA (shRNA) sequences

Claudin-1 shRNA (Open Biosystems)

‘A-10’ Antisense (Clone ID V2LHS_67152): TTCCTCATAAGACACAGTG

‘A-12’ Antisense (Clone ID V2LHS_67150): TCTTGAACGATTCTATTGC

‘C-3’ Antisense (Clone ID V2LHS_67148): TCAGCAAGGAGTCAAAGAC

‘F-7’ Antisense (Clone ID V3LHS_360279): TCTATTGCCATACCATGCT

‘G-11’ Antisense (Clone ID V3LHS_408567): TTTGTAATACCATACTTCA

‘H-4’ Antisense (Clone ID V2LHS_67151): GGCTACGAAAGACACCGAT

CD81 shRNA (Open Biosystems)

‘C-8’ Antisense (Clone ID V2LHS_240779): TATACACAGGCGGTGATGG

‘C-10’ Antisense (Clone ID V2LHS_14888): TACAGTTGAAGGCGACGTG

‘E-8’ Antisense (Clone ID V2LHS_242799): TATTAAATGACGGAGTCAG

‘E-10’ Antisense (Clone ID V3LHS_304175): TGTTCTTGAGCACTGAGGT

‘F-10’ Antisense (Clone ID V2LHS_14889): AACTGCTTCACATCCTTGG

‘H-8’ Antisense (Clone ID V2LHS_14886): TGTGATTACAGTTGAAGGC

H-10’ Antisense (Clone ID V3LHS_304176): AGAACTGCTTCACATCCTT

Appendix V

Principal component analysis

Affymetrix Microarray – Huh-7+CD81 knockdown + Huh-7+Jc1 conditioned media, 72 hours

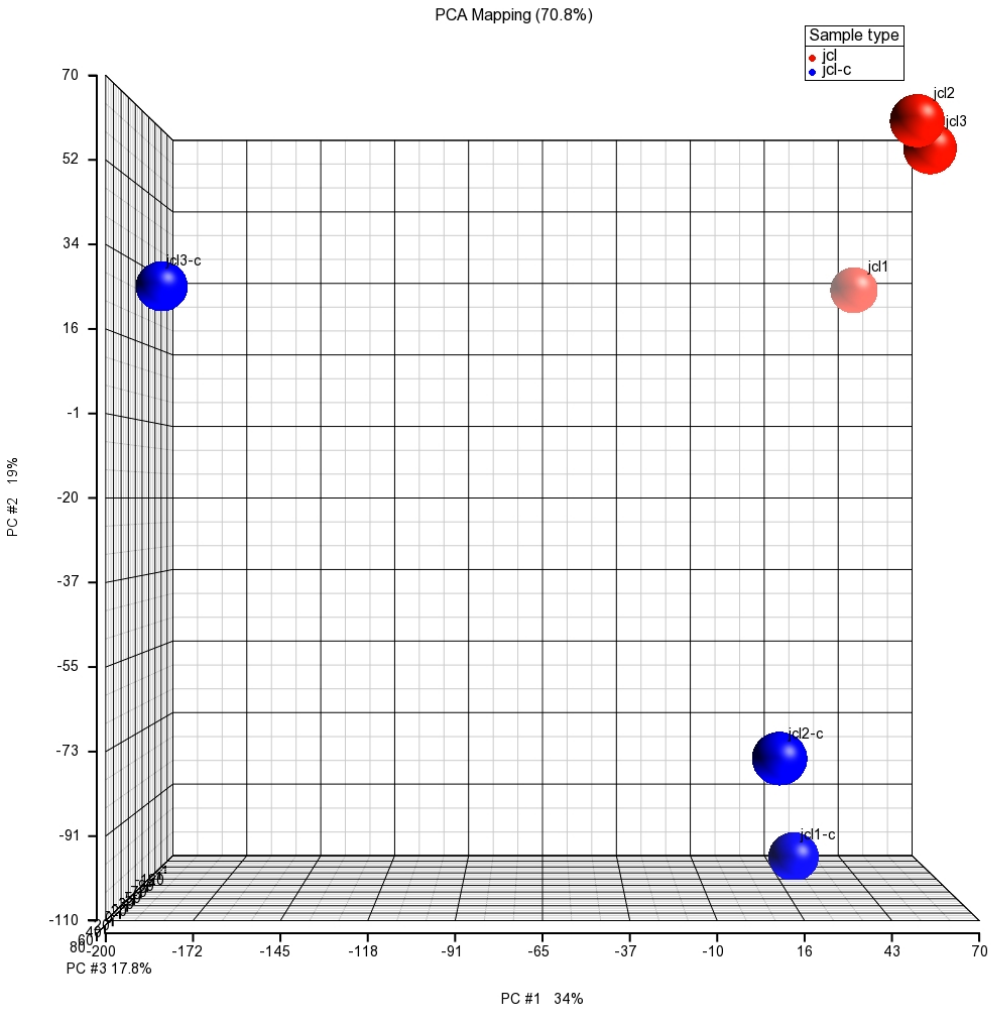

jci = HCV Jc1-infected conditioned media
jci-c = Control conditioned media

Affymetrix Microarray – Huh-7 + HCV-replicon (NNeo-C5B) conditioned media, 72 hours

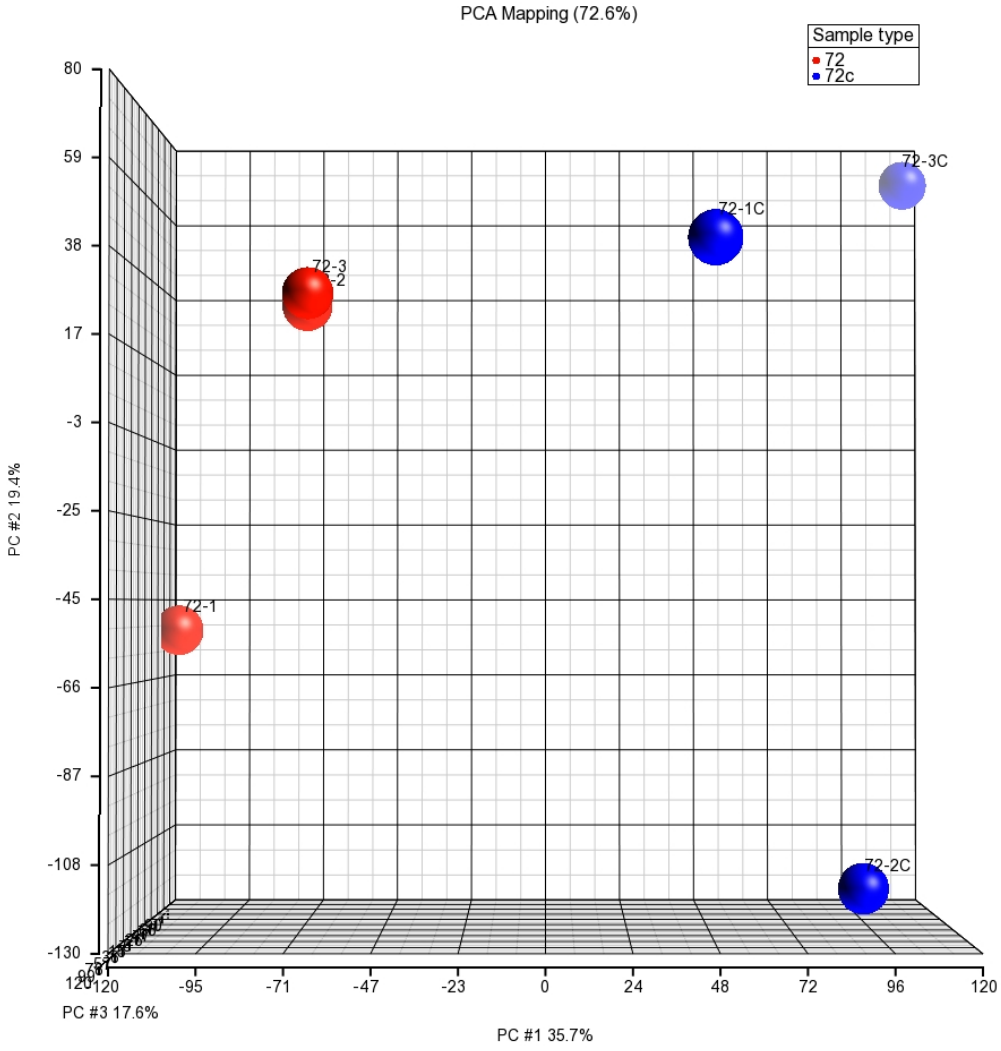

72 = HCV replicon conditioned media
72c = Control conditioned media

Affymetrix Microarray – ΔTIR vs TLR3, Poly I:C, 24 hours

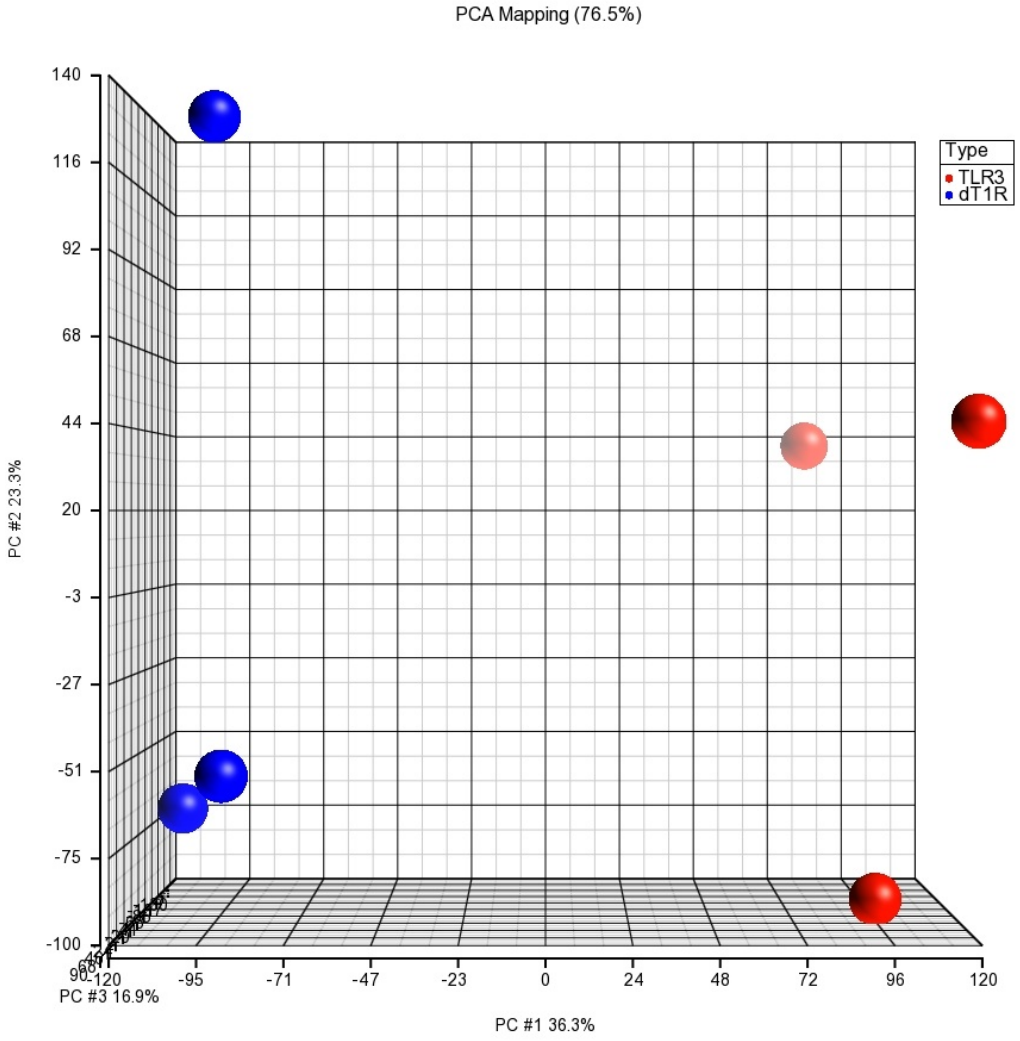

TLR3 = Huh-7+TLR3
dT1R = Huh-7+ΔTIR

Affymetrix Microarray – ΔTIR vs TLR3, HCV Jc1, 72 hours

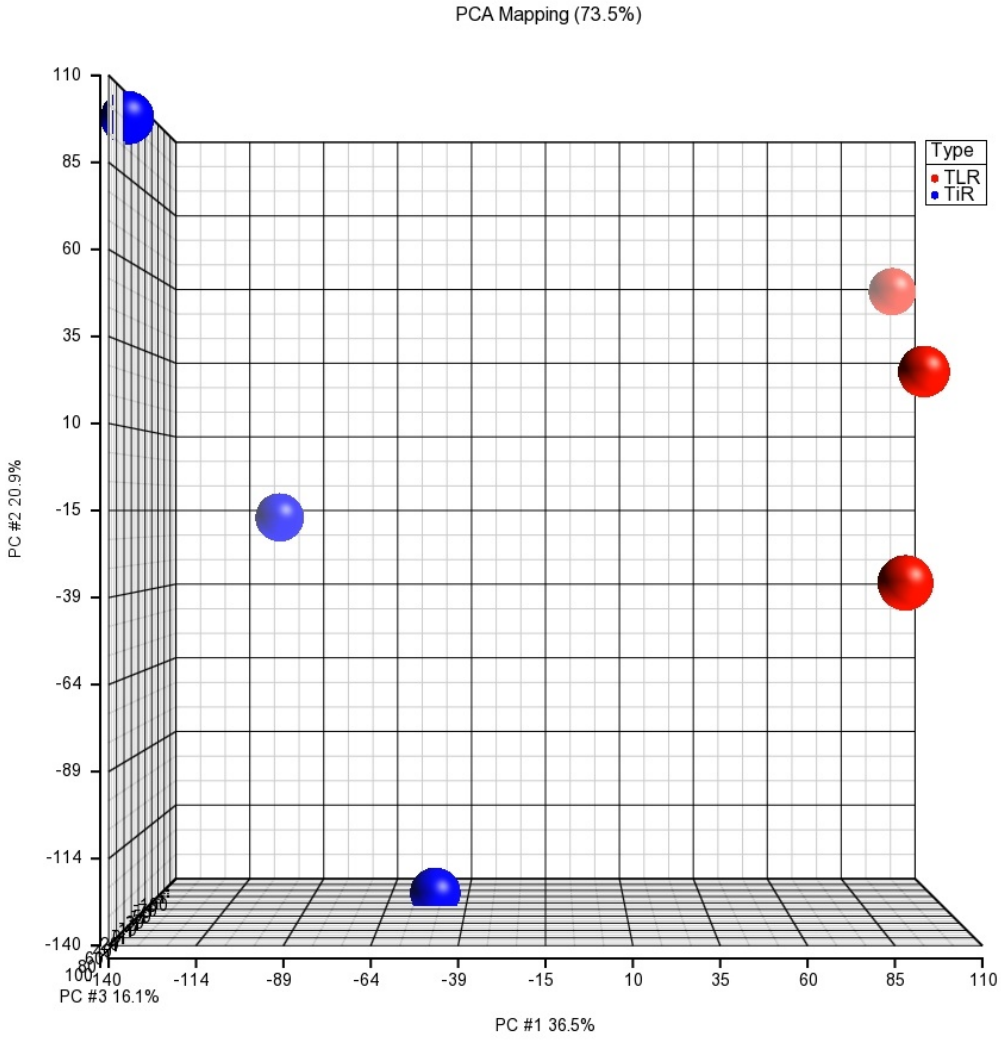

TLR3 = Huh-7+TLR3
TiR = Huh-7+ΔTIR

Affymetrix Microarray – Huh-7+CD81 knockdown hepatocytes following co-culture with HCV-infected Huh-7+TLR3

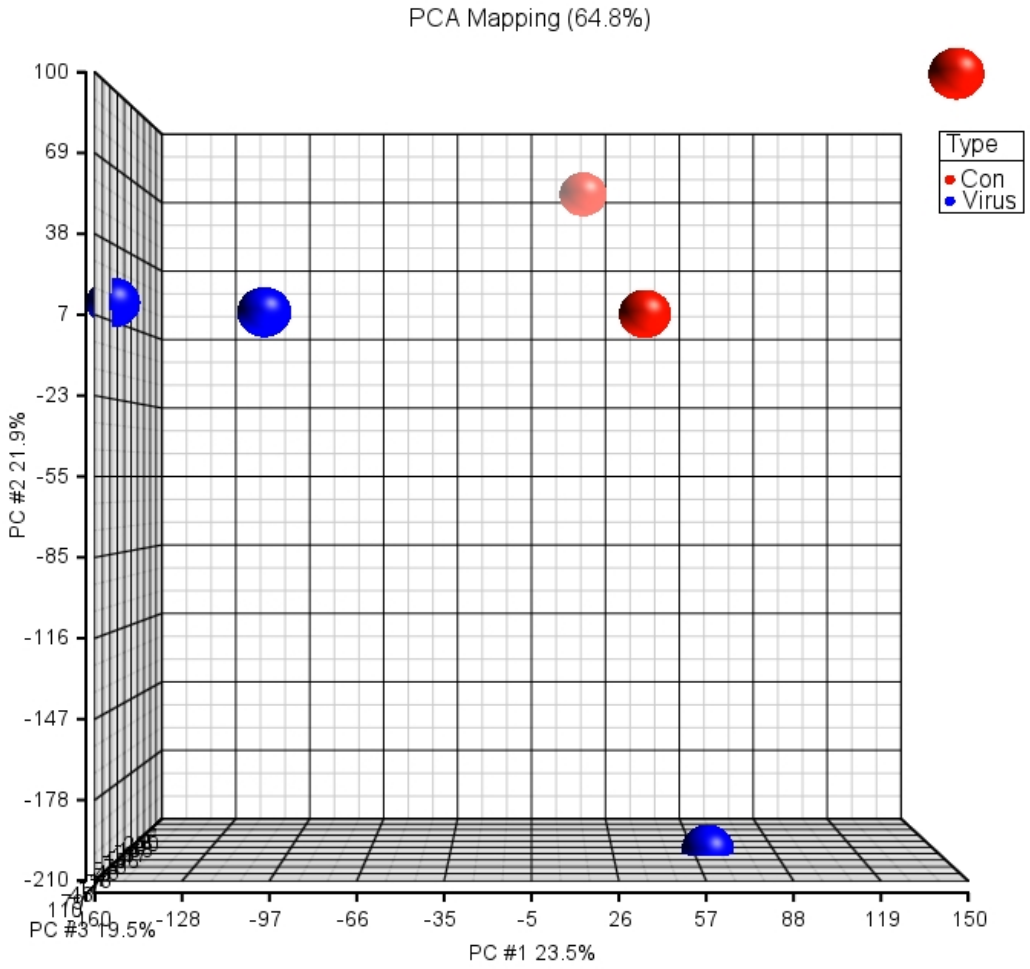

Con = Control
Virus = HCV Jc1-infected

Appendix VI
Human Antiviral Response PCR Array

Gene		Fold change			
		Poly I:C stimulation	*p* value	HCV Jc1 infection	*p* value
AIM2	Absent in melanoma 2	1.6812	ns	1.4575	ns
APOBEC3G	Apolipoprotein B mRNA editing enzyme, catalytic polypeptide-like 3G	1.1258	0.039469	2.2178	ns
ATG5	ATG5 autophagy related 5 homolog (S. cerevisiae)	1.0661	ns	1.7285	0.002573
AZI2	5-azacytidine induced 2	0.9401	ns	1.2875	ns
CARD9	Caspase recruitment domain family, member 9	0.9694	ns	1.7531	ns
CASP1	Caspase 1, apoptosis-related cysteine peptidase (interleukin 1, beta, convertase)	1.4502	ns	2.2747	ns
CASP10	Caspase 10, apoptosis-related cysteine peptidase	1.3035	ns	2.4085	0.004552
CASP8	Caspase 8, apoptosis-related cysteine peptidase	0.9953	ns	1.5463	ns
CCL3	Chemokine (C-C motif) ligand 3	4.6619	0.009179	205.2373	0.001144
CCL5	Chemokine (C-C motif) ligand 5	60.0944	0.001715	41.1888	0.003622
CD40	CD40 molecule, TNF receptor superfamily member 5	2.2487	ns	2.0091	ns
CD80	CD80 molecule	1.4889	ns	1.7713	ns
CD86	CD86 molecule	1.2675	ns	2.4279	0.012008
CHUK	Conserved helix-loop-helix ubiquitous kinase	0.7462	ns	0.9668	ns
CTSB	Cathepsin B	0.7602	ns	1.1895	ns
CTSL1	Cathepsin L1	0.9163	ns	0.4094	ns
CTSS	Cathepsin S	2.159	0.005248	1.4795	0.034935
CXCL10	Chemokine (C-X-C motif) ligand 10	1.171	ns	4.1576	0.000642
CXCL11	Chemokine (C-X-C motif) ligand 11	18.5502	0.007526	19.4157	0.001483
CXCL9	Chemokine (C-X-C motif) ligand 9	15.8444	0.000988	5.638	ns
CYLD	Cylindromatosis (turban tumor syndrome)	0.9499	ns	1.8311	ns
DAK	Dihydroxyacetone kinase 2 homolog (S. cerevisiae)	0.8162	ns	0.9044	ns
DDX3X	DEAD (Asp-Glu-Ala-Asp) box polypeptide 3, X-linked	0.827	ns	0.8901	ns
DDX58	DEAD (Asp-Glu-Ala-Asp) box polypeptide 58	1.3378	ns	2.312	0.004064
DHX58	DEXH (Asp-Glu-X-His) box polypeptide 58	0.4042	ns	1.5787	ns
FADD	Fas (TNFRSF6)-associated via death domain	0.9975	ns	1.1976	ns
FOS	FBJ murine osteosarcoma viral oncogene homolog	0.7283	ns	1.506	0.023632
HSP90AA1	Heat shock protein 90kDa alpha (cytosolic), class A member 1	0.7787	ns	1.0236	ns
IFIH1	Interferon induced with helicase C domain 1	1.6325	0.033484	2.0015	0.001369
IFNA1	Interferon, alpha 1	1.0443	ns	1.8884	ns
IFNA2	Interferon, alpha 2	1.4475	ns	1.0265	ns
IFNAR1	Interferon (alpha, beta and omega) receptor 1	1.1421	ns	0.858	ns
IFNB1	Interferon, beta 1, fibroblast	1.0382	ns	0.3733	ns
IKBKB	Inhibitor of kappa light polypeptide gene enhancer in B-cells, kinase beta	1.0032	ns	1.169	ns
IL12A	Interleukin 12A (natural killer cell stimulatory factor 1, cytotoxic lymphocyte maturation factor 1, p35)	0.3906	0.000017	0.5927	0.003354
IL12B	Interleukin 12B (natural killer cell stimulatory factor 2, cytotoxic lymphocyte maturation factor 2, p40)	0.6493	ns	1.0364	ns
IL15	Interleukin 15	1.3376	0.004471	2.3444	0.024371
IL18	Interleukin 18 (interferon-gamma-inducing factor)	2.6949	0.000706	2.0889	0.001292
IL1B	Interleukin 1, beta	1.8237	0.036425	1.062	ns
IL6	Interleukin 6 (interferon, beta 2)	2.7043	0.003823	4.2362	0.017961
IL8	Interleukin 8	1.9431	0.007808	3.3478	0.000444
IRAK1	Interleukin-1 receptor-associated kinase 1	0.9847	ns	1.1207	ns
IRF3	Interferon regulatory factor 3	0.8273	ns	0.9572	ns
IRF5	Interferon regulatory factor 5	0.6498	ns	0.7533	ns
IRF7	Interferon regulatory factor 7	1.2737	ns	0.9836	ns

Table cont.

Gene		Fold change			
		Poly I:C stimulation	*p* value	HCV Jc1 infection	*p* value
ISG15	ISG15 ubiquitin-like modifier	1.0621	ns	2.0074	0.000138
JUN	Jun proto-oncogene	0.7919	ns	1.1092	ns
MAP2K1	Mitogen-activated protein kinase kinase 1	0.7919	ns	1.2859	ns
MAP2K3	Mitogen-activated protein kinase kinase 3	1.0955	ns	2.206	0.002632
MAP3K1	Mitogen-activated protein kinase kinase kinase 1	0.9154	ns	1.1194	ns
MAP3K7	Mitogen-activated protein kinase kinase kinase 7	0.8071	ns	1.068	ns
MAPK1	Mitogen-activated protein kinase 1	0.5784	ns	0.7244	ns
MAPK14	Mitogen-activated protein kinase 14	1.0407	ns	1.2648	ns
MAPK3	Mitogen-activated protein kinase 3	0.8122	ns	1.0183	ns
MAPK8	Mitogen-activated protein kinase 8	0.8281	ns	0.9198	ns
MAVS	Mitochondrial antiviral signaling protein	0.8731	ns	0.8482	ns
MEFV	Mediterranean fever	0.1659	ns	2.2049	ns
MX1	Myxovirus (influenza virus) resistance 1, interferon-inducible protein p78 (mouse)	1.3352	ns	1.3179	ns
MYD88	Myeloid differentiation primary response gene (88)	0.8873	ns	0.877	ns
NFKB1	Nuclear factor of kappa light polypeptide gene enhancer in B-cells 1	1.1231	ns	1.9295	ns
NFKBIA	Nuclear factor of kappa light polypeptide gene enhancer in B-cells inhibitor, alpha	1.0108	ns	1.7839	0.03139
NLRP3	NLR family, pyrin domain containing 3	1.0608	ns	0.4773	ns
NOD2	Nucleotide-binding oligomerization domain containing 2	2.4949	0.023493	1.252	ns
OAS2	2'-5'-oligoadenylate synthetase 2, 69/71kDa	23.3865	0.019757	3.0062	ns
PIN1	Peptidylprolyl cis/trans isomerase, NIMA-interacting 1	0.6604	0.017567	0.8449	ns
PSTPIP1	Proline-serine-threonine phosphatase interacting protein 1	1.0307	ns	1.8184	ns
PYCARD	PYD and CARD domain containing	1.74	0.010709	1.5486	ns
PYDC1	PYD (pyrin domain) containing 1	0.9139	ns	1.582	ns
RELA	V-rel reticuloendotheliosis viral oncogene homolog A (avian)	0.9134	ns	1.0576	ns
RIPK1	Receptor (TNFRSF)-interacting serine-threonine kinase 1	1.16	ns	1.3368	ns
SPP1	Secreted phosphoprotein 1	2.1047	0.002198	2.6936	0.001869
STAT1	Signal transducer and activator of transcription 1, 91kDa	1.348	ns	1.9352	0.013159
SUGT1	SGT1, suppressor of G2 allele of SKP1 (S. cerevisiae)	0.8301	ns	1.1696	ns
TBK1	TANK-binding kinase 1	0.7464	ns	0.8779	0.033762
TICAM1	Toll-like receptor adaptor molecule 1	0.9042	ns	1.1437	ns
TLR3	Toll-like receptor 3	647.2248	0.000035	1876.7154	0.000467
TLR7	Toll-like receptor 7	0.8555	ns	0.481	ns
TLR8	Toll-like receptor 8	1.0418	ns	1.0265	ns
TLR9	Toll-like receptor 9	0.8885	ns	4.0266	ns
TNF	Tumor necrosis factor	1.0677	ns	1.364	ns
TRADD	TNFRSF1A-associated via death domain	1.0108	ns	0.9554	ns
TRAF3	TNF receptor-associated factor 3	0.8668	ns	1.3587	ns
TRAF6	TNF receptor-associated factor 6	0.753	ns	0.8416	0.004057
TRIM25	Tripartite motif containing 25	1.0578	ns	1.5504	ns

ns not significant

Appendix VII

Affymetrix Microarray – ΔTIR vs TLR3 – Poly I:C

Gene Identifier	Gene Name	Fold Change	adj. *p* value
NM_004139	Lipopolysaccharide binding protein	36.2	0.000021
NM_002985	Chemokine (C-C motif) ligand 5	32.93	0.000083
NM_138938	Regenerating islet-derived 3 alpha	25.01	0.000311
NM_002038	Interferon, alpha-inducible protein 6	24.35	0.000038
NM_017631	DEAD (Asp-Glu-Ala-Asp) box polypeptide 60	19.75	0.000002
NM_030754	Serum amyloid A2	17.1	0.000101
NM_005143	Haptoglobin	15.67	0.000041
NM_001910	Cathepsin E	13.87	0.000041
NM_007231	Solute carrier family 6 (amino acid transporter), member 14	11.68	0.000021
NM_006398	Ubiquitin D	10.89	0.000086
NM_006398	Ubiquitin D	10.82	0.000086
NM_004585	Retinoic acid receptor responder (tazarotene induced) 3	9.54	0.000043
NM_002423	Matrix metallopeptidase 7 (matrilysin, uterine)	9.48	0.000077
NM_000610	CD44 molecule (Indian blood group)	9.44	0.000076
NM_001565	Chemokine (C-X-C motif) ligand 10	8.54	0.000083
NM_002543	Oxidized low density lipoprotein (lectin-like) receptor 1	7.97	0.000522
NM_001085	Serpin peptidase inhibitor, clade A (alpha-1 antiproteinase, antitrypsin), member 3	7.53	0.000021
NM_006417	Interferon-induced protein 44	7.28	0.000156
NM_002960	S100 calcium binding protein A3	7.28	0.000402
NM_020995	Haptoglobin-related protein	7.24	0.000086
NM_002462	Myxovirus (influenza virus) resistance 1, interferon-inducible protein p78 (mouse)	7.24	0.000014
NM_018284	Guanylate binding protein 1, interferon-inducible, 67kDa	7.09	0.000064
NM_002994	Chemokine (C-X-C motif) ligand 5	6.82	0.000014
NM_078625	Vanin 3	6.7	0.000214
NM_004079	Cathepsin S	6.63	0.000181
NM_001486	Glucokinase (hexokinase 4) regulator	6.44	0.000467
NM_001548	Interferon-induced protein with tetratricopeptide repeats 1	6.08	0.000190
NM_005564	Lipocalin 2	6.06	0.000059
NM_014391	Ankyrin repeat domain 1 (cardiac muscle)	5.95	0.000101
NM_001785	Cytidine deaminase	5.85	0.000062
NM_001710	Complement factor B	5.8	0.000043
NM_001710	Complement factor B	5.7	0.000043
NM_001165	Baculoviral IAP repeat-containing 3	5.67	0.000113
NM_001733	Complement component 1, r subcomponent	5.58	0.000021
NM_005195	CCAAT/enhancer binding protein (C/EBP), delta	5.17	0.000055
NM_001710	Complement factor B	5.06	0.000126
NM_006084	Interferon regulatory factor 9	4.95	0.000080
NM_001562	Interleukin 18 (interferon-gamma-inducing factor)	4.92	0.000192
NM_001024465	Superoxide dismutase 2, mitochondrial	4.85	0.000041
NM_000584	Interleukin 8	4.8	0.000101
NM_004665	Vanin 2	4.79	0.000471
NM_002993	Chemokine (C-X-C motif) ligand 6 (granulocyte chemotactic protein 2)	4.71	0.000080

NM_006820	Interferon-induced protein 44-like	4.69	0.000277
NM_003641	Interferon induced transmembrane protein 1 (9-27)	4.61	0.000223
NM_001511	Chemokine (C-X-C motif) ligand 1 (melanoma growth stimulating activity, alpha)	4.57	0.000091
NM_002260	Killer cell lectin-like receptor subfamily C, member 2	4.56	0.000318
NM_007028	Tripartite motif-containing 31	4.55	0.000043
NM_002053	Guanylate binding protein 1, interferon-inducible, 67kDa	4.53	0.000079
NM_152367	Chromosome 1 open reading frame 161	4.46	0.001442
NM_030641	Apolipoprotein L, 6	4.32	0.000098
NM_007028	Tripartite motif-containing 31	4.22	0.000064
NM_016816	2,5-oligoadenylate synthetase 1, 40/46kDa	4.22	0.000126
NM_007028	Tripartite motif-containing 31	4.2	0.000060
NM_005409	Chemokine (C-X-C motif) ligand 11	4.19	0.002152
NM_003812	ADAM metallopeptidase domain 23	4.11	0.000021
NM_017912	Hect domain and RLD 6	4.06	0.000080
NM_201442	Complement component 1, s subcomponent	4.06	0.000086
NM_002160	Tenascin C	3.98	0.000101
NM_016235	G protein-coupled receptor, family C, group 5, member B	3.95	0.000043
NR_015379	urothelial cancer associated 1	3.92	0.000294
NM_022168	Interferon induced with helicase C domain 1	3.91	0.000904
NM_017654	Sterile alpha motif domain containing 9	3.88	0.000190
NM_004613	Transglutaminase 2 (C polypeptide, protein-glutamine-gamma-glutamyltransferase)	3.86	0.000131
NM_014470	Rho family GTPase 1	3.85	0.000070
NM_021199	Sulfide quinone reductase-like (yeast)	3.83	0.000126
NM_139248	Lipase, member H	3.78	0.000324
NM_002089	Chemokine (C-X-C motif) ligand 2	3.74	0.000153
NM_005567	Lectin, galactoside-binding, soluble, 3 binding protein	3.73	0.000059
NM_145343	Apolipoprotein L, 1	3.72	0.000269
NM_021187	Cytochrome P450, family 4, subfamily F, polypeptide 11	3.72	0.000277
NM_006512	Serum amyloid A4, constitutive	3.52	0.000190
NM_030754	Serum amyloid A2	3.51	0.001104
NM_001561	Tumor necrosis factor receptor superfamily, member 9	3.48	0.000062
NM_000354	Serpin peptidase inhibitor, clade A (alpha-1 antiproteinase, antitrypsin), member 7	3.47	0.000312
NM_001031683	Interferon-induced protein with tetratricopeptide repeats 3	3.46	0.000324
NM_002640	Serpin peptidase inhibitor, clade B (ovalbumin), member 8	3.38	0.000195
NM_001775	CD38 molecule	3.35	0.000178
NM_006290	Tumor necrosis factor, alpha-induced protein 3	3.31	0.000235
NM_000700	Annexin A1	3.28	0.000173
NM_000050	Argininosuccinate synthetase 1	3.28	0.000190
NR_024240	major histocompatibility complex, class I, J (pseudogene)	3.27	0.000284
NM_002205	Integrin, alpha 5 (fibronectin receptor, alpha polypeptide)	3.25	0.000219
NR_024320	lipopolysaccharide-induced TNF factor	3.19	0.000451
NM_000433	Neutrophil cytosolic factor 2	3.16	0.000165
NM_006169	Nicotinamide N-methyltransferase	3.13	0.005798
NM_052972	Leucine-rich alpha-2-glycoprotein 1	3.12	0.000080
NM_005460	Synuclein, alpha interacting protein	3.12	0.000471
NM_004370	Collagen, type XII, alpha 1	3.12	0.000235
NM_001531	Major histocompatibility complex, class I-related	3.11	0.000589
NM_001001435	Chemokine (C-C motif) ligand 4-like 1	3.1	0.001267
NM_001001435	Chemokine (C-C motif) ligand 4-like 1	3.1	0.001267

NM_002261	Killer cell lectin-like receptor subfamily C, member 3	3.07	0.000462
ENST00000396451	killer cell lectin-like receptor subfamily K, member 1	3.07	0.009737
NM_014002	Inhibitor of kappa light polypeptide gene enhancer in B-cells, kinase epsilon	3.04	0.000215
NM_002374	Microtubule-associated protein 2	3.03	0.000059
NM_000593	Transporter 1, ATP-binding cassette, sub-family B (MDR/TAP)	3.03	0.000277
NM_001012631	Interleukin 32	3.03	0.000192
NM_005514	Major histocompatibility complex, class I, B	3.02	0.000173
NM_003955	Suppressor of cytokine signaling 3	3	0.000589
NM_003810	Tumor necrosis factor (ligand) superfamily, member 10	3	0.000441
NM_001114309	E74-like factor 3 (ets domain transcription factor, epithelial-specific)	2.98	0.000181
NM_007085	Follistatin-like 1	2.95	0.000113
AL832451	guanylate binding protein 2, interferon-inducible	2.94	0.000021
NM_014467	Sushi-repeat-containing protein, X-linked 2	2.94	0.000182
NM_004048	Beta-2-microglobulin	2.93	0.000080
NM_000600	Interleukin 6 (interferon, beta 2)	2.92	0.000828
NM_001657	Amphiregulin	2.91	0.000625
NM_005514	Major histocompatibility complex, class I, B	2.9	0.000223
NM_012339	Tetraspanin 15	2.9	0.000064
NM_182607	V-set and immunoglobulin domain containing 1	2.89	0.001009
NM_005514	Major histocompatibility complex, class I, B	2.89	0.000190
NM_003965	Chemokine (C-C motif) receptor-like 2	2.88	0.000501
NM_004163	RAB27B, member RAS oncogene family	2.88	0.000437
NR_024240	major histocompatibility complex, class I, J (pseudogene)	2.87	0.000242
NM_006018	Niacin receptor 2	2.86	0.000101
NM_017585	Solute carrier family 2 (facilitated glucose transporter), member 6	2.85	0.000346
NM_000064	Complement component 3	2.84	0.000060
NM_014080	Dual oxidase 2	2.84	0.000702
NM_007293	Complement component 4A (Rodgers blood group)	2.84	0.000131
NM_014831	Lupus brain antigen 1	2.83	0.000978
NM_002116	Major histocompatibility complex, class I, A	2.83	0.000243
XR_018049	argininosuccinate synthetase pseudogene 11	2.82	0.001070
NM_001425	Epithelial membrane protein 3	2.82	0.000126
NM_002229	Jun B proto-oncogene	2.82	0.000324
NM_003335	Ubiquitin-like modifier activating enzyme 7	2.81	0.000076
NM_152703	Sterile alpha motif domain containing 9-like	2.79	0.000386
NM_006187	2-5-oligoadenylate synthetase 3, 100kDa	2.79	0.001376
NM_000602	Serpin peptidase inhibitor, clade E (nexin, plasminogen activator inhibitor type 1), member 1	2.79	0.000064
NM_000715	Complement component 4 binding protein, alpha	2.79	0.000369
NM_172208	TAP binding protein (tapasin)	2.78	0.000258
NM_001251	CD68 molecule	2.78	0.000229
NM_001104554	Progestin and adipoQ receptor family member V	2.77	0.002617
NM_020923	Zinc finger, DBF-type containing 2	2.77	0.003472
NM_003999	Oncostatin M receptor	2.76	0.000076
NM_006622	Polo-like kinase 2 (Drosophila)	2.76	0.000041
NM_002127	Major histocompatibility complex, class I, G	2.76	0.000101
NM_002127	Major histocompatibility complex, class I, G	2.76	0.000101
NM_003225	Trefoil factor 1	2.76	0.000086
NM_000416	Interferon gamma receptor 1	2.75	0.000080
NM_005516	Major histocompatibility complex, class I, E	2.75	0.000182

NM_005516	Major histocompatibility complex, class I, E	2.75	0.000182
NM_031419	Nuclear factor of kappa light polypeptide gene enhancer in B-cells inhibitor, zeta	2.73	0.000489
NM_005516	Major histocompatibility complex, class I, E	2.73	0.000179
NM_001080391	SP100 nuclear antigen	2.73	0.000087
NM_005651	Tryptophan 2,3-dioxygenase	2.73	0.003036
NM_003190	TAP binding protein (tapasin)	2.73	0.000288
NM_002117	Major histocompatibility complex, class I, C	2.72	0.000110
NM_004900	Apolipoprotein B mRNA editing enzyme, catalytic polypeptide-like 3B	2.72	0.000702
NM_003937	Kynureninase (L-kynurenine hydrolase)	2.72	0.000181
NM_003965	Chemokine (C-C motif) receptor-like 2	2.71	0.001056
NM_033049	Mucin 13, cell surface associated	2.71	0.000368
NM_003982	Solute carrier family 7 (cationic amino acid transporter, y+ system), member 7	2.7	0.000086
NM_000716	Complement component 4 binding protein, beta	2.69	0.000235
NM_013451	Myoferlin	2.69	0.000079
NM_002976	Sodium channel, voltage-gated, type VII, alpha	2.69	0.000927
NM_007360	Killer cell lectin-like receptor subfamily K, member 1	2.69	0.000995
NM_017565	Family with sequence similarity 20, member A	2.68	0.000438
NM_021175	Hepcidin antimicrobial peptide	2.68	0.016539
NM_002117	Major histocompatibility complex, class I, C	2.67	0.000086
NM_002116	Major histocompatibility complex, class I, A	2.66	0.000190
NM_006270	Related RAS viral (r-ras) oncogene homolog	2.66	0.000973
ENST00000385827	ncrna:snoRNA_pseudogene chromosome:NCBI36:9:132315066:132315162:1 gene:ENSG00000208562	2.66	0.000181
NM_000503	Eyes absent homolog 1 (Drosophila)	2.65	0.002593
NM_002127	Major histocompatibility complex, class I, G	2.64	0.000076
NM_001001396	ATPase, Ca++ transporting, plasma membrane 4	2.64	0.000348
NM_018964	Solute carrier family 37 (glycerol-3-phosphate transporter), member 1	2.64	0.000464
NM_001955	Endothelin 1	2.63	0.000501
NM_003657	Breast carcinoma amplified sequence 1	2.62	0.000227
NM_198904	Gamma-aminobutyric acid (GABA) A receptor, gamma 2	2.62	0.000310
NM_004120	Guanylate binding protein 2, interferon-inducible	2.61	0.000083
NM_002345	Lumican	2.61	0.000933
NM_001008397	Glutathione peroxidase 8 (putative)	2.61	0.000363
NM_031458	Poly (ADP-ribose) polymerase family, member 9	2.61	0.000337
NM_000104	Cytochrome P450, family 1, subfamily B, polypeptide 1	2.6	0.000064
NM_000331	Serum amyloid A1	2.6	0.003036
NM_000201	Intercellular adhesion molecule 1	2.59	0.000080
NM_005533	Interferon-induced protein 35	2.57	0.000555
NM_002083	Glutathione peroxidase 2 (gastrointestinal)	2.56	0.000091
NM_003764	Syntaxin 11	2.54	0.000872
NM_018295	Transmembrane protein 140	2.53	0.000091
NM_002230	Junction plakoglobin	2.51	0.000363
NM_012413	Glutaminyl-peptide cyclotransferase	2.51	0.000181
NM_022823	Fibronectin type III domain containing 4	2.5	0.000208
NM_005860	Follistatin-like 3 (secreted glycoprotein)	2.49	0.000439
NM_003141	Tripartite motif-containing 21	2.46	0.002678
NM_001657	Amphiregulin	2.46	0.000489
NM_007315	Signal transducer and activator of transcription 1, 91kDa	2.44	0.000113

NM_003118	Secreted protein, acidic, cysteine-rich (osteonectin)	2.43	0.000681
NM_004102	Fatty acid binding protein 3, muscle and heart (mammary-derived growth inhibitor)	2.43	0.000086
NM_014474	Sphingomyelin phosphodiesterase, acid-like 3B	2.42	0.000131
NM_080424	SP110 nuclear body protein	2.41	0.000249
NM_000576	Interleukin 1, beta	2.41	0.001604
NM_002116	Major histocompatibility complex, class I, A	2.41	0.000043
NM_017439	Pigeon homolog (Drosophila)	2.41	0.003660
NM_172208	TAP binding protein (tapasin)	2.4	0.000165
NM_032413	Chromosome 15 open reading frame 48	2.39	0.003758
NM_001012302	Anoctamin 9	2.39	0.000235
NM_004925	Aquaporin 3 (Gill blood group)	2.38	0.000288
NM_000063	Complement component 2	2.37	0.000235
NM_000063	Complement component 2	2.37	0.000235
NM_000063	Complement component 2	2.37	0.000207
NR_015350	KIAA0040	2.36	0.001027
NM_017554	Poly (ADP-ribose) polymerase family, member 14	2.35	0.000091
NM_014314	DEAD (Asp-Glu-Ala-Asp) box polypeptide 58	2.35	0.000751
NM_001008211	Optineurin	2.35	0.000123
NM_014568	UDP-N-acetyl-alpha-D-galactosamine:polypeptide N-acetylgalactosaminyltransferase 5 (GalNAc-T5)	2.34	0.000173
NM_004591	Chemokine (C-C motif) ligand 20	2.34	0.000190
NM_000757	Colony stimulating factor 1 (macrophage)	2.33	0.000465
NM_152680	Transmembrane protein 154	2.32	0.000190
NM_139017	Interleukin 31 receptor A	2.32	0.000501
NM_006291	Tumor necrosis factor, alpha-induced protein 2	2.3	0.000076
NM_021173	Polymerase (DNA-directed), delta 4	2.3	0.037669
NM_005558	Ladinin 1	2.3	0.000064
NM_014795	Zinc finger E-box binding homeobox 2	2.3	0.000756
NM_002276	Keratin 19	2.29	0.000348
NM_032587	Caspase recruitment domain family, member 6	2.29	0.000555
NM_002318	Lysyl oxidase-like 2	2.29	0.001622
NM_002800	Proteasome (prosome, macropain) subunit, beta type, 9 (large multifunctional peptidase 2)	2.29	0.000736
NM_002800	Proteasome (prosome, macropain) subunit, beta type, 9 (large multifunctional peptidase 2)	2.29	0.000736
NM_002800	Proteasome (prosome, macropain) subunit, beta type, 9 (large multifunctional peptidase 2)	2.29	0.000736
NM_005761	Plexin C1	2.27	0.000224
NM_015900	Phospholipase A1 member A	2.26	0.000387
NM_000206	Interleukin 2 receptor, gamma (severe combined immunodeficiency)	2.26	0.001749
NM_003761	Vesicle-associated membrane protein 8 (endobrevin)	2.25	0.000209
NM_001135181	Solute carrier family 5 (sodium/glucose cotransporter), member 9	2.25	0.000467
NM_017720	Signal transducing adaptor family member 2	2.24	0.001370
NM_002192	Inhibin, beta A	2.24	0.000149
NM_001001435	Chemokine (C-C motif) ligand 4-like 1	2.23	0.006357
NM_201524	G protein-coupled receptor 56	2.23	0.000337
NM_007047	Butyrophilin, subfamily 3, member A2	2.23	0.000721
NM_002198	Interferon regulatory factor 1	2.22	0.000101
ENST00000385577	ncrna:snRNA_pseudogene chromosome:NCBI36:7:143514455:143514559:1 gene:ENSG00000208312	2.22	0.019920
NM_017791	Feline leukemia virus subgroup C cellular receptor family, member 2	2.22	0.000120
NM_181785	Solute carrier family 46, member 3	2.21	0.000625

NM_004670	3-phosphoadenosine 5-phosphosulfate synthase 2	2.21	0.000131
NM_032427	Mastermind-like 2 (Drosophila)	2.2	0.001070
NM_000877	Interleukin 1 receptor, type I	2.2	0.000227
NM_014632	Microtubule associated monoxygenase, calponin and LIM domain containing 2	2.2	0.000098
NM_144650	Alcohol dehydrogenase, iron containing, 1	2.19	0.003997
NM_002999	Syndecan 4	2.19	0.000086
NM_021623	Pleckstrin homology domain containing, family A (phosphoinositide binding specific) member 2	2.18	0.000854
NM_176870	Metallothionein 1M	2.18	0.002510
NM_001885	Crystallin, alpha B	2.17	0.001678
NM_001777	CD47 molecule	2.17	0.000345
NM_021572	Ectonucleotide pyrophosphatase/phosphodiesterase 5 (putative function)	2.17	0.003270
NM_175061	JAZF zinc finger 1	2.16	0.000349
NM_024726	IQ motif containing with AAA domain 1	2.16	0.004026
NM_021105	Phospholipid scramblase 1	2.15	0.000427
NM_006952	Uroplakin 1B	2.15	0.001417
NM_006435	Interferon induced transmembrane protein 2 (1-8D)	2.15	0.000721
NM_013431	Killer cell lectin-like receptor subfamily K, member 1	2.15	0.006190
NM_145799	Septin 6	2.15	0.000441
NM_152772	T-complex 11 (mouse)-like 2	2.15	0.002199
NM_005419	Signal transducer and activator of transcription 2, 113kDa	2.14	0.000481
AY699265	microRNA 21	2.14	0.010297
NM_030666	Serpin peptidase inhibitor, clade B (ovalbumin), member 1	2.14	0.000080
NM_005711	EGF-like repeats and discoidin I-like domains 3	2.14	0.000443
NM_006851	GLI pathogenesis-related 1	2.13	0.000337
NM_015149	Ral guanine nucleotide dissociation stimulator-like 1	2.13	0.000687
NM_152309	Phosphoinositide-3-kinase adaptor protein 1	2.13	0.000249
NM_020529	Nuclear factor of kappa light polypeptide gene enhancer in B-cells inhibitor, alpha	2.13	0.000721
NM_002210	Integrin, alpha V (vitronectin receptor, alpha polypeptide, antigen CD51)	2.12	0.000122
NM_005127	C-type lectin domain family 2, member B	2.12	0.001104
NM_003507	Frizzled homolog 7 (Drosophila)	2.12	0.000315
NM_033504	Transmembrane protein 54	2.12	0.000330
NM_005204	Mitogen-activated protein kinase kinase kinase 8	2.12	0.000060
NM_030572	Chromosome 12 open reading frame 39	2.12	0.001646
NM_016445	Pleckstrin 2	2.12	0.000348
NM_014365	Heat shock 22kDa protein 8	2.12	0.000625
NM_017523	XIAP associated factor 1	2.12	0.000400
NM_032962	Chemokine (C-C motif) ligand 15	2.12	0.000300
NM_004566	6-phosphofructo-2-kinase/fructose-2,6-biphosphatase 3	2.11	0.000448
NM_006058	TNFAIP3 interacting protein 1	2.11	0.000235
NM_000655	Selectin L	2.1	0.000447
ENST00000365142	ncrna:misc_RNA chromosome:NCBI36:2:88310203:88310298:-1 gene:ENSG00000202012	2.1	0.032988
NM_052941	Guanylate binding protein 4	2.1	0.000441
NM_006472	Thioredoxin interacting protein	2.1	0.000315
NM_005950	Metallothionein 1G	2.09	0.000181
NM_004688	N-myc (and STAT) interactor	2.09	0.001442
NM_032148	Solute carrier family 41, member 2	2.08	0.000043
NM_001080512	Bicaudal C homolog 1 (Drosophila)	2.08	0.000277
NM_000022	Adenosine deaminase	2.08	0.001150

NM_001040058	Secreted phosphoprotein 1	2.08	0.000098
NM_001145009	Butyrophilin, subfamily 3, member A1	2.07	0.000235
NM_015488	Paroxysmal nonkinesigenic dyskinesia	2.07	0.000390
NM_004285	Hexose-6-phosphate dehydrogenase (glucose 1-dehydrogenase)	2.07	0.000143
NM_005949	Metallothionein 1F	2.06	0.000060
NM_001153	Annexin A4	2.06	0.000086
NM_021727	Fatty acid desaturase 3	2.06	0.000782
NM_145252	Zymogen granule protein 16 homolog B (rat)	2.06	0.000060
NM_198827	G protein-coupled receptor 133	2.05	0.000662
NM_015515	Keratin 23 (histone deacetylase inducible)	2.05	0.002325
NM_003255	TIMP metallopeptidase inhibitor 2	2.05	0.000699
NM_005435	Rho guanine nucleotide exchange factor (GEF) 5	2.04	0.000797
NM_016546	Complement component 1, r subcomponent-like	2.04	0.000368
NM_018950	Major histocompatibility complex, class I, F	2.04	0.000173
NM_177551	Niacin receptor 1	2.04	0.005698
NM_000405	GM2 ganglioside activator	2.04	0.002046
NM_001276	Chitinase 3-like 1 (cartilage glycoprotein-39)	2.04	0.000181
NM_024430	Proline-serine-threonine phosphatase interacting protein 2	2.03	0.000427
NM_003786	ATP-binding cassette, sub-family C (CFTR/MRP), member 3	2.03	0.000381
NM_000214	Jagged 1 (Alagille syndrome)	2.03	0.000249
NM_014988	LIM and calponin homology domains 1	2.03	0.000403
NM_021034	Interferon induced transmembrane protein 3 (1-8U)	2.03	0.000930
NM_001012967	DEAD (Asp-Glu-Ala-Asp) box polypeptide 60-like	2.02	0.000736
NM_153218	Chromosome 13 open reading frame 31	2.01	0.011542
NM_153208	IQ motif containing K	2.01	0.000598
NM_018950	Major histocompatibility complex, class I, F	2.01	0.000076
NM_017439	Pigeon homolog (Drosophila)	2.00	0.001323
NM_001333	Cathepsin L2	-2.00	0.000625
NM_001080443	Kinesin family member 18B	-2	0.000249
NM_020890	KIAA1524	-2.00	0.000378
NM_033305	Vacuolar protein sorting 13 homolog A (S. cerevisiae)	-2.01	0.001015
NM_003384	Vaccinia related kinase 1	-2.02	0.000363
NM_005117	Fibroblast growth factor 19	-2.02	0.000991
NM_173658	Zinc finger protein 660	-2.02	0.000344
NM_145290	G protein-coupled receptor 125	-2.02	0.000300
NM_012112	TPX2, microtubule-associated, homolog (Xenopus laevis)	-2.02	0.000131
NM_145307	Rhotekin 2	-2.03	0.008443
NM_001042551	Structural maintenance of chromosomes 2	-2.03	0.000439
NM_022041	Gigaxonin	-2.03	0.000386
NM_001255	Cell division cycle 20 homolog (S. cerevisiae)	-2.03	0.000420
NM_021052	Histone cluster 1, H2ae	-2.04	0.001325
NM_001130862	RAD51 associated protein 1	-2.04	0.001808
NM_182620	Family with sequence similarity 33, member A	-2.04	0.004319
NM_021195	Claudin 6	-2.04	0.002172
ENST00000387426	ncrna:snoRNA_pseudogene chromosome:NCBI36:15:28722452:28722548:1 gene:ENSG00000210161	-2.05	0.006453
NM_001080449	DNA replication helicase 2 homolog (yeast)	-2.05	0.008443
NM_003167	Sulfotransferase family, cytosolic, 2A, dehydroepiandrosterone (DHEA)-preferring, member 1	-2.05	0.000523
NM_001713	Betaine-homocysteine methyltransferase	-2.06	0.000589
NM_024854	Pyridine nucleotide-disulphide oxidoreductase domain 1	-2.06	0.000189

NM_016426	G-2 and S-phase expressed 1	-2.06	0.001515
NM_005480	Trophinin associated protein (tastin)	-2.06	0.002148
NM_152515	Cytoskeleton associated protein 2-like	-2.06	0.001287
NM_194298	Solute carrier family 16, member 9 (monocarboxylic acid transporter 9)	-2.06	0.000461
NM_031217	Kinesin family member 18A	-2.07	0.000428
NM_006089	Sex comb on midleg-like 2 (Drosophila)	-2.08	0.000194
NM_030941	Exonuclease NEF-sp	-2.08	0.000387
NM_001130688	High-mobility group box 2	-2.08	0.000277
NM_007174	Citron (rho-interacting, serine/threonine kinase 21)	-2.09	0.000447
NM_001875	Carbamoyl-phosphate synthetase 1, mitochondrial	2.09	0.000293
NM_022145	Centromere protein K	-2.1	0.000235
NM_017760	Non-SMC condensin II complex, subunit G2	-2.1	0.000249
NM_014865	Non-SMC condensin I complex, subunit D2	-2.1	0.000249
NM_017769	G2/M-phase specific E3 ubiquitin ligase	-2.11	0.000296
NM_032900	Rho GTPase activating protein 19	-2.11	0.000349
NM_001037540	Sex comb on midleg-like 1 (Drosophila)	-2.11	0.002111
ENST00000388115	ncrna:Mt_tRNA_pseudogene chromosome:NCBI36:16:80712880:80712948:1 gene:ENSG00000210850	-2.11	0.001325
NM_013277	Rac GTPase activating protein 1	-2.11	0.000113
NM_005647	Transducin (beta)-like 1X-linked	-2.12	0.001169
NM_001122679	Odz, odd Oz/ten-m homolog 2 (Drosophila)	-2.12	0.000579
NM_018725	Interleukin 17 receptor B	-2.13	0.000186
NM_005391	Pyruvate dehydrogenase kinase, isozyme 3	-2.13	0.001180
NM_006845	Kinesin family member 2C	-2.14	0.000190
NM_182553	Cornichon homolog 2 (Drosophila)	-2.14	0.001749
NM_173529	Chromosome 18 open reading frame 54	-2.14	0.002688
NM_152311	Clarin 3	-2.14	0.000249
NR_026677	chromosome 9 open reading frame 45	-2.14	0.000439
NM_006733	Centromere protein I	-2.15	0.000269
ENST00000365653	ncrna:misc_RNA chromosome:NCBI36:9:85797667:85797768:1 gene:ENSG00000202523	-2.16	0.011357
NM_018063	Helicase, lymphoid-specific	-2.16	0.001070
NM_001809	Centromere protein A	-2.16	0.000342
NM_001012410	Shugoshin-like 1 (S. pombe)	-2.16	0.000487
NR_026583	Rac GTPase activating protein 1 pseudogene	-2.17	0.000133
NM_001237	Cyclin A2	-2.17	0.000126
NM_001075	UDP glucuronosyltransferase 2 family, polypeptide B10	-2.17	0.006789
NM_001211	Budding uninhibited by benzimidazoles 1 homolog beta (yeast)	-2.18	0.000084
NM_006342	Transforming, acidic coiled-coil containing protein 3	-2.18	0.000190
NM_152562	Cell division cycle associated 2	-2.18	0.000319
NM_003981	Protein regulator of cytokinesis 1	-2.18	0.000143
NM_004219	Pituitary tumor-transforming 1	-2.19	0.000487
NM_001114120	DEP domain containing 1	-2.19	0.001749
ENST00000387066	ncrna:snRNA_pseudogene chromosome:NCBI36:3:12531205:12531303:1 gene:ENSG00000209801	-2.2	0.001131
NM_007280	Opa interacting protein 5	-2.21	0.000612
NM_003509	Histone cluster 1, H2ai	-2.22	0.000075
NM_001994	Coagulation factor XIII, B polypeptide	-2.22	0.000137
NM_005539	Inositol polyphosphate-5-phosphatase, 40kDa	-2.24	0.000467
NM_152527	Solute carrier family 16, member 14 (monocarboxylic acid transporter 14)	-2.24	0.000625

NM_003836	Delta-like 1 homolog (Drosophila)	-2.24	0.000625
NM_033084	Fanconi anemia, complementation group D2	-2.24	0.000355
NM_003318	TTK protein kinase	-2.26	0.000273
NM_000846	Glutathione S-transferase alpha 2	-2.27	0.002696
NM_022766	Ceramide kinase	-2.27	0.001515
NM_001040100	Chromosome 3 open reading frame 57	-2.27	0.000441
NM_030919	Family with sequence similarity 83, member D	-2.27	0.000439
NM_003513	Histone cluster 1, H2ab	-2.28	0.000699
NM_018101	Cell division cycle associated 8	-2.28	0.000219
AK094159	Hypothetical LOC645524	-2.28	0.041110
NM_016195	Kinesin family member 20B	-2.28	0.000697
NM_006101	NDC80 homolog, kinetochore complex component (S. cerevisiae)	-2.29	0.000766
NM_004523	Kinesin family member 11	-2.29	0.000306
NM_001786	Cell division cycle 2, G1 to S and G2 to M	-2.29	0.000791
NM_145290	G protein-coupled receptor 125	-2.29	0.000248
NM_013381	Thyrotropin-releasing hormone degrading enzyme	-2.29	0.003084
NM_001105206	Laminin, alpha 4	-2.3	0.000190
NM_004217	Aurora kinase B	-2.3	0.000765
NM_015310	Pleckstrin and Sec7 domain containing 3	-2.3	0.000182
NM_019593	Hypothetical protein KIAA1434	-2.31	0.000190
NM_020675	SPC25, NDC80 kinetochore complex component, homolog (S. cerevisiae)	-2.31	0.000736
NM_024094	Defective in sister chromatid cohesion 1 homolog (S. cerevisiae)	-2.31	0.000923
NM_006206	Platelet-derived growth factor receptor, alpha polypeptide	-2.31	0.000382
NM_033286	Chromosome 15 open reading frame 23	-2.33	0.000041
NM_001761	Cyclin F	-2.33	0.000126
NM_013296	G-protein signaling modulator 2 (AGS3-like, C. elegans)	-2.33	0.000122
NM_005322	Histone cluster 1, H1b	-2.33	0.000306
NM_031299	Cell division cycle associated 3	-2.33	0.001325
NM_020973	Glucosidase, beta, acid 3 (cytosolic)	-2.34	0.000279
NM_001067	Topoisomerase (DNA) II alpha 170kDa	-2.35	0.000153
ENST00000362530	ncrna:misc_RNA chromosome:NCBI36:2:230631189:230631284:-1 gene:ENSG00000199400	-2.36	0.001485
NM_018131	Centrosomal protein 55kDa	-2.36	0.000276
NM_005630	Solute carrier organic anion transporter family, member 2A1	-2.36	0.000373
NM_199133	Family with sequence similarity 173, member B	-2.36	0.000645
NM_181802	Ubiquitin-conjugating enzyme E2C	-2.36	0.000277
NM_002108	Histidine ammonia-lyase	-2.36	0.000080
ENST00000410579	ncrna:misc_RNA chromosome:NCBI36:1:8779217:8779318:-1 gene:ENSG00000222511	-2.37	0.002427
NM_000059	Breast cancer 2, early onset	-2.38	0.000481
NM_033272	Potassium voltage-gated channel, subfamily H (eag-related), member 7	-2.39	0.000167
NM_170589	Cancer susceptibility candidate 5	-2.39	0.000153
NM_014767	Sparc/osteonectin, cwcv and kazal-like domains proteoglycan (testican) 2	-2.39	0.000441
NM_012291	Extra spindle pole bodies homolog 1 (S. cerevisiae)	-2.41	0.000458
NM_005192	Cyclin-dependent kinase inhibitor 3	-2.42	0.000283
NM_017915	Chromosome 12 open reading frame 48	-2.42	0.000190
NM_173814	Protogenin homolog (Gallus gallus)	-2.42	0.000891
NM_012310	Kinesin family member 4A	-2.42	0.000166
NM_000735	Glycoprotein hormones, alpha polypeptide	-2.43	0.001113
NM_006461	Sperm associated antigen 5	-2.45	0.000224

NM_138555	Kinesin family member 23	-2.46	0.000159
NM_005378	V-myc myelocytomatosis viral related oncogene, neuroblastoma derived (avian)	-2.46	0.000300
NM_014750	Discs, large (Drosophila) homolog-associated protein 5	-2.47	0.000091
NM_019013	Family with sequence similarity 64, member A	-2.47	0.000235
NM_032117	Meiotic nuclear divisions 1 homolog (S. cerevisiae)	-2.48	0.000927
NM_001039841	Rho GTPase activating protein 11B	-2.49	0.001467
NM_032042	Family with sequence similarity 172, member A	-2.53	0.000315
NM_001790	Cell division cycle 25 homolog C (S. pombe)	-2.54	0.000224
NM_005733	Kinesin family member 20A	-2.57	0.000126
NM_004701	Cyclin B2	-2.57	0.000388
NM_014229	Solute carrier family 6 (neurotransmitter transporter, GABA), member 11	-2.62	0.001169
NM_001010893	Solute carrier family 10 (sodium/bile acid cotransporter family), member 5	-2.62	0.001196
NM_005941	Matrix metallopeptidase 16 (membrane-inserted)	-2.62	0.000235
NM_003521	Histone cluster 1, H2bm	-2.63	0.000368
NM_001039752	Solute carrier family 22, member 10	-2.65	0.002515
NM_002417	Antigen identified by monoclonal antibody Ki-67	-2.66	0.001866
NM_145697	NUF2, NDC80 kinetochore complex component, homolog (S. cerevisiae)	-2.67	0.000325
NM_202002	Forkhead box M1	-2.68	0.000431
NM_002539	Ornithine decarboxylase 1	-2.71	0.000101
NM_002497	NIMA (never in mitosis gene a)-related kinase 2	-2.73	0.000441
NM_014875	Kinesin family member 14	-2.74	0.000348
NM_005030	Polo-like kinase 1 (Drosophila)	-2.77	0.000131
NM_021062	Histone cluster 1, H2bb	-2.8	0.000489
NM_001142556	Hyaluronan-mediated motility receptor (RHAMM)	-2.8	0.000190
NM_003840	Tumor necrosis factor receptor superfamily, member 10d, decoy with truncated death domain	-2.81	0.000344
NM_001813	Centromere protein E, 312kDa	-2.81	0.000441
NM_031966	Cyclin B1	-2.84	0.000156
NM_018136	Asp (abnormal spindle) homolog, microcephaly associated (Drosophila)	-2.86	0.000076
NM_018492	PDZ binding kinase	-2.91	0.000192
NM_014783	Rho GTPase activating protein 11A	-2.91	0.000196
NM_006841	Solute carrier family 38, member 3	-2.92	0.000395
NM_018304	Proline rich 11	-3.02	0.000086
NM_001098721	Guanine nucleotide binding protein (G protein), gamma 4	-3.11	0.000131
NM_020242	Kinesin family member 15	-3.13	0.000363
NM_022908	5-nucleotidase domain containing 2	-3.16	0.000080
AL136588	Transcribed locus	-3.29	0.000834
NM_016343	Centromere protein F, 350/400ka (mitosin)	-3.3	0.000174
AB096683	Family with sequence similarity 72, member D	-3.41	0.000131
AB096683	Family with sequence similarity 72, member D	-3.41	0.000137
AB096683	Family with sequence similarity 72, member D	-3.45	0.000131
AB096683	Family with sequence similarity 72, member D	-3.98	0.000983
NM_006061	Cysteine-rich secretory protein 3	-6.69	0.000260

Appendix VIII

Affymetrix Microarray – ΔTIR vs TLR3 – HCV Jc1

Gene Identifier	Gene Name	Fold Change	adj. *p* value
NM_004139	Lipopolysaccharide binding protein	10.87	0.000088
NM_017631	DEAD (Asp-Glu-Ala-Asp) box polypeptide 60	7.76	0.000170
NM_001565	Chemokine (C-X-C motif) ligand 10	5.6	0.000081
NM_021187	Cytochrome P450, family 4, subfamily F, polypeptide 11	4.29	0.000283
NM_001785	Cytidine deaminase	3.97	0.001100
NM_000583	Group-specific component (vitamin D binding protein)	3.4	0.007420
NM_001031683	Interferon-induced protein with tetratricopeptide repeats 3	3.38	0.000283
NM_001001435	Chemokine (C-C motif) ligand 4-like 1	3.34	0.001870
NM_030787	Complement factor H-related 5	2.97	0.001560
NM_005143	Haptoglobin	2.97	0.001150
NM_005807	Proteoglycan 4	2.96	0.000470
ENST00000377050	ubiquitin D	2.94	0.002030
NM_001548	Interferon-induced protein with tetratricopeptide repeats 1	2.84	0.000403
ENST00000477922	maltase-glucoamylase-like pseudogene	2.83	0.001800
NM_020119	Zinc finger CCCH-type, antiviral 1	2.78	0.000258
ENST00000477922	maltase-glucoamylase-like pseudogene	2.77	0.000694
NM_002993	Chemokine (C-X-C motif) ligand 6 (granulocyte chemotactic protein 2)	2.73	0.001320
NM_006512	Serum amyloid A4, constitutive	2.73	0.008010
NM_002984	Chemokine (C-C motif) ligand 4	2.66	0.002010
NM_003733	2-5-oligoadenylate synthetase-like	2.65	0.000694
ENST00000477922	maltase-glucoamylase-like pseudogene	2.64	0.003740
ENST00000477922	maltase-glucoamylase-like pseudogene	2.57	0.001850
NM_001142883	Inositol hexakisphosphate kinase 3	2.55	0.001420
ENST00000477922	maltase-glucoamylase-like pseudogene	2.52	0.051400
ENST00000477922	maltase-glucoamylase-like pseudogene	2.5	0.001600
NM_001547	Interferon-induced protein with tetratricopeptide repeats 2	2.49	0.003080
NM_000584	Interleukin 8	2.49	0.000564
NM_001165	Baculoviral IAP repeat-containing 3	2.48	0.001250
NM_001775	CD38 molecule	2.43	0.000470
NM_021006	Chemokine (C-C motif) ligand 3-like 1	2.43	0.001100
ENST00000477922	maltase-glucoamylase-like pseudogene	2.43	0.000610
NM_006417	Interferon-induced protein 44	2.37	0.010300
NM_177551	Niacin receptor 1	2.32	0.008120
NM_001086	Arylacetamide deacetylase (esterase)	2.31	0.003790
NM_002985	Chemokine (C-C motif) ligand 5	2.31	0.005600
NM_001910	Cathepsin E	2.31	0.000502
ENST00000477922	maltase-glucoamylase-like pseudogene	2.3	0.000470
NR_033807	cytochrome P450, family 3, subfamily A, polypeptide 5	2.3	0.002320
NM_000610	CD44 molecule (Indian blood group)	2.28	0.000283
NM_000715	Complement component 4 binding protein, alpha	2.23	0.000170
NM_004668	Maltase-glucoamylase (alpha-glucosidase)	2.21	0.002240
NM_201442	Complement component 1, s subcomponent	2.19	0.000670
NM_130786	Alpha-1-B glycoprotein	2.18	0.001620

NM_005651	Tryptophan 2,3-dioxygenase	2.17	0.004910
NM_021258	Interleukin 22 receptor, alpha 1	2.15	0.000694
NM_000602	Serpin peptidase inhibitor, clade E (nexin, plasminogen activator inhibitor type 1), member 1	2.13	0.001250
NM_005711	EGF-like repeats and discoidin I-like domains 3	2.12	0.000383
ENST00000477922	maltase-glucoamylase-like pseudogene	2.1	0.002930
NM_005564	Lipocalin 2	2.1	0.001850
NR_028291	vanin 3	2.08	0.000670
NM_004665	Vanin 2	2.07	0.007420
NM_005567	Lectin, galactoside-binding, soluble, 3 binding protein	2.07	0.003430
NM_003999	Oncostatin M receptor	2.05	0.000170
NM_001486	Glucokinase (hexokinase 4) regulator	2.04	0.000081
NM_003064	Secretory leukocyte peptidase inhibitor	2.04	0.000694
NM_207581	Dual oxidase maturation factor 2	2.02	0.002920
ENST00000477922	maltase-glucoamylase-like pseudogene	2.02	0.000194
NR_003717	maltase-glucoamylase-like pseudogene	2.01	0.002220
NM_007231	Solute carrier family 6 (amino acid transporter), member 14	2.01	0.032500
NM_001025195	Carboxylesterase 1 (monocyte/macrophage serine esterase 1)	2	0.000337
NM_006646	WAS protein family, member 3	-2	0.000674
NM_001163335	synaptotagmin-like 5	-2.04	0.002240
NM_016132	Myelin expression factor 2	-2.05	0.009240
NR_024494	breakpoint cluster region pseudogene	-2.05	0.045700
NM_014344	Four jointed box 1 (Drosophila)	-2.06	0.001800
NM_004942	Defensin, beta 4	-2.12	0.039700
NM_000846	Glutathione S-transferase alpha 2	-2.17	0.002920
NM_004750	Cytokine receptor-like factor 1	-2.18	0.000626
NM_006061	Cysteine-rich secretory protein 3	-2.22	0.000814
NM_001045	Solute carrier family 6 (neurotransmitter transporter, serotonin), member 4	-2.6	0.000283
NM_018476	Brain expressed, X-linked 1	-2.66	0.000081
NM_004063	Cadherin 17, LI cadherin (liver-intestine)	-2.81	0.000670
NM_152311	Clarin 3	-3.3	0.000647
NM_014229	Solute carrier family 6 (neurotransmitter transporter, GABA), member 11	-4.69	0.000403

Appendix IX

Affymetrix Microarray – Huh-7+CD81 knockdown hepatocytes following co-culture with HCV-infected Huh-7+TLR3

Gene Identifier	Gene Name	Fold Change	adj. *p* value
NM_000782	cytochrome P450, family 24, subfamily A, polypeptide 1	2.29	0.326
NM_000799	erythropoietin	2.28	0.326
NM_003955	suppressor of cytokine signaling 3	2.06	0.375
NM_025163	phosphatidylinositol glycan anchor biosynthesis, class Z	1.77	0.428
NM_178859	organic solute transporter beta	1.70	0.326
NM_000965	retinoic acid receptor, beta	1.69	0.359
NM_015515	keratin 23 (histone deacetylase inducible)	1.69	0.465
NR_002955	small nucleolar RNA, H/ACA box 14A	1.68	0.428
NM_007028	tripartite motif-containing 31	1.66	0.428
NM_016445	pleckstrin 2	1.63	0.359
NM_003999	oncostatin M receptor	1.46	0.465
NM_000186	complement factor H	1.44	0.359
NM_014849	synaptic vesicle glycoprotein 2A	1.42	0.428
NM_020361	carboxypeptidase A6	1.40	0.465
NM_001009984	chromosome 20 open reading frame 194	1.40	0.331
NM_000602	serpin peptidase inhibitor, clade E (nexin, plasminogen activa	1.38	0.428
NM_003672	CDC14 cell division cycle 14 homolog A (S. cerevisiae)	1.37	0.428
NM_001710	complement factor B	1.35	0.428
NM_004522	kinesin family member 5C	1.34	0.428
NM_000096	ceruloplasmin (ferroxidase)	1.34	0.409
NM_001102416	kininogen 1	1.33	0.428
NM_024980	G protein-coupled receptor 157	1.33	0.428
NM_000628	interleukin 10 receptor, beta	1.31	0.465
NM_004655	axin 2	1.31	0.428
NM_006209	ectonucleotide pyrophosphatase/phosphodiesterase 2	1.31	0.428
NM_002410	mannosyl (alpha-1,6-)-glycoprotein beta-1,6-N-acetyl-glucosaminyltransferase	1.30	0.465
NM_015675	growth arrest and DNA-damage-inducible, beta	1.30	0.342
NM_012435	SHC (Src homology 2 domain containing) transforming protein 2	1.29	0.428
NM_018645	hairy and enhancer of split 6 (Drosophila)	1.28	0.375
NM_001002029	complement component 4B (Chido blood group)	1.28	0.428
NM_000027	aspartylglucosaminidase	1.28	0.465
NM_001160042	IQ motif containing C	1.27	0.460
NM_007293	complement component 4A (Rodgers blood group)	1.26	0.359
NM_016274	pleckstrin homology domain containing, family O member 1	1.26	0.359
NM_002738	protein kinase C, beta	1.26	0.359
NR_027297	homer homolog 3 (Drosophila)	1.26	0.465
NM_024544	mitochondrial E3 ubiquitin protein ligase 1	1.25	0.456
NM_007283	monoglyceride lipase	1.25	0.479
NM_000201	intercellular adhesion molecule 1	1.25	0.465
NM_018004	transmembrane protein 45A	1.24	0.326
NM_001040450	family with sequence similarity 63, member B	1.24	0.428
NM_182943	procollagen-lysine, 2-oxoglutarate 5-dioxygenase 2	1.24	0.359
NM_001003940	Bcl2 modifying factor	1.23	0.428
NM_014603	cerebellar degeneration-related protein 2-like	1.23	0.359
NM_005281	G protein-coupled receptor 3	1.23	0.430
NM_032857	lactamase, beta	1.22	0.326

NM_018948	ERBB receptor feedback inhibitor 1	1.22	0.460
NM_001012967	DEAD (Asp-Glu-Ala-Asp) box polypeptide 60-like	1.22	0.388
NM_000292	phosphorylase kinase, alpha 2 (liver)	1.22	0.465
NM_001063	transferrin	1.22	0.456
NM_138621	BCL2-like 11 (apoptosis facilitator)	1.21	0.326
NM_007243	nurim (nuclear envelope membrane protein)	1.20	0.326
NM_173554	chromosome 10 open reading frame 107	1.20	0.465
NM_001271	chromodomain helicase DNA binding protein 2	1.20	0.428
NM_018341	chromosome 6 open reading frame 70	1.19	0.428
NM_138782	FCH domain only 2	1.19	0.430
NM_017459	microfibrillar-associated protein 2	1.18	0.465
NM_000033	ATP-binding cassette, sub-family D (ALD), member 1	1.18	0.428
NM_001040457	rhomboid domain containing 2	1.17	0.465
NM_001773	CD34 molecule	1.17	0.428
NR_002773	AOC3 pseudogene	1.17	0.380
NM_016083	cannabinoid receptor 1 (brain)	1.17	0.456
NM_198393	testis expressed 14	1.17	0.428
NM_080650	ATP binding domain 4	1.16	0.465
NM_021959	protein phosphatase 1, regulatory (inhibitor) subunit 11	1.16	0.428
NM_021137	tumor necrosis factor, alpha-induced protein 1 (endothelial)	1.16	0.428
NM_017602	OTU domain containing 5	1.16	0.465
NM_020444	KIAA1191	1.16	0.359
NM_004730	eukaryotic translation termination factor 1	1.15	0.428
NM_138704	necdin-like 2	1.15	0.403
NM_013400	replication initiator 1	1.14	0.428
NM_014670	basic leucine zipper and W2 domains 1	1.14	0.409
NM_001130969	nasal embryonic LHRH factor	1.12	0.418
NM_148923	cytochrome b5 type A (microsomal)	1.12	0.465
NM_015123	FERM domain containing 4B	1.12	0.326
NM_014048	MKL/myocardin-like 2	1.12	0.354
NM_024297	PHD finger protein 23	1.11	0.415
NM_153708	receptor (chemosensory) transporter protein 1	1.11	0.465
NM_004849	ATG5 autophagy related 5 homolog (S. cerevisiae)	1.11	0.331
NM_000508	fibrinogen alpha chain	1.11	0.330
NM_000709	branched chain keto acid dehydrogenase E1, alpha polypeptide	1.09	0.326
NM_032039	integrin alpha FG-GAP repeat containing 3	1.08	0.428
NM_015306	ubiquitin specific peptidase 24	-1.03	0.428
NR_001552	testis-specific transcript, Y-linked 16 (non-protein coding)	-1.07	0.428
NM_002010	fibroblast growth factor 9 (glia-activating factor)	-1.09	0.487
NM_015071	Rho GTPase activating protein 26	-1.11	0.326
NM_016065	mitochondrial ribosomal protein S16	-1.12	0.487
NM_130794	cystatin 11	-1.12	0.428
NM_005764	PDZK1 interacting protein 1	-1.13	0.465
NM_182704	selenoprotein V	-1.14	0.430
NM_000710	bradykinin receptor B1	-1.14	0.326
NM_005381	nucleolin	-1.15	0.359
NR_036204	microRNA 4320	-1.16	0.428
NM_002440	mutS homolog 4 (E. coli)	-1.16	0.428
NM_002594	proprotein convertase subtilisin/kexin type 2	-1.17	0.359
NM_000040	apolipoprotein C-III	-1.17	0.465
NM_020297	ATP-binding cassette, sub-family C (CFTR/MRP), member 9	-1.18	0.428
NM_002699	POU class 3 homeobox 1	-1.18	0.354
NR_003194	small nucleolar RNA, C/D box 114-2	-1.18	0.428
NR_028484	chromosome 22 open reading frame 45	-1.18	0.428

U89331	short stature homeobox	-1.18	0.428
NR_003296	small nucleolar RNA, C/D box 115-4	-1.19	0.430
NM_024758	agmatine ureohydrolase (agmatinase)	-1.19	0.426
NR_029966	microRNA 433	-1.19	0.409
NR_029681	microRNA 140	-1.20	0.465
NM_176822	NLR family, pyrin domain containing 14	-1.20	0.465
NM_002677	peripheral myelin protein 2	-1.21	0.428
BC028204	hypothetical protein LOC646241	-1.22	0.428
NM_001173467	Sp7 transcription factor	-1.22	0.483
NM_013356	solute carrier family 16, member 8 (monocarboxylic acid transporter)	-1.22	0.359
NM_181617	keratin associated protein 21-2	-1.23	0.380
NM_001195124	hypothetical protein LOC100288525	-1.23	0.465
NR_026997	chromosome 22 open reading frame 34	-1.23	0.428
NR_030192	microRNA 525	-1.24	0.359
NR_002144	mitogen-activated protein kinase kinase 2 pseudogene	-1.25	0.326
NM_000570	Fc fragment of IgG, low affinity IIIb, receptor (CD16b)	-1.25	0.428
NM_001002035	defensin, beta 108B	-1.27	0.456
NM_031409	chemokine (C-C motif) receptor 6	-1.28	0.460
NM_018327	serine palmitoyltransferase, long chain base subunit 3	-1.28	0.326
NM_207406	BEN domain containing 4	-1.31	0.390
NM_006841	solute carrier family 38, member 3	-1.32	0.359
NM_001245	sialic acid binding Ig-like lectin 6	-1.34	0.430
XR_114960	hypothetical LOC100505805	-1.36	0.465
NM_003986	butyrobetaine (gamma), 2-oxoglutarate dioxygenase (gamma-butyrobetaine hydroxylase) 1	-1.36	0.456
NM_021949	ATPase, Ca++ transporting, plasma membrane 3	-1.37	0.426
NM_173804	transmembrane protein 86B	-1.43	0.426

References

Agnello, V., Abel, G., et al. (1999). Hepatitis C virus and other flaviviridae viruses enter cells via low density lipoprotein receptor. *Proc Natl Acad Sci U S A* **96**(22): 12766-71.

Agnello, V., Abel, G., et al. (1998). Detection of widespread hepatocyte infection in chronic hepatitis C. *Hepatology* **28**(2): 573-84.

Akuta, N., Suzuki, F., et al. (2007). Amino acid substitutions in the hepatitis C virus core region are the important predictor of hepatocarcinogenesis. *Hepatology* **46**(5): 1357-64.

Aloia, A. L., Locarnini, S., et al. (2012). Antiviral resistance and direct-acting antiviral agents for HCV. *Antivir Ther* **17**(6 Pt B): 1147-62.

Alter, M. J. (1995). Epidemiology of hepatitis C in the West. *Semin Liver Dis* **15**(1): 5-14.

Ando, K., Hiroishi, K., et al. (1997). Perforin, Fas/Fas ligand, and TNF-alpha pathways as specific and bystander killing mechanisms of hepatitis C virus-specific human CTL. *J Immunol* **158**(11): 5283-91.

Apolinario, A., Majano, P. L., et al. (2005). Gene expression profile of T-cell-specific chemokines in human hepatocyte-derived cells: evidence for a synergistic inducer effect of cytokines and hepatitis C virus proteins. *J Viral Hepat* **12**(1): 27-37.

Appel, N., Zayas, M., et al. (2008). Essential role of domain III of nonstructural protein 5A for hepatitis C virus infectious particle assembly. *PLoS Pathog* **4**(3): e1000035.

Arnaud, N., Dabo, S., et al. (2011). Hepatitis C virus reveals a novel early control in acute immune response. *PLoS Pathog* **7**(10): e1002289.

Asselah, T., Bieche, I., et al. (2009). Gene expression and hepatitis C virus infection. *Gut* **58**(6): 846-58.

Barba, G., Harper, F., et al. (1997). Hepatitis C virus core protein shows a cytoplasmic localization and associates to cellular lipid storage droplets. *Proc Natl Acad Sci U S A* **94**(4): 1200-5.

Bartenschlager, R., Penin, F., et al. (2011). Assembly of infectious hepatitis C virus particles. *Trends Microbiol* **19**(2): 95-103.

Barth, H., Schafer, C., et al. (2003). Cellular binding of hepatitis C virus envelope glycoprotein E2 requires cell surface heparan sulfate. *J Biol Chem* **278**(42): 41003-12.

Bartosch, B., Dubuisson, J., et al. (2003). Infectious hepatitis C virus pseudo-particles containing functional E1-E2 envelope protein complexes. *J Exp Med* **197**(5): 633-42.

Bataller, R., Paik, Y. H., et al. (2004). Hepatitis C virus core and nonstructural proteins induce fibrogenic effects in hepatic stellate cells. *Gastroenterology* **126**(2): 529-40.

Behrens, S. E., Tomei, L., et al. (1996). Identification and properties of the RNA-dependent RNA polymerase of hepatitis C virus. *EMBO J* **15**(1): 12-22.

Benedicto, I., Molina-Jimenez, F., et al. (2009). The tight junction-associated protein occludin is required for a postbinding step in hepatitis C virus entry and infection. *J Virol* **83**(16): 8012-20.

Benias, P. C., Gopal, K., et al. (2012). Hepatic expression of toll-like receptors 3, 4, and 9 in primary biliary cirrhosis and chronic hepatitis C. *Clin Res Hepatol Gastroenterol* **36**(5): 448-54.

Berres, M. L., Trautwein, C., et al. (2011). Serum chemokine CXC ligand 10 (CXCL10) predicts fibrosis progression after liver transplantation for hepatitis C infection. *Hepatology* **53**(2): 596-603.

Bitzegeio, J., Bankwitz, D., et al. (2010). Adaptation of hepatitis C virus to mouse CD81 permits infection of mouse cells in the absence of human entry factors. *PLoS Pathog* **6**: e1000978.

Blanchard, E., Belouzard, S., et al. (2006). Hepatitis C virus entry depends on clathrin-mediated endocytosis. *J Virol* **80**(14): 6964-72.

Blight, K. J., Kolykhalov, A. A., et al. (2000). Efficient initiation of HCV RNA replication in cell culture. *Science* **290**(5498): 1972-4.

Blight, K. J., McKeating, J. A., et al. (2002). Highly permissive cell lines for subgenomic and genomic hepatitis C virus RNA replication. *J Virol* **76**(24): 13001-14.

Bode, J. G., Ludwig, S., et al. (2003). IFN-alpha antagonistic activity of HCV core protein involves induction of suppressor of cytokine signaling-3. *FASEB J* **17**(3): 488-90.

Boonstra, A., van der Laan, L. J., et al. (2009). Experimental models for hepatitis C viral infection. *Hepatology* **50**(5): 1646-55.

Bowden, D. S. and Berzsenyi, M. D. (2006). Chronic hepatitis C virus infection: genotyping and its clinical role. *Future Microbiol* **1**(1): 103-12.

Brazzoli, M., Bianchi, A., et al. (2008). CD81 is a central regulator of cellular events required for hepatitis C virus infection of human hepatocytes. *J Virol* **82**(17): 8316-29.

Brimacombe, C. L., Grove, J., et al. (2010). Neutralizing antibody-resistant hepatitis C virus cell-to-cell transmission. *J Virol* **85**(1): 596-605.

Brown, R. S. (2005). Hepatitis C and liver transplantation. *Nature* **436**(7053): 973-8.

Bukh, J. (2012). Animal models for the study of hepatitis C virus infection and related liver disease. *Gastroenterology* **142**(6): 1279-1287 e3.

Butera, D., Marukian, S., et al. (2005). Plasma chemokine levels correlate with the outcome of antiviral therapy in patients with hepatitis C. *Blood* **106**(4): 1175-82.

Calle Serrano, B. and Manns, M. P. (2012). HCV's days are numbered: next-generation direct-acting antivirals and host-targeting agents. *Antivir Ther* **17**(6 Pt B): 1133-46.

Carow, B. and Rottenberg, M. E. (2014). SOCS3, a Major Regulator of Infection and Inflammation. *Front Immunol* **5**: 58.

Cerny, A. and Chisari, F. V. (1999). Pathogenesis of chronic hepatitis C: immunological features of hepatic injury and viral persistence. *Hepatology* **30**(3): 595-601.

Chak, E., Talal, A. H., et al. (2011). Hepatitis C virus infection in USA: an estimate of true prevalence. *Liver Int* **31**(8): 1090-101.

Charlton, M. (2005). Recurrence of hepatitis C infection: Where are we now? *Liver Transpl*(11 Suppl 2): S57-62.

Choo, Q. L., Kuo, G., et al. (1989). Isolation of a cDNA clone derived from a blood-borne non-A, non-B viral hepatitis genome. *Science* **244**(4902): 359-62.

Choo, Q. L., Weiner, A. J., et al. (1990). Hepatitis C virus: the major causative agent of viral non-A, non-B hepatitis. *Br Med Bull* **46**(2): 423-41.

Clement, S., Pascarella, S., et al. (2010). The hepatitis C virus core protein indirectly induces alpha-smooth muscle actin expression in hepatic stellate cells via interleukin-8. *J Hepatol* **52**(5): 635-43.

Coenen, M., Nischalke, H. D., et al. (2011). Hepatitis C virus core protein induces fibrogenic actions of hepatic stellate cells via toll-like receptor 2. *Lab Invest* **91**(9): 1375-82.

Croker, B. A., Krebs, D. L., et al. (2003). SOCS3 negatively regulates IL-6 signaling in vivo. *Nat Immunol* **4**(6): 540-5.

Dansako, H., Yamane, D., et al. (2013). Class A scavenger receptor 1 (MSR1) restricts hepatitis C virus replication by mediating toll-like receptor 3 recognition of viral RNAs produced in neighboring cells. *PLoS Pathog* **9**(5): e1003345.

Davis, G. L., Alter, M. J., et al. (2010). Aging of hepatitis C virus (HCV)-infected persons in the United States: a multiple cohort model of HCV prevalence and disease progression. *Gastroenterology* **138**(2): 513-21, 521 e1-6.

de la Fuente, C., Goodman, Z., et al. (2013). Genetic and functional characterization of the N-terminal region of the hepatitis C virus NS2 protein. *J Virol* **87**(8): 4130-45.

Dharancy, S., Malapel, M., et al. (2005). Impaired expression of the peroxisome proliferator-activated receptor alpha during hepatitis C virus infection. *Gastroenterology* **128**(2): 334-42.

Diago, M., Castellano, G., et al. (2006). Association of pretreatment serum interferon gamma inducible protein 10 levels with sustained virological response to peginterferon plus ribavirin therapy in genotype 1 infected patients with chronic hepatitis C. *Gut* **55**(3): 374-9.

Dolganiuc, A., Norkina, O., et al. (2007). Viral and host factors induce macrophage activation and loss of toll-like receptor tolerance in chronic HCV infection. *Gastroenterology* **133**(5): 1627-36.

Dore, G. J., Law, M., et al. (2003). Epidemiology of hepatitis C virus infection in Australia. *J Clin Virol* **26**(2): 171-84.

Dreux, M., Garaigorta, U., et al. (2012). Short-range exosomal transfer of viral RNA from infected cells to plasmacytoid dendritic cells triggers innate immunity. *Cell Host Microbe* **12**(4): 558-70.

Drummer, H. E., Maerz, A., et al. (2003). Cell surface expression of functional hepatitis C virus E1 and E2 glycoproteins. *FEBS Lett* **546**(2-3): 385-90.

Duong, F. H., Filipowicz, M., et al. (2004). Hepatitis C virus inhibits interferon signaling through up-regulation of protein phosphatase 2A. *Gastroenterology* **126**(1): 263-77.

Dustin, L. B. and Rice, C. M. (2007). Flying under the radar: the immunobiology of hepatitis C. *Annu Rev Immunol* **25**: 71-99.

Egger, D., Wolk, B., et al. (2002). Expression of hepatitis C virus proteins induces distinct membrane alterations including a candidate viral replication complex. *J Virol* **76**(12): 5974-84.

Eksioglu, E. A., Zhu, H., et al. (2011). Characterization of HCV interactions with Toll-like receptors and RIG-I in liver cells. *PLoS One* **6**(6): e21186.

El-Shamy, A., Shindo, M., et al. (2013). Polymorphisms of the core, NS3, and NS5A proteins of hepatitis C virus genotype 1b associate with development of hepatocellular carcinoma. *Hepatology* **58**(2): 555-63.

Evans, M. J., Rice, C. M., et al. (2004). Phosphorylation of hepatitis C virus nonstructural protein 5A modulates its protein interactions and viral RNA replication. *Proc Natl Acad Sci U S A* **101**(35): 13038-43.

Evans, M. J., von Hahn, T., et al. (2007). Claudin-1 is a hepatitis C virus co-receptor required for a late step in entry. *Nature* **446**(7137): 801-5.

Fofana, I., Krieger, S. E., et al. (2010). Monoclonal anti-claudin 1 antibodies prevent hepatitis C virus infection of primary human hepatocytes. *Gastroenterology* **139**(3): 953-64, 964 e1-4.

Fofana, I., Zona, L., et al. (2013). Functional analysis of claudin-6 and claudin-9 as entry factors for hepatitis C virus infection of human hepatocytes by using monoclonal antibodies. *J Virol* **87**(18): 10405-10.

Foster, G. R. (2010). Pegylated interferons for the treatment of chronic hepatitis C: pharmacological and clinical differences between peginterferon-alpha-2a and peginterferon-alpha-2b. *Drugs* **70**(2): 147-65.

Foy, E., Li, K., et al. (2005). Control of antiviral defenses through hepatitis C virus disruption of retinoic acid-inducible gene-I signaling. *Proc Natl Acad Sci U S A* **102**(8): 2986-91.

Fried, M. W. (2002). Side effects of therapy of hepatitis C and their management. *Hepatology* **36**(5 Suppl 1): S237-44.

Fried, M. W., Buti, M., et al. (2013). Once-daily simeprevir (TMC435) with pegylated interferon and ribavirin in treatment-naive genotype 1 hepatitis C: the randomized PILLAR study. *Hepatology* **58**(6): 1918-29.

Fried, M. W., Shiffman, M. L., et al. (2002). Peginterferon alfa-2a plus ribavirin for chronic hepatitis C virus infection. *N Engl J Med* **347**(13): 975-82.

Friedman, S. L. (2000). Molecular regulation of hepatic fibrosis, an integrated cellular response to tissue injury. *J Biol Chem* **275**(4): 2247-50.

Friedman, S. L. (2008). Hepatic stellate cells: protean, multifunctional, and enigmatic cells of the liver. *Physiol Rev* **88**(1): 125-72.

Friedman, S. L. (2008). Mechanisms of hepatic fibrogenesis. *Gastroenterology* **134**(6): 1655-69.

Gale, M., Jr. and Foy, E. M. (2005). Evasion of intracellular host defence by hepatitis C virus. *Nature* **436**(7053): 939-45.

Gane, E. (2012). Future perspectives: towards interferon-free regimens for HCV. *Antivir Ther* **17**(6 Pt B): 1201-10.

Gentzsch, J., Brohm, C., et al. (2013). Hepatitis C Virus p7 is Critical for Capsid Assembly and Envelopment. *PLoS Pathog* **9**(5): e1003355.

Gieseler, R. K., Marquitan, G., et al. (2011). Hepatocyte apoptotic bodies encasing nonstructural HCV proteins amplify hepatic stellate cell activation: implications for chronic hepatitis C. *J Viral Hepat* **18**(11): 760-7.

Gong, G., Waris, G., et al. (2001). Human hepatitis C virus NS5A protein alters intracellular calcium levels, induces oxidative stress, and activates STAT-3 and NF-kappa B. *Proc Natl Acad Sci U S A* **98**(17): 9599-604.

Gonzalez-Peralta, R. P., Fang, J. W., et al. (1994). Optimization for the detection of hepatitis C virus antigens in the liver. *J Hepatol* **20**(1): 143-7.

Gosert, R., Egger, D., et al. (2003). Identification of the hepatitis C virus RNA replication complex in Huh-7 cells harboring subgenomic replicons. *J Virol* **77**(9): 5487-92.

Gottwein, J. M. and Bukh, J. (2008). Cutting the gordian knot-development and biological relevance of hepatitis C virus cell culture systems. *Adv Virus Res* **71**: 51-133.

Gouttenoire, J., Penin, F., et al. (2010). Hepatitis C virus nonstructural protein 4B: a journey into unexplored territory. *Rev Med Virol* **20**(2): 117-29.

Gremion, C., Grabscheid, B., et al. (2004). Cytotoxic T lymphocytes derived from patients with chronic hepatitis C virus infection kill bystander cells via Fas-FasL interaction. *J Virol* **78**(4): 2152-7.

Groskreutz, D. J., Monick, M. M., et al. (2006). Respiratory syncytial virus induces TLR3 protein and protein kinase R, leading to increased double-stranded RNA responsiveness in airway epithelial cells. *J Immunol* **176**(3): 1733-40.

Guidotti, L. G. and Chisari, F. V. (2006). Immunobiology and pathogenesis of viral hepatitis. *Annu Rev Pathol* **1**: 23-61.

Hadziyannis, S. J., Sette, H., Jr., et al. (2004). Peginterferon-alpha2a and ribavirin combination therapy in chronic hepatitis C: a randomized study of treatment duration and ribavirin dose. *Ann Intern Med* **140**(5): 346-55.

Hamamoto, I., Nishimura, Y., et al. (2005). Human VAP-B is involved in hepatitis C virus replication through interaction with NS5A and NS5B. *J Virol* **79**(21): 13473-82.

Harris, H. J., Davis, C., et al. (2010). Claudin association with CD81 defines hepatitis C virus entry. *J Biol Chem* **285**(27): 21092-102.

Harris, H. J., Farquhar, M. J., et al. (2008). CD81 and claudin 1 coreceptor association: role in hepatitis C virus entry. *J Virol* **82**(10): 5007-20.

Harvey, C. E., Post, J. J., et al. (2003). Expression of the chemokine IP-10 (CXCL10) by hepatocytes in chronic hepatitis C virus infection correlates with histological severity and lobular inflammation. *J Leukoc Biol* **74**(3): 360-9.

Heiskala, M., Peterson, P. A., et al. (2001). The roles of claudin superfamily proteins in paracellular transport. *Traffic* **2**(2): 93-8.

Helbig, K. J., Ruszkiewicz, A., et al. (2009). Differential expression of the CXCR3 ligands in chronic hepatitis C virus (HCV) infection and their modulation by HCV in vitro. *J Virol* **83**(2): 836-46.

Helbig, K. J., Ruszkiewicz, A., et al. (2004). Expression of the CXCR3 ligand I-TAC by hepatocytes in chronic hepatitis C and its correlation with hepatic inflammation. *Hepatology* **39**(5): 1220-9.

Horner, S. M. and Gale, M., Jr. (2013). Regulation of hepatic innate immunity by hepatitis C virus. *Nat Med* **19**(7): 879-88.

Hsu, M., Zhang, J., et al. (2003). Hepatitis C virus glycoproteins mediate pH-dependent cell entry of pseudotyped retroviral particles. *Proc Natl Acad Sci U S A* **100**(12): 7271-6.

Huang, L., Hwang, J., et al. (2005). Hepatitis C virus nonstructural protein 5A (NS5A) is an RNA-binding protein. *J Biol Chem* **280**(43): 36417-28.

Huang, W., Zhu, G., et al. (2010). Plasma osteopontin concentration correlates with the severity of hepatic fibrosis and inflammation in HCV-infected subjects. *Clin Chim Acta* **411**(9-10): 675-8.

Huang, Y., Feld, J. J., et al. (2007). Defective hepatic response to interferon and activation of suppressor of cytokine signaling 3 in chronic hepatitis C. *Gastroenterology* **132**(2): 733-44.

Hugle, T., Fehrmann, F., et al. (2001). The hepatitis C virus nonstructural protein 4B is an integral endoplasmic reticulum membrane protein. *Virology* **284**(1): 70-81.

Ikeda, M., Abe, K., et al. (2005). Efficient replication of a full-length hepatitis C virus genome, strain O, in cell culture, and development of a luciferase reporter system. *Biochem Biophys Res Commun* **329**(4): 1350-9.

Ikeda, M., Sugiyama, K., et al. (1998). Human hepatocyte clonal cell lines that support persistent replication of hepatitis C virus. *Virus Res* **56**(2): 157-67.

Ikeda, M., Yi, M., et al. (2002). Selectable subgenomic and genome-length dicistronic RNAs derived from an infectious molecular clone of the HCV-N strain of hepatitis C virus replicate efficiently in cultured Huh7 cells. *J Virol* **76**(6): 2997-3006.

Itsui, Y., Sakamoto, N., et al. (2006). Expressional screening of interferon-stimulated genes for antiviral activity against hepatitis C virus replication. *J Viral Hepat* **13**(10): 690-700.

Jacobson, I. M., Gordon, S. C., et al. (2013). Sofosbuvir for hepatitis C genotype 2 or 3 in patients without treatment options. *N Engl J Med* **368**(20): 1867-77.

Jirasko, V., Montserret, R., et al. (2010). Structural and functional studies of nonstructural protein 2 of the hepatitis C virus reveal its key role as organizer of virion assembly. *PLoS Pathog* **6**(12): e1001233.

Jones, C. T., Murray, C. L., et al. (2007). Hepatitis C virus p7 and NS2 proteins are essential for production of infectious virus. *J Virol* **81**(16): 8374-83.

Jones, D. M. and McLauchlan, J. (2010). Hepatitis C virus: assembly and release of virus particles. *J Biol Chem* **285**(30): 22733-9.

Jones, D. M., Patel, A. H., et al. (2009). The hepatitis C virus NS4B protein can trans-complement viral RNA replication and modulates production of infectious virus. *J Virol* **83**(5): 2163-77.

Joyce, M. A. and Tyrrell, D. L. (2010). The cell biology of hepatitis C virus. *Microbes Infect* **12**(4): 263-71.

Kandathil, A. J., Graw, F., et al. (2013). Use of laser capture microdissection to map hepatitis C virus-positive hepatocytes in human liver. *Gastroenterology* **145**(6): 1404-13 e1-10.

Kapadia, S. B., Barth, H., et al. (2007). Initiation of hepatitis C virus infection is dependent on cholesterol and cooperativity between CD81 and scavenger receptor B type I. *J Virol* **81**(1): 374-83.

Kawai, T. and Akira, S. (2008). Toll-like receptor and RIG-I-like receptor signaling. *Ann N Y Acad Sci* **1143**: 1-20.

Kisseleva, T. and Brenner, D. A. (2006). Hepatic stellate cells and the reversal of fibrosis. *J Gastroenterol Hepatol* **21 Suppl 3**: S84-7.

Kosaka, N., Iguchi, H., et al. (2010). Secretory mechanisms and intercellular transfer of microRNAs in living cells. *J Biol Chem* **285**(23): 17442-52.

Kowdley, K. V., Lawitz, E., et al. (2014). Phase 2b trial of interferon-free therapy for hepatitis C virus genotype 1. *N Engl J Med* **370**(3): 222-32.

Krawczynski, K., Beach, M. J., et al. (1992). Hepatitis C virus antigen in hepatocytes: immunomorphologic detection and identification. *Gastroenterology* **103**(2): 622-9.

Krieger, N., Lohmann, V., et al. (2001). Enhancement of hepatitis C virus RNA replication by cell culture-adaptive mutations. *J Virol* **75**(10): 4614-24.

Krieger, S. E., Zeisel, M. B., et al. (2010). Inhibition of hepatitis C virus infection by anti-claudin-1 antibodies is mediated by neutralization of E2-CD81-claudin-1 associations. *Hepatology* **51**(4): 1144-57.

Lagging, M., Romero, A. I., et al. (2006). IP-10 predicts viral response and therapeutic outcome in difficult-to-treat patients with HCV genotype 1 infection. *Hepatology* **44**(6): 1617-25.

Lau, D. T., Fish, P. M., et al. (2008). Interferon regulatory factor-3 activation, hepatic interferon-stimulated gene expression, and immune cell infiltration in hepatitis C virus patients. *Hepatology* **47**(3): 799-809.

Lau, G. K., Davis, G. L., et al. (1996). Hepatic expression of hepatitis C virus RNA in chronic hepatitis C: a study by in situ reverse-transcription polymerase chain reaction. *Hepatology* **23**(6): 1318-23.

Lau, J. Y. and Davis, G. L. (1994). Detection of hepatitis C virus RNA genome in liver tissue by nonisotopic in situ hybridization. *J Med Virol* **42**(3): 268-71.

Lavanchy, D. (2008). Chronic viral hepatitis as a public health issue in the world. *Best Pract Res Clin Gastroenterol* **22**(6): 991-1008.

Law, M. G., Dore, G. J., et al. (2003). Modelling hepatitis C virus incidence, prevalence and long-term sequelae in Australia, 2001. *Int J Epidemiol* **32**(5): 717-24.

Lawitz, E., Mangia, A., et al. (2013). Sofosbuvir for previously untreated chronic hepatitis C infection. *N Engl J Med* **368**(20): 1878-87.

Lee, U. E. and Friedman, S. L. (2011). Mechanisms of hepatic fibrogenesis. *Best Pract Res Clin Gastroenterol* **25**(2): 195-206.

Li, J., Liu, K., et al. (2013). Exosomes mediate the cell-to-cell transmission of IFN-alpha-induced antiviral activity. *Nat Immunol* **14**(8): 793-803.

Li, K., Chen, Z., et al. (2005). Distinct poly(I-C) and virus-activated signaling pathways leading to interferon-beta production in hepatocytes. *J Biol Chem* **280**(17): 16739-47.

Li, K., Foy, E., et al. (2005). Immune evasion by hepatitis C virus NS3/4A protease-mediated cleavage of the Toll-like receptor 3 adaptor protein TRIF. *Proc Natl Acad Sci U S A* **102**(8): 2992-7.

Li, K., Li, N. L., et al. (2012). Activation of chemokine and inflammatory cytokine response in hepatitis C virus-infected hepatocytes depends on Toll-like receptor 3 sensing of hepatitis C virus double-stranded RNA intermediates. *Hepatology* **55**(3): 666-75.

Li, K., Prow, T., et al. (2002). Cellular response to conditional expression of hepatitis C virus core protein in Huh7 cultured human hepatoma cells. *Hepatology* **35**(5): 1237-46.

Li, X. D., Sun, L., et al. (2005). Hepatitis C virus protease NS3/4A cleaves mitochondrial antiviral signaling protein off the mitochondria to evade innate immunity. *Proc Natl Acad Sci U S A* **102**(49): 17717-22.

Liang, Y., Shilagard, T., et al. (2009). Visualizing hepatitis C virus infections in human liver by two-photon microscopy. *Gastroenterology* **137**(4): 1448-58.

Lin, T. I., Lenz, O., et al. (2009). In vitro activity and preclinical profile of TMC435350, a potent hepatitis C virus protease inhibitor. *Antimicrob Agents Chemother* **53**(4): 1377-85.

Lin, W., Tsai, W. L., et al. (2010). Hepatitis C virus regulates transforming growth factor beta1 production through the generation of reactive oxygen species in a nuclear factor kappaB-dependent manner. *Gastroenterology* **138**(7): 2509-18, 2518 e1.

Lin, W., Weinberg, E. M., et al. (2008). HIV increases HCV replication in a TGF-beta1-dependent manner. *Gastroenterology* **134**(3): 803-11.

Lin, W., Wu, G., et al. (2011). HIV and HCV cooperatively promote hepatic fibrogenesis via induction of reactive oxygen species and NFkappaB. *J Biol Chem* **286**(4): 2665-74.

Lindenbach, B. D., Evans, M. J., et al. (2005). Complete replication of hepatitis C virus in cell culture. *Science* **309**(5734): 623-6.

Lindenbach, B. D., Meuleman, P., et al. (2006). Cell culture-grown hepatitis C virus is infectious in vivo and can be recultured in vitro. *Proc Natl Acad Sci U S A* **103**(10): 3805-9.

Lindenbach, B. D., Pragai, B. M., et al. (2007). The C terminus of hepatitis C virus NS4A encodes an electrostatic switch that regulates NS5A hyperphosphorylation and viral replication. *J Virol* **81**(17): 8905-18.

Liu, S., Yang, W., et al. (2009). Tight junction proteins claudin-1 and occludin control hepatitis C virus entry and are downregulated during infection to prevent superinfection. *J Virol* **83**(4): 2011-4.

Lohmann, V., Korner, F., et al. (2001). Mutations in hepatitis C virus RNAs conferring cell culture adaptation. *J Virol* **75**(3): 1437-49.

Lohmann, V., Korner, F., et al. (1999). Replication of subgenomic hepatitis C virus RNAs in a hepatoma cell line. *Science* **285**(5424): 110-3.

Lundberg, A. M., Drexler, S. K., et al. (2007). Key differences in TLR3/poly I:C signaling and cytokine induction by human primary cells: a phenomenon absent from murine cell systems. *Blood* **110**(9): 3245-52.

Lundin, M., Monne, M., et al. (2003). Topology of the membrane-associated hepatitis C virus protein NS4B. *J Virol* **77**(9): 5428-38.

Lupberger, J., Zeisel, M. B., et al. (2011). EGFR and EphA2 are host factors for hepatitis C virus entry and possible targets for antiviral therapy. *Nat Med* **17**(5): 589-95.

Madan, V., Redondo, N., et al. (2010). Cell permeabilization by poliovirus 2B viroporin triggers bystander permeabilization in neighbouring cells through a mechanism involving gap junctions. *Cell Microbiol* **12**(8): 1144-57.

Manns, M. P., McHutchison, J. G., et al. (2001). Peginterferon alfa-2b plus ribavirin compared with interferon alfa-2b plus ribavirin for initial treatment of chronic hepatitis C: a randomised trial. *Lancet* **358**(9286): 958-65.

Mansy, S. S., Nosseir, M. M., et al. (2014). Value of reelin for assessing hepatic fibrogenesis in a group of Egyptian HCV infected patients. *Clin Chem Lab Med* **52**(9): 1319-28.

Marcellin, P., Asselah, T., et al. (2002). Fibrosis and disease progression in hepatitis C. *Hepatology* **36**(5 Suppl 1): S47-56.

Marks, K. M. and Jacobson, I. M. (2012). The first wave: HCV NS3 protease inhibitors telaprevir and boceprevir. *Antivir Ther* **17**(6 Pt B): 1119-31.

Martell, M., Esteban, J. I., et al. (1992). Hepatitis C virus (HCV) circulates as a population of different but closely related genomes: quasispecies nature of HCV genome distribution. *J Virol* **66**(5): 3225-9.

Marusawa, H., Hijikata, M., et al. (1999). Hepatitis C virus core protein inhibits Fas- and tumor necrosis factor alpha-mediated apoptosis via NF-kappaB activation. *J Virol* **73**(6): 4713-20.

Masaki, T., Suzuki, R., et al. (2008). Interaction of hepatitis C virus nonstructural protein 5A with core protein is critical for the production of infectious virus particles. *J Virol* **82**(16): 7964-76.

Matsumoto, M., Funami, K., et al. (2003). Subcellular localization of Toll-like receptor 3 in human dendritic cells. *J Immunol* **171**(6): 3154-62.

McCartney, E. M., Eyre, N. S., et al. (2011). Border patrol intensifies for hepatitis C virus entry. *Hepatology* **54**(4): 1472-5.

McKeating, J. A., Zhang, L. Q., et al. (2004). Diverse hepatitis C virus glycoproteins mediate viral infection in a CD81-dependent manner. *J Virol* **78**(16): 8496-505.

Mee, C. J., Grove, J., et al. (2008). Effect of cell polarization on hepatitis C virus entry. *J Virol* **82**(1): 461-70.

Meertens, L., Bertaux, C., et al. (2008). The tight junction proteins claudin-1, -6, and -9 are entry cofactors for hepatitis C virus. *J Virol* **82**(7): 3555-60.

Meylan, E., Curran, J., et al. (2005). Cardif is an adaptor protein in the RIG-I antiviral pathway and is targeted by hepatitis C virus. *Nature* **437**(7062): 1167-72.

Ming-Ju, H., Yih-Shou, H., et al. (2011). Hepatitis C virus E2 protein induce reactive oxygen species (ROS)-related fibrogenesis in the HSC-T6 hepatic stellate cell line. *J Cell Biochem* **112**(1): 233-43.

Miyanari, Y., Atsuzawa, K., et al. (2007). The lipid droplet is an important organelle for hepatitis C virus production. *Nat Cell Biol* **9**(9): 1089-97.

Miyashita, M., Oshiumi, H., et al. (2011). DDX60, a DEXD/H box helicase, is a novel antiviral factor promoting RIG-I-like receptor-mediated signaling. *Mol Cell Biol* **31**(18): 3802-19.

Miyoshi, H., Moriya, K., et al. (2011). Pathogenesis of lipid metabolism disorder in hepatitis C: polyunsaturated fatty acids counteract lipid alterations induced by the core protein. *J Hepatol* **54**(3): 432-8.

Mohan, N., Gonzalez-Peralta, R. P., et al. (2010). Chronic hepatitis C virus infection in children. *J Pediatr Gastroenterol Nutr* **50**(2): 123-31.

Mohd Hanafiah, K., Groeger, J., et al. (2013). Global epidemiology of hepatitis C virus infection: New estimates of age-specific antibody to HCV seroprevalence. *Hepatology* **57**(4): 1333-42.

Monazahian, M., Bohme, I., et al. (1999). Low density lipoprotein receptor as a candidate receptor for hepatitis C virus. *J Med Virol* **57**(3): 223-9.

Moradpour, D., Englert, C., et al. (1996). Characterization of cell lines allowing tightly regulated expression of hepatitis C virus core protein. *Virology* **222**(1): 51-63.

Moradpour, D., Evans, M. J., et al. (2004). Insertion of green fluorescent protein into nonstructural protein 5A allows direct visualization of functional hepatitis C virus replication complexes. *J Virol* **78**(14): 7400-9.

Moradpour, D., Penin, F., et al. (2007). Replication of hepatitis C virus. *Nat Rev Microbiol* **5**(6): 453-63.

Morikawa, K., Lange, C. M., et al. (2011). Nonstructural protein 3-4A: the Swiss army knife of hepatitis C virus. *J Viral Hepat* **18**(5): 305-15.

Moriya, K., Fujie, H., et al. (1998). The core protein of hepatitis C virus induces hepatocellular carcinoma in transgenic mice. *Nat Med* **4**(9): 1065-7.

Moriya, K., Nakagawa, K., et al. (2001). Oxidative stress in the absence of inflammation in a mouse model for hepatitis C virus-associated hepatocarcinogenesis. *Cancer Res* **61**(11): 4365-70.

Moriya, K., Yotsuyanagi, H., et al. (1997). Hepatitis C virus core protein induces hepatic steatosis in transgenic mice. *J Gen Virol* **78 (Pt 7)**: 1527-31.

Nagaraja, T., Chen, L., et al. (2012). Activation of the connective tissue growth factor (CTGF)-transforming growth factor beta 1 (TGF-beta 1) axis in hepatitis C virus-expressing hepatocytes. *PLoS One* **7**(10): e46526.

Nakabayashi, H., Taketa, K., et al. (1982). Growth of human hepatoma cells lines with differentiated functions in chemically defined medium. *Cancer Res* **42**(9): 3858-63.

Nakano, T., Lau, G. M., et al. (2011). An updated analysis of hepatitis C virus genotypes and subtypes based on the complete coding region. *Liver Int* **32**(2): 339-45.

Napoli, J., Bishop, G. A., et al. (1996). Progressive liver injury in chronic hepatitis C infection correlates with increased intrahepatic expression of Th1-associated cytokines. *Hepatology* **24**(4): 759-65.

Nguyen, H., Sankaran, S., et al. (2006). Hepatitis C virus core protein induces expression of genes regulating immune evasion and anti-apoptosis in hepatocytes. *Virology* **354**(1): 58-68.

Nishitsuji, H., Funami, K., et al. (2013). Hepatitis C virus infection induces inflammatory cytokines and chemokines mediated by the cross talk between hepatocytes and stellate cells. *J Virol* **87**(14): 8169-78.

Okuda, M., Li, K., et al. (2002). Mitochondrial injury, oxidative stress, and antioxidant gene expression are induced by hepatitis C virus core protein. *Gastroenterology* **122**(2): 366-75.

Pal, S., Shuhart, M. C., et al. (2006). Intrahepatic hepatitis C virus replication correlates with chronic hepatitis C disease severity in vivo. *J Virol* **80**(5): 2280-90.

Paradis, V., Mathurin, P., et al. (1996). Histological features predictive of liver fibrosis in chronic hepatitis C infection. *J Clin Pathol* **49**(12): 998-1004.

Park, J., Kang, W., et al. (2012). Hepatitis C virus infection enhances TNFalpha-induced cell death via suppression of NF-kappaB. *Hepatology* **56**(3): 831-40.

Patouraux, S., Bonnafous, S., et al. (2012). The osteopontin level in liver, adipose tissue and serum is correlated with fibrosis in patients with alcoholic liver disease. *PLoS One* **7**(4): e35612.

Pawlotsky, J. M. (2003). Hepatitis C virus genetic variability: pathogenic and clinical implications. *Clin Liver Dis* **7**(1): 45-66.

Pawlotsky, J. M. (2004). Pathophysiology of hepatitis C virus infection and related liver disease. *Trends Microbiol* **12**(2): 96-102.

Perlemuter, G., Sabile, A., et al. (2002). Hepatitis C virus core protein inhibits microsomal triglyceride transfer protein activity and very low density lipoprotein secretion: a model of viral-related steatosis. *FASEB J* **16**(2): 185-94.

Perz, J. F., Armstrong, G. L., et al. (2006). The contributions of hepatitis B virus and hepatitis C virus infections to cirrhosis and primary liver cancer worldwide. *J Hepatol* **45**(4): 529-38.

Phan, T., Kohlway, A., et al. (2011). The acidic domain of hepatitis C virus NS4A contributes to RNA replication and virus particle assembly. *J Virol* **85**(3): 1193-204.

Pietschmann, T., Kaul, A., et al. (2006). Construction and characterization of infectious intragenotypic and intergenotypic hepatitis C virus chimeras. *Proc Natl Acad Sci U S A* **103**(19): 7408-13.

Pietschmann, T., Zayas, M., et al. (2009). Production of infectious genotype 1b virus particles in cell culture and impairment by replication enhancing mutations. *PLoS Pathog* **5**(6): e1000475.

Pileri, P., Uematsu, Y., et al. (1998). Binding of hepatitis C virus to CD81. *Science* **282**(5390): 938-41.

Ploss, A. and Evans, M. J. (2012). Hepatitis C virus host cell entry. *Curr Opin Virol* **2**(1): 14-9.

Ploss, A., Evans, M. J., et al. (2009). Human occludin is a hepatitis C virus entry factor required for infection of mouse cells. *Nature* **457**(7231): 882-6.

Pol, S., Ghalib, R. H., et al. (2012). Daclatasvir for previously untreated chronic hepatitis C genotype-1 infection: a randomised, parallel-group, double-blind, placebo-controlled, dose-finding, phase 2a trial. *Lancet Infect Dis* **12**(9): 671-7.

Poli, G. (2000). Pathogenesis of liver fibrosis: role of oxidative stress. *Mol Aspects Med* **21**(3): 49-98.

Popescu, C. I., Callens, N., et al. (2011). NS2 protein of hepatitis C virus interacts with structural and non-structural proteins towards virus assembly. *PLoS Pathog* **7**(2): e1001278.

Popescu, C. I., Rouille, Y., et al. (2011). Hepatitis C virus assembly imaging. *Viruses* **3**(11): 2238-54.

Preiss, S., Thompson, A., et al. (2008). Characterization of the innate immune signalling pathways in hepatocyte cell lines. *J Viral Hepat* **15**(12): 888-900.

Presser, L. D., McRae, S., et al. (2013). Activation of TGF-beta1 Promoter by Hepatitis C Virus-Induced AP-1 and Sp1: Role of TGF-beta1 in Hepatic Stellate Cell Activation and Invasion. *PLoS One* **8**(2): e56367.

Qadri, I., Iwahashi, M., et al. (2004). Induced oxidative stress and activated expression of manganese superoxide dismutase during hepatitis C virus replication: role of JNK, p38 MAPK and AP-1. *Biochem J* **378**(Pt 3): 919-28.

Raychoudhuri, A., Shrivastava, S., et al. (2011). ISG56 and IFITM1 proteins inhibit hepatitis C virus replication. *J Virol* **85**(24): 12881-9.

Razali, K., Thein, H. H., et al. (2007). Modelling the hepatitis C virus epidemic in Australia. *Drug Alcohol Depend* **91**(2-3): 228-35.

Reynolds, G. M., Harris, H. J., et al. (2008). Hepatitis C virus receptor expression in normal and diseased liver tissue. *Hepatology* **47**(2): 418-27.

Robbins, P. D. and Morelli, A. E. (2014). Regulation of immune responses by extracellular vesicles. *Nat Rev Immunol* **14**(3): 195-208.

Rockey, D. C. and Friedman, S. L. (1992). Cytoskeleton of liver perisinusoidal cells (lipocytes) in normal and pathological conditions. *Cell Motil Cytoskeleton* **22**(4): 227-34.

Roderfeld, M., Weiskirchen, R., et al. (2009). Altered factor VII activating protease expression in murine hepatic fibrosis and its influence on hepatic stellate cells. *Liver Int* **29**(5): 686-91.

Rodriguez-Inigo, E., Bartolome, J., et al. (1999). Histological damage in chronic hepatitis C is not related to the extent of infection in the liver. *Am J Pathol* **154**(6): 1877-81.

Romero-Brey, I., Merz, A., et al. (2012). Three-dimensional architecture and biogenesis of membrane structures associated with hepatitis C virus replication. *PLoS Pathog* **8**(12): e1003056.

Sakai, A., Claire, M. S., et al. (2003). The p7 polypeptide of hepatitis C virus is critical for infectivity and contains functionally important genotype-specific sequences. *Proc Natl Acad Sci U S A* **100**(20): 11646-51.

Sanghavi, S. K. and Reinhart, T. A. (2005). Increased expression of TLR3 in lymph nodes during simian immunodeficiency virus infection: implications for inflammation and immunodeficiency. *J Immunol* **175**(8): 5314-23.

Santolini, E., Pacini, L., et al. (1995). The NS2 protein of hepatitis C virus is a transmembrane polypeptide. *J Virol* **69**(12): 7461-71.

Sato, K., Ishikawa, T., et al. (2007). Expression of Toll-like receptors in chronic hepatitis C virus infection. *J Gastroenterol Hepatol* **22**(10): 1627-32.

Scarselli, E., Ansuini, H., et al. (2002). The human scavenger receptor class B type I is a novel candidate receptor for the hepatitis C virus. *EMBO J* **21**(19): 5017-25.

Schoggins, J. W., Wilson, S. J., et al. (2011). A diverse range of gene products are effectors of the type I interferon antiviral response. *Nature* **472**(7344): 481-5.

Scholle, F., Li, K., et al. (2004). Virus-host cell interactions during hepatitis C virus RNA replication: impact of polyprotein expression on the cellular transcriptome and cell cycle association with viral RNA synthesis. *J Virol* **78**(3): 1513-24.

Schulze-Krebs, A., Preimel, D., et al. (2005). Hepatitis C virus-replicating hepatocytes induce fibrogenic activation of hepatic stellate cells. *Gastroenterology* **129**(1): 246-58.

Schwabe, R. F., Bataller, R., et al. (2003). Human hepatic stellate cells express CCR5 and RANTES to induce proliferation and migration. *Am J Physiol Gastrointest Liver Physiol* **285**(5): G949-58.

Shimakami, T., Hijikata, M., et al. (2004). Effect of interaction between hepatitis C virus NS5A and NS5B on hepatitis C virus RNA replication with the hepatitis C virus replicon. *J Virol* **78**(6): 2738-48.

Shin, J. Y., Hur, W., et al. (2005). HCV core protein promotes liver fibrogenesis via up-regulation of CTGF with TGF-beta1. *Exp Mol Med* **37**(2): 138-45.

Sievert, W., Altraif, I., et al. (2011). A systematic review of hepatitis C virus epidemiology in Asia, Australia and Egypt. *Liver Int* **31 Suppl 2**: 61-80.

Sklan, E. H., Charuworn, P., et al. (2009). Mechanisms of HCV survival in the host. *Nat Rev Gastroenterol Hepatol* **6**(4): 217-27.

Spengler, U. and Nattermann, J. (2007). Immunopathogenesis in hepatitis C virus cirrhosis. *Clin Sci (Lond)* **112**(3): 141-55.

Sprenger, H., Kaufmann, A., et al. (1997). Induction of neutrophil-attracting chemokines in transforming rat hepatic stellate cells. *Gastroenterology* **113**(1): 277-85.

Starr, R., Willson, T. A., et al. (1997). A family of cytokine-inducible inhibitors of signalling. *Nature* **387**(6636): 917-21.

Steinmann, E., Penin, F., et al. (2007). Hepatitis C virus p7 protein is crucial for assembly and release of infectious virions. *PLoS Pathog* **3**(7): e103.

Stiffler, J. D., Nguyen, M., et al. (2009). Focal distribution of hepatitis C virus RNA in infected livers. *PLoS One* **4**(8): e6661.

Sulkowski, M. S., Gardiner, D. F., et al. (2014). Daclatasvir plus sofosbuvir for previously treated or untreated chronic HCV infection. *N Engl J Med* **370**(3): 211-21.

Sumpter, R., Jr., Loo, Y. M., et al. (2005). Regulating intracellular antiviral defense and permissiveness to hepatitis C virus RNA replication through a cellular RNA helicase, RIG-I. *J Virol* **79**(5): 2689-99.

Suzuki, T., Aizaki, H., et al. (2007). Molecular biology of hepatitis C virus. *J Gastroenterol* **42**(6): 411-23.

Takahashi, K., Asabe, S., et al. (2010). Plasmacytoid dendritic cells sense hepatitis C virus-infected cells, produce interferon, and inhibit infection. *Proc Natl Acad Sci U S A* **107**(16): 7431-6.

Tanaka, N., Moriya, K., et al. (2008). PPARalpha activation is essential for HCV core protein-induced hepatic steatosis and hepatocellular carcinoma in mice. *J Clin Invest* **118**(2): 683-94.

Taniguchi, H., Kato, N., et al. (2004). Hepatitis C virus core protein upregulates transforming growth factor-beta 1 transcription. *J Med Virol* **72**(1): 52-9.

Te, H. S. and Jensen, D. M. (2010). Epidemiology of hepatitis B and C viruses: a global overview. *Clin Liver Dis* **14**(1): 1-21, vii.

Tellinghuisen, T. L., Evans, M. J., et al. (2007). Studying hepatitis C virus: making the best of a bad virus. *J Virol* **81**(17): 8853-67.

Terrault, N. A., Dodge, J. L., et al. (2013). Sexual transmission of hepatitis C virus among monogamous heterosexual couples: the HCV partners study. *Hepatology* **57**(3): 881-9.

Thein, H. H., Yi, Q., et al. (2008). Estimation of stage-specific fibrosis progression rates in chronic hepatitis C virus infection: a meta-analysis and meta-regression. *Hepatology* **48**(2): 418-31.

Thomas, D. L. (2012). Highly active anti-hepatitis C therapy: seven lessons from HIV. *Antivir Ther* **17**(6 Pt B): 1183-8.

Timpe, J. M., Stamataki, Z., et al. (2008). Hepatitis C virus cell-cell transmission in hepatoma cells in the presence of neutralizing antibodies. *Hepatology* **47**(1): 17-24.

Tissari, J., Siren, J., et al. (2005). IFN-alpha enhances TLR3-mediated antiviral cytokine expression in human endothelial and epithelial cells by up-regulating TLR3 expression. *J Immunol* **174**(7): 4289-94.

Trajkovic, K., Hsu, C., et al. (2008). Ceramide triggers budding of exosome vesicles into multivesicular endosomes. *Science* **319**(5867): 1244-7.

Tumne, A., Prasad, V. S., et al. (2009). Noncytotoxic suppression of human immunodeficiency virus type 1 transcription by exosomes secreted from CD8+ T cells. *J Virol* **83**(9): 4354-64.

Urtasun, R., Lopategi, A., et al. (2012). Osteopontin, an oxidant stress sensitive cytokine, up-regulates collagen-I via integrin alpha(V)beta(3) engagement and PI3K/pAkt/NFkappaB signaling. *Hepatology* **55**(2): 594-608.

Vieyres, G., Brohm, C., et al. (2013). Subcellular localization and function of an epitope-tagged p7 viroporin in hepatitis C virus-producing cells. *J Virol* **87**(3): 1664-78.

Vieyres, G. and Pietschmann, T. (2013). Entry and replication of recombinant hepatitis C viruses in cell culture. *Methods* **59**(2): 233-48.

Wakita, T., Pietschmann, T., et al. (2005). Production of infectious hepatitis C virus in tissue culture from a cloned viral genome. *Nat Med* **11**(7): 791-6.

Wald, O., Weiss, I. D., et al. (2007). Chemokines in hepatitis C virus infection: pathogenesis, prognosis and therapeutics. *Cytokine* **39**(1): 50-62.

Waller, H., Chatterji, U., et al. (2010). The use of AlphaLISA technology to detect interaction between hepatitis C virus-encoded NS5A and cyclophilin A. *J Virol Methods* **165**(2): 202-10.

Walsh, M. J., Jonsson, J. R., et al. (2006). Non-response to antiviral therapy is associated with obesity and increased hepatic expression of suppressor of cytokine signalling 3 (SOCS-3) in patients with chronic hepatitis C, viral genotype 1. *Gut* **55**(4): 529-35.

Wang, N., Liang, Y., et al. (2009). Toll-like receptor 3 mediates establishment of an antiviral state against hepatitis C virus in hepatoma cells. *J Virol* **83**(19): 9824-34.

Wang, Y., Li, J., et al. (2013). Induction of interferon-lambda contributes to Toll-like receptor-3-activated hepatic stellate cell-mediated hepatitis C virus inhibition in hepatocytes. *J Viral Hepat* **20**(6): 385-94.

Wasmuth, H. E., Tag, C. G., et al. (2009). The Marburg I variant (G534E) of the factor VII-activating protease determines liver fibrosis in hepatitis C infection by reduced proteolysis of platelet-derived growth factor BB. *Hepatology* **49**(3): 775-80.

Watanabe, N., Aizaki, H., et al. (2011). Hepatitis C virus RNA replication in human stellate cells regulates gene expression of extracellular matrix-related molecules. *Biochem Biophys Res Commun* **407**(1): 135-40.

Weber, G. F., Ashkar, S., et al. (1996). Receptor-ligand interaction between CD44 and osteopontin (Eta-1). *Science* **271**(5248): 509-12.

Welbourn, S. and Pause, A. (2007). The hepatitis C virus NS2/3 protease. *Curr Issues Mol Biol* **9**(1): 63-9.

Wilkins, C., Woodward, J., et al. (2013). IFITM1 is a tight junction protein that inhibits hepatitis C virus entry. *Hepatology* **57**(2): 461-9.

Winnard, P. T., Jr., Kluth, J. B., et al. (2007). Development of novel chimeric transmembrane proteins for multimodality imaging of cancer cells. *Cancer Biol Ther* **6**(12): 1889-99.

Witteveldt, J., Evans, M. J., et al. (2009). CD81 is dispensable for hepatitis C virus cell-to-cell transmission in hepatoma cells. *J Gen Virol* **90**(Pt 1): 48-58.

Wong, J. B., McQuillan, G. M., et al. (2000). Estimating future hepatitis C morbidity, mortality, and costs in the United States. *Am J Public Health* **90**(10): 1562-9.

Wozniak, A. L., Griffin, S., et al. (2010). Intracellular proton conductance of the hepatitis C virus p7 protein and its contribution to infectious virus production. *PLoS Pathog* **6**(9): e1001087.

Wu, C. F., Lin, Y. L., et al. (2013). Hepatitis C virus core protein stimulates fibrogenesis in hepatic stellate cells involving the obese receptor. *J Cell Biochem* **114**(3): 541-50.

Xu, L., Hui, A. Y., et al. (2005). Human hepatic stellate cell lines, LX-1 and LX-2: new tools for analysis of hepatic fibrosis. *Gut* **54**(1): 142-51.

Yamaguchi, A., Tazuma, S., et al. (2005). Hepatitis C virus core protein modulates fatty acid metabolism and thereby causes lipid accumulation in the liver. *Dig Dis Sci* **50**(7): 1361-71.

You, L. R., Chen, C. M., et al. (1999). Hepatitis C virus core protein enhances NF-kappaB signal pathway triggering by lymphotoxin-beta receptor ligand and tumor necrosis factor alpha. *J Virol* **73**(2): 1672-81.

Yu, G. Y., Lee, K. J., et al. (2006). Palmitoylation and polymerization of hepatitis C virus NS4B protein. *J Virol* **80**(12): 6013-23.

Zeisel, M. B., Koutsoudakis, G., et al. (2007). Scavenger receptor class B type I is a key host factor for hepatitis C virus infection required for an entry step closely linked to CD81. *Hepatology* **46**(6): 1722-31.

Zeremski, M., Petrovic, L. M., et al. (2008). Intrahepatic levels of CXCR3-associated chemokines correlate with liver inflammation and fibrosis in chronic hepatitis C. *Hepatology* **48**(5): 1440-50.

Zeremski, M., Petrovic, L. M., et al. (2007). The role of chemokines as inflammatory mediators in chronic hepatitis C virus infection. *J Viral Hepat* **14**(10): 675-87.

Zeuzem, S., Berg, T., et al. (2013). Simeprevir increases rate of sustained virologic response among treatment-experienced patients with HCV genotype-1 infection: a phase IIb trial. *Gastroenterology* **146**(2): 430-441 e6.

Zhang, J., Randall, G., et al. (2004). CD81 is required for hepatitis C virus glycoprotein-mediated viral infection. *J Virol* **78**(3): 1448-55.

Zhang, S., Kodys, K., et al. (2013). CD81/CD9 tetraspanins aid plasmacytoid dendritic cells in recognition of hepatitis C virus-infected cells and induction of interferon-alpha. *Hepatology* **58**(3): 940-9.

Zhang, S., Saha, B., et al. (2013). IFN-gamma production by human natural killer cells in response to HCV-infected hepatoma cells is dependent on accessory cells. *J Hepatol* **59**(3): 442-9.

Zheng, A., Yuan, F., et al. (2007). Claudin-6 and claudin-9 function as additional coreceptors for hepatitis C virus. *J Virol* **81**(22): 12465-71.

Zhong, J., Gastaminza, P., et al. (2005). Robust hepatitis C virus infection in vitro. *Proc Natl Acad Sci U S A* **102**(26): 9294-9.

Zhu, X., He, Z., et al. (2014). IFITM3-containing exosome as a novel mediator for anti-viral response in dengue virus infection. *Cell Microbiol* **17**(1): 105-18.